Mesangioblasts promote the regeneration of a stable and organised vasculature in a decellularised intestinal graft

To be submitted for a

Doctorate in Philosophy

Alfonso Maria Tedeschi

University College London

August 2022

I, Alfonso Maria Tedeschi, confirm that the work presented in this thesis is my own. Where information has been taken from other sources I confirm that this has been stated.

Table of Contents

Acronyms

List of figures

List of tables

Abstract

Whole organ tissue engineering has emerged as a viable solution to the lack of organs for transplant, but there is a significant bottleneck in whole organ tissue creation, namely the vasculature. The main cell types that compose the vasculature are endothelial cells and perivascular cells.

Recent efforts used endothelial cells and supporting cells to engineer organs' vasculature. Ott's group published in 2015 a pioneer study introducing this concept and seeding both cell types through both arterial and venous routes in a rat decellularised lung. Nevertheless, still many works attempted organ revascularisation without taking in account the perivascular compound. Moreover, in many works, the presence of the engineered graft has been characterised only after few days in culture *in vitro* and *in vivo* and sustainability over time of the engineered endothelium is another point that need to be addressed

In this context, this work aims to elucidate the mechanisms behind which endothelial cells (Human Umbilical Vein Endothelial Cells, HUVECs) and perivascular cells (Mesoangioblasts, MABs) cross-talk and repopulated the preserved vasculature of a decellularised whole organ.

In this study I report the use of the perivascular compartment as pivotal for generating a vasculature with good barrier function and durability both *in vitro* and *in vivo,* with

poor results obtained instead when only HUVECs were used. In this work I established a perfusable, functional, and long-lasting vasculature with cells organising themselves in a native manner by seeding MABs and HUVECs into the conserved vasculature of a decellularised rat gut.

Impact statement

Whole organ tissue engineering has emerged as an alternative solution to the lack of organs for transplant, yet there is a significant impediment in whole organ tissue creation: the vasculature.

In fact, the delivery of oxygen and nutrients in an avascular tissue would be limited to a few hundred micrometres by gas diffusion, and necrosis would occur in the rest of the graft.

Perivascular cells have a crucial role in the generation and homeostasis of blood vessels , however some gaps still exists in understanding the crosstalk between these two cell types.

Recent efforts used endothelial cells and supporting cells to engineer organs' vasculature.

Nevertheless, still many works attempted organ revascularisation without taking in account the perivascular compound in lung, liver, kidney and intestine. Therefore, still not a consistent and homogenous strategy of organ vascularisation has been established in the field.

In this context, this work aimed at elucidating the mechanisms behind which endothelial cells and perivascular cells cross-talk and repopulated the preserved vasculature of a decellularised whole organ. Insights provided by this study about this

regeneration process will help to reach clinical translation of engineered whole organs since the lack of a functional vasculature is a definitive no-go.

In this work we report the use of the perivascular compartment as pivotal for generating a vasculature with good barrier function and durability both *in vitro* and *in vivo,* with poor results obtained instead when only HUVECs were used.

In particular, by seeding MABs and HUVECs into the preserved vasculature of a decellularised rat intestine, I generated a perfusable, functional, and long lasting vasculature with cells organising themselves in a native manner: endothelial cells lying the vessel drawing a patent endothelium, MABs surrounding them and a smooth muscle layer around the vessel coming from the pericytes precursor. This latter achievement was never reported in previous whole organ re-vascularization studies.

To my knowledge, very little is known, about gut smooth muscle development both in human and in mice. However, none of those theories take in account the possible contribution of a pericyte precursor which is the unexpected result unveiled in our tissue engineered gut vasculature.

Those results corroborate the hypothesis, first proposed by Paolo Bianco, that pericytes are bi-potent progenitors of the vascular smooth muscle and of the extravascular mesodermal derivatives of the tissue in which they reside.

To my knowledge this is the first time that it was proven in the visceral smooth muscle, within a gut tissue engineering model.

Therefore, we found more solid and standardize conditions to address organ revascularisation. We believe these insights should transform the field of vascular tissue engineering and that will fasten the development of tissue-engineered big organs for a broad spectrum of gastrointestinal disorders, nevertheless for their clinical applications.

List of publications

1. Loukogeorgakis S., Shangaris P, Bertin E, Franzin C, Piccoli M, Pozzobon M, Subramaniam S , Tedeschi A[1], Kim AG, Li H, Fachin CG Dias AIBS Stratigis JD, Ahn NJ, Thrasher AJ, Bonfanti P, Peranteau WH, David AL, Flake AW, De Coppi P. In Utero Transplantation of Expanded Autologous Amniotic Fluid Stem Cells Results in Long-Term Hematopoietic Engraftment, Stem Cells 2019

2. F. Pellegata, A, M. Tedeschi and Paolo De Coppi. Whole Organ Tissue Vascularization: Engineering the Tree to Develop the Fruits,. Frontiers 2018

3. B. Palikuqi, D.T Nguyen, G. Li, R. Schreiner, A. F Pellegata, Y Liu, D. Redmond, F. Geng, Y. Lin, J. M G. Salinero, M. Yokoyama P. Zumbo, T. Zhang, B. Kunar, M. Witherspoon, T. Han, A. M.Tedeschi, F. Scottoni, S. Lipkin, L. Dow, O. Elemento, J. Z. Xiang, K. Shido, J. Spence, J. Q. Zhou, R. E Schwartz, P. DeCoppi, S. Y. Rabbany, S. Rafii. Adaptable durable and hemodynamic human vasculogenic endothelial cells for organogenesis and tumorigenesis

4. L. Meran, I. Massie, A.Weston, R. Gaifulina, P.Faull, M. Orford, A. Kucharska, A Baulies, E. Hirst, J. Konig, A.M. Tedeschi, A.Pellegata, S. Eli, B. Snijders, L. Collinson, N. Thapar, G. Thomas, S. Eaton, P. Bonfanti, P. De Coppi, and V.S.W. Li. Engineering transplantable jejunal mucosal grafts using primary patient-derived organoids from children with intestinal failure"

5. S. Loukogeorgakis, N. A. Juffali , J. Jimenez , P. Maghsoudlou , A. Tedeschi , S. Khalaf , A.Khabbush , L. Urbani , M. Platé , C. G. Fachin , A. I. Bradley, D. S. Dias , N. Sindhwani , J. Toelen , P.Carmeliet , S. M Janes, P De Coppi, J. Deprest. Prenatal VEGF nano-delivery reverses congenital diaphragmatic hernia-associated pulmonary abnormalities SUBMITTED, Manuscript under revision

Chapter 1

Introduction

1.1. Short bowel syndrome

1.1.1. Anatomy of the intestine

The intestine is composed of two major segments that form a continuous tube, the small intestine and the large intestine. The small intestine begins at the pylorus (just after the stomach) and ends at the ileocecal valve, which is where the large intestine start ending with the anus. The small intestine is furtherly subdivided into three main segments. Starting from that one proximal to the stomach to the distal: the duodenum, followed by the jejunum and then the ileum. The large intestine begins at the caecum, followed by the ascending colon, the transverse colon, the descending colon and the rectum, terminating with the anus. Small and large intestine differ a lot in term of size. Whilst the small intestine has a total length of 6-7 meters consisting of multiple loops, the large intestine has a wider diameter but a shorter length (1.5 meters) (Figure 1.1) (Mowat and Agace 2014).

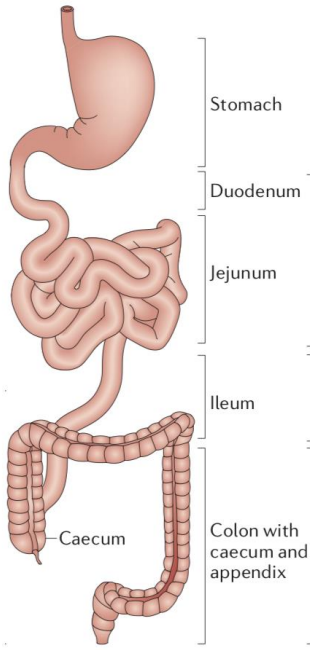

Figure 1.1: Intestine gross anatomy. Picture adapted from Mowat and Agace 2014 that shows the anatomy of the intestine (Mowat and Agace 2014)

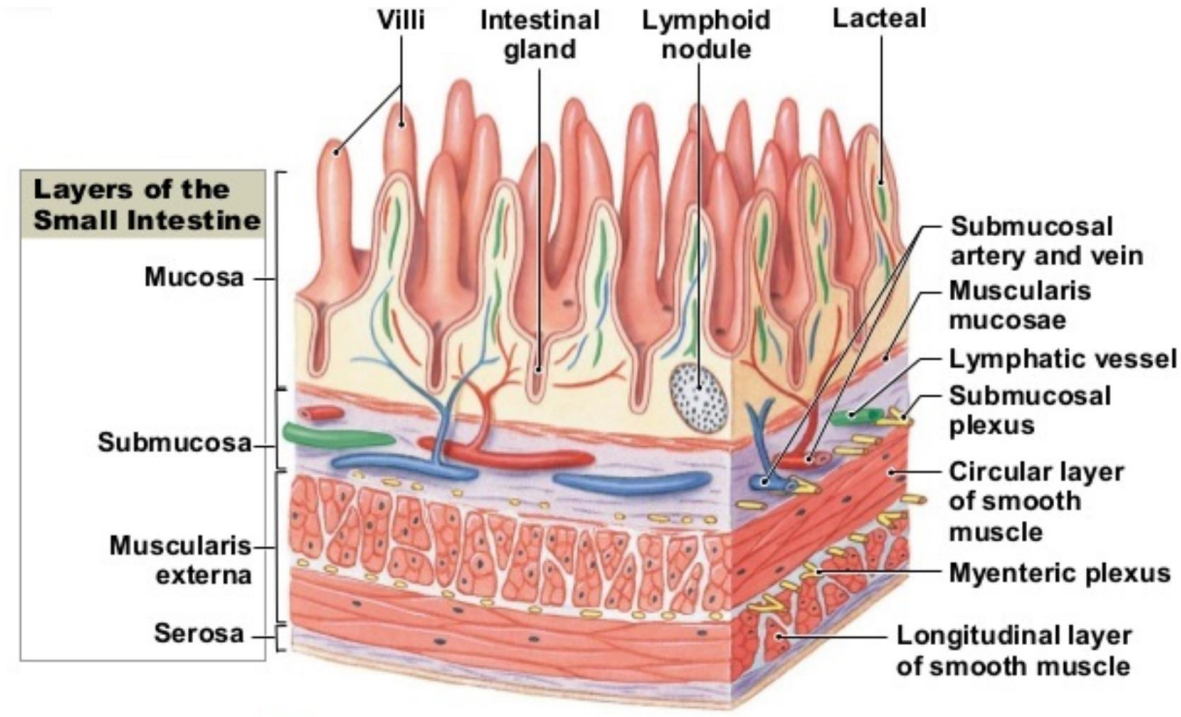

Figure 1.2: Histology of the small intestine. Subdivision of the intestine wall into the four main layers: mucosa, submucosa, muscularis externa, serosa. Picture taken from https://socratic.org/questions/from-the-lumen-outward-what-are-the-layers-of-the-gastrointestinal-tract

Histologically, the intestine is a multi-stratified organ composed of different layers. The first layer on the luminal surface is the mucosa, a specialised epithelium lying on the *lamina propria*. Deeper down lies the *muscolaris mucosae,* a thin layer of muscle cells that separate the mucosa from the sub-mucosa. The submucosa is adjacent to the *muscolaris externa* and contains the submucosal plexus of the Enteric Nervous System (ENS), and the majority of the blood and lymphatic vessels. The *muscolaris externa* consists of two muscle layers, an inner circular and an outer longitudinal, with the myenteric plexus of the of the ENS located between them (Figure 1.2) (Gerritsen et al 2011).

The small intestine and large intestine again differ for the presence or not of villi, finger-like projections which extend into the lumen that are present in the small intestine only and increase the surface area of digestively active epithelium (Mowat and Agace 2014). The surface epithelium is continuously renewed by immature cells arising from invaginations known as the crypts. The vast majority of these cells are absorptive enterocytes but there are also Paneth cells, goblet cells and neuroendocrine cells. All those cells have a fast turn-over (4-5 days) and, except for Paneth cells which move downwards to the base of the

crypt, newly formed epithelial cells move upward and acquire their specific digestive and absorptive function only at the base of the villus. The journey of those cells carry on up to the tip of the villus where they get extruded and ejected into the intestinal lumen (Figure 1.3) (Mowat and Agace 2014) .

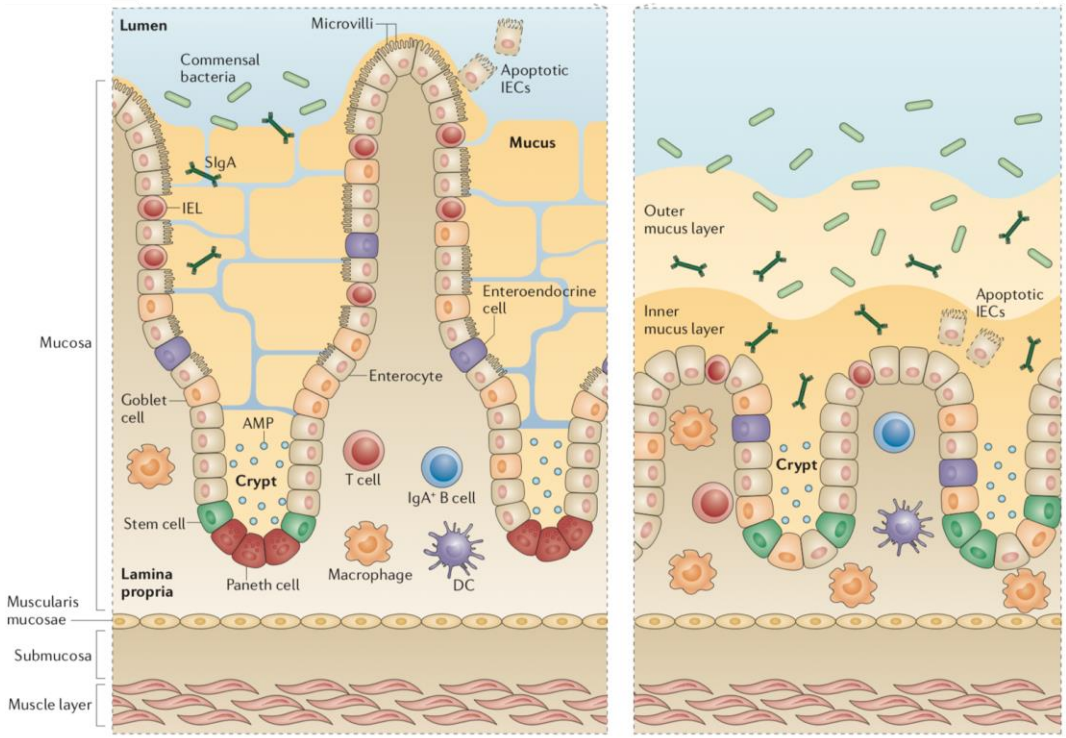

Figure 1.3: Schematic organisation of the small and large intestine epithelium. Picture adapted from Mowat and Agace 2014 showing the epithelial compartment of the small and large intestine. (Mowat and Agace 2014)

1.1.2 Pathophysiology of SBS

Paediatric short bowel syndrome (SBS) is a serious condition that occurs in children with congenital or acquired reduction in the length of the small intestine. The congenital SBS is a rare disorder in which the mean length of the small intestine is substantially reduced when compared to its normal counterpart. Acquired SBS is normally caused by surgical resection of the small intestine for the treatment of Crohn disease, trauma, malignancy, radiation, or mesenteric ischemia but the most common aetiology includes necrotizing enterocolitis (NEC) (Höllwarth et al. 2017).

. SBS results in excessive liquid loss, nutrient malabsorption, electrolyte abnormalities, increased susceptibility to infections, parenteral nutrition associated complications and affects weight gain and growth. If not treated, SBS is debilitating

and can lead to death. Parenteral nutrition (PN) has demonstrated a decreased mortality and enhanced quality of life in children affected with SBS. However, if this treatment is carried out for prolonged amount of time, it is associated with a variety of complications including significant liver disease. Restoring enteral autonomy and reducing long-term dependence on parenteral support represents the primary goal of treatments and this is carried out by increasing the absorptive potential of the remnant intestine (Chandra and Kesavan 2018).

SBS is currently defined as requiring PN for more than 60 days following intestinal resection or having a bowel length that is less than 25% of predicted.(Merritt et al. 2017). The incidence of SBS is 24.5 per 100,000 live births with a greater incidence in preterm infants (Höllwarth et al. 2017).

The minimum length of bowel required for autonomous enteral function in infants is approximately 40 cm with an intact ileocecal valve (Goulet et al. 1991). However, the length of remnant small intestine is not the only factor that plays a role in the ability of a child with SBS to emancipate from parenteral support. Indeed, the site of intestinal resection causes a customised interruption of the proximal-distal gradient of digestion leading to specific types of malabsorption in patients with SBS (Merritt et al. 2017).

Patients who carry out a proximal resections (i.e. jejunum) are more likely to have a transient but significant gastric acid hypersecretion (Kumpf 2014) due to the loss of a number of humoral mediators and secretin feedback inhibition mechanisms that normally regulate gastrin and gastric acid secretion.

However, patient with proximal resection unlikely experience a strong nutrient and electrolytes unbalance due to the capacity of the remaining ileum and intact colon to compensate the lack of the resected tissue. After resection indeed, the colon has the potential to become a vital digestive and absorptive organ (Tappenden 2014).

Loss of significant liquid and electrolyte absorptive capacity occurs, instead, in child lacking the ileum, due to the lower compensative capacity of the jejunum. Moreover

the ileum is the site of bile acid and vitamin B12 absorption, and slows intestinal transit through a primary inhibitory feedback mechanism known as the “ileal brake”(Current treatment paradigms in pediatric short bowel syndrome n.d.). Furthermore, loss of the ileum reduces production of peptide YY and glucagon-like peptide-1, which have an inhibitory effect on intestinal motility, leading to a decrease in intestinal transit time (Kumpf et al. 2014).

The presence of the ileocecal valve (ICV) is another crucial player and its maintenance or not can influence the emancipation of the child from parenteral nutrition (Demehri et al. 2015). The ICV perform the function of a barrier to prevent bacterial translocation of colonic contents and slows intestinal transit time. Loss of the ICV promotes small intestinal bacterial overgrowth which increase SBS symptoms (Demehri et al. 2015).

Following resection, the remnant bowel undergoes a process known as intestinal adaptation. This is a natural compensatory response involving morphologic and functional changes that the remnant bowel undergoes in order to increases absorptive surface area and improves absorption. This process involves the increase in villous height and crypt depth, increased bowel calibre, increase in enterocyte number, hyperplasia of intestinal epithelium and increased expression of epithelial transporter proteins (Kelly, Tappenden, and Winkler 2014).

1.1.3 Management of SBS

In all SBS patients, the objective of treatment is to increase the adaptation process throughout time in order to acquire enteral autonomy, limit problems, and provide an adequate quality of life. The main goal of the current treatment for SBS is to allow the remnant bowel to maximise adaptation in order to restore enteral autonomy. Long-term PN is indeed the primary medical therapy utilized in the immediate postoperative period in SBS. PN therapy attempts to replete calories and nutrients intravenously,

bypassing the enteral circuit while it heals. However, this can lead to several problems such as catheter-associated infection, vascular thrombosis, and intestinal failure associated to liver disease (Current treatment paradigms in pediatric short bowel syndrome n.d.). In the case of congenital SBS, the PN Therapy may last shorter time since the paediatric intestine develops with the kid and may re-establish its normal size. A resection of the intestine and acquired SBS may be more problematic since it occurs in older children or adults, and various therapies, such medical treatments or surgical interventions, must be considered.

Medical treatments can involve hormonal agent able to increase intestinal absorption, or anti-motility agents able to slow intestinal transit time and allow increased absorption of nutrients and fluids (Current treatment paradigms in pediatric short bowel syndrome n.d.). However, despite aggressive medical management, some patients may never recover their bowel function in order to leave PN. These patients require surgical management.

The non-transplant surgical procedure to treat SBS falls in two categories: the ones aiming at prolonging intestinal transit time and those aiming at increasing the functional intestinal absorptive surface area. Longitudinal intestinal lengthening and tailoring (LILT) [Bianchi procedure]) and serial transverse enteroplasty (STEP) are the standard operations for increasing intestinal surface area, promoting intestinal function (Figure 1.4-1.5)(Kishore 2014).

In many cases this might not be enough, and the only solution remains intestinal transplantation which is treated in the next chapter.

The future of SBS therapeutics might be found also in a completely artificial or artificially generated and harvested gut. The advancement of bioengineering technology and molecular medicine has drawn researchers' attention to the prospect of employing tissue-engineered small intestines (TESI). In the clinical setting, it would be difficult, if not impossible, to produce human neonatal intestine organoids, particularly for autologous stem cell transplantation. This is especially true in the case

of congenital SBS, when removing a portion of the intestine from a new-born with a short gut might raise problems. In the instance of acquired SBS, a section of the intestine might be used as a cell source for a tissue engineering technique.

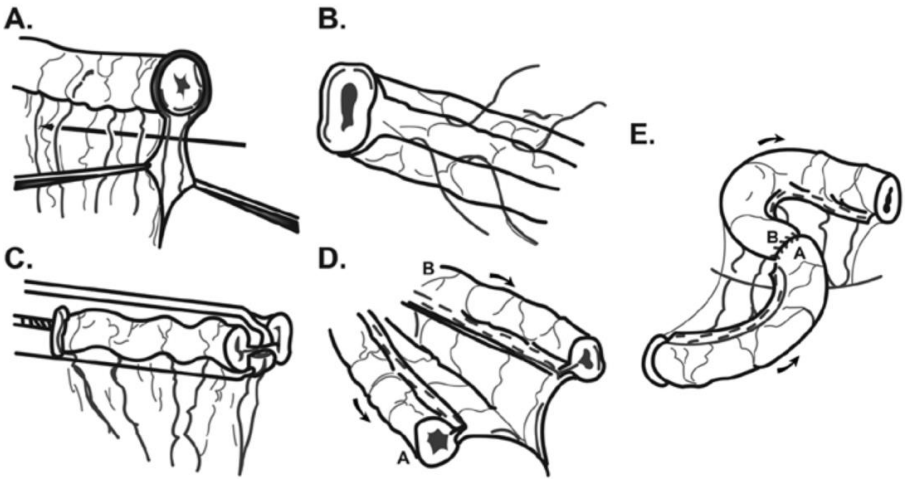

Figure 1.4: Diagram showing the longitudinal intestinal lengthening and tailoring (LILT) procedure, originally described by Bianchi. **(A)** Creation of the avascular space along the mesenteric border of a dilated loop of bowel; **(B)** view of avascular space; **(C)** splitting of the bowel lengthwise; **(D)** view of newly created hemi-loops; **(E)** isoperistaltic anastomosis of hemi-loops. From Kishore 2014

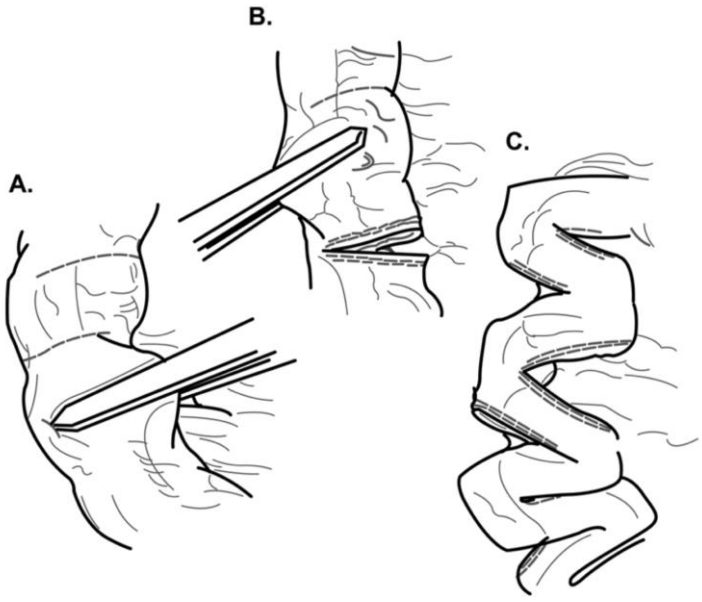

Fig 1.5: Diagram showing the serial transverse enteroplasty (STEP) procedure. staples are fired perpendicular to the long axis of the bowel in a zig- zag pattern to make and close incisions and thereby reduce lumen diameter and lengthen the bowel. The first**(A)** and second **(B)** staples are placed; **(C)** with the appropriate placement of multiple staples, the bowel is extended and tapered. From Kishore 2014

1.1.4 Intestinal Transplantation

Worldwide, only approximately 200 allogeneic intestinal transplants occur each year due to both donor shortage and the technical challenges inherent in the procedure. In children aged 1–18 years, 5-year survival rates from intestinal transplants are significantly lower (46–76%) when compared with renal (95–96%), liver (77–86%) and heart (72–77%) transplants(Howell and Wells n.d.) (Figure 1.6).

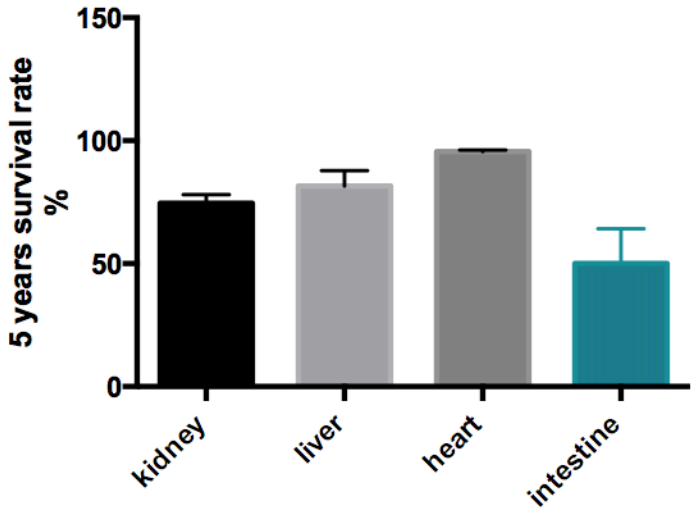

Fig 1.6: Graphic showing the degree of success of intestinal transplantation compared to other organs. Data retrieved from Howell, J. C. & Wells, J. M. Generating intestinal tissue from stem cells: potential for research and therapy. doi:10.2217/rme.11.90.

The reason of this figures is that intestinal transplant recipients generally require more profound immunosuppression than patients receiving other solid organs because of the higher immunogenicity of the intestine. In the intestine, indeed, resides most of the innate immune system of hour body making it the organ with the higher antigen presenting capacity of our body. Due to the strong presence of the donor immune system, the immunosuppression therapy is the crucial factor of outcome in intestinal transplantation (Garg et al. 2011).

Following early transplantation attempts, deaths were most commonly a consequence of acute graft rejection and subsequent sepsis associated multi-organ failure (Middleton and Jamieson 2005), However, even with standard immunosuppression protocol, such as the combination of azathioprine, prednisolone, and antilymphocyte globulin, Graft versus host disease occurs in 50% of the cases (Garg et al. 2011).

The introduction of tacrolimus, a potent new calcineurin inhibitor, marked the next major step in allowing clinical intestinal transplantation to become a reality. Early rejection was then superseded by infection as the main cause of death, (Middleton and Jamieson 2005) indicating the need to refine the target of immunological suppression to reduce infection while avoiding rejection.

In these cases increasing immunosuppression might be the only solutions but not without consequences: a natural consequence of transplantation of an organ exposed to external microorganisms in the presence of profound immunosuppression is the susceptibility of the recipient to local and systemic infections (Garg et al. 2011). Prophylactic interventions, such as systemic and local (selective gut decontamination) administration of antimicrobial agents have proven ineffective, leading instead to the emergence of multi-resistant organisms (Troppmann and Gruessner 2001). Another problem due to strong immunosuppression is the lymphoproliferative disease. Therapies to this problem might include reduction or cessation of immunosuppression which lead to rejection or graft loss (Troppmann and Gruessner 2001).

1.2. Whole organ tissue engineering

1.2.1 Concept of the Whole organ tissue engineering

Tissue engineering (TE) represent a promising tool to overcome the hurdles of organs transplantation. TE aims at repairing a tissue or an organ that has lost its function by creating biological equivalent through the combination of cells, scaffold matrices and stimuli delivered

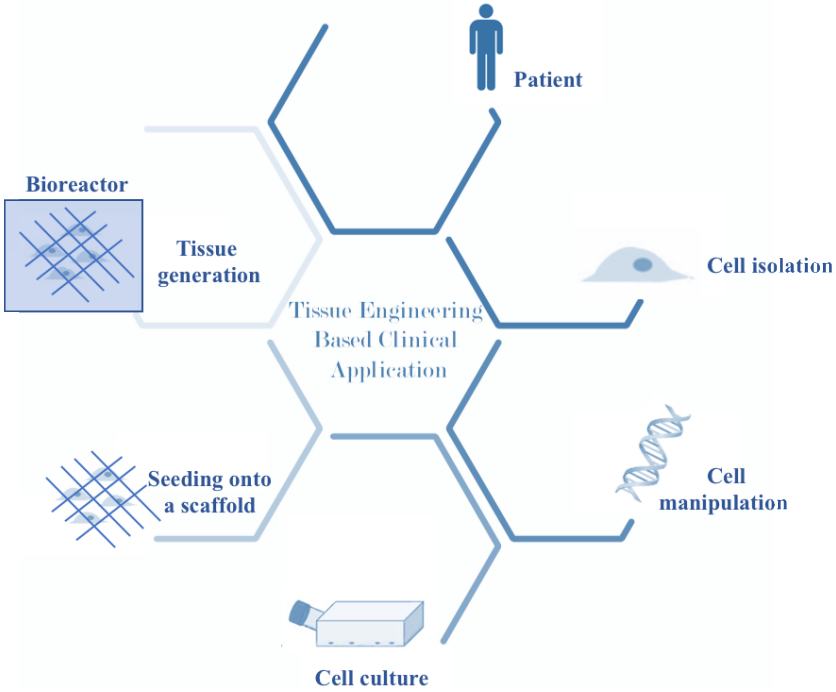

Fig 1.7: whole organs tissue engineering workflow. Schematic showing all the steps of organ tissue engineering from the cell isolation to the delivery into the patient.

through a bioreactor to the growing organ *in vitro* (Langer and Vacanti 1993). The first stage of all TE approaches involves removing cells from the patient and expanding them, with or without a differentiation step. Although cell biologists have been isolating and culturing cells from living tissue since the beginning of the 20th century, these monolayer cell cultures were typically 2D with cells exposed to a liquid interface, diffusion of soluble factors into the culture media, limited cell to cell interaction and

high stiffness of the plastic substrate leading to cell spreading(Hussey, Dziki, and Badylak 2018). Those features do not resemble at all the ones that cells encounter in vivo. Multicellular organisms require a 3D framework that provide structural integrity to the organism, full cell to cell interaction, gradient of soluble factors that delineate specific microenvironments. In fact, the tremendous progress in tissue engineering and regenerative medicine over the past few decades can be largely attributed to the development of biomaterials designed to exert mechanical and biochemical cues that guide cell behaviour, with the general strategy to combine cells with 3D biodegradable scaffolds to create replacement tissues (Figure 1.7).

1.2.2 Decellularised Matrix Scaffolds

The Extracellular Matrix (ECM) is a fibrous network of proteins, proteoglycans and glycosaminoglycans arranged in a tissue-specific 3D architecture that provides cells and tissues with topographical signalling cues, structural and elastic properties and a medium for diffusion and convection of nutrients and oxygen (Geckil et al. 2010). In addition to its structural and mechanical functions, the ECM also serves as an adhesive substrate not only for cell attachment and migration (Mecham et al. 2012), but , also for the sequestration of growth factors and morphogens (Hynes et al. 2009), resulting in the establishment of specialized local microenvironments that contribute to the differentiation and maintenance of tissue-specific cell phenotypes and functions.

Given the complexity and incomplete understanding of ECM composition and structure, designing and fabricating an ECM scaffold that fully mimics the biochemistry and architecture of native tissue ECM are currently not possible. In order to maintain structural feature and some environmental cues of the organs, tissue engineering recently moved to decellularised scaffold. Decellularisation consist in the complete removal of the whole cellular compartment of the tissue or organ while

preserving its extracellular matrix (Gilpin and Yang 2017). This technique allows the generation of a scaffold that preserve the structural, biological and mechanical function of the matrix, acting as a natural template of the organ to be engineered. This is important considering that composition and cell interaction with the matrix is tissue specific and for this reason contribute to tissue functionality (Badylak et al. 2002).

Acellular matrices allow cellular growth and their functional differentiation into the desired phenotype. In addition, the removal of all the cellular compartment leads to the removal of immunogenic material, avoiding the chances of eliciting an immune response even in the case of xenogeneic transplantation (Fishman et al. 2013).

The first stage of decellularization protocols usually consists of flushing cells with deionized water in order to alter their osmotic pressure, finally causing their lysis. Afterwards, the most robust decellularization methods usually combine the effects of chemical, enzymatic and physical agents (Lee et al. 2017).

Chemical agents are used to solubilize cytoplasmic and nuclear components. Several types of detergents and solubilizing agents have been used for this purpose: non-ionic detergents, such as TritonX-100, have a mild effect on tissue architecture, as they disrupt lipid-lipid and lipid-protein bonds while maintaining protein conformation. On the contrary, ionic detergents, such as Sodium Deoxysulfate or Sodium Deoxycholate (SDC), often alter protein-protein interactions (Seddon, Curnow, and Booth 2004). Although being effective for complete removal of cellular components, ionic agents have been reported to damage native tissue architecture to various extents (Gilbert, Sellaro, and Badylak 2006). However, the readout that some chemicals have on the decellularization process is tissue-specific and is time and dose dependent (Ozeki et al. 2006.) For instance, compared effect of various detergents on oesophageal decellularization, proves that tissues treated with SDC show superior mechanical properties and lower DNA remnants if compared to tissues processed with TritonX-100 (Ozeki et al. 2006).

Enzymatic agents include proteases and nucleases (Gilbert, Sellaro and Badylak, 2006). Trypsin, for instance, is protease applied in decellularization protocols, as being able to separate cellular material from the ECM in a wide range of tissues. However, prolonged exposure to trypsin has been shown reduce the contents of ECM proteins and glycosaminoglycans, and therefore alter the native tissue architecture. Endonucleases or exonucleases, instead, are widely used to lyse the genetic material (Gilbert, Sellaro and Badylak, 2006).

Physical methods may be further combined with the above-mentioned agents to further disrupt cell membranes and those include mechanical pressure, sonication, freezing and thawing (Gilbert, Sellaro and Badylak, 2006).

The first scientific report demonstrating a crude decellularization technique was published in 1948 (Riley 1948). In this early study, researchers showed that acellular homogenates can be prepared by pulverizing muscle tissue at −70°C to remove cellular components. Following this first decellularization approach, isolation of the basement membrane of blood vessels (Meezan et al. 1975)and isolation of the ECM of the liver (Rojkind et al. 1980) were reported.

In those reports all the samples were treated with deionized water, deoxyribonuclease and SDC, and continuous stirring was applied to favour release of cellular components. Afterwards, Gamba et al. modified the original protocol adjusting reagent timings and including cyclic repeats to manufacture muscle-derived matrices(Gamba et al. 2002)

In 2006, Marzaro et al. used the hereafter known as “Detergent-Enzymatic” treatment (DET) for the development of porcine oesophageal scaffolds, describing maintenance of ECM architecture and angiogenic factors (Marzaro et al. 2006). The same methodology was applied to obtain an acellular scaffold from pig oesophagus, confirming this is a gentle, efficient technique which preserve the structure of the tissue while removing cellular and nuclear material both in small and big animals (Totonelli et al. 2013).

This decellularization techniques provided the basis for more advanced decellularization techniques, for example, perfusion decellularization, which preserves not only the overall 3D ECM morphology but also an intact vascular tree, providing a route for the reseeding of site-specific cells. Perfusion decellularization was first demonstrated in 2008 with the decellularization and recellularization of a whole rat heart (Ott et al. 2008)

With this technique, our group was the first to report a rat intestinal scaffold preserving the crypt-villi axis on the luminal side (Figure 1.8) (Totonelli et al. 2012).

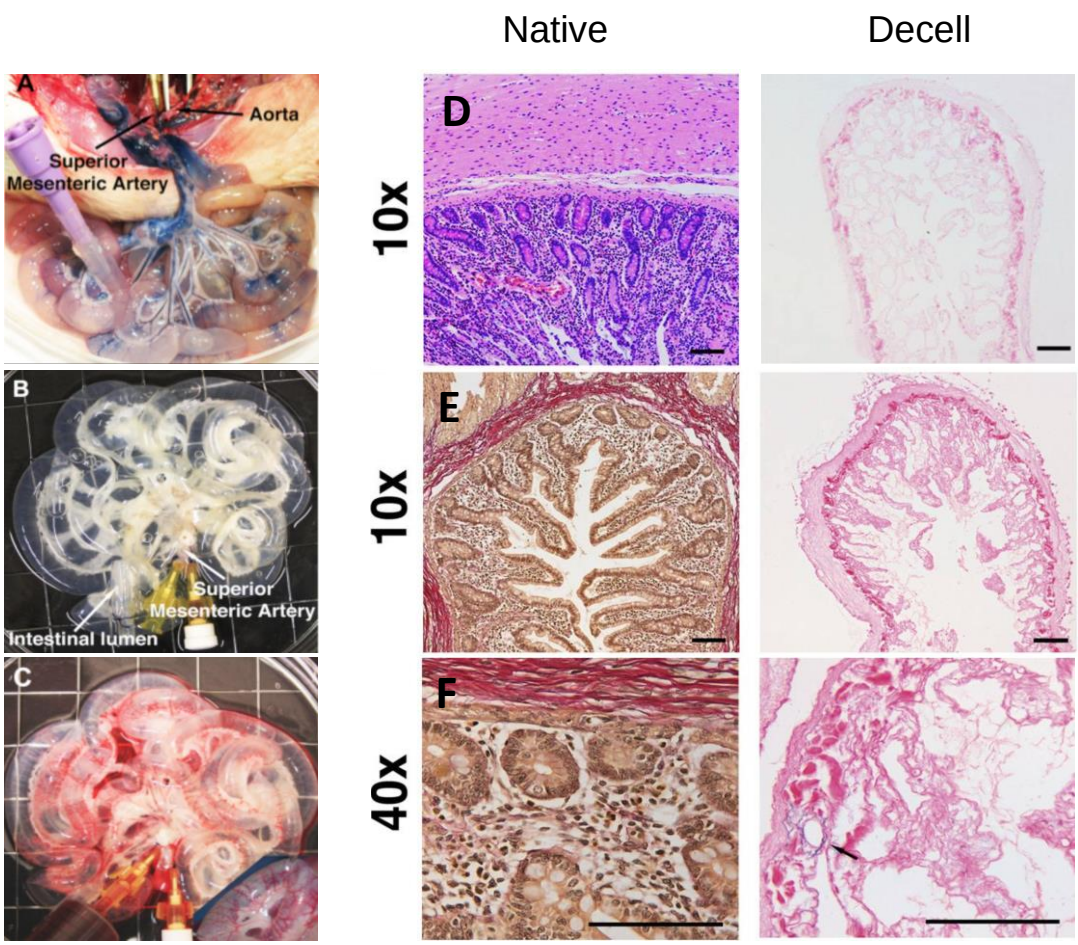

Fig. 1.8: Decellularization of rat small intestine with detergent-enzymatic treatment. Macroscopic images prior **(A)** and following **(B)** one cycle of decellularization. Perfusion with Rosso Ponceau **(C)** dyes display the patency and distribution of vasculature. **(D)** Haematoxylin and Eosin **(**H&E) staining confirms the absence of nuclei and demonstrates preservation of structure following 1 cycle of treatment compared to fresh tissue. **(E-F)** Elastica Van Gieson (EVG) staining confirms the preservation of the elastin component around the blood vessels (black arrow). (From Totonelli et al. 2012)

Interestingly, in the same paper of 2012, it has been shown that among the different compartments preserved within the decellularised intestine, the extracellular matrix of the vasculature optimally retains its structure (Totonelli et al. 2012). This latter achievement results fundamental in the context of whole organ tissue engineering and organ grafting since the delivery of oxygen and nutrients in an avascular tissue

would be limited to a few hundred micrometres by gas diffusion, and necrosis would occur in the rest of the graft (Jain et al. 2005).

1.3. Vascular tissue engineering

1.3.1 Vascular architecture

Vascular system is essential for the homeostasis and growth of every living tissues and organisms. This system consists of arteries, capillaries and veins through which the circulating blood reaches each cell delivering nutrients, oxygen and removing metabolic waste. The gas and metabolic exchange take place in the capillaries which spatial frequency is around 100-300 μm due to oxygen diffusion limit. (Lauridsen et al. 2014). Moreover, circulation permits endocrine communication between cells, the blood indeed carries soluble factors and proteins reaching cells and tissues beyond the diffusion barrier (Orlando et al. 2012).

Blood vessels range in size and include micro vessels (<1mm), small vessels (1–6 mm), and large vessels (>6 mm in diameter) (Hammer et al. 2014).

As the distance and resistance of tissue changes, the vascular structure varies to perfuse each district. Arteries require a thick and stable structure to handle the high pressure of the blood coming from the heart and reaching the distal regions. Looking at the arteries cross section three main layers (or tunics) are recognisable: tunica intima (luminar layer), tunica media (middle region) and tunica adventitia (outside layer) (Figure 1.9).

Endothelial Cells (EC) monolayer covers luminal surface of tunica intima, which prevents the formation of thrombi.

The tunica media, is made of vascular smooth muscle cells (vSMC) and elastic connective tissue, both these layers are involved in regulation and maintenance of the blood pressure.

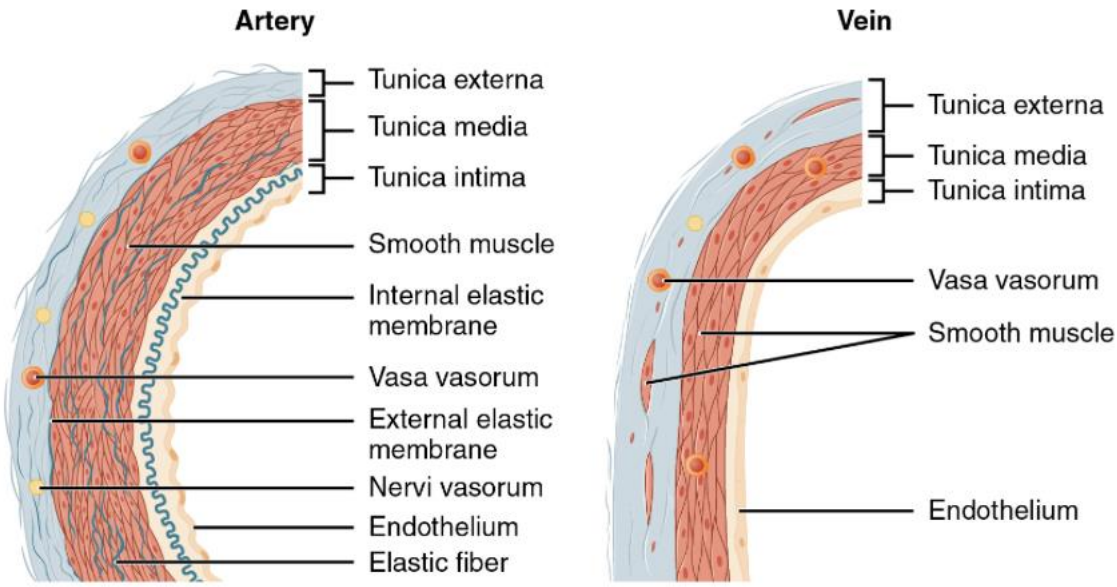

Fig 1.9: large vessel in cross-section. Picture adapted from: https://en.wikipedia.org/wiki/File:2102_Comparison_of_Artery_and_Vein.jpg showing the different layers of large vessel in cross-section: Tunica intima, tunica media, tunica externa

The middle tunica has a nerve supply regulating the vasoconstriction. Fibrous connective tissue forms the tunica externa, the outer layer, that is absent in the arterioles, the connection between arteries and capillaries. Smooth muscle layer is essential for the regulation of the diameter and to prevent rupture or bursting (Kumar et al. 2014). The underlying layers, tunica media and adventitia, are composed of extracellular proteins (such as collagen, elastin, Proteoglycans (PGs) and Glycosaminoglycans (GAGs)) (Figure 1.9).

Veins maintain the same three-layers structure with few differences, the inner layer of veins is smooth endothelium but at intervals this lining is folded to form valves that prevent backflow of blood. The last two layers are quite thin respect to arteries because veins do not regulate blood pressure that is besides very low (Figure 1.9) (Orlando et al. 2012).

Microvasculature includes capillary, pre and post capillary that unlike the mechanically stronger large vessels are characterized by thin walls that facilitate molecular diffusion (Kumar et al. 2014). Lumen surface is covered by a single layer of endothelial cells. The basement membrane around these cells is diffent from the big vessel`s one indeed it is composed by a heterogeneous protein matrix of collagen (type IV), lamin, pelecan and other proteins. The creation and stabilisation of this membrane is due to either ECs and Pericytes.

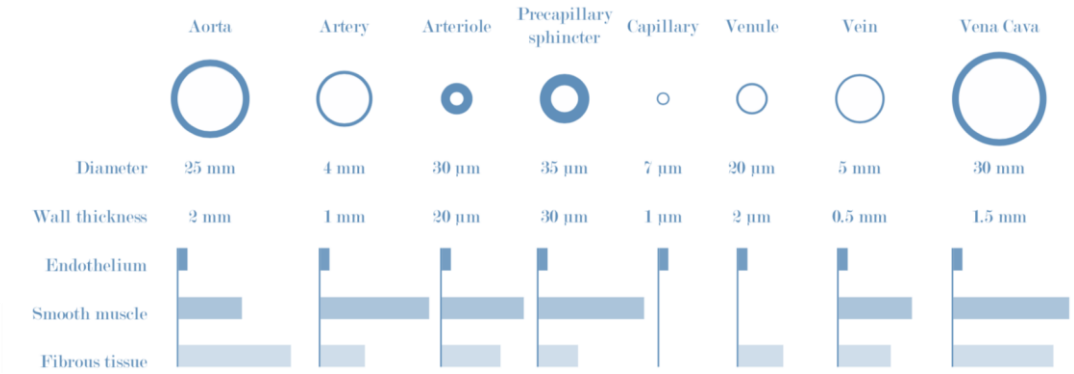

Fig 1.10: Size and composition of the vasculature. Picture adapted from Hammer 2014 showing the differences in and compositions of different compartment of the vasculature.

In figure 1.10 is shown a schematic that summarise the differences in size and composition of the different compartment of the vasculature described in this paragraph. (Figure 1.10).

1.3.2 Endothelial cells:

Origins and markers.

Since the early stages of EC research, it has been contemplated that both EC and haematopoietic cells come from a common progenitor calls “haemangioblast”. This hypothesis was first proposed by Murray in 1932 and it was based on the close developmental association of the haematopoietic and endothelial lineage within the chicken embryo’s blood island (structures around the developing embryo which lead

to different parts of the circulatory system) (Murray et al 1932). This initial association was corroborated in more modern studies showing that embryonic stem cells isolated from mice and human can differentiate down to Blast colony-forming cells, a type of progenitor with both haematopoietic and vascular potential (Kennedy et all 2007).

Further insights about the fact that EC originates from the haemangioblast has been given by receptors studies. Foetal liver kinase 1 (FLK-1) has been identified in primitive and more mature haematopoietic cells as well as in a wide variety of non-haematopoietic tissues (Matthewes et al 1991). In particular functional analysis of FLK-1 revealed that FLK-1 is expressed in blood islands in mouse embryos and is therefore pivotal in regulating both vasculogenesis and angiogenesis (Millauer et al. 1993). In fact, FLK-1 gene-deficient mice failed to generate blood island and therefore EC and Haematopoietic cells (Shalaby, et al. 1995).

Finally, cell sorting confirmed that FLK-1 positive cells represent the earlies precursors of embryonic haematopoiesis and that FLK-1+ VE-Cadherin+ cells demark a diversion point of haematopoietic and EC lineage (Nishikawa et al 1998).

Other important markers are VEGF receptors 1-3; they interact with FLK-1 and are crucial for blood vessel formation (Nesmith et al 2017). In addition to the VEGF receptor pathway, the angiopoietin (Angpt)-Tie is another EC-specific ligand-receptor signalling pathway necessary for embryonic cardiovascular and lymphatic development (Eklund et al 2017). Cell adhesion molecules (CAM) make up a significant group (at least a couple of dozen) of endothelial markers, which are involved in homo or hetero-philic binding with other cells or with the extracellular matrix. Important examples of these molecules are the Platelet endothelial cell adhesion molecule 1 (PECAM-1, CD31) (Frigo et al. 2016). Finally, VWF is an important component of haemostasis, binding platelets at sites of endothelial damage (Valentijn et al. 2013).

Endothelial cells functions.

The endothelium forms a semi-permeable barrier between the blood and the surrounding tissue. This permeability can be distinguished into basal permeability, which occurs at the level of the capillary, and induced permeability, which is more associated with inflammation, which mainly involves post capillary venules (Aird et al. 2007).

Moreover, fluid and small molecules can follow different routes to pass across the barrier compared to big macromolecules. The first ones can move passively across the barrier via a paracellular route, whereas the second ones use an intracellular route. The paracellular route can be involved also in a state of acute or chronic inflammation or other cases (such diabetes, tumour metastasis, ischemia etc), vascular endothelial growth factor (VEGF) and reactive oxygen species induce endothelial cell retraction, which increases the intercellular space and subsequently the permeability to solute and plasma proteins (Muller et al 2013).

The transcellular path, instead, can involve a receptor dependent or independent mechanism which causes invagination of the plasmatic membrane that can shuttle macromolecules from the blood to the interstitium (Muller et al 2013).

Another important endothelial function is the Leukocyte trafficking. The passage of leukocytes from the circulation to the surrounding tissue is crucial for immune response, wound repair and inflammation. Under normal condition leukocytes don't bind to endothelial cells. Following activation, leukocytes start a multi-step cascade that involves their adhesion to endothelial cells, rolling and arrest of the leukocytes and finally their transmigration (Feletou et al. 2011)

This activation process mostly depends on the expression of the selectin family of adhesion molecules, in both endothelial cells and leukocytes. Constitutively, this gene is very poorly expressed but, following activation, is up-regulated, also predominantly

in the endothelial cell of post-capillary venules. E- and P-selectin mediate leukocyte adhesion and rolling at the site of inflammation (Feletou et al. 2011).

Slowly rolling leukocytes are activated by endothelial chemokines, leading to conformational changes in integrins, a superfamily of adhesion receptors expressed by the leukocytes. Integrins interact with their ligands on the endothelial cells belonging to the immunoglobulin family, such as platelet–endothelial cell adhesion molecule (PECAM-1), vascular cell adhesion molecule (VECAM-1), intercellular adhesion molecule (ICAM-1) or junctional adhesion molecule (JAM) (Feletou et al. 2011).

Trans-endothelial migration occurs preferentially via inter-endothelial junctions (paracellular pathway), although a transcellular route has also been observed.

The migration through the inter-endothelial junctions must involve the rupture of the selectin bonds on the endothelial surface and the establishment of new bonds on the margin of the endothelial cells. The activation of leukocytes reduces selectin binding and favours the integrin-mediated associations.

A common function of the endothelium is to maintain blood in a fluid state, and to promote limited clot formation when there is a breech in the integrity of the vascular wall. On the anticoagulant side, ECs express tissue factor pathway inhibitor (TFPI), heparan, thrombomodulin, endothelial protein C receptor (EPCR), tissue-type plasminogen activator (t-PA), ecto-ADPase, prostacyclin, and nitric oxide. On the procoagulant side, ECs synthesize tissue factor, plasminogen activator inhibitor (PAI)-1, von Willebrand factor (vWF) (Aird et al. 2001).

Delivering oxygen and nutrient, regulating the transportation of inflammatory cells and orchestrating the coagulation of blood is only a minimal portion of the functions of EC. EC can sustain the homeostasis the homeostasis of resident stem cells and guide the regeneration and repair of adult organs without causing fibrosis. Tissue specific EC can carry out these tasks by supplying the repopulating cells with stimulatory and

inhibitory growth factor, morphogens and other extracellular matrix component collectively called angiocrine factors. (Butler et al. 2010, Nolan et al. 2013).

For instance, pathophysiological stress or tissue loss can activate EC that release specific inflammatory angiocrine signals to quiescent- specific stem cells, which drive regeneration in order to re-establish homeostatic conditions.

Haematopoietic is one of the fields in which it has been find evidence of this behaviour. It has been shown, indeed, that bone marrow derived EC cells can expand human umbilical cord blood-derived CD34+ cells *ex vivo.* (*Rafii et al. 1994; Rafii et al. 1995).*

After this initial prove of concept, heterotypic primary EC isolated from other organs (such brain, heart and foetal tissue) have been shown to promote the proliferation of mouse, (Li et al. 2003). human (Chute et al. 1999) and primate (Brandt et al. 1999) haematopoietic stem cells. Those initial studies were carried out in presence of serum which contains an over physiological dose of growth factors and therefore could mask the influence of EC to regulate the proliferation of the cells. More recent co-culture studies in serum-free conditions has facilitate the identification of angiocrine factors that orchestrate the self-renewal and differentiation of Haematopoietic stem cells. (Seandel et al. 2008; Poulos et al. 2015)

EC dependent regeneration has been proven also in other organs. In the liver, for instance, sinusoidal EC cells can orchestrate either regeneration or re-establish its recovery by fibrosis. The angiocrine contribution of liver sinusoidal EC to liver regeneration can be observed after surgical resection of 70% of the liver mass, which induce regeneration from through the remaining liver. Initially, liver sinusoidal EC have the role to stimulate the expression of pro-hepatic factors such Wnt2, hepatic growth factor (HGF), Transcription Growth Factor α TGFα and connective tissue growth factor to boost the regeneration of the liver (LeCouter et al 2003). In a second phase they promote proliferative angiogenesis to meet the metabolic demand of the newly growth liver. (Wang et al. 2012).

Angiocrine signals drive regeneration also of Pancreas after injury by supplying BMP2 and BMP4 (Talavera-Adame et al 2015) and of lung through the production of growth factors such MMP-14 (Ding et al. 2011).

Finally, the idea that an endothelial niche orchestrate also myogenesis comes from studies in which EC were shown to facilitate striated muscle formation from pluripotent cells. Moreover, satellite cells are positioned in proximity of EC and co-culture studies showed that EC support cycling of these satellite cells by production of angiocrine factors such IGF1, HGF, FGF2 and PDGF-BB. (Rafii et al. 2016).

1.3.3. Vasculogenesis and angiogenesis

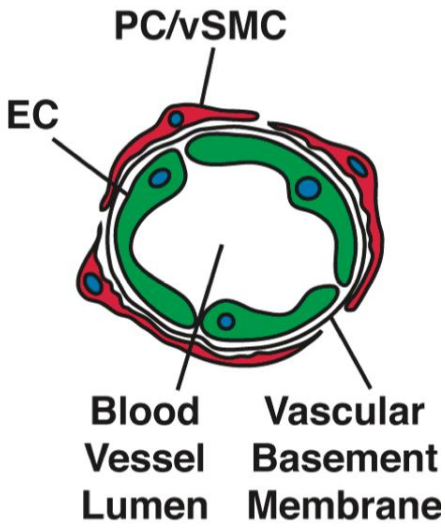

Fig 1.11: Microvasculature composition. Picture retrieved from Bergers and Song 2005 showing the two main cell types of the microvasculature.

The organ's microvasculature is critical for transporting nutrients, blood cells, oxygen, and waste materials. Angiogenesis and neovascularisation work together to create this intricate network of vessels. This network is composed of different interacting cell types, endothelial cells (EC) lining the vessel wall, and perivascular cells or mural cells, mainly composed by pericytes and vascular smooth muscle cells (vSMC) (Figure 1.11). These processes are crucial during growth and development, injury,

repair and remodelling, since these rely on the interactions between the microvasculature and its microenvironment (Bergers and Song 2005).

The process of neovascularisation (or vasculogenesis) refers to the formation of new vessel from recruitment and differentiation of progenitor cells. It is a process, therefore, more present in the embryo but occurs also in the adult life thanks to endothelial progenitor cells coming from the bone marrow through a mechanism called angioblast mobilization (Carmeliet, et al. 2000). This so-called post-natal vasculogenesis is characterized by the mobilization of bone marrow-derived or tissue-resident EPCs into the bloodstream in response to certain cytokines or tissue ischaemia. Circulating EPCs are then recruited into sites of neovascularization, where they are incorporated into the vascular endothelial lining and differentiate *in situ* into endothelial cells (Murasawa et al 2005).

Angiogenesis refers to the formation of new vessels through migration and proliferation of ECs from pre-existing vessels (Figure 1.12). Two distinct mechanisms of angiogenesis have been described: sprouting and intussusception.

Intussusceptive angiogenesis is caused by the insertion of interstitial cellular columns into the lumen of pre-existing vessels. The subsequent growth of these columns and their stabilization results in partitioning of the vessel and remodelling of the local vascular network (Risau et al. 1987; Risau et al. 1997). During intussusception, endothelial cell proliferation is not required, which ultimately makes it a rapid process that occurs within hours or minutes if compared with sprouting angiogenesis.

Sprouting angiogenesis entails two successive phases: neo-vessel growth and neo-vessel stabilization. The initial phase requires selection of ECs from an existing blood vessel in order to form the new vessel, while at the same time their surrounding ECs must remain quiescent. According to the current theory, during this process ECs differentiate into 3 specialized cell types with distinct phenotypes during angiogenesis.

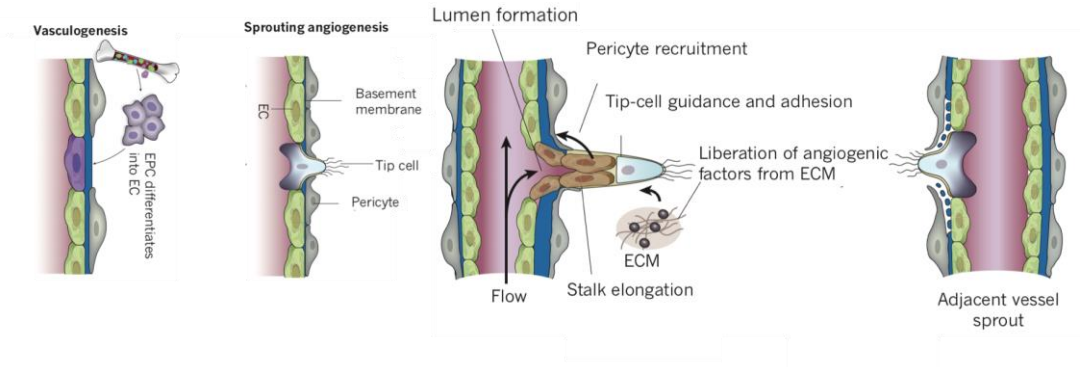

Fig 1.12 Schematic showing the two main strategy of vessel formation: Vasculogenesis and angiogenesis. On the left is shown the vasculogenesis as the recruitment of bone-marrow-derived and/or vascular-wall-resident endothelial progenitor cells (EPCs) that differentiate into endothelial cells. On the right is shown the sprouting angiogenesis: Tip cells navigate in response to guidance signals coming from the apoxic tissue released on the Extra-Cellular Matrix (ECM), such Vascular Endothelial Growth Factor (VEGF). Stalk cells behind the tip cell proliferate, elongate and form a lumen, and sprouts fuse to establish a perfused neo-vessel. Proliferating stalk cells attract pericytes and deposit basement membranes to become stabilized. Picture adapted from Carmeliet et al. 2011.

First, a single ‘tip cell’ develops in response to VEGF-A. This EC is able to break down the basal lamina, it emerges from its parent blood vessel and becomes the leading cell of the sprouting vessel. Their response to VEGF signalling includes extending large filopodia that allow for guidance and sensing of the newly formed vessel, as well as the release of molecular signals that recruit stromal cells for vessel stabilization. The second cell type occur directly behind the migrating tip cell and under influence of the adjacent tip cell it differentiates into ‘stalk cells’ that proliferate and bridge the gap between the tip cell and the parent vasculature. These “stalk cells” are responsible for tube and branch formation, thus assuring the expansion of the vascular structure in response to VEGF-A. Stalk cells also collaborate in the basement membrane deposition and establish junctions with adjacent cells to strengthen the integrity of the novel sprout. Stalk cells also generate the blood vessel lumen through the formation of intra-cellular vacuoles (Gerhardt et al. 2003; Dejana et al. 2009). The third cell type involved in this model are ‘phalanx cells’, which are

the ECs directly behind the ‘stalk cells. Phalanx cells no longer proliferate, express tight junctions and make contact with mural cells (Bergers and Song 2005) (Pitulescu et al. 2017). The neo-vessel formation includes lumen formation within the endothelial sprout, and formation of loops by anastomoses of sprouts.

The stabilization phase consists of arrest of endothelial cell proliferation, reconstruction of a basement membrane around the neo-capillary, and coverage of the immature capillary with pericytes stabilization. (Benjamin et al, 1998).

The functionality, correct extension, and morphology of the new vessels depend on the balance between stalk cell proliferation and tip cell guidance. Phenotypic specialization of endothelial cells in each of those types depends, in turn, on the balance between proangiogenic factors and endothelial proliferation suppressors (Geudens et al. 2011).

The first signal mediating the ECs sprouting and proliferation is a hypoxic signal coming from the avascular tissue. Indeed, tissue-derived VEGF-A is produced by the avascular tissue and, by linking its endothelial receptor VEGFR2, starts the finely regulated Notch signalling that induces endothelial fate (Pitulescu et al. 2017).

1.3.4. Notch signalling:

The Notch family of receptors and their ligands control endothelial cell sprouting during embryonic vascular development. Four Notch receptors (Notch 1, 2, 3 and 4) are expressed in mammals. These receptors are large trans-membrane proteins and all Notch receptors' extracellular domains comprise up to 36 EGF-like domains that are repeated in tandem. These domains mediate the dimerisation process, and domains 11 and 12 in particular are critical for inhibiting cis-activation when a Notch ligand is present on the same cell membrane (Cordle et al., 2008). Five Notch ligands have been identified, including Jagged1, Jagged2, Delta like ligand (Dll)1, Dll3 and Dll4. In the vasculature, Notch 1 and 4 are expressed by the endothelium, whereas Notch 3 functions in smooth muscle cells (Patel-Hett and DAmore 2011). When a

ligand binds to a receptor, it induces a proteolytic cleavage by secretase. As a result, the Notch intracellular domain (NICD) of the Notch protein is liberated in the cytosol and it translocate within the nucleus. Once within the nucleus, NICD interacts with DNA-binding proteins (such as the transcription factor RBP-J), positively and negatively regulating the transcription of a diverse set of downstream targets (Gridley, 2007).

Notch activity regulates embryonic vascular development, angiogenesis, adult vasculogenesis and arterial-venous specification (Hofmann and Iruela-Arispe, 2007; Regan and Majesky, 2009).

VEGFR2 activity, in particular, upregulates expression of the Notch ligand Dll4. In turn, Dll4-mediated activation of Notch suppresses tip cell behaviour in trailing stalk ECs, which form the base of sprouts. Dll4–Notch signalling is opposed by the ligand Jagged1, which is predominantly expressed by stalk and capillary ECs, and promotes vascular maturation (Pitulescu et al. 2017). In the same study by Pitulescu, they proved that Dll4–Notch signalling induces an endothelial fate switch towards arterial ECs the angiogenic growth front, showing that this pathway regulates also arterial-venous specification (Pitulescu et al. 2017)

Newly formed sprouts adhere to each other and form a new, lumen-containing vessel. Endothelial cells then secrete growth factors, partly to attract pericytes that envelop the vessel wall, and promote vessel maturation.

Notch signalling appears to be crucial also during skeletal muscle differentiation. As in this study I will use a cell source coming from skeletal muscle biopsies and used for muscle regeneration studies (the mesoangioblast), it is relevant for this thesis to highlight the Notch contribution to skeletal muscle specification.

It has long been recognised that active Notch signalling suppresses myogenic differentiation. This has been shown in the murine myoblast cell line C2C12 (Kopan et al., 1994; Lindsell et al., 1995; Nofziger et al., 1999) as well as primary satellite cells (Wen et al., 2012).

Notch controls satellite cell activation during quiescence, niche colonisation, and myogenic differentiation in adult muscle (Brohl et al., 2012; Conboy and Rando, 2002; Mourikis et al., 2012; Mourikis and Tajbakhsh, 2014).

Notch signalling is crucial for normal developmental myogenesis. Depletion of Notch signalling leads to a premature exhaustion of the satellite cell pool, leading to an impairment of muscle regeneration (Schuster-Gossler et al., 2007; Vasyutina et al., 2007).

Importantly, Cappellari et al. demonstrated that DLL4 and PDGF-BB activation causes embryonic myoblasts to transition to the perivascular lineage without erasing its myogenic memory (Cappellari et al. 2013). This suggests that bidirectional plasticity between these two cell types exists in the embryo.

1.3.5. PDGF-BB:

PDGF-BB appears to be the crucial player in the recruitment of pericytes to newly formed vessels (Betsholtz 2004).

This molecule regulates cell proliferation and is important during angiogenesis, when it works as a powerful mitogen on fibroblasts, smooth muscle cells, and other cell types (Heldin, 1992). The PDGF family is split into two subtypes based on the makeup of their polypeptide chains: PDGF-A and PDGF-B. These chains are made up of a sequence of 100 amino acid residues that share 60% homology (Heldin and Westermark, 1999). PDGF-A and B associate in hetero- and homo-dimers (i.e. PDGF-AA, PDGF-BB, PDGF-AB) able to bind to three dimeric receptors: PDGFRα, PDGFRαβ and PDGFRβ.

PDGF-B and its receptor PDGFr are required for pericyte recruitment in the CNS, kidneys, and cardiovascular system (Leveen et al., 1994; Lindahl et al., 1997; Tallquist et al., 2003)

During angiogenesis in embryos and adults, PDGF-BB is expressed by the sprouting capillary endothelial cells, whereas its receptor, PDGFRβ, is localized on pericytes, which suggests a paracrine signalling circuit between the two cell types.

Endothelial cells attract mesodermal progenitors to the pericyte destiny during vascular development by secreting PDGF-BB. (Hellstrom et al. 1999)

Moreover, as mentioned in the previous paragraph, it has been reported that developing endothelium can convert committed myoblast to pericytes, likely through Dll4 and PDGF-BB (Cappellari et al. 2013). This shows that Notch ligands and PDGF-BB can regulate not only the recruitment but also drive the differentiation of cells during endothelial development and maturation.

Therefore, whereas VEGF is important for the growth phase, transforming growth factor (TGFβ), platelet-derived growth factor (PDGF-BB), angiopoïetin-1, and their respective receptors are essential for the stabilization phase, as confirmed by both functional knockout of their genes in vivo and a number of *in vitro* observations (Beck and D'Amore, 1997).

1.3.6. Vascularization strategies

The role of the vasculature is not limited only to guarantee graft survival. It exerts an organ function by being the major point of communication between the organ and the rest of the body, for instance this happens in organs that exerts an exocrine function, and the vasculature allows the organ to sense the body and to deliver to the body its products (Jain et al. 2005). Moreover, endothelial cells produce angiocrine factors, orchestrating finely many organ specific functions and stem cells renewal (Butler, Kobayashi, and Rafii 2010, Nolan et al. 2013).

Moreover, the endothelial layer should also match the specific typology of the target organ in terms of endothelial pattern such as normal, fenestrated or sinusoidal, and in terms of phenotype (Rafii, Butler, and Ding 2016).

In order to exploit its function, the vasculature should however be connected to the host vasculature. The graft should promote a rapid ingrowth of host vasculature over a period short enough to avoid tissue necrosis of the graft.

For instance, vascularization could be achieved prior to orthotopic transplantation, temporarily wrapping the engineered construct into highly vascularized tissues *in vivo* (Rivron et al. 2008)(Rouwkema, Rivron, and van Blitterswijk 2008). As an example, muscle and omentum flaps have been demonstrated to successfully foster formation of new vessels by several weeks (Rouwkema, Rivron and van Blitterswijk, 2008; Saxena et al. 2010)

Nevertheless, this is not possible without the need of a second surgery which aim at transferring the construct to the ultimate defect site. This eventuality greatly hampers the use of this solution in clinic (Rouwkema, Rivron and van Blitterswijk, 2008; Tan et al. 2012). In order to overcome this weakness, ideally the scaffold should be able *per se* to promote vasculature invasion following transplantation.

In line with this idea, an alternative method developed in the field involves the use of angiogenic factors. Indeed, certain signalling molecules, such as VEGF and FGF, are known to drive vessel development, while others, such as PDGF and TGF, play a key role in stabilising the newly formed networks (Tan *et al.*, 2012)

In our laboratory, the vascular issue was approached when a stem cells based engineered trachea was replaced in a child. In this occasion the omental sheet was pulled from the stomach to the graft to allow the revascularisation of the graft (Figure 1.13). In this particular case the only ingrowth of the vessel of the host into the graft was sufficient to guaranty its survival (Elliott et al. 2012). However, this strategy was possible as cartilage is a tissue with hypoxic features and a different outcome would be for big organ engineering.

.

A very promising solution is referred to as "*in vitro* pre-vascularization". This is represented by formation of ex novo functional vascular network within the engineered scaffold before transplantation , which may be anastomosed immediately at the moment of organ grafting. (Elliott et al. 2012).

All this observation together should give an idea of how of how crucial regenerating an organ's vasculature is for whole organ tissue engineering, which is currently a huge gap that separates the science from clinical translation.

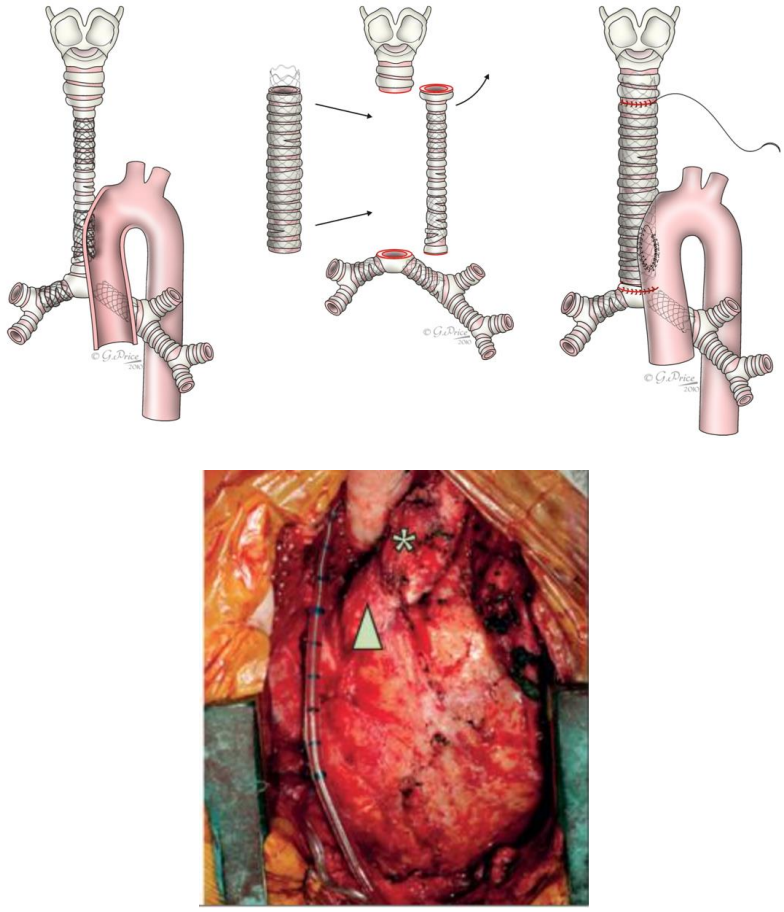

Fig 1.13: Schematic of the successful replacement of a stem cell based engineered trachea on an 8 years old child. During surgery the airway was found to be severely stenotic with multiple stents including one entering the ascending aorta. The old homograft trachea was removed and replaced by the engineered graft. The aortic defect was closed with a bovine pericardial patch and air leaks sealed. Before closing, an omental wrap was brought up to cover the graft. The graft sits in the anatomical position to the right of the ascending aorta. Picture adapted from Elliot et al.2012.

1.4. Cell source for vascular tissue engineering

Microvasculature is an essential compartment of the organ, needed for the delivery of nutrients, oxygen and for the removal of waste products. This intricate network of vessels is generated by angiogenesis and neovascularization processes. These processes are crucial during growth and development, injury, repair, and remodelling, since these rely on the interactions between the microvasculature and its microenvironment (Bergers and Song 2005). The microvasculature is composed of various types of interacting cells, endothelial cells (ECs) lining the vessel wall, and perivascular cells or mural cells, composed mainly of pericytes (PC) and vascular smooth muscle cells (vSMC), which layer larger vessels and regulate the blood afflux to the organ.

When it gets to engineering the vasculature of an organ, the most important and difficult part to rebuilt is the microvasculature, consisting of ECs and PCs, and the vSMC layer.

Determining the best cell source to reconstruct the different anatomical structures of the vasculature tree within a whole organ is a crucial step. This section will focus on the different strategies that have been published in the literature and that have shown potential for use in whole organ tissue engineering.

1.4.1. Endothelial cells

One of the main issues towards the delivery of vascularized tissue engineered organs is to choose a suitable endothelial cell source. This is particularly significant because adult endothelial cells show an impaired proliferative potential after expansion. In

tissue engineering the key aim is to harvest primary cells with minimum invasion, to culture and expand these cells returning a high yield, sufficient to colonize the organ. Even after extensive *in vitro* expansion, should retain their basic functions, for example endothelial cells should inhibit blood clotting while promoting anastomosis to the host vasculature. With this aim in mind, different cell sources have been investigated ranging from primary isolated adult cells to cells differentiated from stem or progenitor cells.

Normally, to harvest adult endothelial cell is required the involvement of large diameter vessels. For this reason, harvesting ECs from patients remains a problem of great concern with significant complications. Endothelial progenitor cells (EPCs) can be separated from peripheral blood, providing a potential source of autologous cells that can be quickly processed. EPCs were firstly described by Asahara et al. who identified a hematopoietic population capable of eliciting postnatal vasculogenesis in adult peripheral blood (Asahara et al. 1997).

Blood-derived EPCs have already been used to endothelialize synthetic vascular grafts in several studies (He et al. 2003; Shirota et al. 2003). Grafts lined with these EPCs have been implanted *in vivo* into a canine carotid model. After 30 days, 11 out of 12 grafts remained patent, with cells lining the surface showing features of a mature EC phenotype (He et al., 2003). Umbilical cord blood (Murga, Yao, and Tosato 2004) and bone marrow (Hamilton, Maul, and Vorp 2004) could represent additional sources of autologous vascular progenitor cells. Several studies have shown that bone marrow–derived cells functionally contribute to neoangiogenesis during wound healing and limb ischemia (Majka et al. 2003), endothelialisation of vascular grafts (Shi et al. 1998) and organ vascularization (Otani et al. 2002). In this regard, in 2004 Schimidt et al seeded differentiated human umbilical cord blood derived EPCs on vascular scaffolds and reported the formation of neo-tissue in both biomimetic and static *in vitro* environments. These tissues were characterized as endothelial

monolayers with related functions (e.g., the production of eNOS indicating features of functional endothelium) (Schmidt et al. 2004)

However, significant controversies exist over the identity and role of EPCs: evidence suggests that hematopoietic stem cells (HSCs) and EPCs (Pardanaud et al. 1989; Risau et al. 1988) are derived from a common precursor (named hemangioblast) (Flamme et al. 1992). In the embryonic yolk sac, vasculogenesis involves growth and fusion of multiple blood islands that ultimately give rise to the yolk sac capillary network (Takayuki et al. 1999); this network differentiates into an arteriovenous vascular system (Takayuki et al. 1999). The integral relationship between the elements that circulate in the vascular system (the blood cells) and the cells that are principally responsible for the development of the vessels themselves (endothelial cells [ECs]) is implied by the composition of the embryonic blood islands. The cells destined to generate hematopoietic cells are situated in the centre of the blood island and are termed hematopoietic stem cells. Endothelial progenitor cells (EPCs), or angioblasts, are located at the periphery of the blood islands, and will give rise to the vasculature structure. In addition to this spatial association, hematopoietic stem cells and EPCs share certain antigenic determinants, including Flk-1, Tie-2, Sca-1, and CD34. These progenitor cells have consequently been considered to derive from a common precursor, putatively termed a hemangioblast. (Takayuki et al. 1999).

Even if this terminology was proposed almost a century ago to describe the common origin of haematopoietic/endothelial progenitor cells (Murray et al. 1932), the existence of haemangioblast was proved only two decades ago by Asahara and colleagues (Asahara et al. 1997), whom successfully isolated “endothelial progenitor cells” (EPCs) from the human peripheral blood. They showed that CD34+ cells derived from the peripheral circulation formed endothelial colonies, based on the ability of these colonies to incorporate acetylated LDL, expression of PECAM and Tie-2 receptor, and production of nitric oxide by VEGF stimulation. In addition to

derivation of an endothelial precursor from the marrow, their study also demonstrates the possibility of vasculogenesis in the adult.

Following studies in a canine model corroborated the idea that vasculogenesis is not only restricted to early embryogenesis, but may play a physiological role, or may contribute to the pathology of vascular diseases in adults. (Shi et al. 1998). Therefore, the best characterised source of EPCs are HSCs coming from the bone marrow and mobilised into the peripheral blood by chemokines such as vascular endothelial growth factor (VEGF), basic fibroblast growth factor 2 (bFGF-2), stromal-cell-derived factor-1 (SDF-1) or granulocyte macrophage-colony-stimulating factor (GM-CSF), which are synthesised by ischaemic tissues. (Takahashi et al. 1999; Askari et al. 2003; Ceradini et al. 2004).

Autologous bone marrow cells have been delivered to thousands of patients with ischaemic heart disease, on the premise that these populations contain functional EPCs, with conflicting results (Nowbar et al. 2014). One potential explanation for the lack of consistent therapeutic benefit is that bone marrow is not the origin of circulating EPCs. Indeed, although late-outgrowth endothelial cells can be readily isolated from cord and peripheral blood (Yoder et al. 2007), it has been impossible to obtain endothelial cells from bone marrow cultures. (Tura et al 2013). These findings suggest that circulating EPCs arise from an alternative niche in the vessel wall.

In a recent report, Takeshi at all studied the origin of EPC in people with sex-mismatched bone marrow transplantation. Although endothelial cells could be obtained from a circulating progenitor and were capable of clonal expansion, these cells did not share the genotype of the transplanted bone marrow (Takeshi et al 2019). This paper concludes that EPCs in circulation do not originate from the bone marrow causing a paradigm shift that lead to a re-evaluation of our approach to harness EPCs for therapeutic vascular regeneration. Moreover, the rarity and poor expansion potential of these cells make them unsuitable for scaled-up production. For this reason, alternative sources for patient-specific ECs would be of value.

More recently induced pluripotent stem cells (iPSc) have been broadly investigated as a promising cell source for ECs. Significant in this field is the contribution of Mummery's group which described the production of iPSC-derived ECs and injected those cells into a zebrafish model, reporting formation of new vessels and successful anastomose to the host vasculature (Orlova et al., 2014) (Figure 1.14). Here, iPSC-derived ECs were able to outperform HUVECs, which were so far considered the gold standard in EC research. While the use of of iPSC-derived ECs is generating a lot of interest and many clinical trials using iPSC are being planned (Roku et al. 2016), a lot of concerns exists about the clinical use of ECs derived from iPSC due to their capacity to form teratoma *in vivo* and their limited clinical use for macular degeneration in the retina (Grber et al. 2015; Cossu et al. 2017)

1.4.2 1.3. Human umbilical cord endothelial cells (HUVECs) in vascular tissue engineering.

Other non-invasive sources of adult human ECs are cadaveric vessels and the umbilical vein (Bourke et al., 1986). So far, Human umbilical vein endothelial cells (HUVECs) have been the gold standard in EC research. They are, in fact, easy to access and are able to deliver high yield following isolation. However, HUVECs have also shown several limitations, like poor engraftment and anastomosis after transplantation in various animal models.

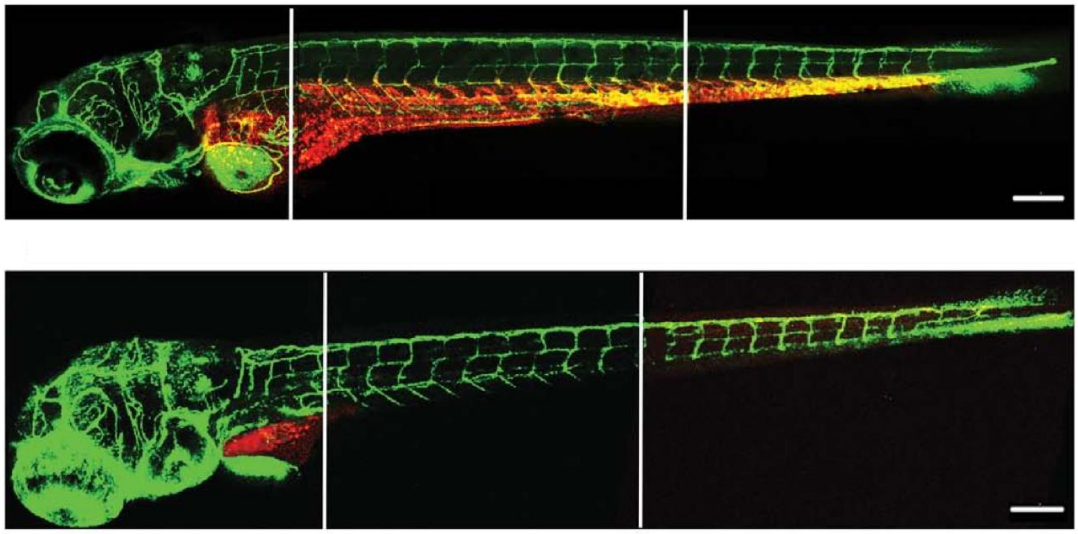

Fig 1.14: 48 hours post implantation of iPSC derived ECs and HUVECs in zebrafish. iPSC–ECs (in red) integrated within the major vascular structure of the zebrafish (GFP; in green) embryos, whereas HUVEC integration was poor (in red). Picture retrieved from (Orlova et al., 2014).

In 2004, HUVECs and mesenchymal cells were embedded in a three-dimensional fibronectin-type 1 collagen gel and then transplanted around the omental sheet into mice, with the aim to create long-lasting blood vessels. In this experiment, HUVECs were able to form tubes that connected to the host vasculature allowing perfusion. However, HUVECs alone showed limited capacity to form vessels and failed to survive long term; furthermore, the functionality of the vasculature over a long period of time was not assessed in this study (Koike et al. 2004). More recently, Mummery's group reported that HUVECs were unable to integrate the xenograft model into the vasculature of zebrafish but were connected to the vasculature or dispersed throughout the embryo. Therefore, HUVECs alone are an inadequate source of cells for vascular tissue engineering, making it necessary to investigate other options (Orlova et al. 2014). To overcome the inabilities of HUVECs alone to regenerate the vasculature in tissue engineered constructs, more and more groups are exploring the possibilities to co-culture of EC and perivascular cells as a better system, essential for regenerating a functional vascular tree. Even though co-culturing the two cell type

this is not novel strategy, a lot of work remains to be done in order to bridge this approach into organ tissue engineering using primary adult cells. Indeed, as it will be extensively explained in the paragraph “state of the art of whole organ vascular tissue engineering”, HUVECs alone have been exploited for the re-vascularisation of several organs such us liver, kidney, as well as the intestine, but only poor attempts were made to rebuild the perivascular compartment.

Finding a strategy which allow to improve the performances of adult primary cells such HUVECs, without the use of genetic modifications, would be of great interest for tissue engineering, making the potential clinical translation easier to reach, reason why we explored this possibility in this thesis work.

In this context, the work proposed by Rafii’s group has been of relevance in the field. The researchers identified a way to directly convert somatic cells to functional endothelial cells. Interestingly, the approach has been performed with human mid-gestation lineage-committed amniotic fluid derived cells which have been converted into a phenotypically stable and expandable population of vascular ECs without transition through a pluripotent state (Ginsberg et al. 2015).

Recently, the idea that ECs only serve to line simple passive “tubing” systems is coming to an end, as their role is more complex than simply delivering oxygen and nutrients, and includes modulating the coagulation of blood, regulating the transportation of inflammatory cells and serving as gatekeepers of cellular metabolism (Carmeliet and Jain 2011). Tissue-specific microvascular capillary networks perform complex physiological functions, such as preserving the homeostasis of resident stem cells and directing the reconstruction and recovery of adult organs preventing fibrosis. More data exists to support the theory that ECs generate angiocrine hormone, producing inhibitory and stimulatory tissue-specific signals for stem cell regeneration (Butler, Kobayashi, and Rafii 2010; Nolan et al. 2013). With this in mind, the discovery of an acceptable endothelial niche may support the development of tissue engineered constructs that rely on the use of stem cells,

providing the ideal environment to recapitulate the diverse signalling networks capable of driving the restoration of organs.

1.4.3. Pericytes

ECs are the main component of the vasculature which have been extensively studied and characterized, while pericytes are key regulators of angiogenesis. Although paternity of pericytes is generally assigned to Rouget in 1874 (Rouget 1874), rouge cells have been called perycites by Zimmermann in 1923, due to their anatomical position close to the endothelial layer (Zimmermann, 1993.). Because of their particular location and cytoplasmic processes, pericytes are generally considered responsible for stabilising the vessel wall and controlling endothelial cell proliferation, playing a key role in angiogenesis (Ribatti et al. 2011). However, they are not the only cells on a peri endothelial location. They indeed share this localization with vascular smooth muscle cells, fibroblast and macrophages and often they can be confused with those (Armulik et al, 2011). Although everyone adopted the view that pericytes belong to the same lineage of vSMCs, it is widely accepted that there is no singular molecular marker that enables us to distinguish them unequivocally from vSMCs or other mesenchymal cells. Marker expression is not the most useful tool to identify pericytes also because it is transient and is not consistent among all pericytes: indeed, different pericytes display a different markers profile and this expression can change throughout the life of the same cell (Armulik et al., 2011). However, although showing differential expression patterns according to stages and origins, it is agreed that pericytes express several mesenchymal markers such as CD44, CD90, CD105. They also express Smooth muscle a-actin (aSMA) neural/glia antigent 2 (NG2), platelet-derived growth factor receptor-b (PDGFr-b) and alkaline phosphatase (AP) (Capplellari et al.2013).

aSMA is a marker widely used to identify pericytes but is also known to be expressed by smooth muscle cells and myofibroblasts (Nehls et al., 1992; Ronnov-Jessen and Petersen, 1996). NG2 is a chondroitin sulphate proteoglycan strongly expressed by pericytes during angiogenesis and can bind FGFβ, PDGF-AA, plasminogen and angiostatin (Abboud, 1995). However, NG2 is commonly expressed by other cell types than pericytes, such as immature neural stem cells capable of differentiation into neurons or glia. PDGFr-β is localised in the pericyte membrane and has a crucial role in the recruitment of these cells by the endothelium during angiogenesis (Betsholtz, 2004).

Finally, Alkaline phosphatases (APs) are a group of glycoproteins able to hydrolyse a large range of monophosphate esters. The first evidence linking AP expression to the capillaries, was published in 1965 (Mizutani and Barrnett, 1965). In humans, four AP isoforms have been recognised while there are only three in the mouse (Stefkova etal., 2015). AP is histochemically traceable in the mouse embryo as early as the 2-4 cell stage (Mulnard and Puissant, 1987). The tissue nonspecific isoform (TnAP) is conserved across the species and its sequence (composed of 12 exons) encodes for an enzyme expressed by a subset of pericytes of the skeletal muscle (Grim and Carlson, 1990; Safadi et al., 1991) bone and heart (Schultz-Hector et al., 1993). AP-positive cells have been easily isolated from skeletal muscle and cultured *in vitro*, showing mesenchymal morphology and pericyte marker expression (Levy et al., 2001).In conclusion, is impossible to fully define pericytes identity due to their heterogeneity and promiscuity of markers, and the only definition relies to their anatomical localization. The current definition of pericytes refers to cells located in the vascular basal membrane as seen through electron microscopy (Miller and Sims 1986). Nevertheless, this definition loses strength during angiogenesis, embryogenesis and tissue regeneration, when identify pericytes on the bases of their location becomes very difficult. It is also widely accepted that pericytes are more frequent in the proximity of micro-vessels (capillaries, venules, and terminal

arterioles), where they share the basal membrane with endothelial cells, and are connected by tight, gap, and adherent junctions. Indeed, a single pericyte can be connected with several endothelial cells by cell protrusions that wrap around, and along the blood vessel (Gerhardt and Betsholtz 2003; Kovacic and Boehm 2009). However, the discovery of sub-endothelial pericyte-like cells in large vessels questioned this definition (Díaz-Flores et al. 2009).

An increasing number of studies suggest that pericytes may be the progenitor of vSMCs and may constitute multipotent progenitor cells like adipocyte (Olson and Soriano 2011), osteoblast, chondrocytes (Collett and Canfield 2005), and skeletal muscle progenitor cells (Dellavalle et al. 2007). This resembles the behaviour of mesenchymal stem cells (MSCs) and therefore it has led to the concept of a perivascular niche of MSCs (Armulik et al., 2011). Paolo Bianco's laboratory has argued in support of this theory, and on the widely shared view that MSCs are ubiquitous in human connective tissue, defined by common *in vitro* phenotype and coinciding with ubiquitous pericytes. They were pioneers in the concept that ubiquitous MSCs with equal capacities do not exist, but that "tissue-specific" mesodermal progenitors can be recruited into a mural cell fate, providing a plausible mechanism by which pericytes are generated, and how they act as a local progenitor cell source (Sacchetti et al. 2016b).

Together, these findings provide evidence that pericytes are a valuable tool for regenerative medicine as they can help restore the vascular smooth muscle layer, which is necessary for a healthy and mature endothelium (Bergers and Song 2005) as well as the mesodermal compound of the tissue from which they originate. Nonetheless, the hypothesis that these cells will contribute to the regeneration of the smooth muscle compartment of organs due to their inherent ability to differentiate into vSMCs, which is not clearly distinguishable from non-vascular smooth muscle cells, cannot be excluded.

Regardless their origin, it is largely accepted that perivascular cells play an important role during the early phases of angiogenesis. Although initial endothelial cell sprouts may develop without the involvement of pericytes, pericytes are among the first cells to invade newly vascularized tissues and are found to be on the growing front of endothelial sprouts. Pericytes can suppress endothelial growth, migration and micro-vessel stabilization (Bergers and Song, 2005; von Tell, Armulik, and Betsholtz, 2006), moreover, pericyte involvement has also been directly implicated in conferring capillary resistance to regression *in-vivo.* For this reason, an increasing number of studies are focusing on these cells type for the purpose of vascular tissue engineering.

1.4.4. Mesoangioblasts

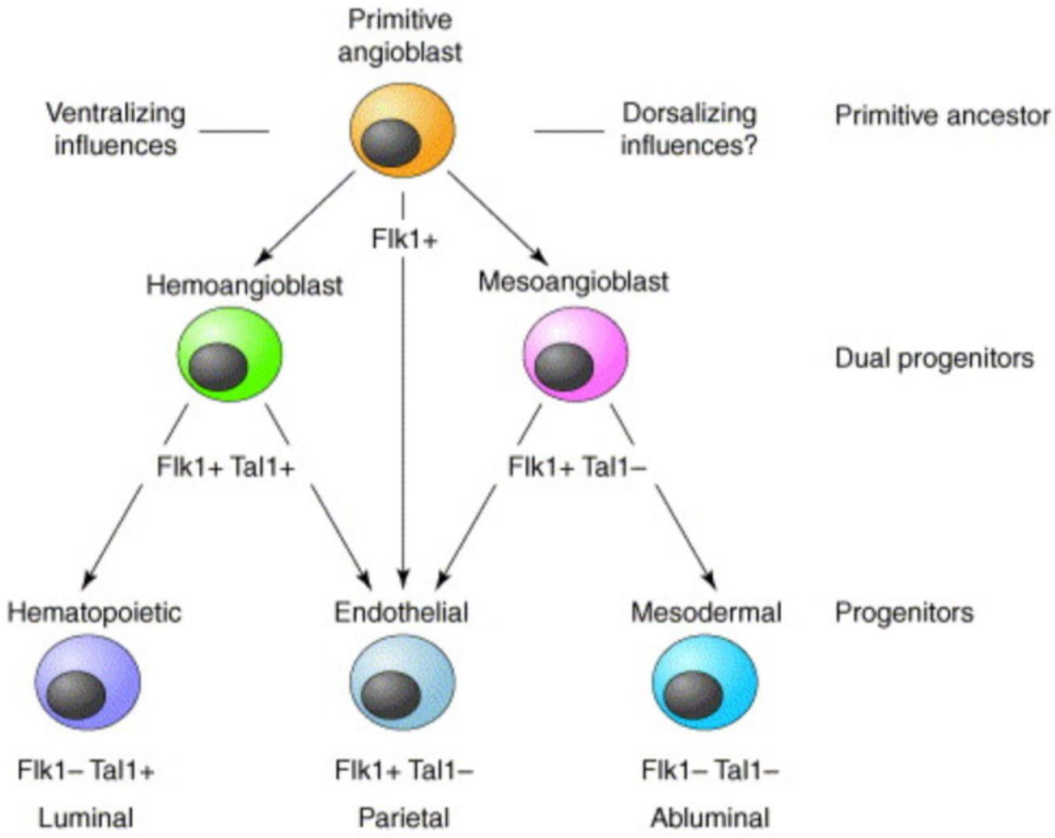

Fig 1.15 Schematic explaining the origins of the embryonic mesoangioblast. Picture retrieved from (Cossu et al. 2003). The schematic represent the theory formulated by Cossu where asymmetric division of a primitive ancestor (angioblast) would generate both the hemoangioblast (which gives rise to the hematopoietic system and endothelial precursors) and mesoangioblast (which would generate mesodermal progenitors and endothelial precursors).

A pioneering study by Bianco and Cossu groups reported that cells isolated from the embryonic murine dorsal aorta and assigned to the perivascular lineage (CD34, Flk-1, SMA and c-Kit expression) can generate vascular and extravascular mesodermal derivatives *in-vivo*. The current theory sees the mesoangioblast coming from a “angiopoietic” ancestor, common to hemoangioblast. According to the theory proposed by Cossu et al., asymmetric division of primitive angioblasts would generate both hematopoietic and “solid-phase” mesodermal progenitors, as well as endothelial

precursors into the vessel parietal niche (Figure 1.15) (Cossu et al. 2003). For this reason, these cells have been named mesoangioblasts (MAB) (Minasi et al. 2002).

Similar cells have been subsequently isolated from murine (Sampaolesi et al. 2003), canine (Sampaolesi et al. 2006) and human skeletal muscle biopsies (Dellavalle et al. 2007) and resulted capable to contribute to skeletal muscle regeneration also upon intraarterial delivery. The latest postnatal cells share anatomical location, capacity to grow in culture and mature into mesodermal lineages, under specific culture conditions (Tonlorenzi et al. 2007). However, differently from their foetal counterpart both mouse and human postnatal mesoangioblasts lose their endothelial features, and are therefore considered “pericyte derived” cells. It is likely that these in situ progenitors might derive from the foetal mesoangioblasts, although this hypothesis has not been formally established yet (Tonlorenzi et al. 2007).

Moreover, mesoangioblast isolated from human skeletal muscle biopsies express Alkaline Phosphatase and are able to differentiate down the smooth muscle lineage (default function of a pericyte) and skeletal muscle (as mesodermal lineage of origin) (Dellavalle et al. 2011). Postnatal muscle-derived pericytes undergo myogenesis with no need of co-cultured skeletal myoblasts, differently from their foetal counterpart: indeed, as postulated by Cossu et al., foetal cells within developing vessels might await to be instructed by specific environmental cues, whereas adult cells have already been addressed to a specific fate (Cappellari et al. 2013).

Due to their easy accessibility from skeletal muscle tissue biopsies, and their standardised culture conditions (Dellavalle et al. 2007; Cossu and Biressi 2005; Tagliafico et al. 2004), these cells are currently used in a clinical trial for treating muscular dystrophy (Cossu et al. 2016) and represent a powerful cell source for clinical translation purposes.

Similarly, to what I have discussed above, pericytes could be derived from pluripotent stem cells. Recently a protocol was established to derive MAB-like stem / progenitor cells from human and murine iPSCs (Gerli et al. 2014). Relevantly, defined conditions

for simultaneous derivation of ECs and PCs from hiPSCs of different tissue origin with high efficiency have also been defined (Orlova et al., 2014).

1.4.4. Vascular Smooth Muscle Cells

From a whole organ tissue engineering perspective, the overall range of differently sized vessels which form the vascular tree must be regenerated because microvasculature alone cannot support organ function. Smooth muscle cells, which represent the main difference between microvasculature and larger vessels, have a crucial role in delivering vasculature function. They are responsible for vaso-motiliy and contribute to the biomechanical blood flow response (Neff et al. 2011). Consequently, derivation and culture of vascular smooth muscle cells (VSMC) represent a significant step toward regeneration of the whole-organ vasculature.

Most SMC markers are either structural components or regulators of their contractile apparatus. SMC express smooth muscle a-actin (aSMA), smooth muscle 22a (SM22), calponin, caldesmon, smooth muscle myosin heavy chain and smoothelin. Moreover, functional contractility is the most robust indicator of contractile phenotype. (Beamish et al. 2010).

Different approaches have been exploited to find a suitable and reliable cell source that could give rise to the vascular smooth muscle compartment. While for blood vessel tissue engineering a great deal of effort has been made to create a smooth muscle (Tresoldi et al. 2015), the field of whole organ revascularization has concentrated on regenerating pericytes to provide a robust microvasculature for the engineered constructs.

One of the most studied sources of VSMCs are mesenchymal stem or stromal cells. Zhao et al published a foundational paper which combined decellularised scaffolds and MSCs. The authors were able to derive ECs and VSMCs from bovine MSCs and they produced tissue-engineered arteries which were transplanted into the sheep

model as a carotid artery interposition for 5 months (Zhao et al. 2010). A study published by Jung et al. offers another case where human MSCs were used to build a scaffold-free graft that contained a mature smooth muscle layer (Jung et al. 2015). Thanks to their fast processing, adipose dependent stem cells (ADSCs) provide another commonly used source of VSMCs alongside MSC. Nonetheless, under the correct biochemical and biomechanical conditions these cells are able to give rise to a mature smooth muscle phenotype that features contractility (Harris et al. 2011). Transforming growth factor-beta 1 (TGFβ) seems to be the principal pathway involved in this process. Indeed, in a similar study, ADSCs were induced to differentiate into VSMCs through TGFβ and bone morphogen growth factor. The human VSMCs derived from ADSCs were seeded on small calibre vascular graft. The resulting vessel wall had a dense and well organized structure similar to the one of physiological vessels (Wang et al. 2010).

Ott's laboratory published a remarkable example of delivering the smooth muscle layer in a whole organ. In their study, the co-seeding of HUVECs and human MSCs, as perivascular supporting cells, in decellularised rat lung scaffolds resulted in a broad re-endotheliazation, but more interestingly, in the same work, they regenerated the lung vasculature using both endothelium and vSMCs with cells derived from human inducible pluripotent stem cells, showing how these cells can represent another valuable source of VSMCs (Ren et al. 2015).

Furthermore, vSMCs, as mentioned above, are supposed to feature a common ancestry with pericytes, making the sources of PCs presented in the previous paragraph a potential cell population for the derivation of the smooth muscle. In particular, mesoangioblasts, which are an easily accessible cell population are already used in the clinic (Cossu et al. 2016), can give rise to a smooth muscle phenotype (Tagliafico et al. 2004), making them an ideal candidate for regeneration of the smooth muscle vascular layer. Another option which has been investigated, is

the direct recruitment of VSMC in-vivo. This approach worked for blood vessels of 5–6 mm in diameter (Pellegata et al. 2015; Syedain et al. 2017).

To summarize, a fully functional and mature vasculature requires both endothelial and mural cells. Many studies focused on blood vessel tissue engineering have demonstrated the importance of this coexistence. However, as it will be discussed furtherly in the next chapter, most of the attempts to regenerate the vasculature in whole organs have been carried out using only ECs. Knowledge from recent studies, and from this thesis, support the use of different cell types together, suggesting that the co-culture is more appropriate approach to address whole organ revascularization.

This PhD thesis address the vascular regeneration in the contest of a whole gut tissue engineering model. For this reason, I would like to make a digression about the visceral smooth muscle, taking in account that no differences have been ever reported between visceral and vascular smooth muscle. Therefore, this thesis will discuss how vessel associate progenitor could serve as a source of smooth muscle cells for both compartments.

The cellular origin of the visceral smooth muscle is not clear yet according to the literature. Torihashi et al. and Kluppel et al. reported the presence of a cKit+ progenitor able to give rise to both longitudinal smooth muscle (LMC) and the myenteric interstitial cells of Cajal (ICC) (Torihashi et al. 1997; Kluppel et al. 1998). The authors discovered with two different approaches the common origin of ICC and LMC and they observed ICC maintaining the expression of cKit and LMC losing its expression and differentiating into smooth muscle cells. According to their theory, the cell fate would depend on their proximity to the Enteric Neural Cells (ENCs) which produces stem-cell-factor (the endogenous ligand of cKit). Cells that are close to ENCs would stimulate the cKit pathway and differentiate into ICC, on the contrary more distant cells would lose this marker and become LMC (Figure 1.16)

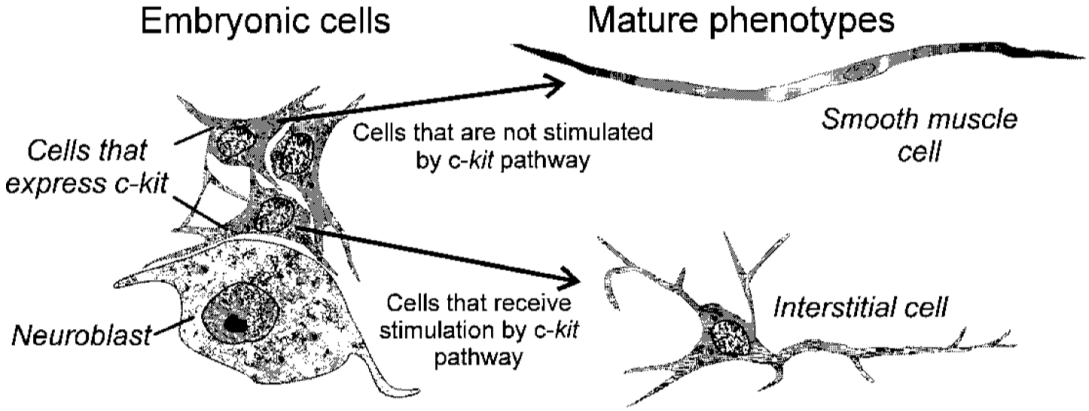

Fig 1.16: Theory of ICC and LMC development from a common origin. Schematic describing the current theory of visceral smooth muscle development that report the presence of a cKit+ progenitor able to give rise to both longitudinal smooth muscle (LMC) and the myenteric interstitial cells of Cajal (ICC). From Torihashi et al. 1997.

A second theory identify mesothelial cells (a type of epithelial cells that lies on the coelomic cavity) to have an important role in the generation of visceral smooth muscle (Rinkevich et al. 2012). Mesothelial cells of many organs seem to undergo an epithelial-mesenchymal transaction, a process by which coelomic epithelial cells convert to a mesenchymal cell phenotype and migrate to contribute to the vascular smooth muscle of the intestine (William et al 2005). Rinkevich et al. demonstrated, by genetic lineage tracing, that mesothelial cells have an important role also in the visceral smooth muscle generation both in development and post-natal growth (Rinkevich et al. 2012). This thesis will discuss this topic in the discussion section.

1.5. State of the art of neo-vascularization in whole organ tissue engineering

1.5.1 Liver

In the contest of vascular tissue engineering, the liver represents one of the most investigated organs. This is due not only to the significant clinical need, but also because it is slowly becoming evident how endothelial cells could play an active role in its regeneration. It is well established, indeed, that endothelial cells support liver organogenesis during embryogenesis before circulation occurs (Lammert, Cleaver, and Melton 2001).

Recently, the Rafii's group described how the niche of liver sinusoidal endothelial cells sustains liver regeneration through the release of angiocrin factors (Ding et al. 2010). This founding demonstrates that liver tissue engineering cannot be achieved without first recapitulating its vascular compartment.

A study of 2013 by Takebe et al showed how the transplantation of vascularised liver buds were able to resemble the organ function (Takebe et al. 2014a). This was a proof of principle that a whole tissue engineered liver with vascular compound could recapitulate the organ function in human.

The main strategy to re-vascularise liver constructs is the injection of endothelial cells, primarily HUVECs, into the portal vein of the decellularised liver (Baptista et al. 2011; Shirakigawa, Takei, and Ijima 2013; Takebe et al. 2014; Bao et al. 2015; Verstegen et al. 2017). In 2011 Baptista published a pioneering study where livers from different species were perfused with detergent to selectively remove tissue cellular components while preserving the extracellular matrix components and intact vascular network. The vascular network was used to reseed human foetal liver epithelial cells and HUVECs. These cells engrafted in their native locations within the decellularised organ and displayed their typical endothelial and hepatic markers expression.

Moreover, the authors demonstrated that the newly formed vasculature did not leak when labelled dextran was injected (Baptista et al., 2011).

In another study HUVECs were seeded and cultured for 3 days in decellularised rat livers using a bioreactor; the perfusion culture allowed cells survival and the cells prevented blood leakage upon *in-vitro* reperfusion (Shirakigawa et al., 2013).

HUVECs were also used to reconstruct the vasculature of pig livers. The authors functionalized pig decellularised scaffolds with heparin over 3 days prior seeding of the cells. With this technique, they demonstrated how the liver did not cause sudden thrombosis when grafted in the infra-hepatic space (Bao et al., 2015). Also Atala's group used MS1 endothelial cells to re-vascularize porcine livers which were able to sustain perfusion for 24h after Orthotopic liver transplant *in vivo* (Ko et al. 2015). In addition, the endothelial cell line EA HY926 was used to recellularize an acellular pig liver lobe, coated with heparin gel that facilitated cell adhesion and grafting. Dynamic culture for 10 days resulted in an even distribution of cells and the scaffold did not cause thrombosis when it was grafted heterotopically into pigs for 1 h (Hussein et al. 2016).

It is important to highlight that in Bao et al. and Hussein et al. the heparin treatment prior seeding enhanced the capacity of the vascularised scaffold to be perfused *in vivo (*Bao et al., 2015, Hussein et al., 2016). However both studies had a very short time point *in vivo* (up to 1h post implantation) and patency of the newly formed vasculature has never been assessed for longer time point which are more relevant for the clinical translation of this system.

A totally different approach was used by Kadota et al. that co-seeded bone marrow MSCs and hepatocytes in a decellularised rat liver model. Published data suggest that MSCs support liver development and regeneration, but here the authors also showed that the cells produced pro-angiogenic factors that were able to promote the ingrowth of host vasculature into the scaffold. With this approach they sustained a orthotopic transplantation for up 1h *in vivo* (Kadota et al. 2014). Promoting the

ingrowth of the host vasculature into the scaffold is a strategy used also in the study by Zhao et al., where hepatocytes were embedded into collagen gel prior subcutaneous implantation for 7 days (Zhao et al. 2010). However, these experiments did not evaluated the long-term perfusion of the constructs, and all the methods used were limited in the size of the graft as the blood vessel's expansion was not rapid enough to support human size tissues, while preventing necrosis. Therefore, in general, transplantation of engineered livers has never exceeded 3 days *in vivo*.

On this regards, the work by Shaheen et al. appears very relevant; the authors re-vascularized decellularised whole porcine livers with HUVECs and implanted them heterotopically into immunosuppressed pigs, showing that the vasculature was able to sustain perfusion for up 15 days (Shaheen et al. 2019). Other studies have tried to overcome the hurdle of the long-term functionality of reconstructed vasculature, by injection of rat sinusoidal endothelial cells into rat liver scaffold. Thanks to Doppler ultrasound the authors were able to detect blood flow after 8 days post implantation (Meng et al. 2019).

1.5.2. Kidney

Because of its filtration function, the kidney represent another organ of which vasculature does not only provide nutrients and oxygen, but it is vital to its function.

The literature around kidney revascularisation is vast and variegated.

The first attempt to engineer the vascular compartment of this organ was performed by repopulating decellularised rat kidneys by using HUVECs and rat neonatal kidney cells; the authors achieved a spatial distribution of endothelial cells into the vessels, which resemble the native glomerula. Importantly, the engineered kidneys were orthotopically implanted in a mouse/rat/rabbit model for a short period of time (not clearly stated in the methods of the article), and there was no cloth formation after the anastomosis of both vascular pedicles of the graft. Importantly, the authors showed

a selective engraftment of cells on the bases of the native ECM structure: glomerular areas predominantly repopulated with podocytes, while tubular structures repopulated with tubular epithelial cells with re-established polarity (Song et al. 2013). These data strengthen the value of using native ECM to promote regeneration in tissue regeneration, as it was shown to promote cell migration to their anatomical location.

The advantages of using native ECM constructs were also observed when Bonandrini et all. The authors seeded embryonic stem cells through the artery of a decellularised rat kidney. After 72 hours, they showed how cells lost the pluripotency and differentiated towards mesoderm derived endothelial progenitors (Bonandrini et al. 2014). In another study, Du et al. seeded iPSC-derived Pax-2^{+} progenitors and iPSC-derived endothelial cells. Interestingly, the presence of endothelial cells upregulated the expression of genes related to renal development into the progenitor cells. Moreover, they observed that glomeruli were recellularized only in the area where also endothelial cells were presents, corroborating the idea that endothelial cells are pivotal for organ regeneration (Du et al. 2016).

1.5.3. Intestine

To date, only a small number of papers focus on the revascularisation of tissue engineered intestine. Recently, decellularised segment of rat intestine were repopulated with iPSC-derived epithelial cells for 14 days and HUVECs were added for 3 days (Kitano et al. 2017.). The intestine was subsequently implanted in a heterotopic mouse model consisting of a subcutaneous graft in the neck, anastomosed to the vasculature and provided of two-end stomas. The graft was maintained for 4 weeks, and its functionality was assessed by delivering nutrients into the lumen of the engineered intestine, via the stoma. Even though absorption of nutrient into the rat blood stream was observed, the authors could not rule out a

possible free diffusion from the acellular areas of the scaffold which was not completely re-epithelialized. Moreover, patency of the engineered blood vessels was not directly assessed, and the repopulation of perivascular compartment was not attempted.

In an article from MacNeil's group, human dermal microvascular endothelial cells and human dermal fibroblasts were injected into the vasculature of a decellularised rat intestine, were successfully engrafted (Dew et al. 2016). Evidence of activation of endothelial tip-cell selection and active sprouting angiogenesis, showed by Dll4 staining, support the use of this technology to study angiogenesis *in vitro*.

Because of the paucity of studies, there are still many aspects that need to be addressed before we will be able to achieve a functional revascularisation of a tissue engineered intestine. For example, endothelial coverage must reach nearly 100% to avoid blood coagulation; such efficient re-endothelialisation has not been achieved yet, remaining the main hurdle in the field. Moreover, none of the reports here discussed provided an extensive functional analysis of the engineered blood vessels. Finally, it is very important to highlight that in order to achieve a fully functional intestine, engineering of the lymphatic tissue also has to be considered and there is still very limited literature on the topic (Koike et al. 2004).

1.5.4. Lung

The lung is another organ in which the vasculature is pivotal to its function, being the gas exchange strictly dependent by the presence of a functional vascular compartment.

The first attempt of decellularizing and repopulating a whole lung was done in 2010 by Cortiella et al. The authors produced and used whole murine cellular lungs to support development of engineered lung tissue from murine embryonic stem cells. As for other organs, the authors noticed site-specific engrafting and differentiation of

cells, highlighting the importance of scaffold-associated cues in guiding embryonic stem cells differentiation toward specific lineages (Cortiella et al. 2010). In a more recent study, the same group demonstrated the feasibility of producing bioengineered lungs for clinical use by using primary adult lung alveolar epithelial cells and vascular cells to repopulate avascular paediatric lung scaffolds. Bioengineered paediatric lungs contained well repopulated vascular compartment and types I and II alveolar epithelial cells. However no *in vivo* analysis were performed (Nichols et al. 2017).

A report from 2014 of Ott's group, reported decellularization of rat, pig and human lungs, and cyto-compatibility of these matrices assessed by seeding either epithelial cells or HUVECs on decellularised tissue slices (Gilpin et al. 2014). The same research group has also achieved the repopulation of both the endothelial and perivascular compartments in a rat decellularised lung, by seeding cells (either HUVECs and hMSC, or iPSC-derived ECs and PCs) through both arterial and venous routes (Ren et al. 2015). With this strategy, a 75% endothelial coverage was reached, leading to a good barrier function. However, lungs orthotopic implantation *in vivo* was performed only for a short period (3 days) and *in vivo* characterization was limited at showing the presence of cells and perfusability of the scaffold. In two later studies, the same group proved scalability to human size, by decellularizing pig and human lungs and seeding epithelial and endothelial cells. However, the perivascular compartment was not reseeded and scaffold were orthotopically transplanted only for 1h, showing a poor gas exchange (Gilpin et al. 2016; Zhou et al. 2017).

Perivascular component repopulation was achieved by Doi et al. by using rat adipose-derived stem/stromal cells which differentiated towards pericyte and repopulated, together with endothelial cells, decellularised rat lungs. Repopulated lungs were orthotopically transplanted in rats for 3h showing that the presence of perivascular cells avoided oedema formation (Doi et al.,2017). Results obtained so far are encouraging, however, lung re-endothelialization still lacks *in vivo* transplantation results which exceed 3 days.

1.5.5. Heart

Reconstitution of tissue engineered heart vasculature is less explored and there is a discrepancy on the cells used as well as the delivery methods.

The first attempt to re-vascularize a decellularised heart was performed in the rat by Taylor's group. Rat aortic endothelial cells were seeded onto decellularised rat hearts via perfusion of the aorta. After 1 week of perfusion culture in a bioreactor, cells repopulated coronaries and showed metabolic activity (Ott et al. 2008). Similar methodology was used by Yasui et al.. this time heart aortas were seeded with rat neonatal endothelial cells alongside rat neonatal cardiomyocytes and fibroblasts. Even though the authors reported contraction, cell distribution was not even (Yasui et al. 2014). Other studies proved the possibility of achieving a native-like cell distribution by injecting cells through the inferior vena cava and brachiocephalic artery. Robertson et al., were able to achieve better repopulation using this seeding route, and they proved reduced incidence of blood clothing in a heterotopic animal model (Robertson et al. 2014).

Scaling up to human size was conducted by Waymann et al. and Sanchez et al. The first report showed that neonatal cardiac seeded onto the decellularised pig heart scaffold and cultured for 10 days in a the bioreactor, were able to re-endothalialise the coronary tract (Weymann et al. 2014). In the second report, HUVECs were used to repopulate decellularised human heart scaffold slices. Endothelial migration to the right compartment (such endocardium and vasculature) was achieved. However, it is important to highlight that both works did not include *in vivo* implantation experiments and complete revascularization of atria, ventriculi and valves was not achieved.

1.6 Aims of the project

Gut transplantation is an effective treatment for patients with short-bowel syndrome. However, long-term outcomes are compromised by rejection and chronic immunosuppression.

Whole organ tissue engineering has emerged as a promising solution to overcome the shortage of organs for transplant, however there is a strong bottleneck in the engineering of whole organs which is the vasculature.

Many research have tried organ revascularization without taking the perivascular compartment into consideration. Nonetheless, in the arena of whole organ tissue engineering, very little attention is devoted to cell location and behaviour when both endothelial and mesenchymal cells are employed. Furthermore, in several studies, the existence of the cell in the construct was identified only after a few days of culture, and the presence of the designed graft was identified only after a few days of *in vivo* implantation. As a result, another issue that must be addressed is the modified endothelium's long-term viability. Therefore, human umbilical vein endothelial cells (HUVECs) and paediatric mesoangioblasts (MABs) (a subset of pericytes) will be co-cultured to unveil the mechanisms behind their crosstalk. Cells will be also co-seeded within the vasculature of an acellular rat intestine using a customised bioreactor to describe the mechanism of revascularization within a tissue specific ECM. In-vivo heterotopic model will be set up to assess anastomosis and durability of the engineered vasculature (Figure 1.17).

In this context, these are the aims of this PhD project:

1. Elucidate the mechanisms behind endothelial cells (HUVECs) and perivascular cells (MABs) interact *in vitro*

2. Standardize the protocol and the conditions that allow HUVECs and MABs to repopulate the preserved vasculature of a decellularised whole organ such as the rat intestine.
3. Regenerate the endothelial, perivascular and smooth muscle compartments of the preserve vasculature of a decellularised rat intestine.
4. Asses the functionality of the newly formed vasculature
5. Validating the long-term durability and maturation of the newly formed vasculature in a heterotopic *in vivo* model

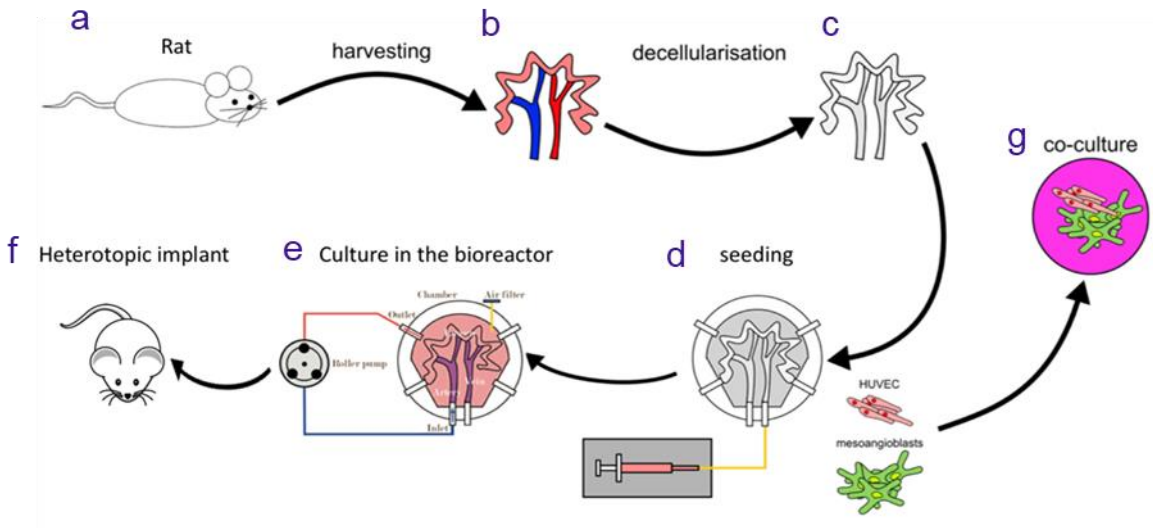

Fig 1.17: Overview of the project. the schematic shows the project methodology: Rat intestine was harvested preserving mesenteric artery and vein (a-b). Intestine was decellularised using an established that preserved the vascular tree (c). Human Umbilical Cord Endothelial Cells (HUVECs) and Mesangioblasts (MABs) were perfused into the scaffold inside a custom-made bioreactor (d). Media were delivered by perfusion for 7 days (e) prior heterotopic implant in mice (f). In parallel, the two cell types were co-cultured together or independently in vitro to evaluate angiogenic capability and unveil mechanisms of their cross talk (g).

Chapter 2

Materials and Methods

2.1. Cell culture

Human Umbilical Vein Endothelial cells (HUVECs) were purchased from GIBCO (GIBCO cat. no. C-015-10C) and cultured on flasks pre-coated with Ultrapure water 0.1% gelatine (Millipore, ES-006-B) in complete endothelial media (EGM-2 with supplements, Lonza, CC-3162). EGM-2 medium was implemented with 10% Fetal Bovine Serum (FBS, Gibco; 10270-106), 1% L-glutamine and 1% penicillin-streptomycin. Cells were passaged when they reached 70-80% confluency, by treatment with an enzymatic mix (TripLE, Gibco; 12563-029) for 5 minutes at 37º degrees, before sub-culturing or seeding in the scaffolds. Each lot of cells was validated by the company using immunohistochemical analysis to assess the expression of Von Willebrand factor (vWf) and CD31 antigens, and for the absence of α-actin. Human mesoangioblasts (MABs) were isolated from paediatric skeletal muscle biopsies from patients aged from 1 week to 8 years old. Tissue biopsies were collected after informed consent was obtained, during surgeries at the Great Ormond Street Hospital, London, in accordance with ethical approval by the NHS Research Ethics Committee, REC Ref: 11/LO/1522. The Committee was constituted in accordance with the Governance Arrangements for Research Ethics Committees and complied fully with the Standard Operating Procedures for Research Ethics Committees in the UK. Cells were isolated according to a previously published protocol (Tonlorenzi et all. 2007) with modifications (Urbani and Camilli 2017).

Firstly, muscle biopsies were washed with Phosphatase Buffer Saline (PBS, Gibco; 10010015) to get rid of residual blood and dissected into 2mm pieces trying to identify portions with small vessels. Eventual adipose tissue was removed. From five to seven tissue fragment were transferred into 60mm dishes pre-coated with 1:100 Growth Factor (GF)-reduced Matrigel (BD 354230). After 1-3 hours, 1ml of cell

medium was added carefully and incubated overnight at 37 °C. 2ml of fresh medium was added to each dish following 24h. 2-4 days after plating of the biopsies pieces, cultures were examined in order to evaluate cell outgrowth from the tissue. If not ready, each dish was supplemented with additional 2ml of medium. Cell outgrowth timing was sample-specific and varied from 5 to 12 days. When cells reached the optimal density, they were detached using 0.5% trypsin/EDTA (Sigma; 25200-072), transferred to tissue culture treated flasks (Thermo Scientific, Nunc) and expanded. Muscle fragments were replated up to four times till complete depletion occurred.

MABs were cultured in Megacell DMEM media (Sigma M3942) containing 5% FBS 1% L-glutamine, 1% penicillin-streptomycin, FGF-2 (5ng/ml) (Gibco; AA10-155), 1% non-essential amino acids (Gibco; 11140050) and 0.1mM 2-mercaptoethanol. Cells were passaged when they reached at 70% confluence by treatment with TripLE for 5 minutes at 37º degrees, before seeding in scaffolds or used for experiments on plastic.

Human MABs and HUVECs were stably transduced with lentivirus to express Green Fluorescent Protein (GFP) or mCherry. 6 well plates were seeded at 3x10^4 cells / cm^2 plate density and allowed to adhere overnight. Growth medium (Megacell or EGM2) was supplemented with a solution of lentiviral vector containing GFP or mcherry under a constitutive promotor. Cells were left over night in incubation and then washed with fresh media prior fluorescence-activated cell sorting (FACS) to isolate only the GFP^+ or $mcherry^+$ population for downstream experiments.

GFP^+ MABs and HUVEC were co-cultured in 24 well plates (Nunclon) at a 1:5 cell ratio (MABs:HUVEC); control wells were plated with only MABs or HUVEC only. All cells were cultured in EGM2 10% FBS for up to 7 days.

For smooth muscle differentiation MABs were treated with differentiation medium composed by high glucose DMEM (Gibco; 11039-21) enriched with L glutamine, 1%

penicillin-streptomycin, 2% horse serum (Gibco 26050088), and 5ng/ml TGFβ (Sigma T7039-50UG), provided fresh daily for one week.

Table 1: List of biopsies of human MABs isolated and used in this work.

biopsy	Age donor	Muscle origin	Pathology	Genetic abnormality
02	6 years	Head temporalis	Congenital deafness	no
03	1 week	Neck strap muscle	Benign neck tumour	no
04	8 years	Head temporalis	Ear surgery	no
05	9 months	Abdomen	---	no

Cells transduction

Human MABs and HUVECs were transduced using a lentivirus received kindly provided by Dr. Colin Butler. This lentivirus was previously manufactured to contain ZsGreen fluorescent protein under the EF1-alpha promoter as shown in Fig 2.1.

$5x10^4$ cells were plated into T25 flasks (Nunc) and left to adhere overnight in 5ml of media (Megacell for MABs and EGM2 for HUVECs). Upon 24h, Polybrene was supplied at 4ug/ml 15min prior to virus addition to increase the efficiency of transduction.

To test increasing M.O.I., serial dilutions of virus were prepared and added to the cells. After 8h at 37°C, cells were washed, fed with fresh medium, and left to recover until confluence prior to passaging.

FACS analysis was performed to establish transduction efficiency, as percentage of ZsGreen^{+} cells. Moreover, ZsGreen^{+} cells were sorted to obtain a pure population of transduced cells. Briefly, cells were trypsinized for 5 min, centrifuged, washed in HBSS and filtered through a 40µm cell strainer cap. Lastly, ZsGreen^{+} cells were resuspended with 400µl of 2% FBS in HBSS and sorted using FACS-Aria (BD, Bioscience). Non-transduced cells were used as negative control. Upon sorting ZsGreen^{+} cells were harvested in 5ml of medium and replated at $2x10\text{^}3$ cells / cm^2 density.

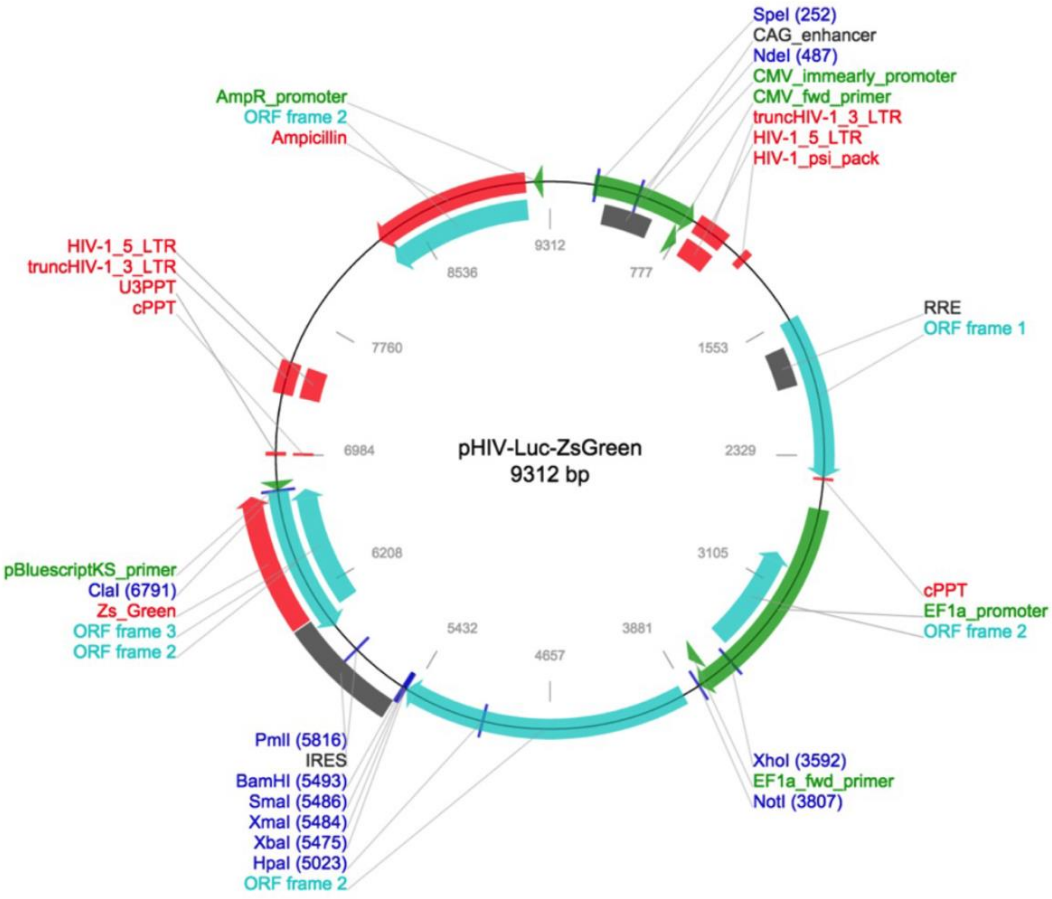

Fig 2.1 Schematic of ZsGreen lentiviral vector. This vector was used for transduction of cells. This lentivirus was previously engineered to incorporate the ZsGreen fluorescent protein under the control of the EF1-alpha promoter.

2.2. Functionalised plates

For experiments on functionalised plates, MABs were plated on dishes coated with Dll4 (R&D Systems; 1389-D4) and/or Jagged1 (R&D Systems 1277-JG) (both 10 mg/ml) and grown in Megacell medium supplemented w/o PDGF-BB (Sigma-Aldrich; P4056) at a concentration of 50 mg/ml.

2.3. qPCR

RNA extraction was performed with RNeasy kits (Qiagen, Germany; 74004), following manufactorer's instructions. Extracted RNA was quantified with a Nanodrop 2000 (Thermo scientific) and reverse transcribed using with Improm RT kit (Promega, USA; A3800) using a BioRad T100 thermocycler and following the standard manufacturers' procedure. Samples were then processed for quantitative real time PCR using Real Time Master Mix (Promega, USA; A600A). qRT-PCRs were performed in triplicate on samples obtained from three independent experiments. GAPDH was used as house-keeping gene for each run. Data analysis was performed with Microsoft Excel and GraphPad Prism 6 using the ΔΔCt / fold increase method (Schmittgen and Livak 2008). Data were presented as mean ± standard deviation (SD).

Table 2: List of primers used for the qPCR

Gena	Sequence	Annealing T (°C)	Brand
Notch1 FW	TGGACGCCGCTGTGAGTCA	55	Sigma NM_017617
Notch1 REV	TGGGCCCGAGATGCATGTA	55	Sigma NM_017617
Notch3 FW	GTCGTGGCTACACTGGACCT	60	Sigma NM_000435
Notch3 REW	AATGTCCACCTCGCAATAGG	60	Sigma NM_000435
HeyI FW	CACCTGAAAATGCTGCACAC	60	Sigma NM_001141945
Hey1 REV	ATGCTCAGATAACGGGCAAC	60	Sigma NM_001141945
aSMA FW	GTT TGA GAC CTT CAA TGT CCC	55	Sigma NM_001141945
aSMA REW	CGA TCT CAC GCT CAG CAG TGA	55	Sigma NM_001141945
SM22 FW	CCAACAAGGGTCCATCCTACG	60	Sigma NM_001001522
SM22 REW	ATCTGGGCGGCCTACATCA	60	Sigma NM_001001522
Calponin FW	GGG AAG GTG AAA GAA GGC AT	60	Sigma NM_001299
Calponin REW	GAG AGC AGA GAT TAC AGG GT	60	Sigma NM_001299
GAPDH FW	AGGTCGGTGTGAACGGATTTG	60	Sigma NM_002046
GAPDH REW	TGTAGACCATGTAGTTGAGGTCA	60	Sigma NM_002046

2.4. RNA-sequencing and bioinformatic analysis.

Resulting fastq files were checked for quality (FastQC v0.11.5) and processed using the Digital Expression Explorer 2 (DEE2) workflow. Adapter trimming was performed with Skewer (v0.2.2) (Jiang et al. 2014). Further quality control done with Minion, part of the Kraken package (Davis et al. 2013). The resultant filtered reads were mapped to mouse reference genome GRCm38 using STAR aligner (Dobin et al. 2013) and gene-wise expression counts generated using the “-quantMode GeneCounts”

parameter. After further filtering and quality control, R package edgeR was used to calculate FPKM and perform differential expression analysis.

Principal Component Analysis was performed on mean-centered log2(FPKM+1) using MATLAB R2017a (The Mathworks). DEGs between MABs cultured alone in 2D and in 3D were selected using a mixed criterion based on uncorrected p-value < 0.05, a fold change (FC) > 1.5, and average log2(CPM) > 3. DEGs between MABs cultured in 2D alone or with HUVEC were selected using an FDR-corrected p-value < 0.01, a FC > 2, and average log2(CPM) > 3. Functional enrichment analysis was performed using the web-based tool Enrichr (Kuleshov et al. 2016) within Gene Ontology-Biological Process database. Enrichment analysis of Reactome pathways was performed using ReactomePA (YU et al. 2016). Bioconductor package. Gene set hierarchical clustering and heatmap visualization was performed using median-centered FPKM data, with correlation distance and complete linkage in MATLAB. A selection of smooth muscle markers was annotated from Andrew et al. 2001. Proteins playing a role as receptor-ligand pairs were taken from Ramilowski et al 2015. Receptor-ligand pairs were visualized using Cytoscape v. 3.8 (Shannon et al. 2003): briefly, all pairs containing either a receptor or a ligand as MABs DEG between 2D culture alone and in co-culture with HUVEC were plotted. To avoid false positives due to HUVEC contamination in MABs samples from co-culture, only DEGs up-regulated in co-culture with an expression equal or higher than in HUVEC were included.

Gene expression data are publicly available on Gene Expression Omnibus database GEO, http://www.ncbi.nlm.nih.gov/geo) under the GEO IDs: GSExxx

2.5. Angiogenic assay

For the network formation assays, cell culture dishes were coated with GF-reduced Matrigel at 37°C for 30 minutes. MABs and HUVECs were then seeded independently or together (ratio 1:5) on the Matrigel coated dishes at a density of 3x10^4 cells / cm^2.

The number of network branches, junctions, and length of the segments were quantified after 19h to assess the stability and quality of the networks, by imaging 5 fields of view of any well and using a plug in of image-J (angiogenesis analyser).

2.6. Scanning Electron Microscopy (SEM)

Unseeded and seeded scaffold samples were fixed in 2.5% Glutaraldehyde (Sigma G5882) in 0.1 M Phosphate Buffer for 24 h at 4 °C. The samples were then submitted for SEM microscopy which was carried out at the facility of Scanning Electron Microscopy in the main campus, UCL.

2.7. Harvest

Intestines from 300-350g weight Sprague-Dawley male rats (between 6-12 months old) were processed as following for production of intestine scaffolds: the mesenteric artery and mesenteric vein were exposed, and all collateral branches were individually closed with silk suture 0.7 thread before being cannulated with a 24-gauge surgical cannula. The lumen of the intestine tract, perfused by the mesenteric vasculature, was cannulated with a silicon tube, and then cleaned. Intestines were placed and sewed onto a silicone base to maintain orientation and morphology of the vessels.

2.8. Decellularisation procedure

The lumen of the intestine and the mesenteric artery were perfused using a Masterflex L/S variable speed roller pump at a speed of 1ml/min. The decellularisation protocol consisted of one cycle of perfusion of deionised water at 4°C for 24h, 4% sodium

deoxycholate (SDC, Sigma D6750) at room temperature (RT) for 4h. Then deionised water was perfused again, for 1h at RT, and 2000kU DNase-I (Sigma EN0521) in 1M NaCl (Sigma 78579) were perfused at RT for 3h, as previously described (Totonelli et al., 2012). Decellularised scaffolds were then irradiated using 5-Gy gamma ray source overnight, and then preserved at 4°C in PBS with 1% penicillin streptomycin. Blue dye was perfused via the mesenteric artery and portal vein to macroscopically assess the preservation of the vascular tree.

2.9. DNA quantification

Fresh or decellularised tissue was cut and 10-15 milligrams of each sample were used for DNA extraction using DNase blood and tissue kit, Qiagen, and quantification. The DNA was extracted following the manufacturer`s instruction. Briefly, the sample were digested in digestion buffer and proteinase. Using alcohol, the DNA was purified and the amount present in each sample was measured by determining absorbance at 260 nm using a NanoDrop machine, Thermo scientific 1000 (Thermo Scientific). For all the quantification at least three biological and technical replicates were analysed.

2.10. Protein quantification

Collagen content was evaluated using Total Collagen Assay kit, QuickZyme, Biosciences. Wet pieces of both fresh and decellularised tissue with a weight around 10-20 milligrams were digested in 6M hydrochloric acid at 95 °C overnight. Collagen content was measured spectrophotometrically with the Infinite microplate reader (Tecan) at the wavelength of 570nm.

Glycosaminoglycan (GAG) content was analysed using the BLYSCAN GAG assay kit (Biocolor, B1000). The tissue was digested with 5mL of papain digestion solution; samples were incubated for one overnight at 65°C. Then, they were mixed with 1,9-dimethyl-methylene blue dye and reagents from the kit. Finally, the absorbance at 656 was measure using Infinite microplate reader (Tecan).

Elastin content was quantified using the FASTIN elastin assay (Biocolor, F2000) according to the manufacturer`s instruction. Briefly, the sample were homogenized, and elastin lysed in 0.25 M oxalic acid, then three different incubations were performed at 95°c to complete the elastin extraction. Absorbance was determinate at 555 nm using Infinite microplate reader (Tecan).

2.11. Histology

Samples were fixed in 4% Paraformaldehyde (PFA; Sigma 158127) solution in PBS, dehydrated in graded alcohols, paraffin embedded and sectioned at 5µm. Tissue slides were stained with Haematoxylin and Eosin (H&E, Thermo, Sigma 517-28-2), Masson's trichrome (MT, kit RAL diagnostics, GT15-1KT), Picrosirius Red (PR, kit Abcam, AB150681) for collagen staining, Elastic Van Gieson (EVG, Merck Millipore,132755) for staining elastin and Alcian Blue (AB, Sigma B8438) for staining Glycosaminoglycans (GAGs).

2.12. Immunohistochemistry

After rehydration of paraffin-embedded sections, the slides underwent an antigen retrieval treatment. For immunohistochemistry, Dako envision kit was used (Dako north America). Primary antibody Collagen I (Abcam, AB6308, 1:50 dilution) Collagen

IV (Novabio, NB120-6586, 1:200 dilution), Laminin (Abcam, AB11575, 1:250 dilution), Fibronectin (Santa Cruz, SC59826, 1:50 dilution) were used.

2.13. Cell Seeding into the decellularised rat intestinal scaffold

Decellularised rat intestine was mounted asymmetrically in the bioreactor chamber. Prior seeding, the vasculature tree was primed with 1 mL of EGM-2 supplemented with 10% FBS, gently injected through a 1 mL syringe (BS Plastipak) connected to the canulated mesenteric artery. HUVECs and MABs were harvested and strained with a 70μm cell strainer (Falcon) before the seeding onto decellularised rat intestine via the mesenteric artery and portal vein using a 1ml syringe. The seedings were carried out with 1ml cell suspension solution in medium (EGM2) injected half through the mesenteric artery and half through the mesenteric vein access. Approximatively 40ml of pre-warmed EGM2 with 10% FBS medium, was added into the bioreactor chamber and fluidic circuit.

The bioreactor culture was allowed through a close circuit in which media was withdrawn from the chamber and re-pumped back into the bioreactor chamber through the canulated mesenteric artery (Fig B). Continuous perfusion of media through the mesenteric artery was carried out using a roller pump at a speed of 1ml/min for 7 days, with media changes every other day.

2.14. Immunofluorescence on plastic

MABs in co-culture with HUVECs were fixed in 4% PFA for 10 minutes before washing with PBS. Cells were then incubated in 0.1% Triton-X 100 (Tx; Sigma) for 5 minutes, followed by 5 min washes with PBS before blocking with 5% donkey serum (Sigma D9663-10ML) for 2 hours. Primary antibodies were diluted in the blocking

solution with addition of 0.5% Tx to allow permeabilization, and incubated at 4°C overnight (O/N). Primary antibody buffer was washed using PBS before secondary antibody solution was added. Secondary antibodies were diluted in the same solution used for primary antibodies. Slides were incubated with Alexa Fluor secondary antibodies (Invitrogen) for 45 minutes at RT before washing with PBS. Nuclei was stained with DAPI (Abcam ab228549) and slides were covered with a coverslip using mounting medium (Abcam, ab104139), before images were taken.

Stained cells were imaged using Zeiss AX10 fluorescence microscope AX10 equipped with a camera. Each slide was imaged in four randomly selected, different fields of view, and the number of positive stained cells out of total cell number was counted using Fiji-ImageJ. The final count of positive cells was expressed as average value over four counts. Images were merged and processed using Fiji-ImageJ. List of primary and secondary antibodies used is shown in Table 3.

2.15. Immunofluorescence - whole mount tissue

Seeded scaffolds were fixed in 4% PFA O/N at 4°C and then washed with PBT $^{+/+}$ (PBS, CaCl2; Sigma, MgCl2; Sigma and Tween 20; Sigma). Blocking solution consisted of PBS $^{+/+}$ with 10% donkey serum ; scaffolds were incubated in blocking solution for at least 2 hours. Primary antibodies were diluted in the blocking solution with addition of 0.5% Tx to allow permeabilization, and incubated for 24-48h at 4°C. Slides were incubated with Alexa Fluor secondary antibodies (Invitrogen) at 37°C for 2 hours, washed and mounted with Vectashield mounting medium containing DAPI (Vector Labs H1200). Stained tissues were imaged using a confocal microscope (Zeiss LSM 710 inverted confocal microscope). Primary and secondary antibodies used are listed in Table 2.

2.16. Quantification of cell coverage of blood vessels

Whole mount stainings were imaged with confocal microscope in order to obtain a picture of 4mm^2 of scaffold in 4 different z-point throughout the thickness of the scaffold. The channels were split using Fiji-ImageJ and only the channel where the endothelial cells were stained was used to calculate the coverage. The stack was flattened using the function “Z-project” and “MAX intensity” of Fiji-ImageJ. The signal of all the images was adjusted in the same way and the final image was converted in 8-bit image to be analysed with threshold tool of Fiji-ImageJ. The following setting were established for all the pictures (low: 40; up: 255).. The ratio of pixels in black/number of total pixels was calculated to evaluate the blood vessels coverage.

2.17. Vascular permeability

The revascularisation efficiency was tested with a fluorescence assay; the assay was performed on native intestine, on scaffold after decellularization and on scaffold after revascularization. A solution with EGM2 media containing 0.2 mg/mL of Fluorescent isothiocyanate-dextran 500 kDa (Sigma FD500S, compound fluorescent at 488 nm), was injected, from a syringe placed 1,5 m above, through the Mesenteric Artery using gravity speed, creating a pressure potential equal to:

$$\Delta p = \rho * g * \Delta h = 1000\ \frac{kg}{m^3} * 9.8\ \frac{m}{s^2} * 1{,}5\ m = 14.7\ kPa$$

The intestinal lumen was closed with connectors and the fluid inside the scaffold was collected straight away to measure the absorbance, indicating the level of leaking of the vessel into the lumen.

2.18. LDL Uptake

To monitor the efficiency of revascularisation and perfusion, Low Density Lipoprotein, LDL (Alexa Fluor, Life technologies, L23380) was added in the media at the concentration of 10um/ml and incubated for three hours in static condition after one day of FBS deprivation. The scaffold was then fixed with PFA and visualized using a confocal microscope. Thresholding technique previously described was used to quantify the patency of the repopulated scaffold.

2.19. TNAP-AP-CREERT2:R26R model experiments

Transgenic mice, expressing an inducible CreERT recombinase, under the transcriptional control of a pericyte-specific promoter (TNAP) were crossed with Rosa-26 NGZ reporter mice. New-born pups, 1 and 3 months old mice were used for the analysis. Mice received an intraperitoneal subcutaneous injection of Tamoxifen 0.25 mg volume; 25 µl were injected into pups and 100 µl in adult mice. Mice were culled at 3 and 30 days after injections.

2.20. X-gal whole mount staining

Murine intestines were fixed with 4% PFA for 1 hour at RT. After, they were incubated in X-gal solution (Sigma 11680293001) O/N at 37 °C, then were washed and dehydrated with increasing sucrose concentration (10–20% and 30%) for 20 minutes and then frozen in Optimal Cutting Temperature compound (O.C.T. Sakura Finetek 4583). 7 µm thick sections were generated using a Leica cryostat and used for immunohistochemistry analysis.

2.21. MABs *in vivo* transplantation

To examine the potential for MABs to differentiate into smooth muscle cells within the native intestinal microenvironment *in vivo*, transplantation experiments were performed. For transplantation, immunodeficient Rag2-/-;γc-/-;C5-/- mice were anaesthetized with a 2–5% isoflurane:oxygen gas mix for induction and maintenance and buprenorphine 0.1 mg/Kg was administered at the induction for anaesthesia and as analgesic. Under aseptic conditions, laparotomy was performed to expose the caecum and terminal ileum. Using the caecum as a morphological landmark, GFP^+-labelled MABs were transplanted to the serosal surface of the terminal ileum (last 5 cm) via 30G syringe needle. Subsequently, the exteriorised bowel was returned to the abdomen and the laparotomy incision was closed. Transplanted mice were allowed to recover. Animals were sacrificed 4 weeks post-transplantation and the intestines were collected.

2.22. Heterotopic transplant in mouse omentum

NOD-SCID-gamma (NSG) female mice, aged between 8 and 12 weeks, were anaesthetized with a 2-5% isoflurane-oxygen gas mix for induction and maintenance. Buprenorphine 0.1 mg/Kg was administered at the induction for analgesia. Under aseptic conditions a midline laparotomy was performed. The stomach was externalized from the incision and the omentum stretched from the great curvature. A segment of the engineered intestine was then enveloped in the omentum, using 8/0 Prolene suture to secure the closure of the omental wrap. The stomach and the omentum were placed back in the abdomen and the laparotomy closed using 6/0 Vicryil suture. Animals were allowed to normally eat and drink immediately after surgery and no further medications were administered during the post-operative periods. Animals were sacrificed after 1 week or 4 weeks for further analysis.

2.23. Intra-venous injection of anti-human VE-caderin

After 1 week or 4 weeks from omental implantation, mice were intravenously injected with fluorescently labelled anti- human VEcadherin, then euthanized after 10 minutes (to avoid diffusion). Grafts were retrieved together with the omental envelope and fixed in 4% PFA, washed in PBS, dehydrated in 30% sucrose overnight, embedded and frozen in O.C.T. with ice-cold isopentane (Sigma) and stored at −80 °C.

7–10 μm thick sections were generated using a Leica cryostat and slides were stored at −20 °C. Slides were stained, mounted and prepared for imaging .

Table 3: Antibodies used for immune staining

Antibody	Raised in	Species of reactivity	Company and catalogue number	Concentration used
CD31	Mouse	Human	Invitrogen MA5-13188	1:50
Pdgfrβ	Rabbit	Human, mouse	Abcam Ab32570	1:50
SM22	Goat	Human, mouse	Abcam AB10135	1:1000
Calponin	Mouse	Human, mouse	Sigma C2687-2ML	1:500
Smooth muscle MHC	Rabbit	Human, mouse	Abcam AB82541	1:100
ASMA	Mouse	Human, mouse	Abcam AB7817	1:100
hVE-Cad	Rabbit	Human	Life Technologies 361900	1:100
Ki67	Rabbit	Human, mouse	Abcam AB15580	1:100
Caspase3	Rabbit	Human, mouse	Cell Signalling,9661	1:100

	Collagen I	Mouse	Human, mouse, rat	Abcam AB6308	1:50
	Collagen IV	Rabbit	Human, mouse, rat	Novabio NB120-6586	1:200
	Laminin	Rabbit	Human, mouse, rat	Abcam AB11575	1:250
	Fibronectin	Rabbit	Human, mouse, rat	Santa Cruz SC59826,	1:50

2.24 Statistics

Data were expressed as mean ± S.E.M. Statistical significancy was determined by two-tailed Student's t-test; one-way "analysis of variance" (ANOVA) and two-way ANOVA with post-hoc Bonferroni test. A p-value of less than 0.05 was considered significant; all statistical analysis was performed using GraphPad Prism6 (GraphPad Software).

Chapter 3

Results

HUVECs promote smooth muscle differentiation of MABs through a Dll4 – Notch3 pathway

3.1 Introduction

One of the main features of this work is the decision to take in account also the perivascular compartment, together with Endothelial cells (EC), in order to engineer the vasculature of a whole organ. Pericytes can suppress endothelial growth, migration and micro-vessel stabilization (Bergers and Song, 2005; von Tell et al., 2006), moreover, pericyte involvement has also been directly implicated in conferring capillary resistance to regression in-vivo. Therefore, they appear to be a pivotal compound when it gets to vascular tissue engineering. Because of their capacity to differentiate down to smooth muscle under canonical TGFβ pathway activation, mesoangioblasts have been chosen as the best choice to produce the perivascular compartment of the preserved vasculature of a decellularised intestinal scaffold.(Dellavalle et al. 2007, Cossu and Biressi 2005, Tagliafico et al. 2004): indeed, another goal of this PhD study is to restore the vascular smooth muscle layer, which is thought to be required for a healthy and mature endothelium (Bergers and Song, 2005). Moreover, these cells are currently used in a clinical trial for dystrophy (Cossu et al. 2016) and therefore represent a powerful tool for our clinical translation purposes. Indeed, *in vivo* skeletal muscle regeneration using human Mesoangioblast isolated from postnatal limb muscles has shown promising results, and their potential to produce smooth muscle cells for therapeutic applications has also been explored in a recent publication from our group. (Urbani and Camilli et al. 2017).

With regard of the endothelial cells compartment, Human Umbilical Vein Endothelial cells (HUVECs) has been taken in account. Although this cell source has shown many limitations, it still represents the gold standard in EC research. We decided to employ HUVECs because the long term aim of this project is creating a functional intestine for clinical translation and at present they are the endothelial source easier to access and able to deliver high yield following isolation which is a crucial point for big organs

tissue engineering. Even if this choice might sound controversial given the fact that in the literature HUVECs alone result not capable of regenerating the vasculature in a tissue engineering setup, the co-culture of EC and perivascular cells is becoming a well-established idea for regenerating a functional vascular tree. Moreover, I cannot ignore the promising results of when HUVECs were put together mesenchymal supporting cells. When HUVECs and mesenchymal cells were embedded in a three-dimensional fibronectin-type 1 collagen gel and then inserted into mice they were able to form tubes that connected to the host vasculature and remained patent up to 1 year (Koike et al., 2004). If this idea in one hand is not novel, in the other hand there is a lot of work to be done to integrate this strategy into organ tissue engineering using primary adult cells. In fact, although this is an established concept, only poor attempts have been made using a co-culture between endothelial cells and pericytes to re-vascularize a whole organ.

Finding a strategy that allows adult primary cells, such as HUVECs, to increase their performance with minimal manipulation would be of significant relevance for tissue engineering and would make clinical translation easier. For this reason, they have been employed as an endothelial cell source in this thesis.This chapter outlines the behaviours of those two cell types in co-culture. In particular I investigated on the mechanisms of their crosstalk that drive smooth muscle differentiation by MABs. Moreover, taking in account the fact that Tissue Engineering studies require long period of culture into a bioreactor, in this chapter I also highlight how the presence of MABs improve HUVECs durability *in vitro* and that the co-culture system is the best way to approach the whole organ re-vascularization that I will face in the next chapter.

.

3.2. Isolation and characterization of human mesoangioblasts (MABs) and human umbilical vein endothelial cells (HUVECs)

Human mesoangioblasts (MABs) were isolated by another PhD Student (Carlotta Camilli) with success from four skeletal muscle biopsies, harvested during surgeries from paediatric patients aged from 1 week to 8 years old, as summarized in Table 1. Cell outgrowth from muscle fragments appeared to be strongly donor-specific, as it varied from 5 to 12 days. As soon as local serum consumption occurred, due to the high cell density surrounding tissue fragments, cells initiated to fuse and immature muscle fibres were visualized, as shown in Figure 3.1b. Therefore, in order to prevent differentiation events and to maintain the pool of progenitor cells, MABs were trypsinized and further expanded in culture prior to characterization and freezing.

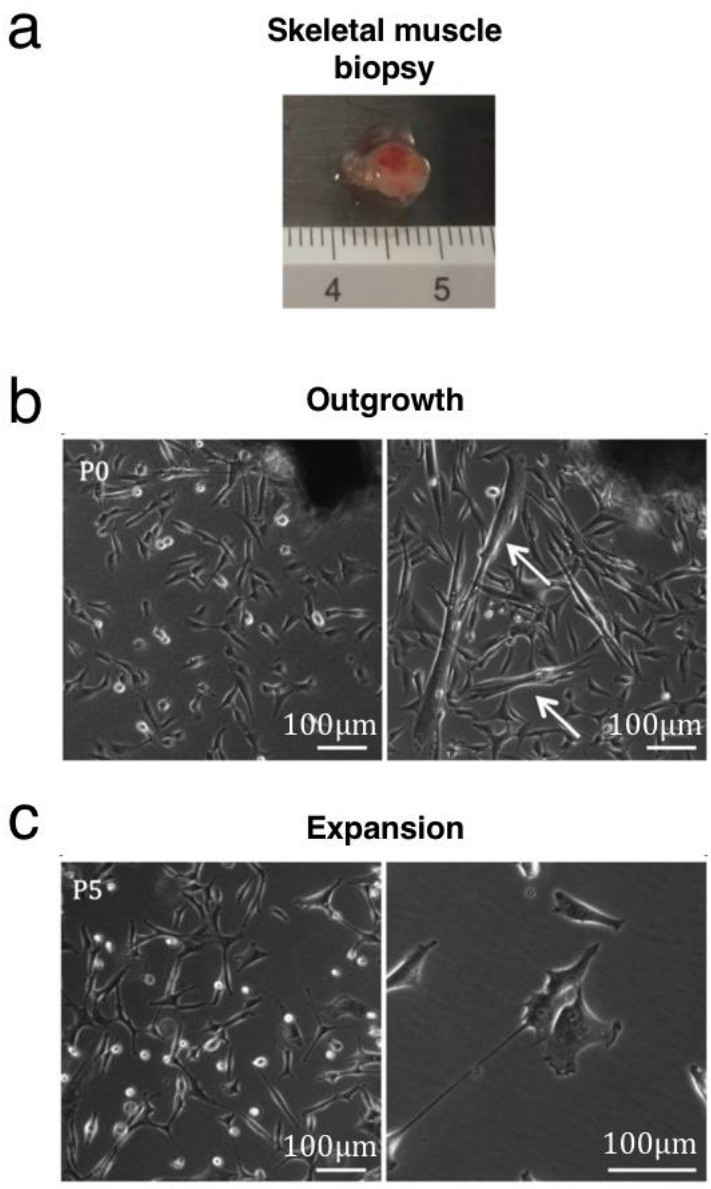

Fig 3.1: Panel representing the isolation and expansions of Mesoangioblasts (MABs). a. Representative skeletal muscle biopsy used for the isolation of MABs. **b**. representative outgrowth of cells (P0) from muscle fragments following 5 days of culture in PM and spontaneous formation of myotubes (white arrows) due to local depletion of serum. **c**. appearance of MABs in culture (P5) as small, triangular and highly refractile cells or roundish floating cells.

As already described (Tonlorenzi *et al.*, 2007), the use of selective growth medium encouraged gradual enrichment of MABs and loss of other muscle cell types, such as satellite cells, myoblasts and fibroblasts (Figure 3.1c). Cultured MABs appeared as small, triangular and highly refractile adherent cells or as round floating cells.

Expanded MABs were characterized by immunofluorescence (and FACS analysis by Carlotta Camilli) for the expression of pericyte markers. As reported before, pericytes form a highly heterogeneous population of perivascular cells that do not feature truly specific markers, as MyoD is for skeletal muscle, and exhibit only some of their markers at any given time (Cappellari and Cossu 2013). MABs displayed, at high frequency and level, neural/glia antigen-2 (NG2), αSMA and PDGF receptor β (PDGFRβ), as noticed by immunostaining (Figure 3.2).

On the other hand, the expression of alkaline phosphatase (AP) was uneven within cultured cell isolates as verified by FACS analysis (28.7 ± 15.4%) (Fig.3.3). FACS analysis also showed frequent expression of NG2 (80.7 ± 17.5%), CD44 (99.6 ± 0.05%) and CD90 (88.6 ± 10.7%), variable positivity for CD146 (58.7 ± 12%) and PDGFRβ (64.6 ± 37.5%), and no expression for CD45 (0.5 ± 0.3%) and CD34 (0.8 ± 1.2%).

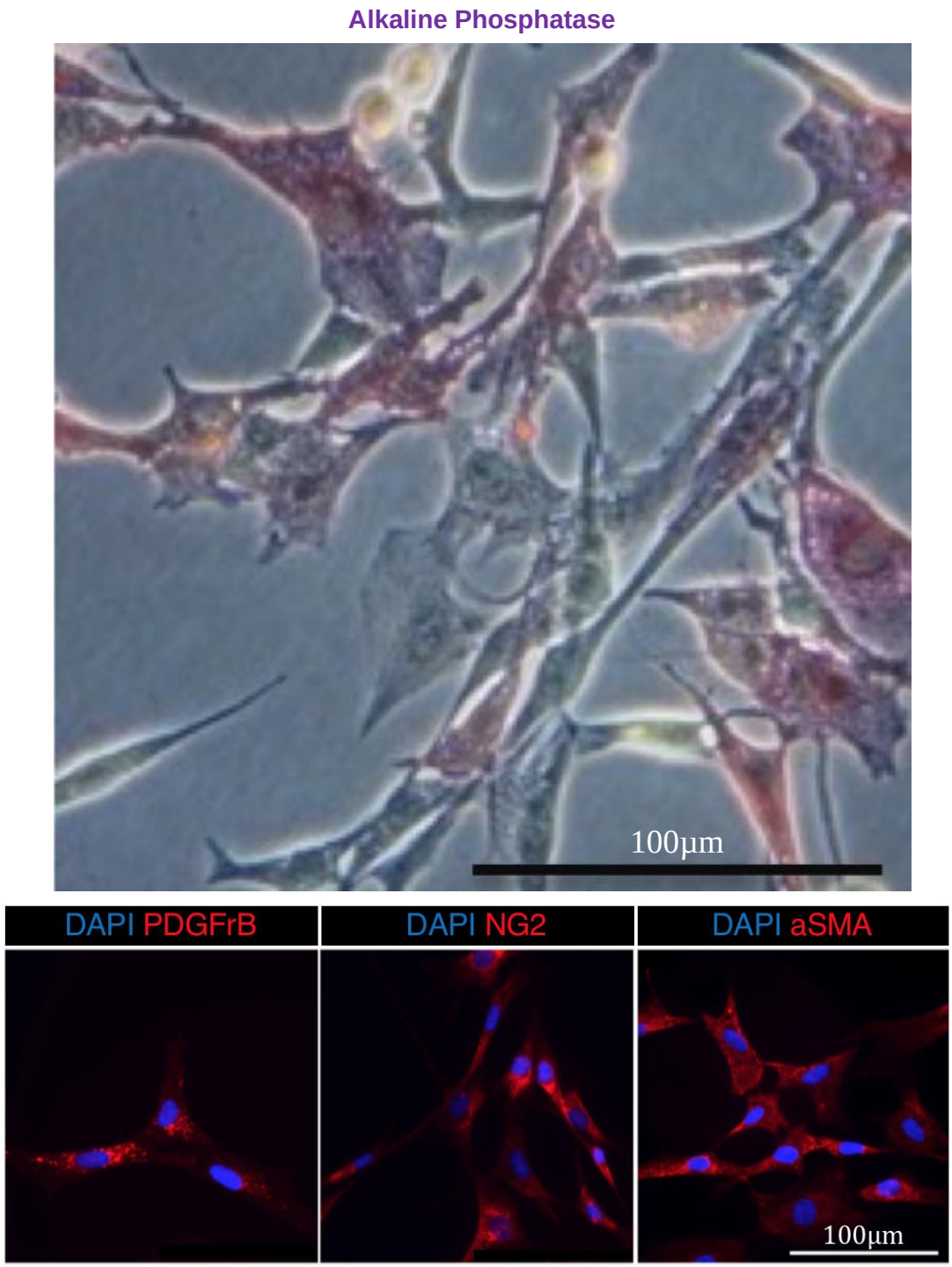

Fig.3.2 Human Mesoangioblast phenotype *in vitro*. Enzymatic assay reveals positivity for Alkaline Phosphatase (AP) while immunofluorescence indicates expression of αSMA, PDGFRβ and NG2**.**

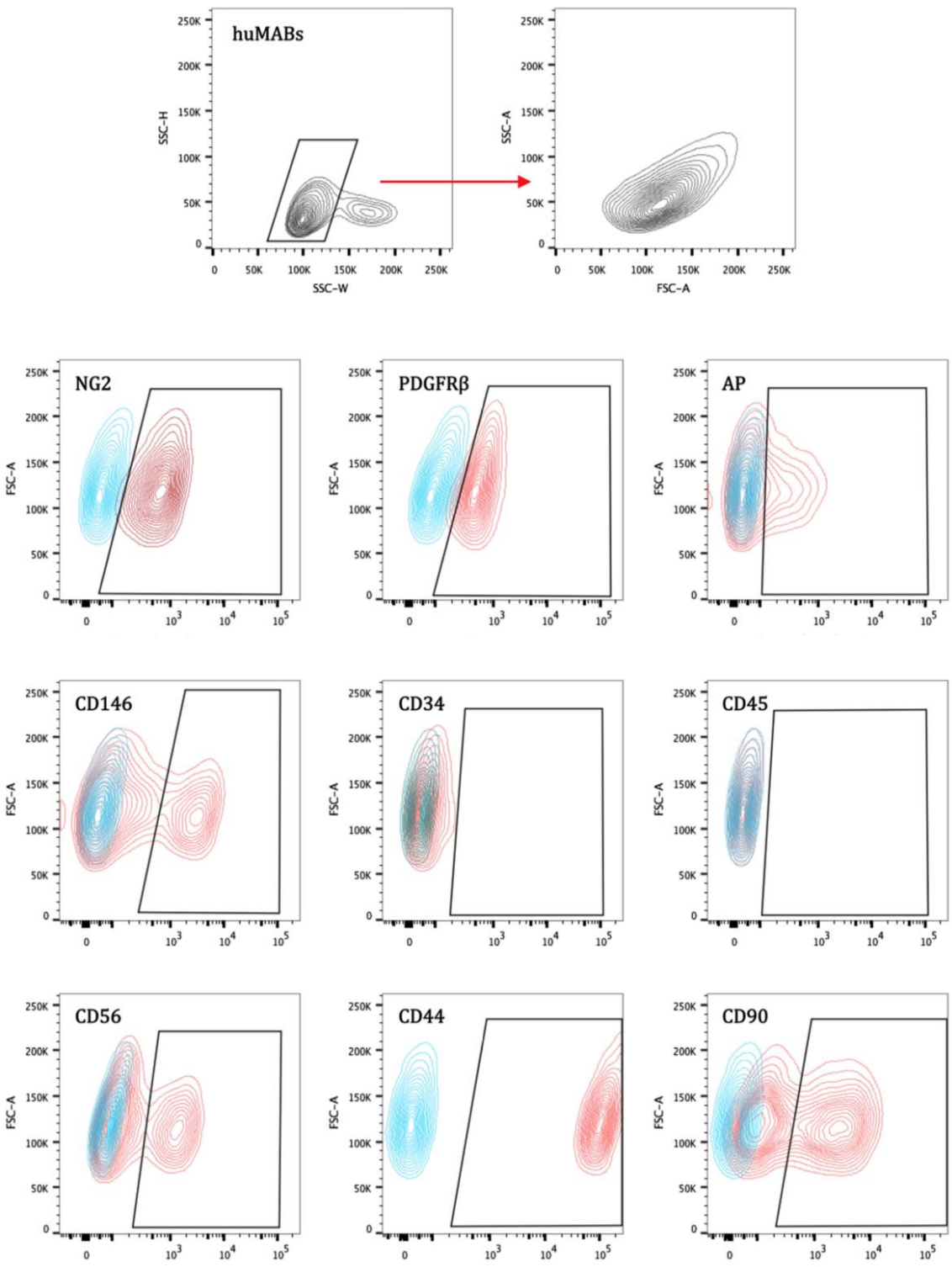

Fig. 3.3: Human Mesoangioblasts express pericyte and mesenchymal markers. Representative FACS analysis, performed at P6 on huMABs#2, confirms positivity for NG2 (97,5%), PDGFRβ (98.7%), AP (30%), CD146 (26.3%), CD56 (32.2%), CD90 (50.5%) and CD44 (100%) while no positivity was detected for CD45. A few cells expressed CD34 (4.2%). Physical parameters reveal a quite heterogeneous cell population.

Muscle-derived MABs were further characterized for the ability to differentiate into skeletal and smooth muscle cells *in vitro* (both by Carlotta Camilli and me). Specifically, cells were stimulated to undergo skeletal muscle differentiation upon exposure to low serum. From 2 to 5 days after medium switch, MABs initiated to fuse generating mature myotubes expressing the adult isoform of myosin heavy chain (MyHC) (Figure 3.4).

Moreover, the capability of MABs to differentiate towards smooth muscle cells was assessed (both by Carlotta Camilli and me) by means of daily exposure to TGFβ. MABs progressively turned into typical enlarged cells until smooth muscle markers were detected. In particular, Calponin was visualized by immunostaining following 7 days of treatment (Figure 3.5), in the large majority of cell population.

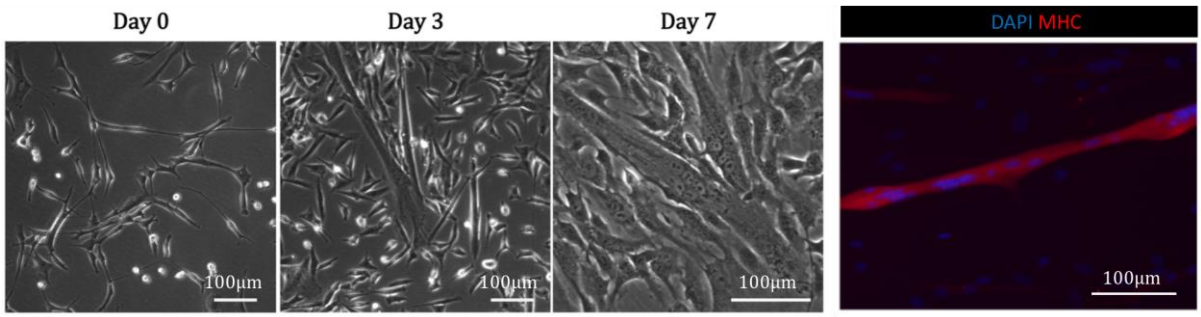

Fig.3.4: *In vitro* skeletal muscle differentiation of human Mesoangioblasts. Representative skeletal muscle differentiation performed at P6 on MABs02. From left to right, upon treatment with low serum, MABs started to fuse until generating mature myotubes at about day. On the very right panel is shown an immunofluorescence for expression of MyHC at day 7.

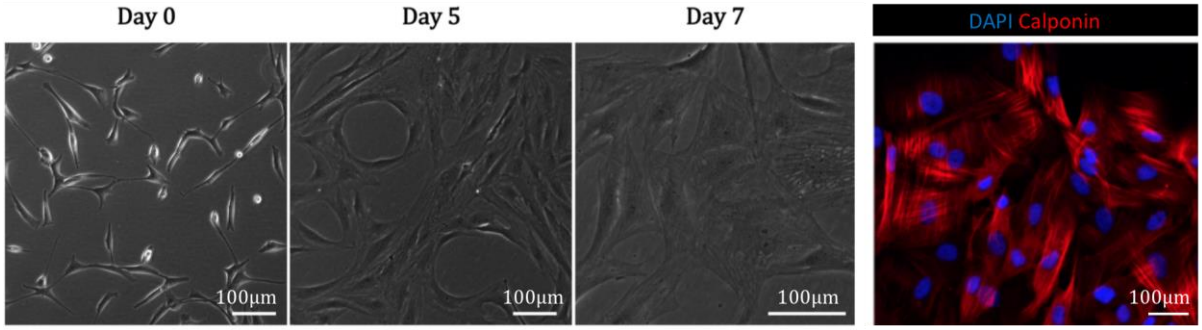

Fig.3.5: *In vitro* smooth muscle differentiation of human mesoangioblasts. Representative smooth muscle differentiation performed at P6 on MABs02. From left to right, following daily treatment with Transforming Growth Factor beta (TGFβ) (5ng/ml), MABs gradually turned into enlarged and striated cells. In the very right panel, an immunofluorescence confirms expression of Calponin at day 7

Human Umbilical Vein Endothelial cells (HUVECs) were purchased from GIBCO (GIBCO cat. no. C-015-10C). Each lot of cells were previously tested using immunohistochemical methods for the presence of von Willebrand factor (vWf) and CD31 antigen, and for the absence of a-actin. They were cultured in complete endothelial media (EGM-2) as described in the materials and method section. Initially endothelial cells assume a round collocation “in the flask as shown in Fig. 3.6 (Figure 3.6). Changing media every 3 days, cell confluency is achieved in 6-7 days, with a 1,200 cells/cm^2 seeding density. When confluent HUVECs show contact inhibition and “cobblestone appearance” (tightly packed polygonal ECs) in phase-contrast microscopy (Figure 3.6).

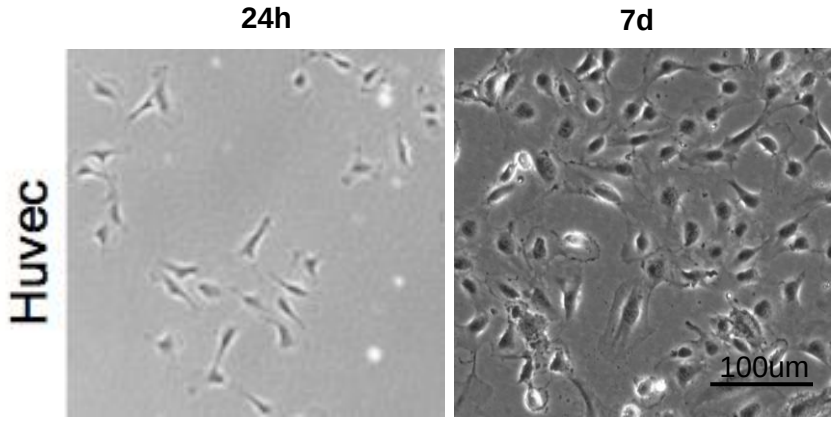

Fig 3.6: Bright field of HUVECs in culture at 24h and 7 days. In plastic, EC shows a circular collocation and they assume a “cobblestone appearecen” when they reach confluency.

3.3. HUVECs promote smooth muscle differentiation by MABs

MABs transfected with a lentiviral vector carrying GFP protein and HUVECs were cultured independently or together (Figure 3.7). Cells in co-culture orientated themselves in a peculiar rounded disposition that persisted up to 7 days, whilst the plate with MABs only was totally confluent at 7 days (Figure 3.7). Moreover, in presence of HUVEC, MABs expressed smooth muscle markers such SM22 and Calponin. On the contrary, when MABs were cultured alone, smooth muscle differentiation did not occur. (Figure 3.7).

a

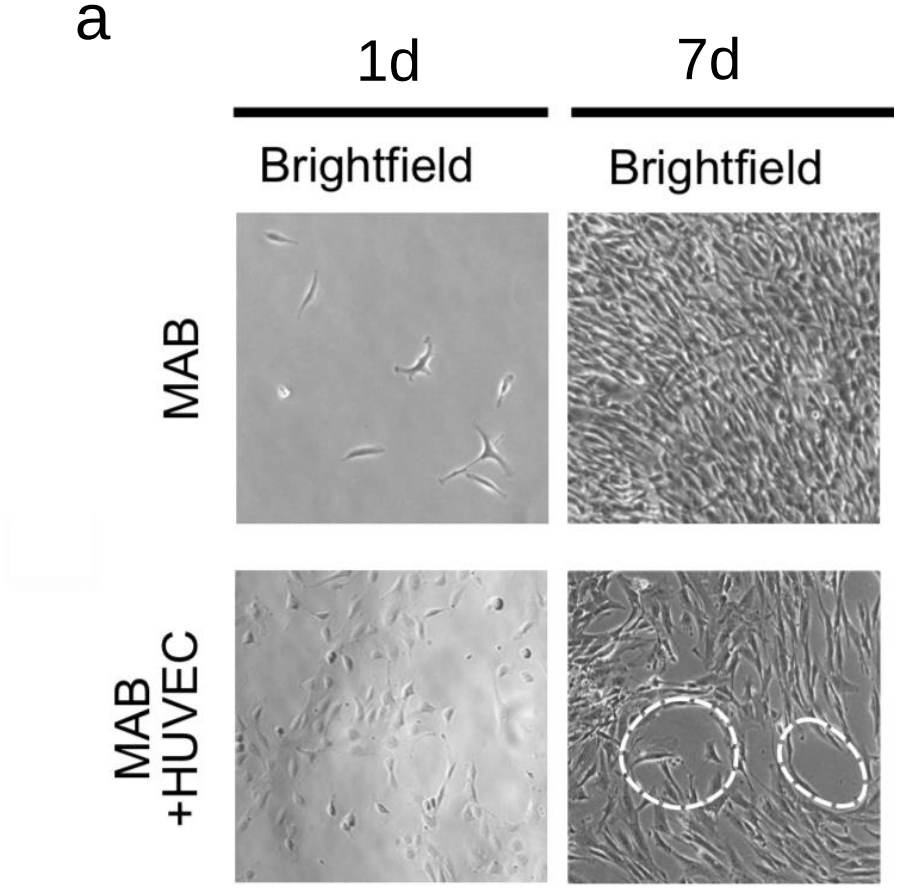

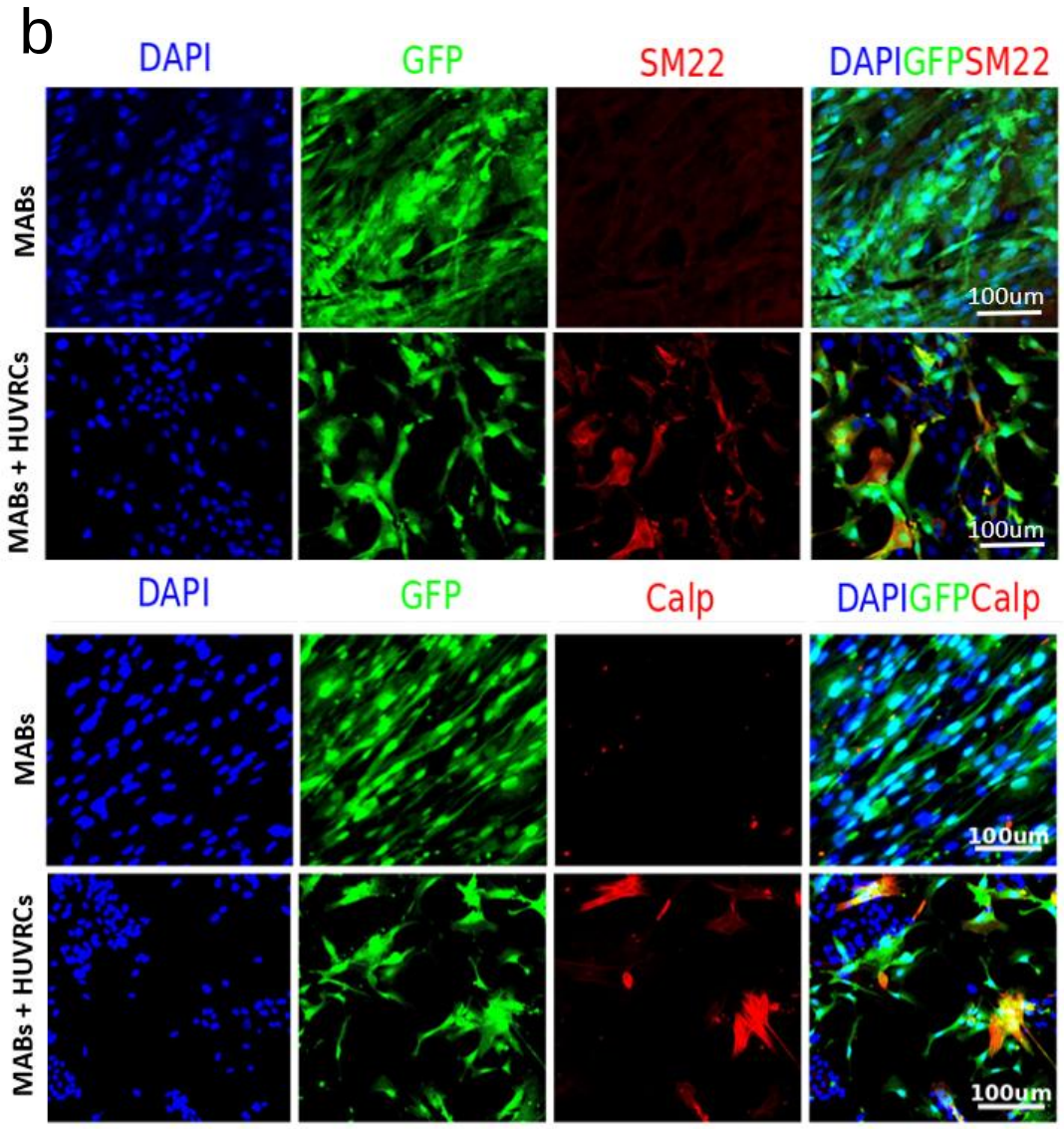

Fig 3.7: co culture of HUVECs and MABs. a bright field of MABs02 cultured undeendently or in co-culture with HUVECs at 1 day and 7 days. As displied in the dashed circle, cells in co-culture dispose themselves in peculiar rounded disposition that is kept up to 7 days. **b** immunostaining immages of MABs GFP+ (in green) cultured independently or in co-culture with huvecs (unstained blu nuclei), stained for SM22 or Calponin (in red)

3.4. Smooth muscle differentiation results independent from TGFβ pathway and rather depends from endothelial derived notch stimulation

Interestingly MABs' smooth muscle differentiation driven by HUVEC was independent from TGFβ, a pivotal factor for smooth muscle differentiation of MABs (Dellavalle et al. 2007). Indeed, addition of TGFβ inhibitor into the co-culture did not decrease significantly the expression of smooth muscle markers compared to the normal co-culture in figure 3.7 (Figure 3.8a). To be more specific, figure 3.8's control is the co-culture (with no other conditions) shown in figure 3.7. Another control of this experiment is the co-culture in the presence of TGFi, which eliminates the possibility that EC activate the TGF pathway, which is known to be critical for smooth muscle differentiation. Subsequently, MABs were cultured with HUVECs Jagged1 -/- or with HUVECs in presence of Dll4 antibody or a combination of the 2 conditions to deplete Notch pathway (Figure 3.8a). Interestingly, when jagged1 was ablated I did not observe and significant decrease of smooth muscle markers, when Dll4 or both ligands were absent, MAB smooth muscle differentiation was completely inhibited (Figure 3.8a-c).

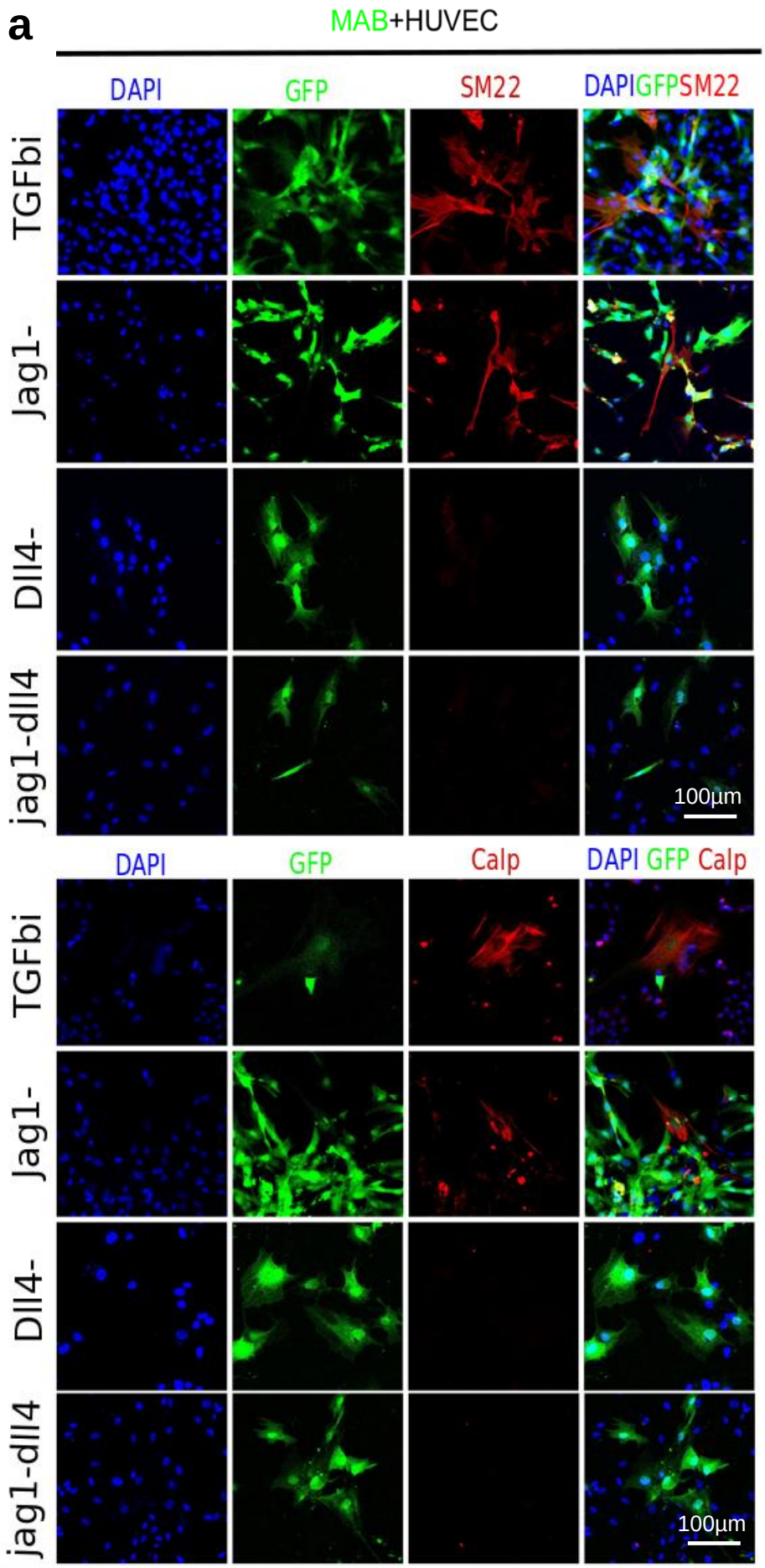
a
MAB+HUVEC
DAPI
GFP
SM22
DAPIGFPSM22
TGFbi
Jag1-
Dll4-
jag1-dll4
100μm
DAPI
GFP
Calp
DAPI GFP Calp
TGFbi
Jag1-
Dll4-
jag1-dll4
100μm

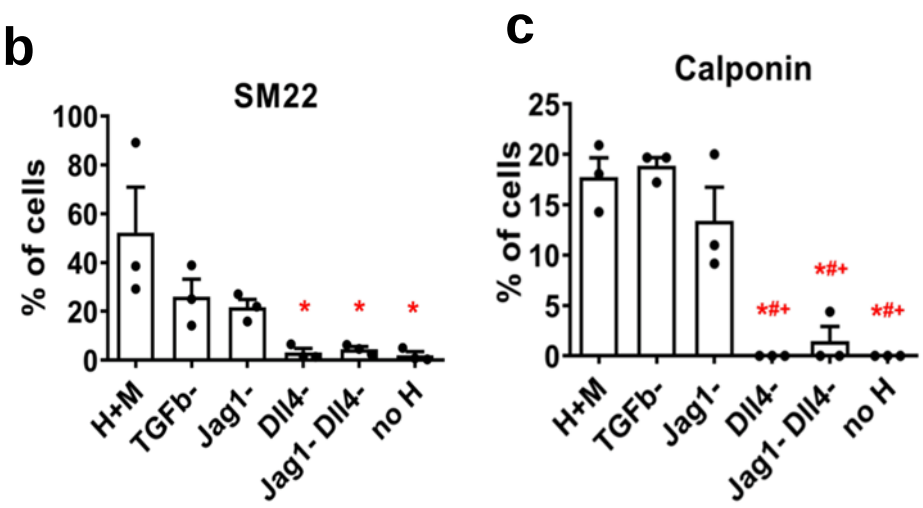

Fig. 3.8: a From top to bottom, immunofluorescence staining for SM22 and Calponin of MABs02 cultured with HUVECs in presence of Transforming Growth Factor beta (TGFβ) inhibitor, MABs cultured with HUVECs Jagged 1 -/- or with HUVECs in presence of Dll4 antibody or a combination of the 2 conditions. These panels show, from left to right, single channels of DAPI (in blue) MAB's GFP signal (in green), Staining for SM22 and Calponin (in red) and merges of the 3 signals. **b-c.** Cell counting of sm22 and calponin positive cells over number of MABs. Statistic was established with 3 biological replicates of MABS (n=3: 02-03-05); one-way Anova was performed; P value <0.0001;

To further investigate the role of the ligands, MABs were cultured in dishes coated with the Notch ligand Dll4 and jagged1 and in the presence or absence of PDGF-BB (being a paracrine factor released by endothelial cells to recruit pericytes) (Figure 3.9). MABs cultured in presence of TGFβ were used as a positive control. I observed that MABs exposed to Dll4, Dll4 and jagged1 phenotypically resemble MABs in smooth muscle differentiative medium (TGFβ) with also expression of calponin. Some features were also present in MABs exposed to jagged1, however, no similarities were observed between MABs cultured in the smooth muscle medium and the one exposed to PDGF-BB only (Figure 3.9). The findings were also validated by qPCR which revealed an enhanced expression of smooth muscle markers (aSMA, SM22, Calponin) in the MABs treated specifically with Dll4 or a combination of the two notch ligands, and not with only Jagged1or PDGF-BB (Figure 3.8). Moreover. this phenomenon appeared strictly associated to Notch3 receptor (and not Notch1) (Figure 3.9b).

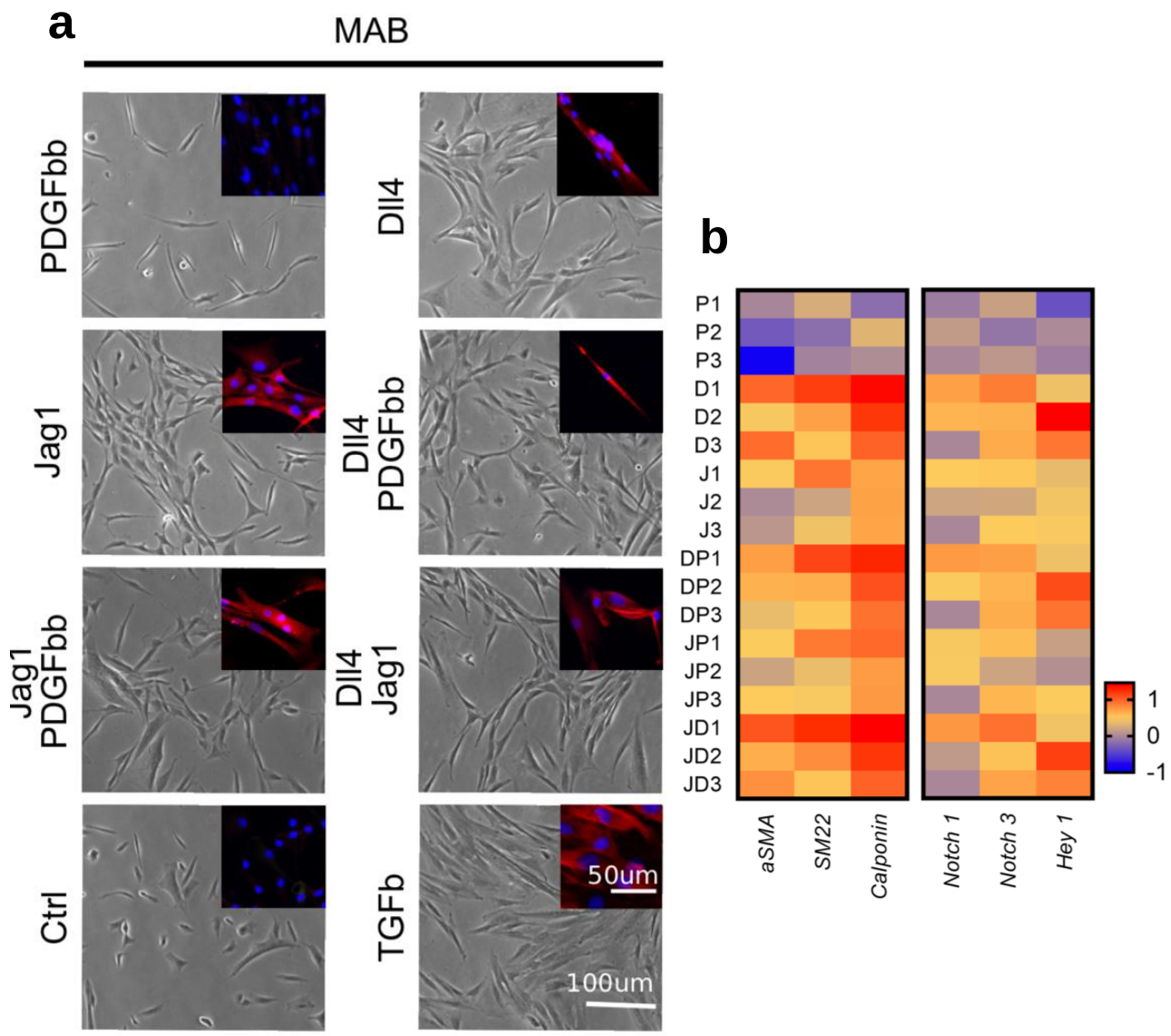

Fig. 3.9. Bright field images of MABs cultured on dishes coated with Dll4, jagged1, Dll4 and jagged1, and w/o PDGF-BB, MABs were also cultured in normal condition and in presence of Transforming Growth Factor beta (TGFβ) as negative and positive control. In the inserts there are confocal images of the same plates stained for calponin (in red). **b**. qPCR for smooth muscle markers (aSMA, SM22, Calponin) and NOTCH pathway (Notch1, Notch3, Hey1) on RNAs extracted from the plates in the panel a. Statistic was established with 3 biological replicates of MABS (n=3: 02-03-05);

Table4. Original qPCR data.

aSMA	CTRL	P	D	DP	J	JP	JD
	1	0.972967	10.268810	5.419367	2.961494	3.016416	12.725980
	1	0.473811	2.893718	4.307732	1.042193	1.575186	4.504201
	1	0.134951	9.743811	2.342923	1.265341	3.218208	6.395568
SM22	CTRL	P	D	DP	J	JP	JD
	1	1.827779	16.415070	15.005410	8.767298	8.272511	19.562420
	1	0.661378	5.266048	4.552153	1.586875	2.386602	6.555303
	1	0.907005	3.498272	3.422547	2.586861	2.887852	3.456428
CALP	CTRL	P	D	DP	J	JP	JD
	1	0.661889	28.085290	21.318620	5.045002	10.134220	34.584360
	1	2.070088	17.830680	13.333650	5.236577	5.625560	17.883120
	1	1.071485	10.814900	9.084162	5.039666	5.745674	10.814900
Notch1	CTRL	P	D	DP	J	JP	JD
	1	0.827985	5.097765	5.463582	3.222605	2.901827	5.611413
	1	1.372175	4.157416	2.959281	1.612713	2.881605	1.325552
	1	1.200000	4.533400	3.654000	1.956500	2.989900	2.122420
Notch3	CTRL	P	D	DP	J	JP	JD
	1	1.479543	7.442936	5.173232	3.363356	3.767041	8.499704
	1	0.745476	4.252344	4.079797	1.682744	1.593767	3.544994
	1	1.287481	4.549479	4.454790	3.199395	4.044616	4.977233
Hey1	CTRL	P	D	DP	J	JP	JD
	1	0.4179036	2.559428	2.559428	2.316375	1.472849	2.660969
	1	1.021746	29.194680	12.583370	2.711983	1.124456	14.205920
	1	0.843009	7.986093	8.350083	2.949282	3.039090	7.055165

original qPCR data of the 3 biological replicates (from top to bottom MABs02-03-05) for Asma, SM22,CALP, Notch1, Notch3, Hey1.

In table 4 are reported the original qPCR data of the 3 biological replicates. The variability of the experiment doesn't allow to establish a statistic significance and therefore more experiments would be needed, however these data shows a clear trend of differentiation towards smooth muscle markers when Dll4 and Jagged1 are involved.

3.5 RNA sequencing unveils pathways involved in HUVECs and MABs crosstalk

We used RNA sequencing to learn more about the transcriptional alterations caused by the above-mentioned phenotypic cross-talk between HUVECs and MABs. Mesangioblasts GFP+ and HUVECs mCherry+ were cultivated separately or combined in 2D (on plastic) and 3D (in matrigel) for 7 days. After 7 days of culture, the coculture samples were sorted for GFP+ and mCherry+ to isolate the endothelium and Mesangioblast populations. As a result, both the cells in single culture and the

cells from the co-culture underwent RNA sequencing, which was conducted by one of our collaborators at the Ansary Stem Cell Institute in the United States and analysed by Camilla Luni (at the ShanghaiTech University, Institute for Advanced Immunochemical Studies). The results of principal component analysis (PCA) revealed that the primary differences within the first principal component were between MABs and HUVECs, as predicted, and that MABs exhibit a distinct transcriptional shift within HUVEC co-culture (second principal component) (Fig. 3.10a). On the contrary, the effect of MABs culture within Matrigel (3D culture system, Fig. 3.10a), produces smaller transcriptional changes.

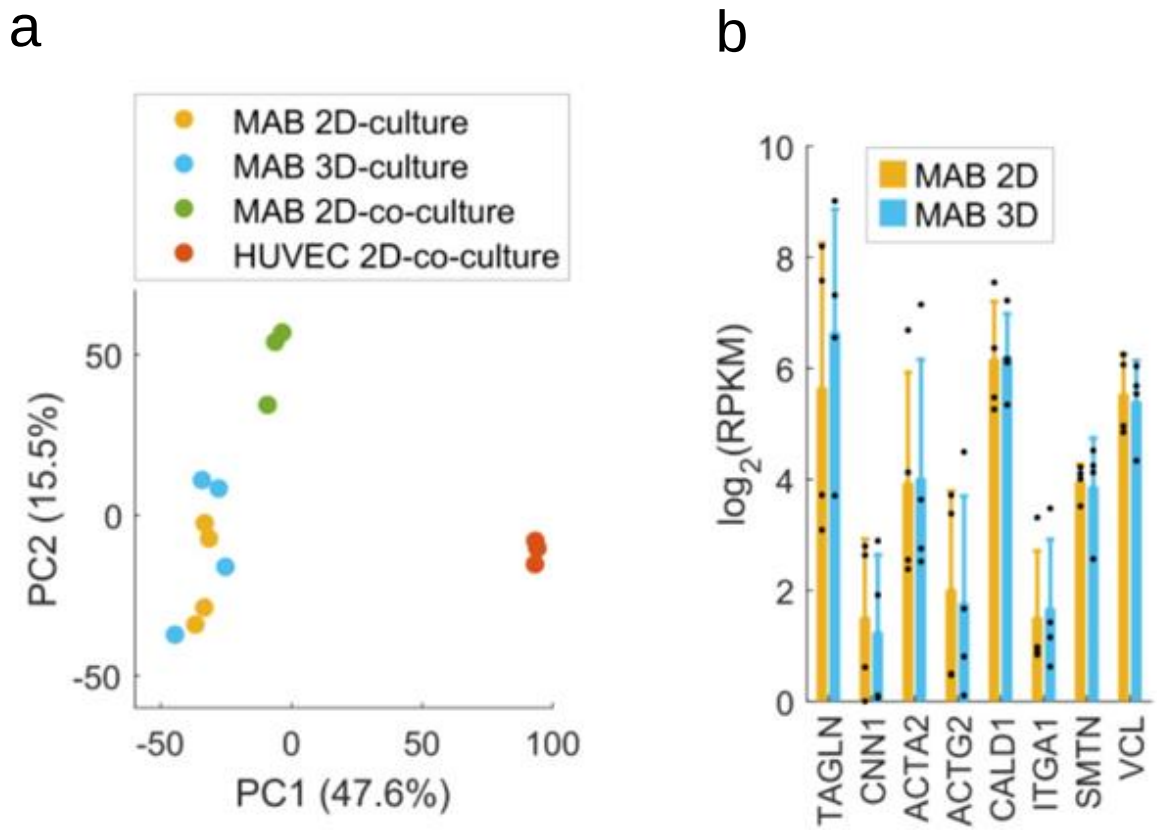

Fig 3.10: Cell sequencing of in vitro co-cultures of MABs and HUVEC. Major transcriptional changes of MABs under 2D and 3D-culture and co-culture with HUVECs highlight their interplay with the extracellular environment. **a.** Principal Component Analysis of MABs cultured alone in 2D or in 3D, and MABs and HUVECs co-cultured in 2D. **b.** Expression of smooth muscle markers in MABs cultured alone in 2D and 3D. Dots: values of single replicates. Error bars: standard deviation (n=4).

We further investigated other distinct molecular differences among MABs in 2D and 3D cultures. Typical smooth muscle markers (Solway et al. 2005) were expressed similarly in the two culture systems (Fig. 3.10b). The main differences were related to genes involved in extra-cellular matrix deposition, including COL11A1 and FBN2 up-regulated in 3D, and degradation, including MMP1 and MMP16 up-regulated in 2D (Fig. 3.11a-b).

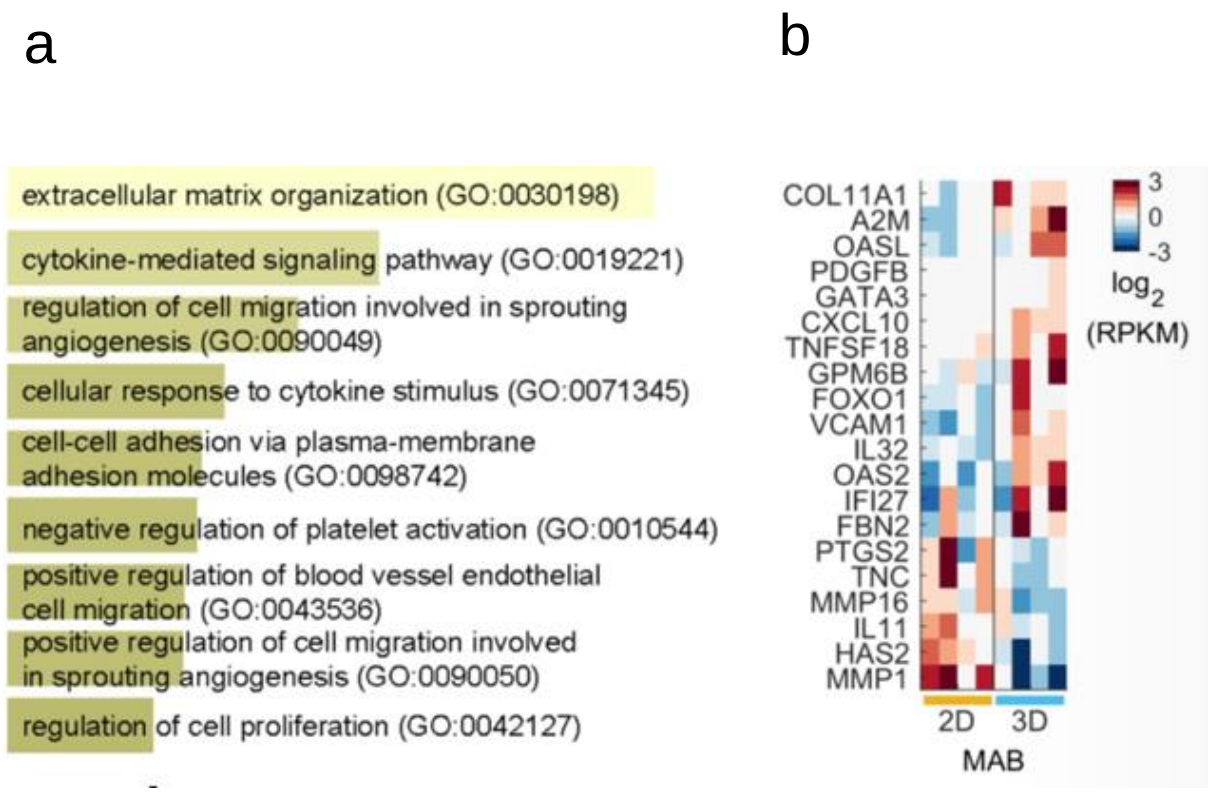

Fig 3.11: Cell sequencing of in vitro co-cultures of MABs and HUVEC shows differences in Extracellular matrix deposition and degradation genes. **a**. Results from the enrichment analysis of MABs DEGs between 2D- and 3D-culture within the Gene Ontology-Biological Process database. Length of bars and lightness of colour represent high statistical significance. All categories with adjusted p-value < 0.05 are shown. Full results are reported in Supplementary Table S1. **b.** Hierarchical clustering of genes from the categories in (3.10a) having an adjusted p-value < 0.01, i.e. the first two categories. Median-centred log2(FPKM) are shown.

To unravel the molecular differences between vascular wall components, we analysed the RNA-seq data of the two cell types, mCherry-labelled HUVECs and GFP-labelled MABs, after co-culture and FACS-sorting. Expression of selected genes shows the distinct separation of the two sub-populations with negligible cross-contamination (Fig. 3.12a). In presence of HUVECs, MABs differentially expressed 350 genes (of these 209 were up regulated in co-culture). Differential expression was most significantly related to platelet degranulation and NOTCH signalling (Fig. 3.12c). Notably, NOTCH1 and NOTCH3 were not differentially expressed, with NOTCH3 expression level almost three-fold higher than NOTCH1 (Fig. 3.12b). MABs activated this pathway in co-culture as demonstrated by higher expression of downstream players (HEY1 and histone deacetylases). Moreover, MABs also significantly up-regulated NOTCH ligand JAG1 in co-culture (Fig. 3.12b). Thus, the cross-talk between HUVECs and MABs is mediated through bidirectional NOTCH signalling.

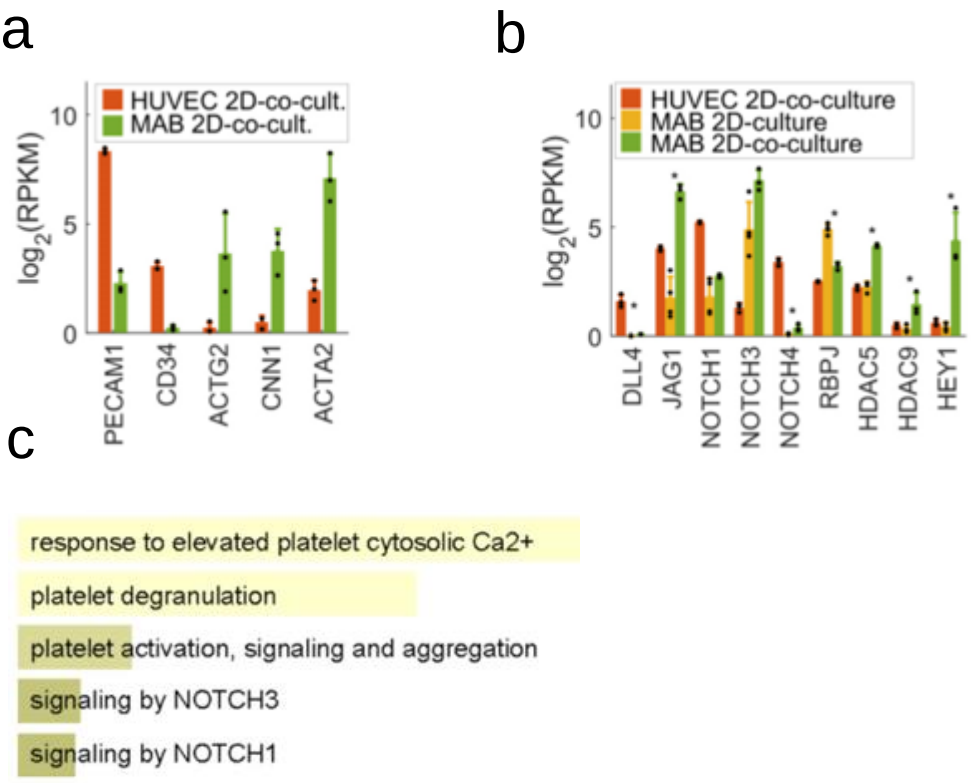

Fig 3.12: Cell sequencing of MABs co-cultured with HUVEC shows MABs upregulation of NOTCH pathway **a**.Expression of endothelial (PECAM1, CD34) and smooth muscle (ACTG2, CNN1, ACTA2) markers in the MABs and HUVECs samples derived from 2D-co-culture experiments. Dots: values of single replicates. Error bars: standard deviation (n=3). **b.** Expression of NOTCH pathway genes in the indicated samples. Dots: values of single replicates. Error bars: standard deviation (n=3 or 4). Asterisks indicate DEGs between MABs cultured alone in 2D and in co-culture. **c.** Results from the enrichment analysis of MABs DEGs between 2D-culture alone and 2D-co-culture with HUVECs within the Reactome Pathways database. Length of bars represent high statistical significance. Most significant categories with adjusted p-value < 0.05 are shown

Then, we conducted a more in-depth investigation to determine the parameters that are modified during cell-cell cross-talk when MABs are cultivated alongside HUVECs. Figure 3.13a shows the differential expression of ligands and receptors expressed in MAB cells when cultivated alone and in co-culture. In Fig. 3.13b, we illustrate how these players are involved in known receptor-ligand interactions and how several of

them are strong candidates for HUVEC-MAB interactions. HUVECs, for example, exhibit numerous receptors for FGF1 and IL1B, ligands that are up-regulated in MABs in co-culture but not expressed by HUVECs. FGF1 has previously been linked to angiogenesis (Beenken et al. 2009; Mori et al. 2013). Given these results are derived from high-throughput data, they await further experimental confirmation, but could represent important reference data for future studies.

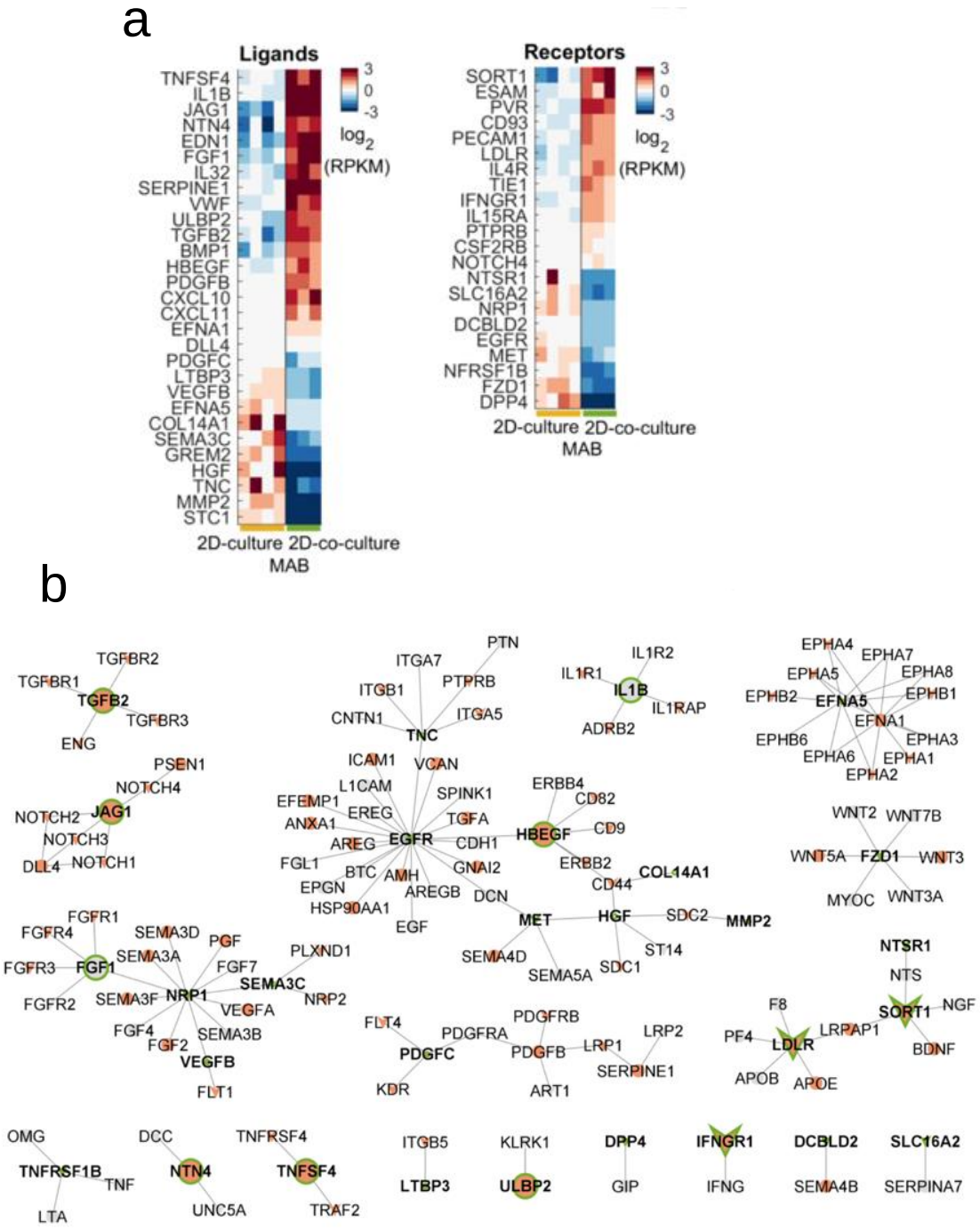

Fig. 3.13: Differential expression of ligands and receptors expressed in MAB cells when cultivated alone and in co-culture. a. Hierarchical clustering of MABs DEGs between 2D-culture alone and 2D-co-culture with HUVECs identified as receptors (left) and ligands (right). **b.** Receptor-ligand interaction network between MABs and HUVECs. V-shaped symbols: receptors; ellipses: ligands. Red-filled symbols: genes expressed by HUVECs. Green-edge symbols with bold label: MABs DEGs between 2D-culture alone and 2D-co-culture with HUVECs; large and small symbols identify DEGs up- and down-regulated in MABs in the co-culture system, respectively. Edges: receptor-ligand interactions (Ramilowski et al. 2015)

3.6. MABs located in a pericyte position supporting vessel-like structure in a Matrigel assay

HUVEC marked w/o mCherry were cultured independently or in co-culture with Mesoangiobasts (MABs) marked w/o GFP in a ratio 5:1 in a growth factor reduced Matrigel coating and EBM2 media implemented with FBS (a basal media for endothelial cells without any growth factor) (Figure 3.14a). Characteristically, MABs located in a pericyte position supporting long-term vessel-like structure formation (Figure 3.14a).

a

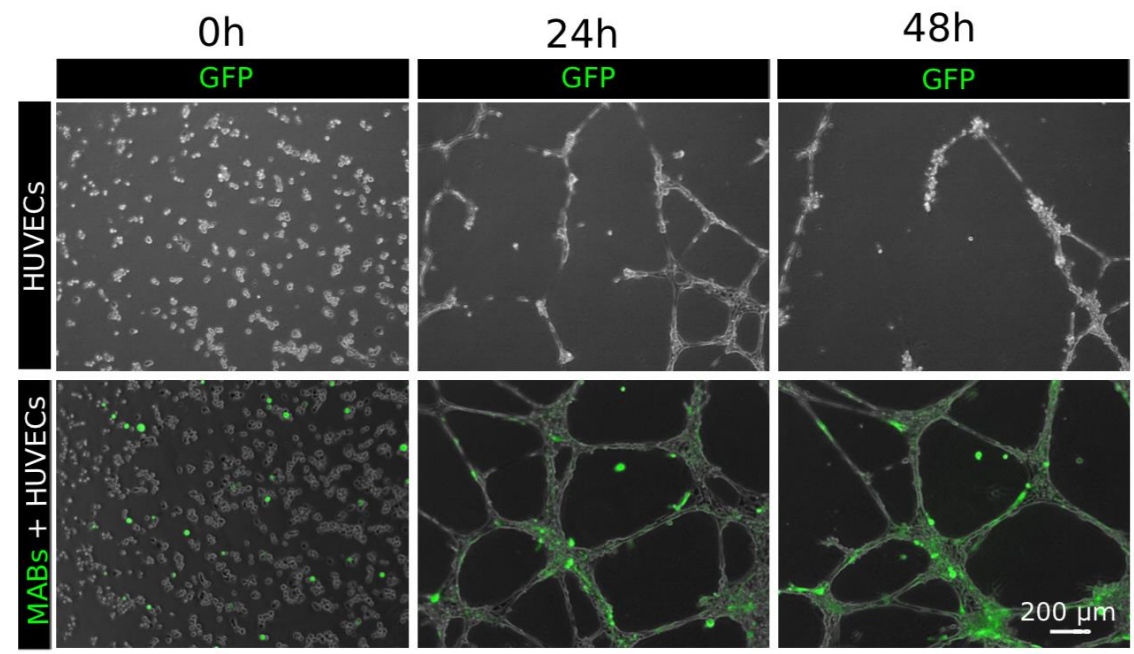

b

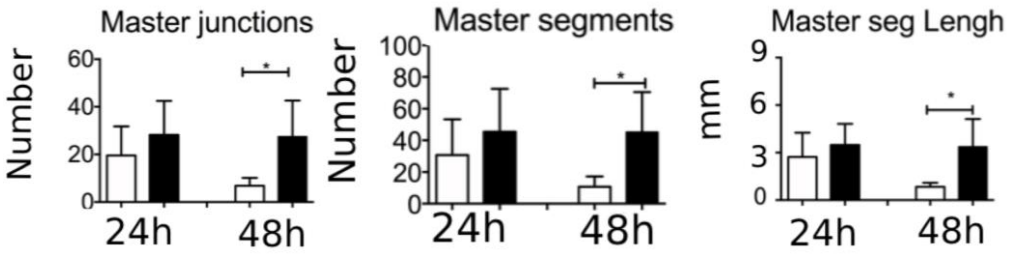

Fig. 3.14: a. Confocal images of MABs (green) and HUVECs in Matrigel cultured together at 1:5 ratio, or independently in a media without growth factor (EBM2). HUVECs branched with MABs positioned in perithelial position supporting angiogenesis. **b**. pictures of 5 field of view of any well and conditions were taken and put through an angiogenesis analyser, a plug in of ImageJ. All the angiogenesis parameters (Master junctions, Master segments, Master segments length) were higher when HUVECs were co-cultured with MABs and became statistically significant at 48h as the HUVECs only web regressed. The figure shows the results obtained with HUVECs and MABs05. Statistic was established with 3 biological replicates of MABS (n=3: 02-03-05); one-way Anova was performed; P value = 0.0142. The other biological replicates (MABs02-03) are shown in the Appendix figure 3.14.

I evaluated the capacity to form tubes, through an angiogenesis analyser (plug-in of ImageJ) and according to different parameters such number of master junctions, number of master segments and the length of different segments (Figure 3.14b). After 24h, the network of HUVECs only started shrinking with a significant cell's death while the network of the HUVEC co-cultured with MABs was maintained with significant differences appearing already after 48h (Figure 3.14). The presence of MABs increased HUVECs durability up to 28 days whilst only debris would appear in the group with only HUVECs (Figure 3.15). In particular, after 7 days, only debris would form in wells where only HUVECs had been cultured. Cells in the wells containing MABs and HUVECs began to organize into spheroid forms, showing still a significant link between these two cell types. Furthermore, MABs would over-proliferate in other parts of the Matrigel, more evidently from day 14 when MABs reach confluency (Fig 3.15). Despite the loss of the geometrical vessel-like organisation characteristic of the culture at 48 hours, the co-culture allowed the cells to survive for another 28 days and the interaction between MABs and HUVECs was maintained. Immunofluorescence imagery using MABs-GFP and HUVECs-mCherry has been included to support this latest statement (Figure 3.16)

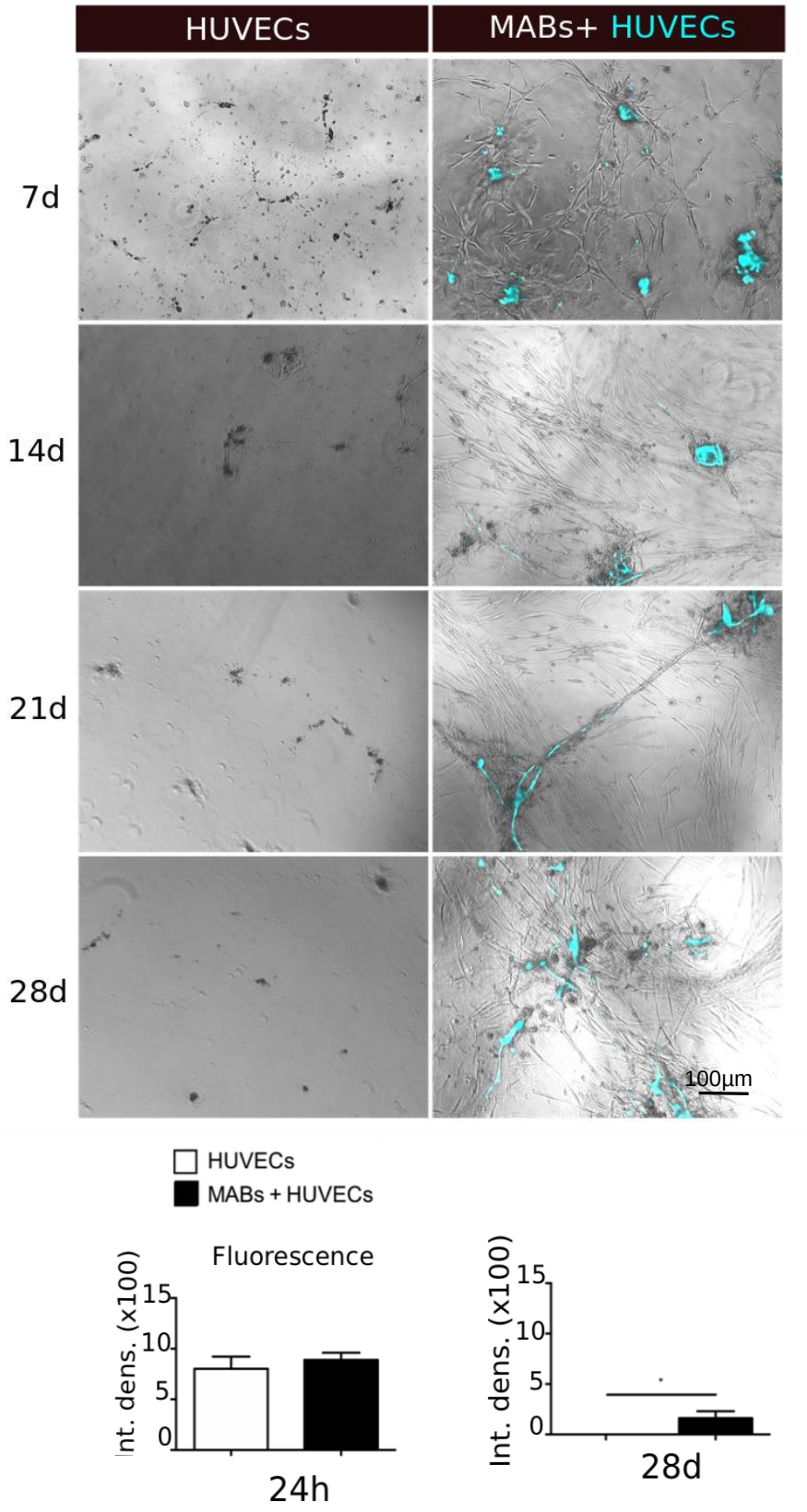

Fig. 3.15: Confocal images of MABs and HUVECs (cyan) in Matrigel cultured together at 1:5 ratio, or independently in a media without growth factor (EBM2) kept for 28 days. HUVECs persisted only in the well with MABs.. The figure shows the results obtained with HUVECs and MABs05. Pictures

of wells in the 2 conditions were taken and put ImageJ to calculate the fluorescence. Experiment was performed with 3 biological replicates of MABS (n=3: 02-03-04). The other biological replicates (MABs02—03) are shown in the Appendix figure 3.15.

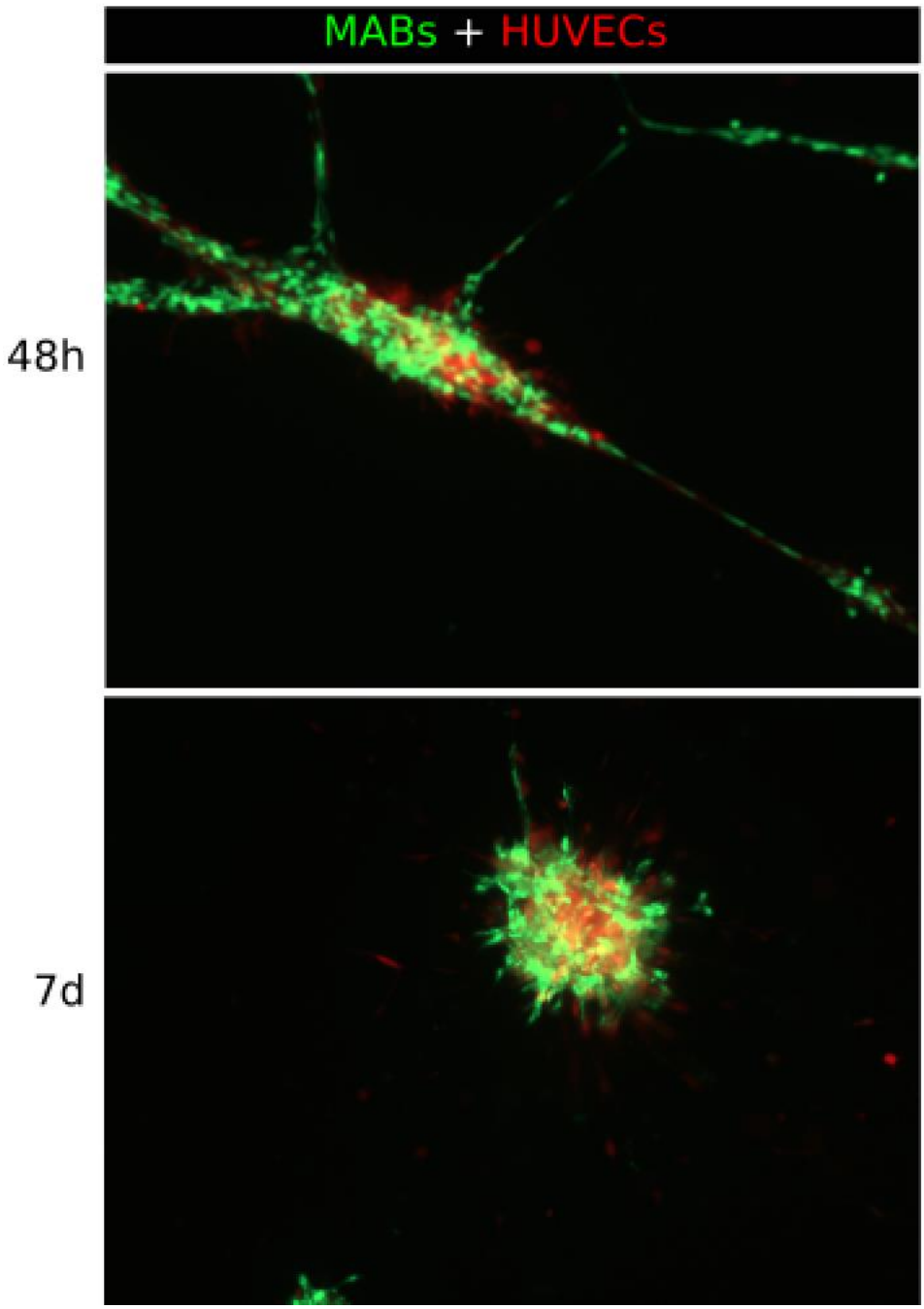

Fig 3.16: Confocal images of MABs GFP (in green) and HUVECSs mCherry (in red) in Matrigel cultured together at 1:5 ratio in a media without growth factor (EBM2) at 48h and 7 days. Images shows the interaction between MABs and HUVECs is maintained even after the loss of canonical vessel like structure organisation at 7 days. The figure shows the results obtained with HUVECs and MABs05. The other biological replicates (MABs02-03) are shown in the Appendix figure 3.16.

3.7. Scan electron microscopy analyses

Scan Electron Microscopy (SEM) of the networks in Matrigel showed endothelial cells and mesoangioblast in their natural disposition and patent lumen were observed. Functional vessels formation was also evident from the presence of tight junctions between HUVECs (Figure 3.17).

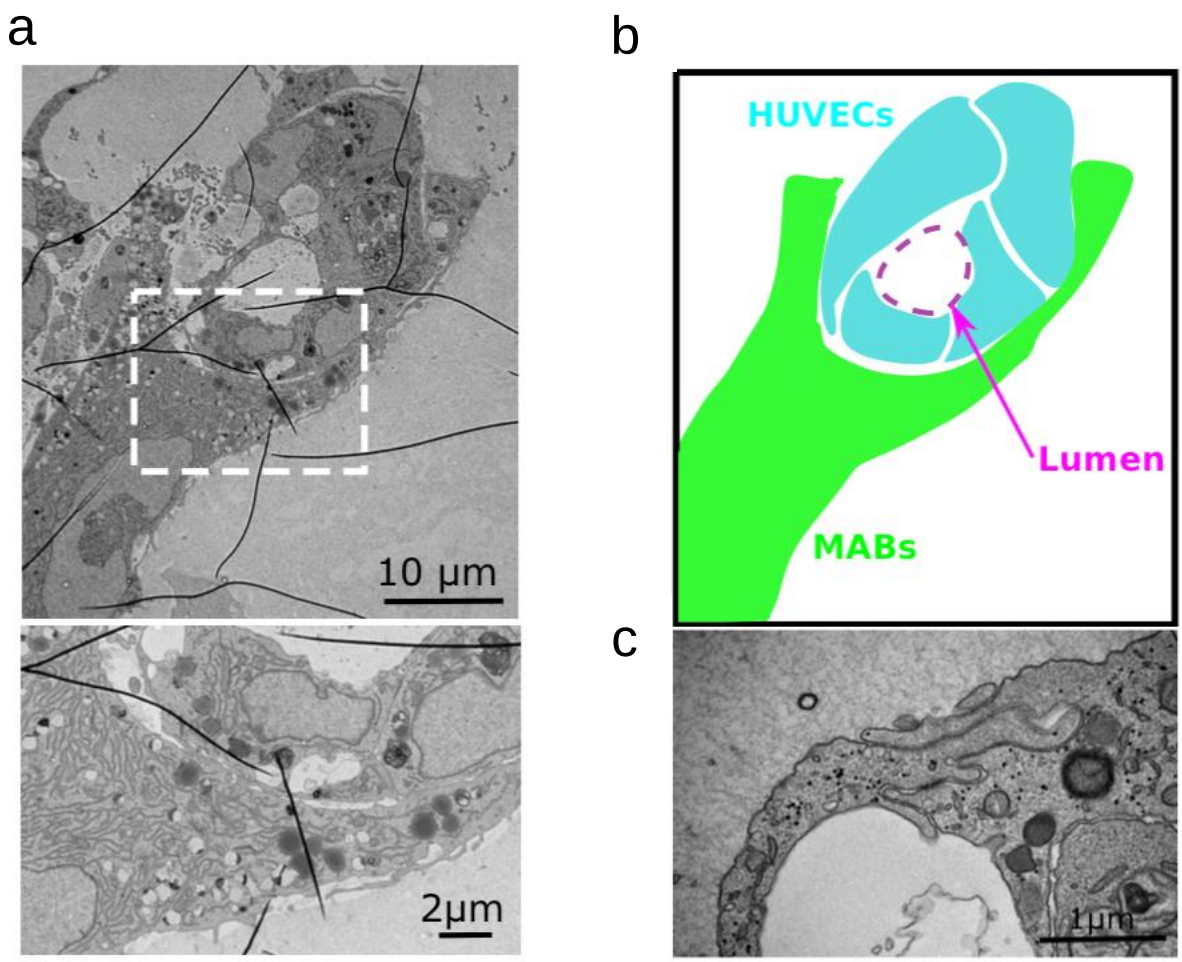

Fig. 3.17: Scan Electron Microscopy image showing HUVECs defining a lumen and MABs05 surrounding them as in their natural disposition. **a**. In the dashed area is highlighted the interaction between MABs and HUVECs which is also the higher magnification picture showed below. **b**. schematic representing the cell disposition in the panel a: HUVECs in cyan colour, MABs in green and dashed magenta line highlighting the lumen. **c**. Scan Electron Microscopy image showing thigh junctions between endothelial cells. Experiment was performed with 3 biological replicates (n=3: 02-04-05).

3.8. Discussion

The utilisation of a dependable and conveniently accessible cell source is a key milestone in tissue engineering. Human Mesoangioblasts (MABs), blood vessel-associated bi-potent mesodermal progenitors (which are considered a subset of pericytes), were proposed in this study. (Minasi et al. 2002; Dellavalle et al. 2011). The name Mesoangioblast come from the fact that embryonically they are isolated from the embryonic murine dorsal aorta and assigned to the perivascular lineage (CD34, Flk-1, SMA and c-Kit expression), however they are also capable to generate in-vivo both vascular and extra vascular mesodermal derivatives. This capability is lost in the adult counterpart: they are only able to generate the extravascular compound losing the endothelial features and therefore are consider pericytes.

Mesoangioblast that can be easily harvested via simple skeletal muscle biopsies, isolated and expanded in GMP conditions using an established SOP, differentiated towards either skeletal muscle or smooth muscle, the latter via TGFβ administration and previously used in a clinical trial (Dellavalle et al. 2007) (Cossu and Biressi 2005) (Tagliafico et al. 2004) (Cossu et al. 2016).

. The capability of MABs to differentiate down to smooth muscle is another important feature of interest to us. In 2017 Urbani and Camilli also exploited their potential to generate smooth muscle for clinical applications. Theirs is the first work to show smooth muscle regeneration using mesoangioblasts and decellularised scaffolds in conjunction with daily TGFβ treatment. All of these factors combine to make MABs an excellent source for replicating the vascular smooth muscle compartment of the macrovasculature.

Human Umbilical Vein Endothelial Cells (HUVECs) have been selected to generate the endothelial compartment in this work.

Prior to attempt at the repopulation of the vascular compound of the preserved vasculature of a decellularised rat intestine I wanted to understand the behaviour of

MABs and HUVECs in co-culture. This work, indeed, aims at elucidating the mechanisms behind which endothelial cells and perivascular cells cross-talk and repopulated the preserved vasculature of a decellularised whole organ. Understanding the process at the base of vascular maturation is crucial to truly reach clinical translation of engineered whole organ.

For co-culture experiments I decided to use EGM2 media (widely used for endothelial expansion), in order to resemble the culture conditions that I would have established into the scaffold. In fact, I wanted to prioritise the endothelial proliferation in this set-up. Moreover, in preliminary analyses I observed that HUVECs die in Megacel (traditional MABs' culture media)

These data show that HUVECs influence the behaviour of MABs triggering them to differentiate down to smooth muscle. After seven days of co-culture of HUVECs and MABs in plastic in EGM2 medium, MABs expressed smooth muscle markers such as SM22 and Calponin. In the negative control in which MABs were cultured independently in EGM2 media, they did not express smooth muscle marker. This allowed us to understand that MABs behave normally in this culture conditions. Moreover, I excluded the possibility that any effect on MABs was due to some component in the media and not the presence of endothelial cells.

Surprisingly, this event occurred in the absence of TGFβ supplementation, which is the conventional route utilised to induce MAB smooth muscle development. (Arianna Dellavalle, Sampaolesi, Tonlorenzi, et al. 2007) (Cossu and Biressi 2005) (Tagliafico et al. 2004). TGFβ may be produced by endothelial cells and guide MABs smooth muscle development even if it is not present in the EGM medium. To test this, I co-cultured HUVECs and MABs in the presence of a TGFβ inhibitor and found that smooth muscle generation was not significantly reduced, but that there were still a large number of differentiated Calponin positive cells.

Cappellari et al. showed in 2013 that combining Dll4 and PDGF-BB converts committed skeletal myoblasts to pericytes while leaving their myogenic memory

intact. My idea, which was inspired by this work, was that NOTCH ligands and PDGF-BB are also involved in the process of MABs smooth muscle development. Dll1 and Dll4, in particular, were considered since they are the two notch ligands found in the endothelium. To prove this hypothesis we knew that one of our collaborators could provide a cell line knock out for jagged 1. Unfortunately there wasn't another cell line also knock out for dll4 and therefore we use the antibody. We are aware that this could be a weakness of this experimental design but it was the best way in our hands to test our hypothesis.

As a result, I co-culture MABs with Jagged1 -/- HUVECs, or HUVECs in the presence of Dll4 antibodies, or a combination of the two. I did not detect a significant decrease in smooth muscle markers when Jagged1 was knocked out, but MAB smooth muscle differentiation was completely inhibited when Dll4 or both ligands were knocked out. However, Dll4 is an important endothelial component and its lack may affect other cellular compounds that lead endothelial cells to lose the capacity to drive MABs smooth muscle differentiation. Therefore, I sectioned the problem by coating Notch ligand Dll4 and jagged1 in the presence or absence of PDGF-BB in tissue culture dishes. Culturing MABs on those coated dishes I mimicked the endothelial Notch signal without taking in account all the other endothelial compounds. qPCR analyses shows a trend by MABs to differentiate towards smooth muscle following Dll4 - Notch 3 axes. The experiment's variability prevents establishing statistical significance, thus further studies are required; nonetheless, these findings reveal a clear tendency of differentiation toward smooth muscle markers when Dll4 and Jagged1 are involved. This was implemented by our sequencing data that showed how the transcriptional profiles of alone-cultured MABs and co-cultured MABs clearly separate and feature several differentially expressed genes.

In this chapter I also want to report a strategy that allows adult primary cells, such as HUVECs, to increase their performance without the need of genetic alterations, in order to promote and facilitate tissue engineering's clinical translation. In particular I

outline how a co-culture approach can improve HUVECs' performances in term of angiogenesis and long-term durability.

Therefore, I cultured HUVEC independently or in co-culture with MABs in a growth factor reduced Matrigel coating and EBM2 media (a basal media for endothelial cells without any growth factor) implemented with FBS. In this set-up HUVECs without the addition of any cues, except for 3D environment of the Matrigel, started forming an interconnected web of tubing that resemble the microvasculature. In normal conditions those vessels like structure would start regressing after 24 hours till when they would completely disappear after 4-5 days.

In the co-culture MABs disposed themselves in a perivascular location supporting the vessel like structure and keeping them in culture for a longer time point up to 28 days. SEM studies indicated an even stronger similarity between those structures and blood vessels. In fact, endothelial cells forming a patent lumen and MABs around them could be seen as in their natural environment. Other endothelial characteristics such as tight connections between endothelial cells and endothelial cells, as well as MABs, were also identified.

Surprisingly, each angiogenic parameter had a greater value in the co-culture at 24h, a difference that became statistically significant at 48h when the HUVECs network collapsed instead. The stabilizing effect of mesenchymal cells on HUVECs is not a concept completely novel. In reality, HUVECs and mesenchymal cells were implanted into mice in 2004 after being embedded in a three-dimensional fibronectin-type 1 collagen gel. HUVECs were able to construct tubes that linked to the host vasculature in this experiment and stayed patent for up to a year. (Koike et al., 2004).

However, whole organ tissue engineering often require long period of culture into the bioreactor and therefore is important to make sure that vessel like structures can be maintained for long time points also in *in vitro.* Surprisingly the co-culture system was able to elongate endothelial durability for up to 28 days which was never reported in previous reports.

How the implementation of this co-culture approach into organ vasculature engineering will allow the generation of an organised, patent and functional vascular tree will be treated in the next chapters.

Chapter 4

Co-injection of HUVECs and MABs results in a functional endothelial coverage into the preserved vasculature of an intestinal scaffold

4.1. Introduction

Understanding the regeneration processes that occur into the preserved vasculature of a decellularised whole organ is crucial to truly reach clinical translation of engineered whole organ since the lack of a functional vasculature is the main limitation that separate tissue engineering from clinic.

No much is known about the mechanisms and conditions that enable endothelial cells and perivascular cells to crosstalk and repopulated the preserved vasculature of a decellularised whole organ.

Moreover, the field display remarkable confusion in term of how to achieve this aim.

In fact, although many basic science works suggest that the perivascular compartment is important for vascular regeneration, homeostasis and functionality, (Koike et al., 2004 Bergers and Song, 2005; von Tell et al., 2006), still many works attempted organ revascularisation without taking in account the this compound in lung (Baptista et al., 2011; Shirakigawa et al., 2013; Takebe et al., 2014; Bao et al., 2015; Verstegen et al., 2017), kidney (Song et al. 2013, Du et al. 2016). and intestine (Kitano et al. 2017.).

Therefore, still not a consistent and homogenous strategy of organ vascularisation has been established in the field.

This chapter aims to elucidate the conditions for obtaining a patent, functional and long-lasting endothelium in a rat decellularised intestine.

4.2. Manufacture of the decellularised intestinal scaffold

Decellularised intestinal scaffolds were produced adapting the protocol already reported by Totonelli 2012. Upon harvesting (by Aslan Gjinovci) from 200-300gr Sprague Dawley male rats, a fragment of intestine was cannulated through the mesenteric artery and vein and then connected to a peristaltic pump for perfusion of

DET solutions through the lumen and the cannulated vasculature. A complete intestinal decellularization was obtained after 1 cycle of DET, as previously by Totonelli 2012 and 32hs treatments were sufficient to generate a translucent and white-pale acellular matrix preserving the original size and morphology.

The successful outcome of the decellularization process was assessed by DAPI Staining, H&E and DNA quantification (Figure 4.1a-c). Presence of the main collagens of the matrix were assessed with different histology. Picro-sirius red staining, show maintenance of collagen fibres after the decellularization process. Alcian blue staining shows the evident reduction of the Gags content on the matrix as the quantification confirms. The Verhoeff–Van Gieson staining proves that the content of elastine is maintained. Furthermore, the Masson`s trichrome confirms the maintenance of collagen and other fibres amount and morphology while the cellular component is not visible in any scaffold pictures. (Fig.4.1 d). The maintenance of the principal component of the ECM was confirmed by Immunohistochemistry. In particular collagen I, collagen IV, fibronectin and laminin were conserved along the scaffold after the decellularization, maintaining the matrix characteristic outline. (Figure 4.1d, e).

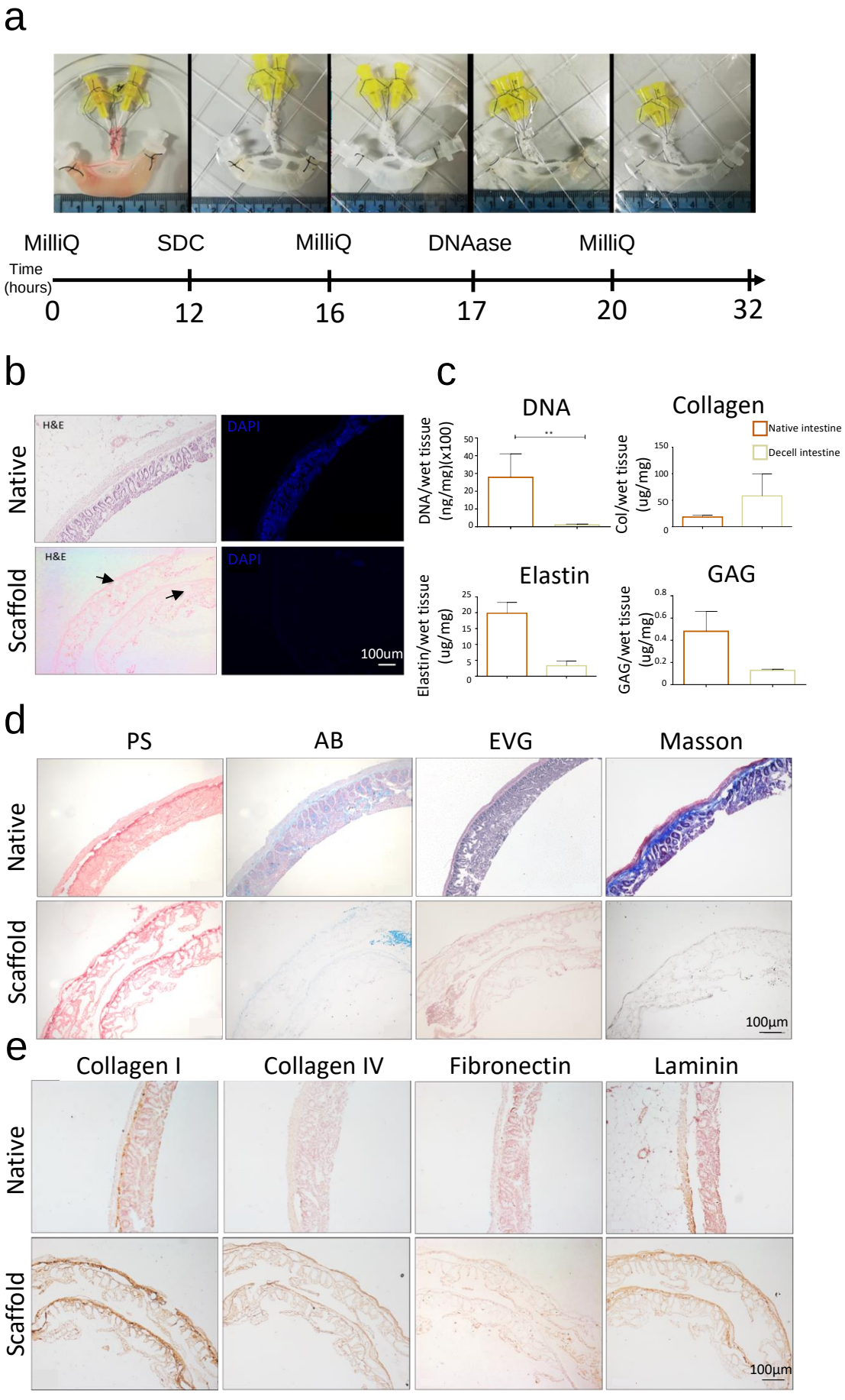
a
MilliQ
SDC
MilliQ
DNAase
MilliQ
Time (hours)
0
12
16
17
20
32
b
Native
Scaffold
H&E
DAPI
100um
c
DNA
DNA/wet tissue (ng/mg)(x100)
Collagen
Col/wet tissue (ug/mg)
Native intestine
Decell intestine
Elastin
Elastin/wet tissue (ug/mg)
GAG
GAG/wet tissue (ug/mg)
d
PS
AB
EVG
Masson
Native
Scaffold
100µm
e
Collagen I
Collagen IV
Fibronectin
Laminin
Native
Scaffold
100µm

Fig 4.1. Decellularization characterization: a. Schematic showing the decellularization process (adapted from Totonelli 2012) and the macroscopic look of the intestines at any step of the procedure. **b**. Images of Haematoxylin and Eosin (H&E) and DAPI staining of section of intestines before and after decellularization show the complete removal of the cellular compartment and maintenance of the vascular compound (as indicated by the arrows). **c**. DNA quantification of the intestine before and after decellularization show reduction of the genetic component to 80 ng DNA/mg. Collagen, elastin and GAG quantifications show permanence of this components in the Extracellular Matrix (ECM) of the intestines after decellularization. **d.** from left to right, Picro-sirius red staining, Alcian blue staining, Verhoeff–Van Gieson, Masson`s trichrome, show respectively maintenance of the collagen component, reduction of GAG content, maintenance of elastin, maintenance of collagen and other fibres amount and morphology. **e.** from left to right, images of immune histochemistry of collagen I, collagen IV, fibronectin and laminin, show that those components were conserved after the decellularization. Decellularization analyses were performed with 3 biological replicates (intestines coming from 3 different rats; n=3); Mann-Whitney tests was performed. GAG's P value= 0.0238; DNA's P value= 0.0079; Collagen's P value= 0.1.

4.3. Seeding into the preserved vasculature of a decellularised intestinal scaffold

To assess the cell capacity to repopulate the decellularised vascular network of the intestine, a suspension of media and cells were seeded into the preserved vasculature of the acellular scaffold. I wanted to understand also whether a co-culture approach was more beneficial of seeding only HUVECs, and if I were able to resemble the results obtained *in vitro* in the Matrigel essay described in the previous chapter. Therefore, the suspensions of media and cells were containing either only HUVECs or MABs and HUVECs in a ratio 1:5 and they were seeded into the mesenteric artery and vein of the acellular scaffold (Figure 4.2). Stereomicroscope images taken immediately after the seeding showed GFP+ cells distributing evenly into the preserved vasculature of the acellular intestine (Figure 4.2b).

a

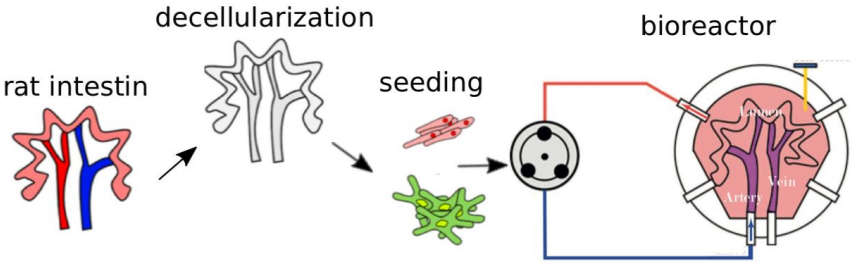
decellularization
bioreactor
rat intestin
seeding

b

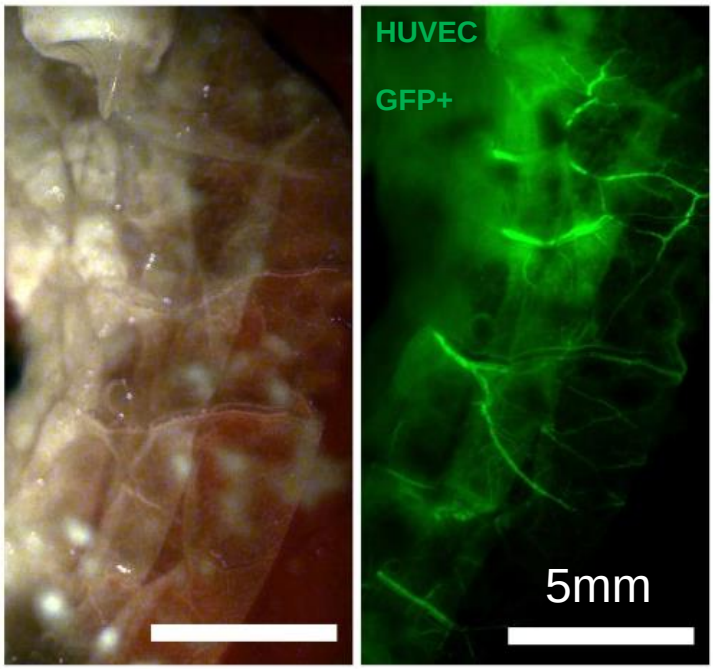
HUVEC
GFP+
5mm

c

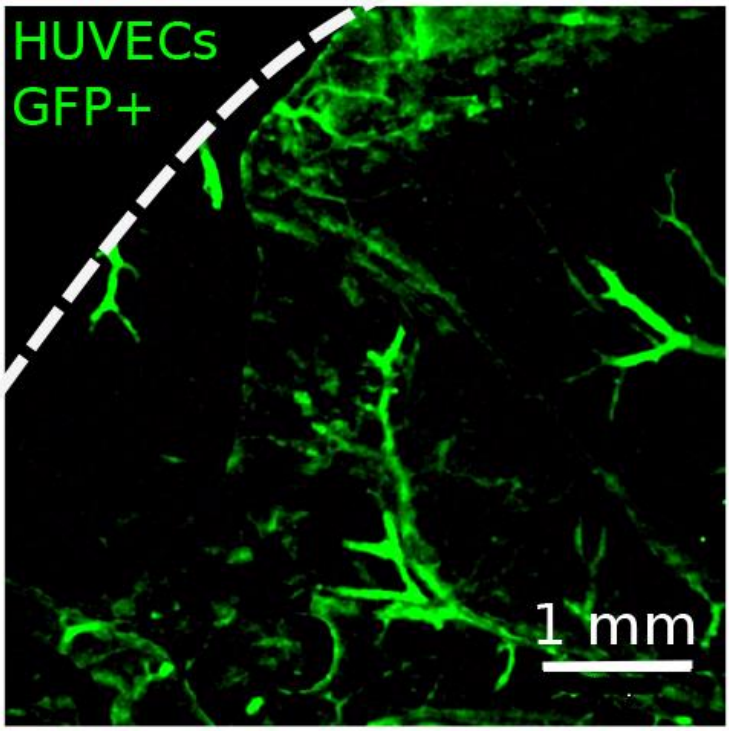
HUVECs
GFP+
1 mm

Fig. 4.2. Schematic showing the phases of the experiments into the scaffold from the harvest to the seeding of MABs and HUVECs into the preserved vasculature of the decellularised rat intestine. **a.** The bioreactor set up consist in a pump retrieving media form the filled chamber of the bioreactor and flowing it into the artery. This dynamic culture initiated 24 hours after the seeding and terminated after 7 days of forward perfusion through the mesenteric artery. **b-c.** Immediately after seeding from the mesenteric artery and vein, stereomicroscope images in fluorescence were taken. The left panel of figure b shows the bright field of the decellularised rat intestinal wall and in the right panel is the stereomicroscope image in fluorescence of the same region of the scaffold. The scaffold shows to be perfused by a suspension of media and cells (HUVECs GFP+) reaching the distal vasculature in the intestinal wall, as seen in these photos.

After the seeding, intestines were mounted on the chamber of a custom-made bioreactor (designed and manufactured by Alessandro Pellegata and Simone Russo) and the cannula of the artery was connected to a pump system that would retriever the media from the chamber itself and make it flow through the artery. After 7 days of dynamic culture into the bioreactor, intestines were retrieved and immunostaining for PDGFRβ and CD31 was performed to detect the presence of MABs and HUVECs into the scaffold (Figure 4.3 a). The endothelial coverage was calculated as number of black pixels over number of total pixels of the CD31 channel and normalised to the CD31 channel of the native tissue (Figure 4.3 a-b).

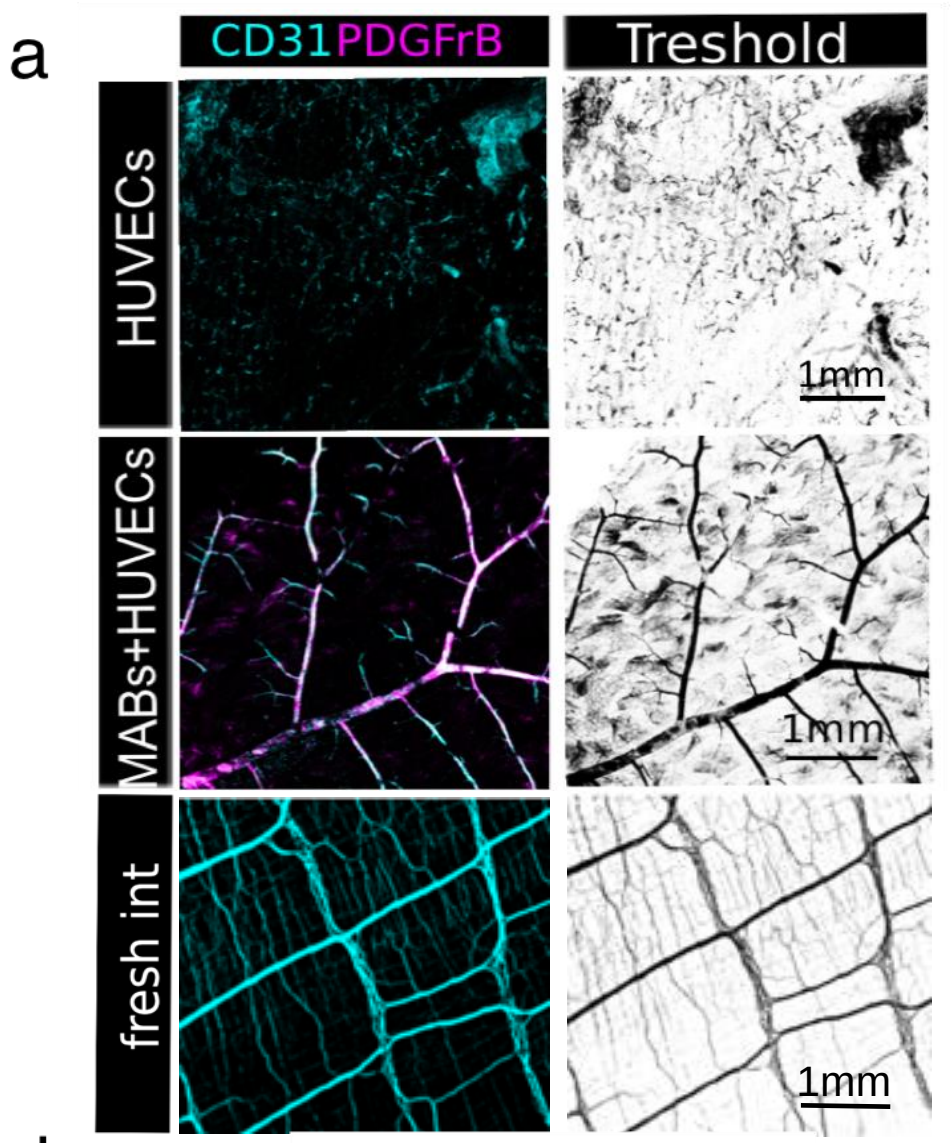
a
CD31PDGFrB
Treshold
HUVECs
MABs+HUVECs
fresh int
1mm
1mm
1mm

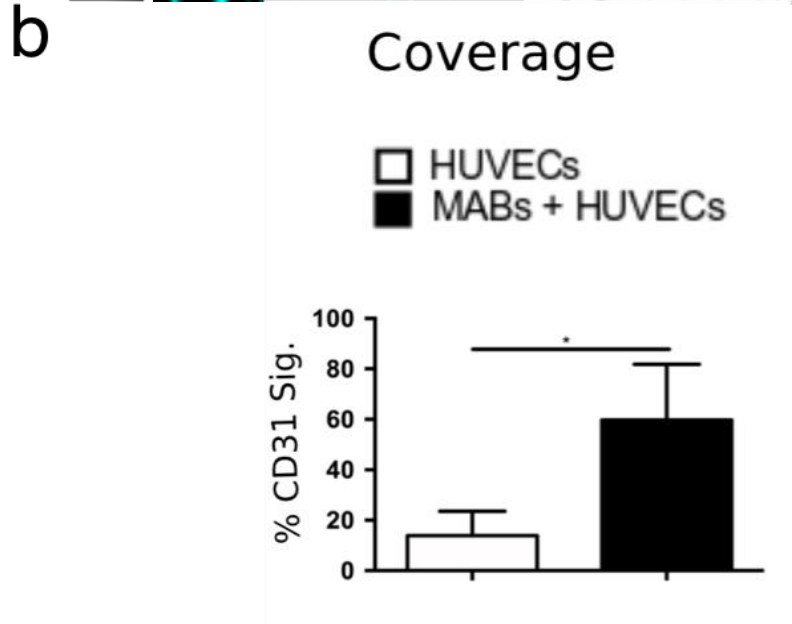
b
Coverage
HUVECs
MABs + HUVECs
% CD31 Sig.
100
80
60
40
20
0
*

Fig. 4.3 Endothelial coverage into the preserved vasculature of a decellularised rat intestine. a. whole mount staining for PDGFRβ and CD31 (staining respectively MABS and HUVECs) were performed on scaffold co-seeded with HUVECs only (top panels) or HUVECs and MABs (bottom panels), and they were imaged through confocal microscope. The images are representative of 4 mm^2 of scaffold (tile scan 5 field of view times 5 at 20x magnification). Those imaged were thresholded through ImageJ in the same way to calculate the coverage **b.** once the images where thresholded, the coverage was calculated as number of black pixels over number of total pixels and normalised to the value obtained from the native tissue). HUVECs showed to perform better when MABs were present in the scaffold and reached around 75% of vascular coverage. The representative pictures of the co-seeding in the figure were performed with MABs05 but experiment was performed with 4 MABs biopsies (n=4; MABs02-03-04-05). Representative pictures of the other biopsies are shown in the appendix figure 4.3. For the quantification of the coverage unpaired T test with equal SD was performed. P value= 0.0213.

Similarly to what observed in 2D and 3D culture, when HUVECs and MABs were injected together, they achieved a better coverage into the scaffold after 7 days of dynamic culture, whilst HUVECs injected alone appeared scattered into the scaffold, could not organise themselves to replace the decellularised vascular structure and were mostly unable to survive after injection (as confirmed by the strong presence of Cleavage Caspase3 in the scaffold with only HUVECs, (Figure 4.4).

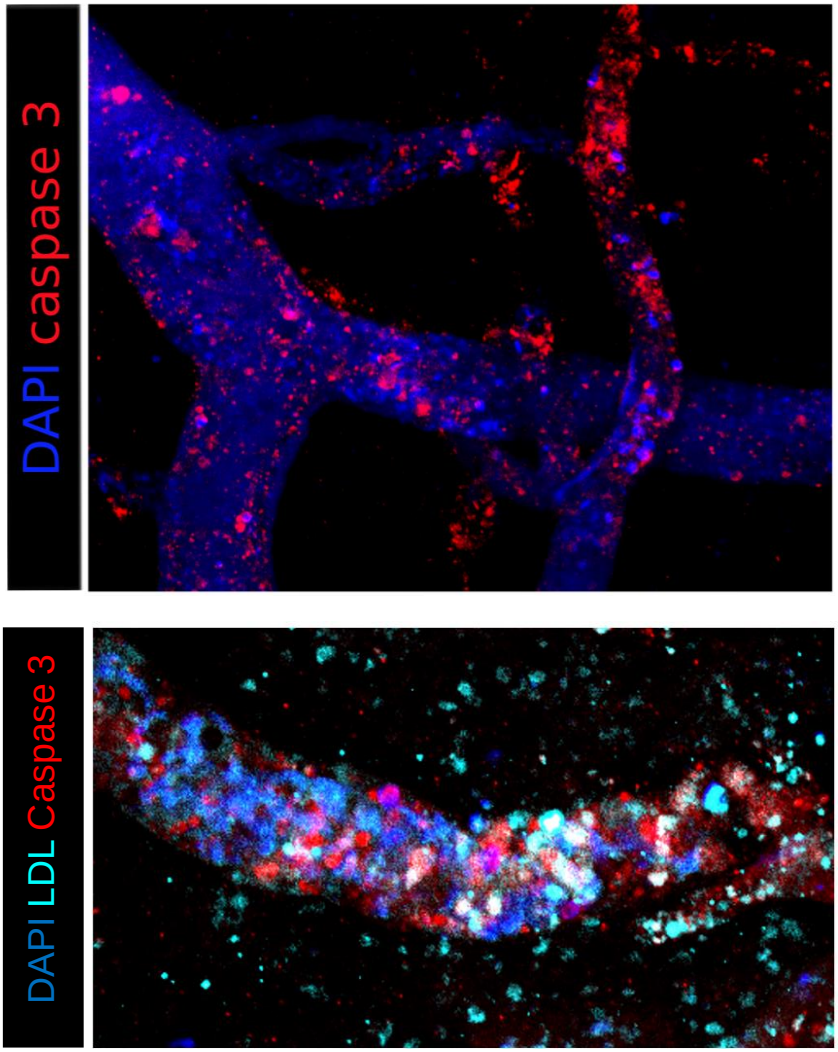

Fig.4.4: whole mount Cleavage Caspase 3 staining on scaffold seeded with only HUVECs. Representative confocal image of a scaffold seeded with only HUVECs showing strong presence of Cleavage Caspase 3 (in red), indicating high cell death. In the bottom panel is a confocal image of another region of the scaffold after incubation of LDL and allowed its intake from Endothelial cells (in cyan) and Caspase 3 staining in red.

4.4. Assessment of vessel patency after re-endothelialisation

In order to assess the patency of the newly formed vasculature I took advantages of the capacity of endothelial cells to uptake LDL. Therefore, I used a fluorescently labelled LDL and I injected it through the mesenteric artery and vein of the re-populated vasculature. Endothelial cells that had been in contact with the solution

would uptake ldl and it would result in a fluorescent signal after washing out the solution. Since this would occur only if the ldl passed through the lumen of the endothelium, this is an excellent way to assess how much of the repopulated endothelium is actually perfused. Importantly, vessels injected with HUVECs and MABs were patent, as demonstrated by assessing fluorescent labelled LDL uptake after 7 days of dynamic. Orthogonal projection of Z-stack images allowed us to delineate the patent lumen with inner layer of LDL+ endothelial cells surrounded by PDGFRβ+ pericytes (Fig. 4.5).

At low magnification, I could assess the degree of perfusion of vasculature using the same strategy used for quantifying endothelial coverage showing that the scaffolds seeded with both HUVECs and MABs were perfusable at the 60% (close to 100% of the repopulated area) (Fig. 4.5 b-c). Scaffold seeded with HUVECs only were not able to perform in the same way (Fig. 4.5 b-c).

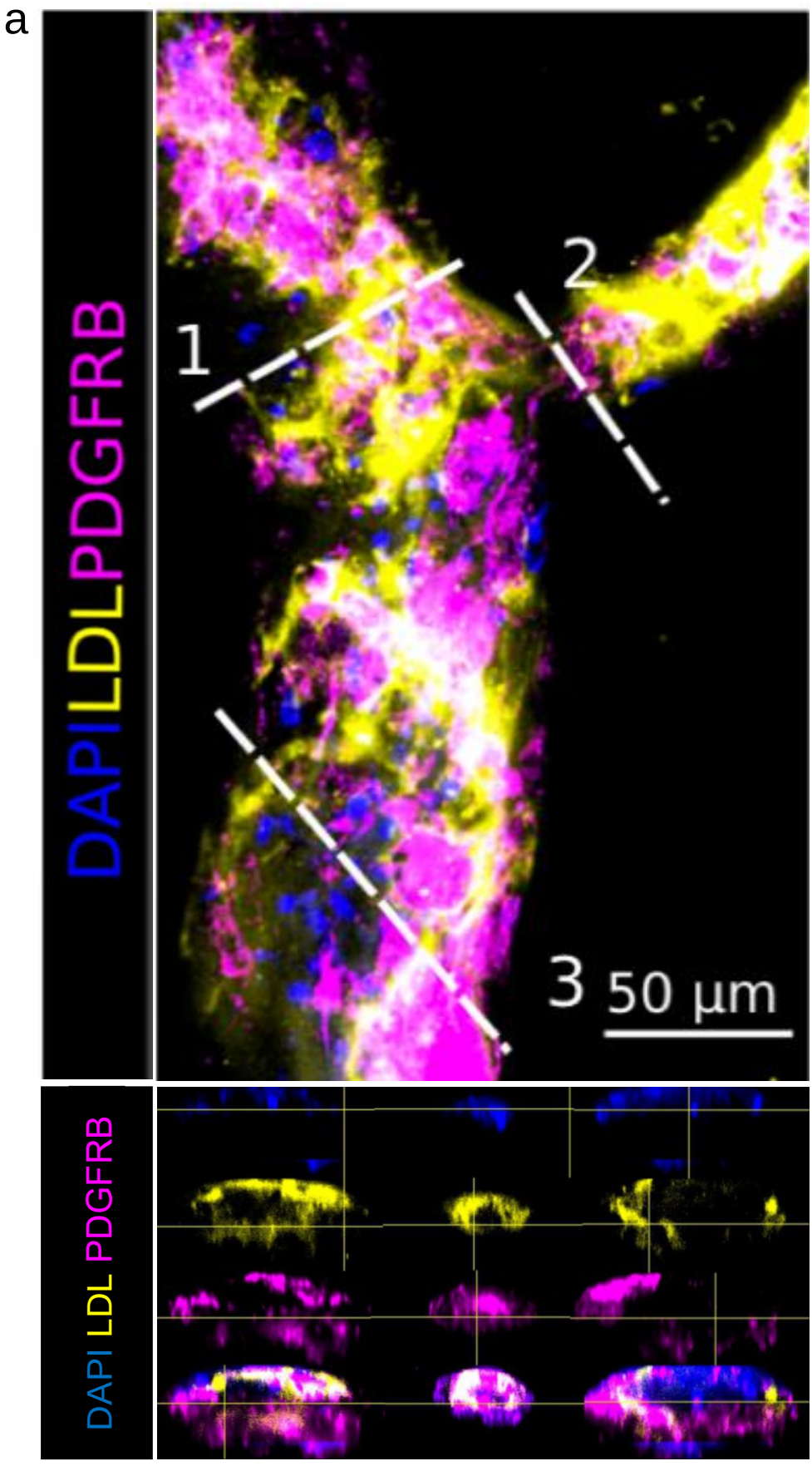
a
DAPI LDL PDGFRB
1
2
3
50 µm
DAPI LDL PDGFRB

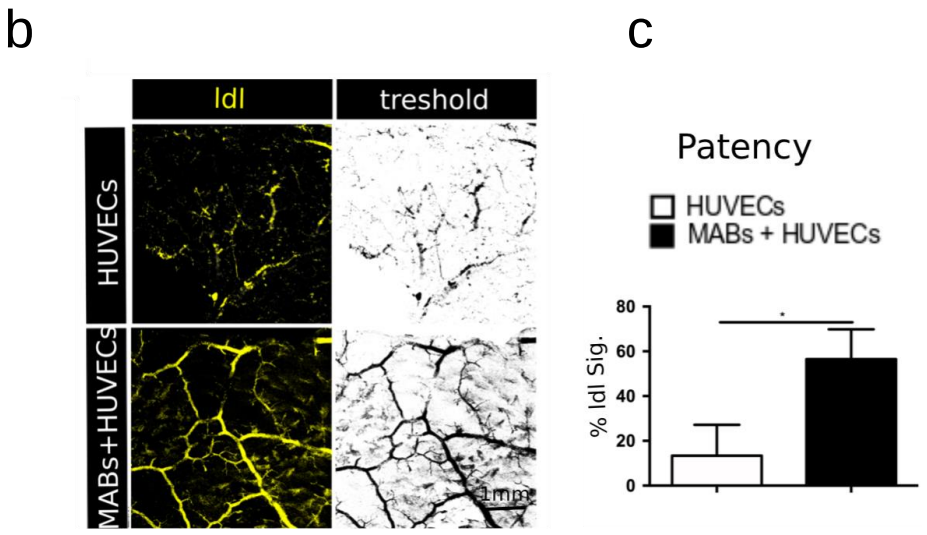

Fig.4.5: Assessment of the vessel patency after re-vascularization. a. injection of labelled LDL through the mesenteric artery and vein of the re-populated vasculature reveals presence of endothelial cells (yellow, since they have uptaken the fluorescent LDL), and the areas of the scaffold that are perfused. Presence of MABs05 was assessed though PDGFRβ staining (magenta). Orthogonal views of the dashed areas of the z-stak confocal images shows the vasculature featuring a patent lumen with endothelial cells lying the vessel and Pericytes surrounding it. In the bottom panels of figure 5a are displayed the individual channels of the 3 lumen dashed above.). Representative pictures of the other biopsies are shown in the appendix figure 4.5a **b.** confocal images representative of 4 mm^2 of scaffold (tile scan 5 field of view times 5 at 20x magnification). Those imaged were thresholded through ImageJ in the same way as I previously described for the endothelial coverage. **c.** Once the images where thresholded, the patent area was calculated as number of black pixels over number of total pixels and normalised to the value obtained from the fresh intestine cd31 signal (in fig 4.3 a).

The representative pictures of the co-seeding in the figure were performed with MABs05 but experiment were performed with 3 biological replicates (n=4; MABs02-03-05). Representative pictures of the other biopsies are shown in the appendix figure 4.5b. For the patency an unpaired T test with equal SD was performed. P value= 0.0087.

4.5. Permeability of the newly formed vasculature

One of the most important function of the endothelium is to promote the formation of a barrier. I investigated whether the decellularised scaffold had the capacity to restrain small-weight molecules such as a solution of

fluorescent dextran delivered inside the vascular compartment. After gravimetric perfusion through the vascular tree, the fluorescent solution was collected inside the intestinal lumen and fluorescence was measured indicating the amount of dextran passed from the vasculature to the lumen (Figure 4.6).

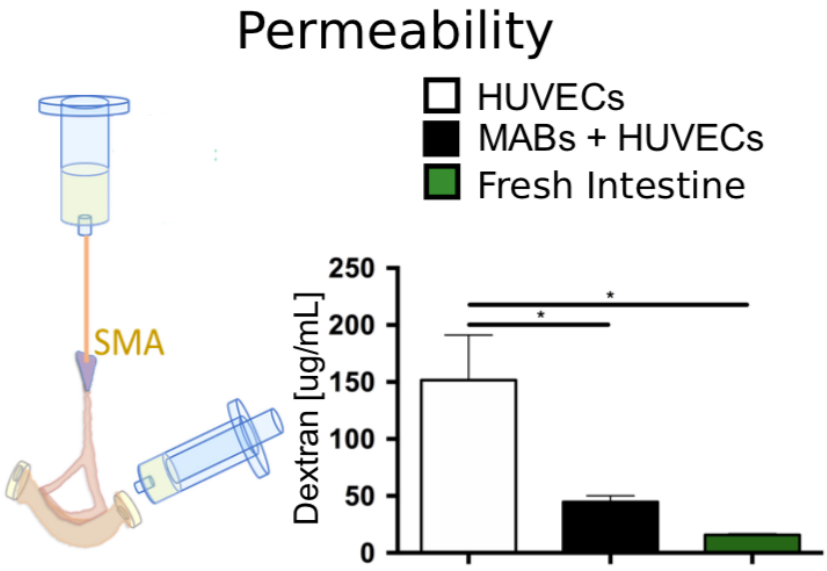

Fig.4.6: Vascular permeability. gravimetric perfusion through the superior mesenteric artery (SMA) of a fluorescent solution of dextran. The solution retrieved inside the intestinal lumen was used to measure its fluorescence and have an estimation of the amount of dextran passed from the vasculature to the lumen. Quantifications shows that scaffolds co-seeded with MABs and HUVECs display a degree of permeability like freshly isolated intestines and they significantly perform better of the scaffold seeded with only HUVECs. For this experiment 3 biopsies of MABs were used (n=3: MABs02-03-05). One way Anova was performed. P value= 0.0008

My data revealed that the leakage of dextran in the intestinal lumen is significant lower in the scaffold receiving both HUVEC and MAB when compared to the scaffold seeded with HUVECs alone. Moreover, scaffold repopulated with MABs and HUVECs retain small molecules similarly to the intestine freshly isolated (Figure 4.6).

4.6. Discussion

Recent efforts used endothelial cells and supporting cells to engineer organs' vasculature. Ott's team released a pioneering research in 2015 that introduced this idea and seeding across both arterial and venous channels in a rat decellularised lung. (Ren et al. 2015). With this strategy, they reported a 75% endothelial coverage leading to a good barrier function. The characterization of repopulated scaffolds in this work was limited to assessing the presence of cells and barrier functions, but little was reported about the mechanisms that lie between endothelial and perivascular cells in organ re-endothelialisation: whether perivascular cells had a beneficial effect on re-endothelialisation in this context was not elucidated. Nevertheless, still many works attempted organ revascularisation without taking in account the perivascular compound.

Ott's laboratory itself published two later studies in the lung to prove scalability to human size decellularizing pig and human lungs and using epithelial and endothelial cells. In those occasions the perivascular compartment was not taken in account (Gilpin et al., 2016; Zhou et al., 2017). Seeding HUVECs only was the main re-vascularisation strategy used also in many works in the liver (Baptista et al., 2011; Shirakigawa et al., 2013; Takebe et al., 2014; Bao et al., 2015; Verstegen et al., 2017), kidney (Song et al. 2013, Du et al. 2016). and intestine (Kitano et al. 2017.).

The latter paper is a work published by Ott's laboratory where decellularised segment of rat intestine were repopulated with iPSC-derived epithelial cells for 14 days and HUVECs for 3 days (Kitano et al. 2017). Even though this is a study published after the one published in lung in 2015, they did not account for the perivascular compound, and additional imitations of this work will be reviewed later in this paragraph. The number of publications published following Ren et al. 2015 that address entire organ re-vascularization without the participation of a perivascular cell source reflects the

field's uncertainty and lack of understanding of how the perivascular compound is critical to regenerate an organ vasculature.

The first intent of this PhD thesis is clarifying this issue and our outcomes remarkably encourage the use of a co-culture approach to address organ re-vascularization.

In fact, the goal of this study is to repopulate and evaluate the vasculature of a rat gut. As a result, I investigated if the findings obtained in plastic were equally applicable to the preserved vasculature of a decellularised rat gut.

I developed a seeding method that allowed cells to distribute evenly throughout the scaffold. Moreover, my data shows that by co-seeding MABs and HUVECs is possible to achieve a better coverage compared with the seeding of HUVECs only. HUVECs, when they were seeded without the support MABs, appeared scattered in the scaffold and they displayed remarkable cells death after 7 days of dynamic culture onto the bioreactor. On the contrary the presence of MABs allow the system to outperform the previous strategy. The co-culture allowed the endothelium to be stable after 7 days of dynamic culture and that resulted in a better endothelial coverage. This was consistent with the results in Matrigel.

The strategy used to quantify the endothelial coverage is an improvement compared to the strategy used in previous report. Ren et al., for example, reported a 75 percent endothelial coverage on repopulated lung slices by assessing the coverage of the CD31 signal over the Collagen IV (a vasculature specific collagen) signal. This is an excellent approach to assess how much of the decellularised vascular scaffold is repopulated by CD31 endothelial cells, but it does not provide an understanding of the conditions across the whole scaffold because the experiment was done on slices. The endothelial coverage in this work was performed on whole mount staining by thresholding the CD31 signal and it was calculated as the number of black pixels over number of total pixels of the CD31 channel, and normalised to the CD31 channel of the native tissue.

This give us a more precise way to calculate the coverage throughout the whole scaffold ruling out the possibility to make overestimations.

One of the main hurdles of the vascular tissue engineering is the possibility of recreating a lumenalised endothelium. These data show that seeding HUVECs and MABs into the preserved vasculature of a decellularised intestine resulted in HUVECs lining the vessels while MABs surrounded them and disposed themselves in a typical perivascular position. The vasculature was also patent in many areas of the scaffold. However, perfusability of the scaffold requires a quantitative analysis since it must be guaranteed throughout the whole scaffold. In a previous report, Kitano et al. addressed this issue by injecting a fluorescently labelled solution of dextran to identify the area of the scaffold that would be perfuse by it. (Kitano et al. 2017).

In the contest of vascular regeneration of decellularised organs this cannot be a good approach. The rational of using decellularised organ is indeed that they maintain their physiological architecture including the vasculature. The preserved vasculature of decellularised organ is fully patent and it represent a free path for seeding cells.

As a result, injecting fluorescent dextran on a sparsely repopulated scaffold, such as one seeded exclusively with HUVECs (as utilised by Kitano et al 2017), would result in a high degree of perfusion. The field must employ a technique that allows us to determine how much of the vasculature is repopulated and perfused.

In order to do so I took advantages of the capacity of endothelial cells to uptake LDL. Therefore, I used a fluorescently labelled LDL and I injected it through the mesenteric artery and vein of the re-populated vasculature. Endothelial cells that had been in contact with the solution would uptake LDL and it would result in a fluorescent signal after washing out the solution. Because this would only happen if the ldl went through the endothelium's lumen, it's a great technique to see how much of the repopulated endothelium is truly perfused.

Finally, one of the most important function of the endothelium is to promote the formation of a barrier. Scaffold repopulated with MABs and HUVECs retained small

molecules similarly to the intestine freshly isolated and therefore were able to outperform scaffold seeded only with HUVECs.

Finally, in this chapter, I discuss how the perivascular compartment may be utilised to generate a patent vasculature with high barrier function and endurance, as opposed to the unsatisfactory results achieved when just HUVECs were employed. As a result, the co-culture method appears to be the optimum option for whole-organ vascular tissue engineering.

Chapter 5

Pericytes contributes to generate the vascular smooth muscle and the visceral smooth muscle in the intestinal acellular scaffold

5.1. Introduction

Smooth muscle cells, which represent the main difference between microvasculature and larger vessels, have a crucial role in delivering vasculature function. They deliver vaso-motiliy and contribute to the biomechanical blood flow response (Neff et al., 2011). However, the field of whole organ revascularization has concentrated on regenerating pericytes which are important for a robust microvasculature but not much has been done to recapitulate the smooth muscle layer. The derivation and culture of vascular smooth muscle cells would represent a significant step toward regeneration of the whole vasculature. I know that MABs are able to differentiate down to smooth muscle by stimulating the canonical TGFβ pathway (Minasi et al. 2002) (A. Dellavalle et al. 2011).

However, in chapter 3 I established that MABs can also differentiate down towards smooth muscle without TGFβ administration when they are in co-culture with HUVECs.

One of the issues I wanted to address was whether this capability was maintained in the scaffold. As a result, in this chapter, I evaluated MABs' ability to create the smooth muscle layer inside the preserved vasculature of the decellularised rat gut.

The fact that smooth muscle cells derived from MABs precursor colonised not only the vascular smooth muscle layer but also portions of the scaffold belonging to the visceral smooth muscle was an unexpected finding of this experiment. In this chapter, I investigated MABs' contribution to visceral smooth muscle development *in vitro* (in the scaffold) and *in vivo.* In addition, I unveiled in mice an alternative route of visceral smooth muscle generation that involve vessel associated precursors cells.

5.2. HUVECs smooth muscle differentiation of MABs and their migration within the scaffold

Z-stack confocal images of whole mount staining for CD31 - PDGFRβ and CD31-SM22 revealed that cells seeded in the decellularised intestine were able to recapitulate a similar behaviour to the one I observed in 2D and 3D. In particular, PDGFRβ positive cells (undifferentiated pericytes) were located in a peripheral position surrounding CD31 positive endothelial cells (HUVEC) that laid the vasculature (Figure 5.1).

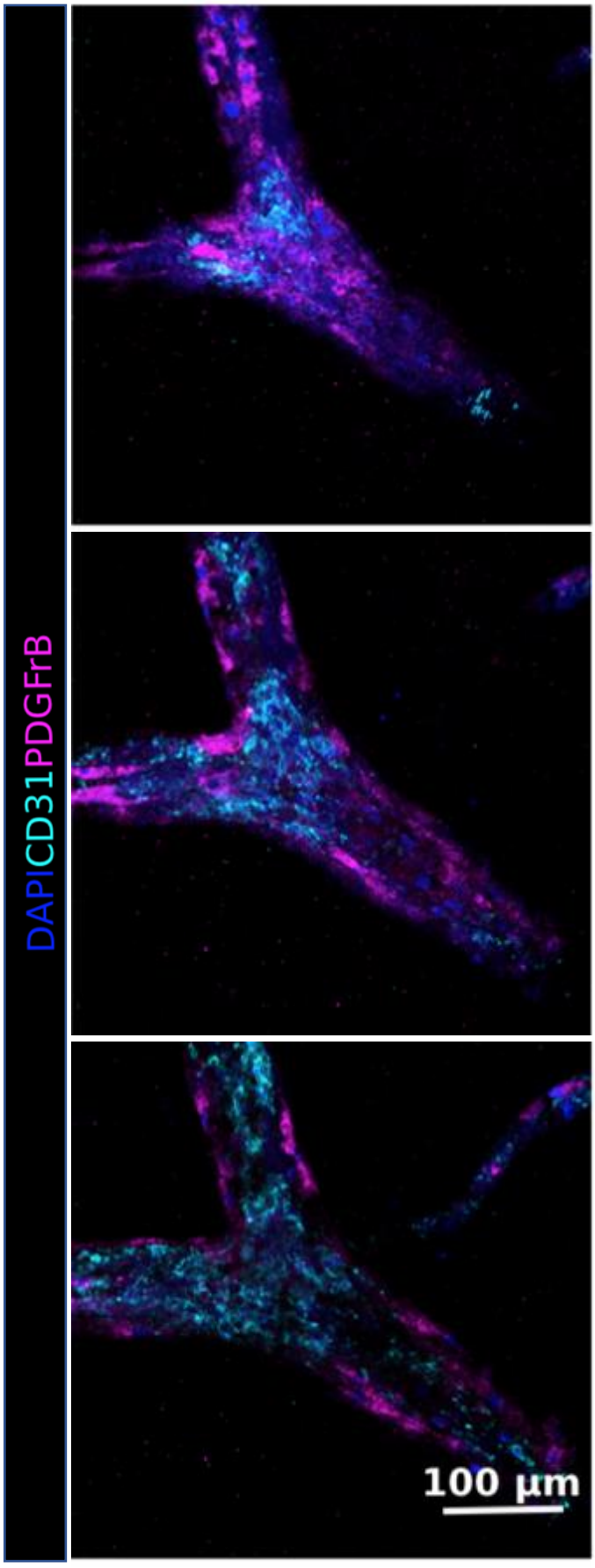
DAPICD31PDGFrB
100 µm

Fig 5.1: Different Z-points' confocal images of the re-vascularized scaffold with both MABs and HUVECs. The seeding and culture of both MABs05 and HUVECs inside the preserved vasculature of the intestinal scaffold resulted in MABs (shown as positive for PDGFRβ) surrounding the vessel and endothelial cells (shown as positive for CD31) lining the lumen. Seedings were performed with 3 MABs biological biopsies (n=3: MABs02-04-05). Other representative pictures showing undifferentiated pericytes surrounding endothelial cells are displayed in Appendix figure 4.5a.

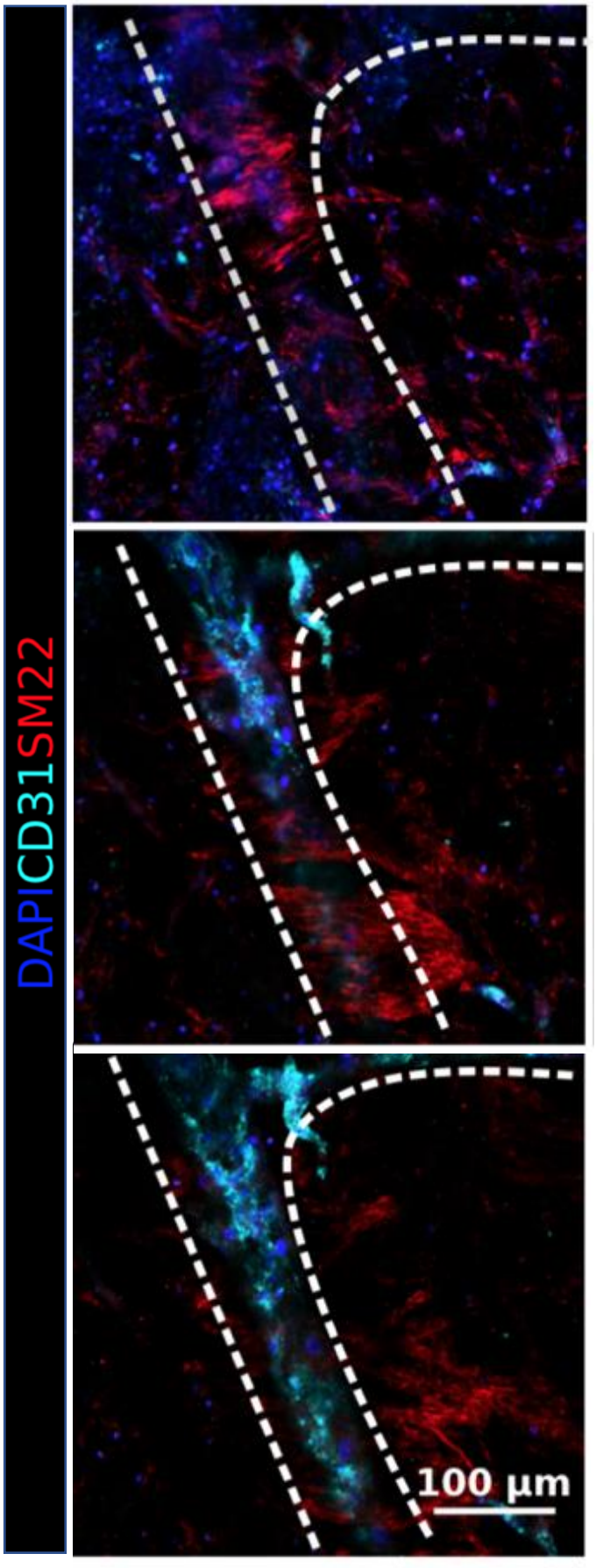
DAPICD31SM22
100 µm

Fig. 5.2: Different Z-points' confocal images of the re-vascularized scaffold with both MABs and HUVECs Different Z-points' confocal images of SM22 staining proves MABs05 to be able to differentiate down to smooth muscle into the scaffold. This SM22 population can migrate outside the vasculature occupying different region of the scaffold whilst the PDGFRβ (fig. 6.1) remain relocated. Seedings were performed with 3 MABs biological replicates (n=3: MABs02-04-05). Additional figures showing smooth muscle present in the scaffold obtained with the other MABs biopsies are shown in Appendix figure 5.2.

Interestingly SM22 positive cells appears to migrate outside the defined vasculature structure and to dispose themselves at various distances within the scaffold (Figure 5.2).

Using four colour confocal images I could defined the 3D organisation of the injected cells after dynamic culture. I observed from inside-out, a perfusable (ldl+) endothelium, surrounded by PDGFRβ+ perycites and a SM22 differentiated population surrounding both the vessel and disposing themselves on the compartment normally belonging to the visceral smooth muscle of the intestine (Figure 5.3).

This finding was confirmed also by the presence of smooth muscle MHC into the scaffold (Figure 5.4)

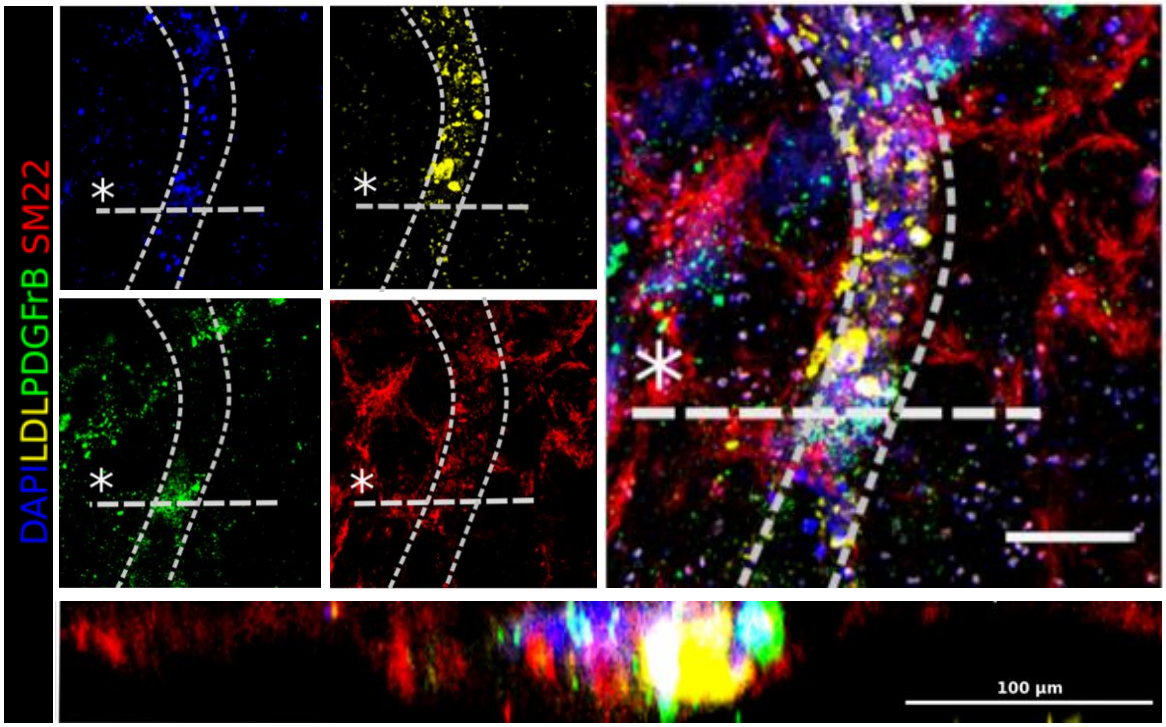

Fig. 5.3: Four colour confocal images and orthogonal view of a representative re-vascularized vessel. The dashes highlights the shape of the vessel and the area of the orthogonal projection: from inside-out, I observe a perfusable (ldl+) endothelium, surrounded by PDGFRβ+ pericytes and a SM22 differentiated population surrounding the vessel. Moreover, the SM22 population is able to migrate out and dispose itself on the compartment normally belonging to the visceral smooth muscle of the intestine. In the figure, MABs05 was used. Seedings were performed with 3 MABs biological replicates (n=3: MABs02-04-05). Other representative pictures of scaffold seeded with other MABs biopsies and perfused by fluorescently labelled LDL are showed in Fig5.5, Appendix Figure 5.5 and Appendix figure 5.2.

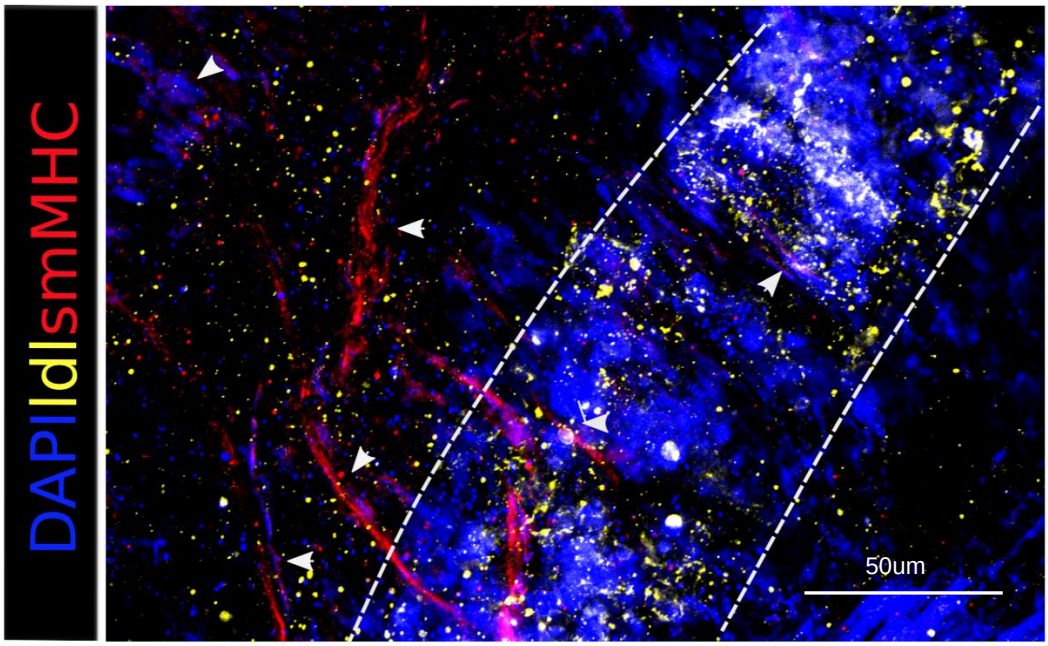

Fig. 5.4: Confocal image of a re-vascularized vessel showing presence of mature smooth muscle marker such smooth muscle MHC (white arrows). Seedings were performed with 3 MABs biological replicates (n=3: MABs02-04-05)

Importantly, MABs injected alone were neither able to differentiate into smooth muscle, as observed in 2D culture, nor to migrate outside the vasculature of the intestine (Figure 5.5).

This data reinforce the idea proposed by Paolo Bianco (Sacchetti et al. 2016a) that MABs as pericytes can contribute not only to the vascular smooth muscle but also to mesodermal derivative of the tissue they, in this case visceral smooth muscle .

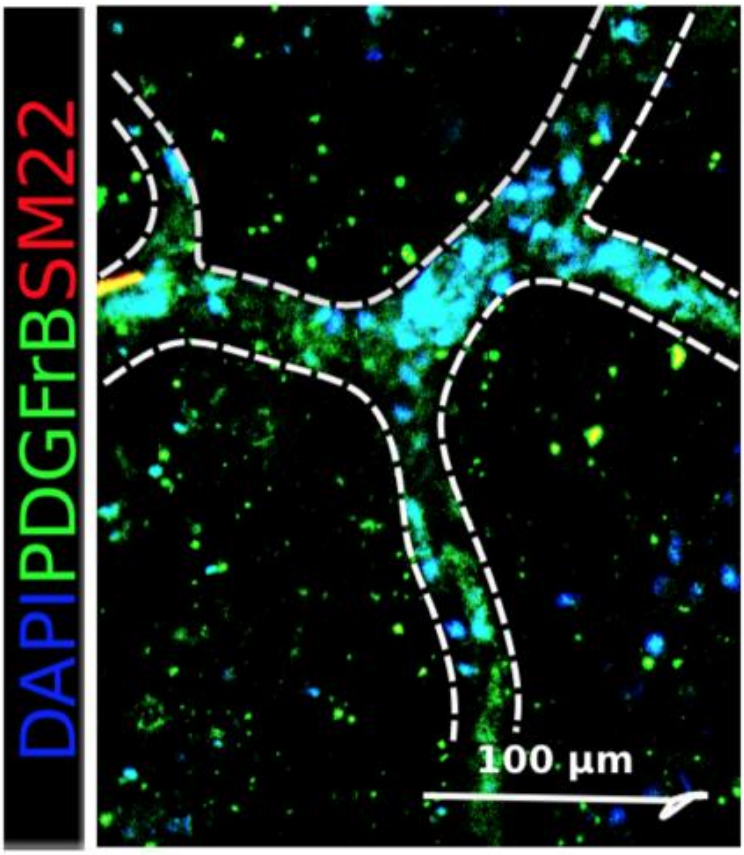

Fig. 5.5: Confocal image of a scaffold injected only with MABs in absence of HUVECs. The dashes highlight the shape of the vessels. Mesoangioblast appeared relegated around the vasculature and no SM22 was observed in the area normally belonging to the visceral smooth muscle of the intestine

5.3. TNAP-AP-CREERT2:R26R model reveal that pericytes contribute to visceral smooth muscle.

To investigate whether this phenomenon is present during post-natal visceral smooth muscle formation, I took advantages of a TN-AP-CreERT2:R26R mouse model present in a collaborator lab (Giulio Cossu's). This model allowed us to trace the fate of Alkaline Phosphatase (AP) (as pericyte marker) positive cells in the intestine after tamoxifen injection (Figure 5.6). Tamoxifen is widely used for the induction of genomic recombination in mice (double-)transgenic for floxed genes and Tamoxifen specific estrogen receptors (ER) coupled to Cre-recombinase. Therefore,

tamoxifen injections will result in a Cre-dependent recombination which allow the expression of LacZ (a gene which encode for the β -galactosidase enzyme) in the cells expressing also AP. X-gal staining can provide a visual assay of LacZ activity: β -Galactosidase cleaves X-gal into galactose and 5-bromo-4-chloro-3-hydroxyindole; this second compound is then oxidized into 5,5' -dibromo-4,4' -dichloro-indigo. As its name suggests, this final product is blue in colour. Tamoxifen injection was performed in Giulio Cossu's lab by Francesco Galli for 5 consecutive days. After either 3 days or 1 month, intestines were retrieved and fixed with 4% PFA and shipped to us.

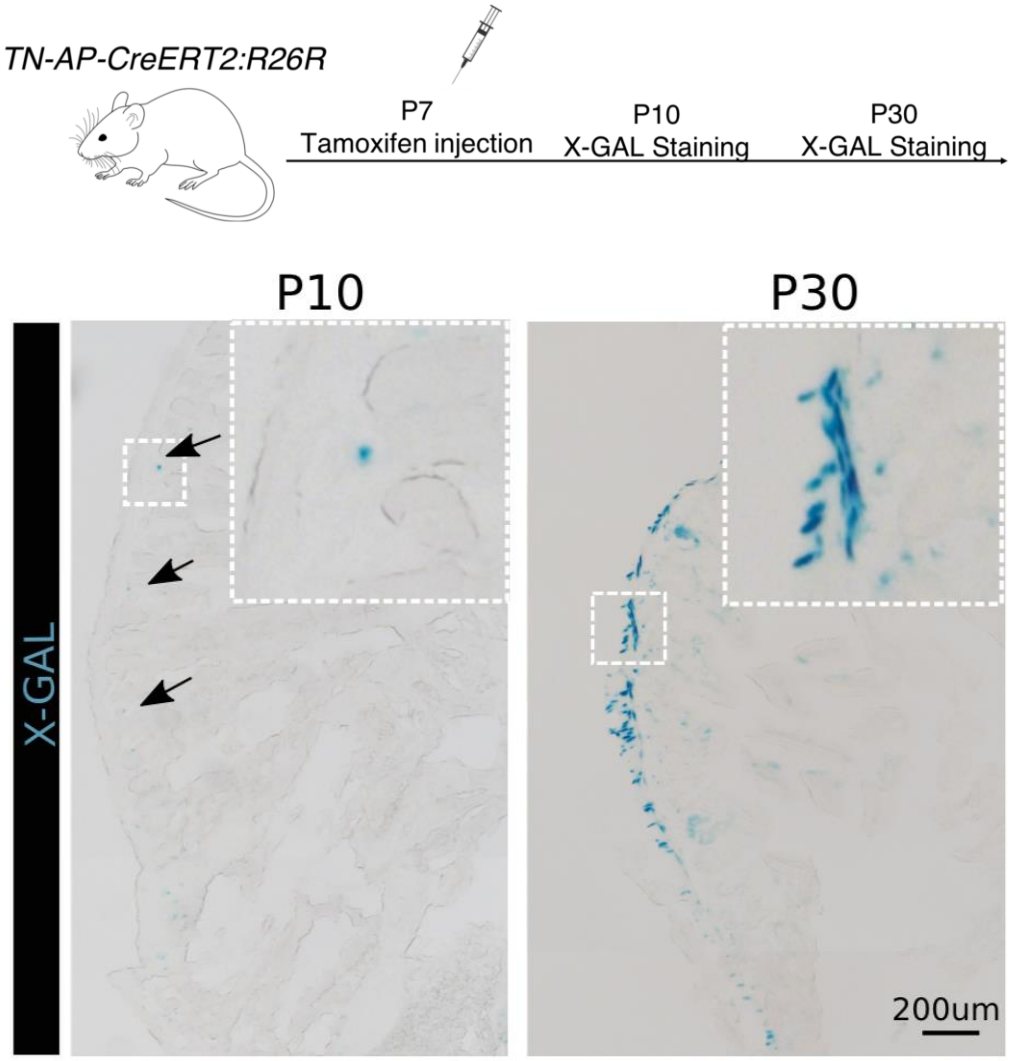

Fig 5.6: X-gal whole mount staining of intestine retrieved at 3 days post injection (left) and 30 days post injection (right). The dashed squares are showed in higher magnification at the top right corner of the image. 3 days post injections cells appear to be only in the submucosal layer where majority of blood vessel are. 30 days post injections they appear to be in the visceral smooth muscle layer. 3 biological replicates (3 TNAP-AP-CREERT2:R26R mouse) were used for these analyses (n=3)

X-gal whole mount staining were performed to track the presence of AP positive cells, then samples were embedded in OCT and sliced at the cryostat to be looked and imaged at the microscope. Cross-sections of X-gal staining of intestine retrieved at 3 days post injection revealed AP cell only in the submucosal layer where majority of blood vessel are, in line with their perycitarial identity (Figure 5.6).Interestingly at P30

AP positive cells were observed laying the visceral smooth muscle layer as confirmed by counterstaining with SM22 (Figure 5.6- 5.7).

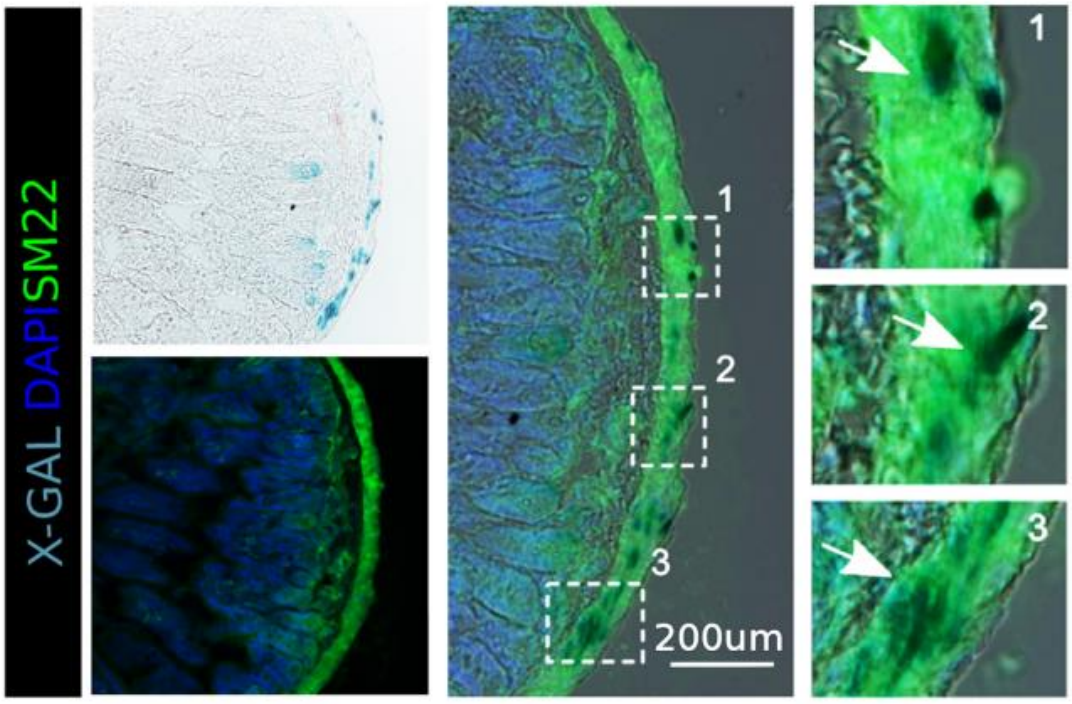

Fig 5.7: Whole mount x-gal counterstained with SM22 IF staining. Counterstaining with SM22 reveal that X-gal positive cells (White arrows) lays on the smooth muscle layer of the intestine. The dashed squares are shown in higher magnification on the very right panels. 3 biological replicates (3 TNAP-AP-CREERT2:R26R mouse) were used for these analyses (n=3)

In order to rule out the possibility that AP positive cells represents pericytes in the microvasculature of the visceral smooth muscle and not the differentiated smooth muscle cells, high magnification images were taken to observe their phenotype. Immunohistochemistry for smooth muscle MHC were performed and I could easily distinguish the two visceral smooth muscle layers: longitudinal and circular. This analysis revealed the presence of AP positive cells both in the longitudinal a circular smooth muscle and they followed the orientation of the corresponding layers (Figure 5.8). In order to investigate whether this phenomenon is present also in adult mice, two months old mice were also induced with tamoxifen and sacrificed after one month.

Intestines were retrieved, fixed and shipped to us by Francesco Galli. Since I did not expect to see a big number of cells in the adult mice, I preferred to image a whole open fragment of intestine and not in cross-section as in the previous analysis. However, the epithelial and submucosa layer would have masked the visibility of the smooth muscle cells at the microscope. Therefore, mucosa and submucosa layer were peeled away by Ben Cairns and X-gal staining were performed only on the remaining visceral smooth muscle layers. Images of whole mount x-gal staining counterstained for smooth muscle MHC shows the presence of AP positive cells differentiated into smooth muscle also in the adult mice (Figure 5.9).

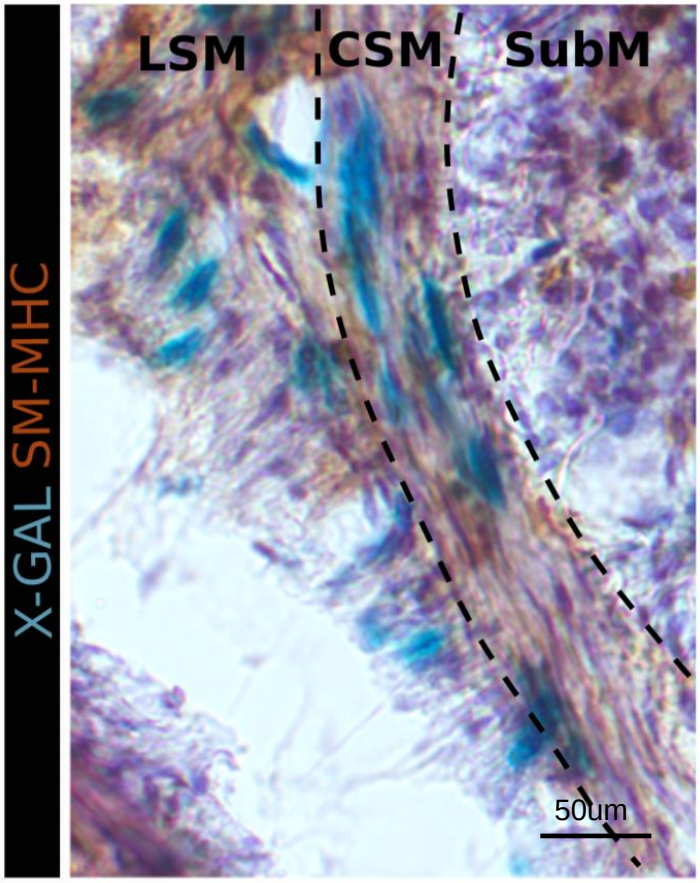

Fig 5.8: High magnification image of whole mount staining for X-gal and smooth muscle MHC on section of intestine of TN-AP-CreERT2:R26R mouse, 30 days post injections of tamoxifen. AP positive cells appear both in the longitudinal and circular smooth muscle (LSM/CSM) and they followed the orientation of the corresponding layers.

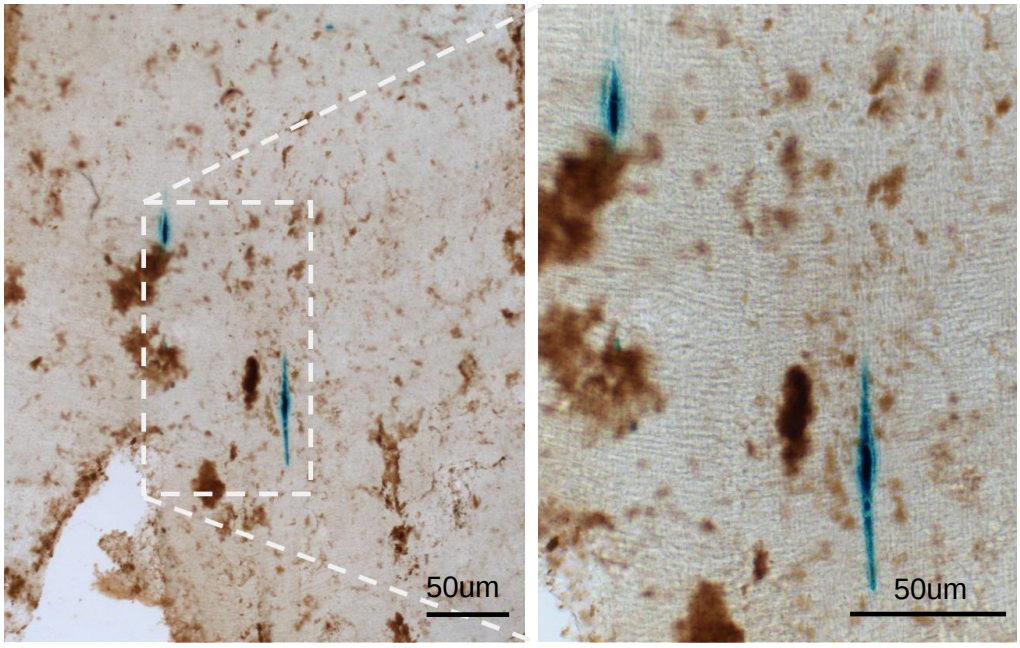

Fig 5.9: X-gal and smooth muscle MHC whole mount staining performed only on the visceral smooth muscle layers of TN-AP-CreERT2:R26R 2-month-old mice, 30 days after tamoxifen injection. presence of AP positive cells differentiated into smooth muscle are confirmed also in the adult mice. The dashed square in the left image is shown in a higher magnification in the right image.

5.4. Human MABs injected in the intestinal smooth muscle if immunocompromised mice contribute to the generation of the visceral smooth muscle

As a final proof of principle that human skeletal muscle MABs can contribute to generate also the visceral smooth muscle of the intestine and therefore being an optimal source for the tissue engineering also of this compound, human MABs GFP+ were injected into the visceral smooth muscle of immunocompromised ($Rag2^{-/-}$;$\gamma c^{-/-}$;$C5^{-/-}$) mice by Conor McCann. After one month intestines were retrieved, the smooth muscle layers were isolated and whole immunofluorescence for smooth muscle MHC was performed. Significantly, after one month post injection human MABs integrate into the visceral smooth muscle layer expressing the mature smooth muscle marker smooth muscle MHC. (Figure 5.10)

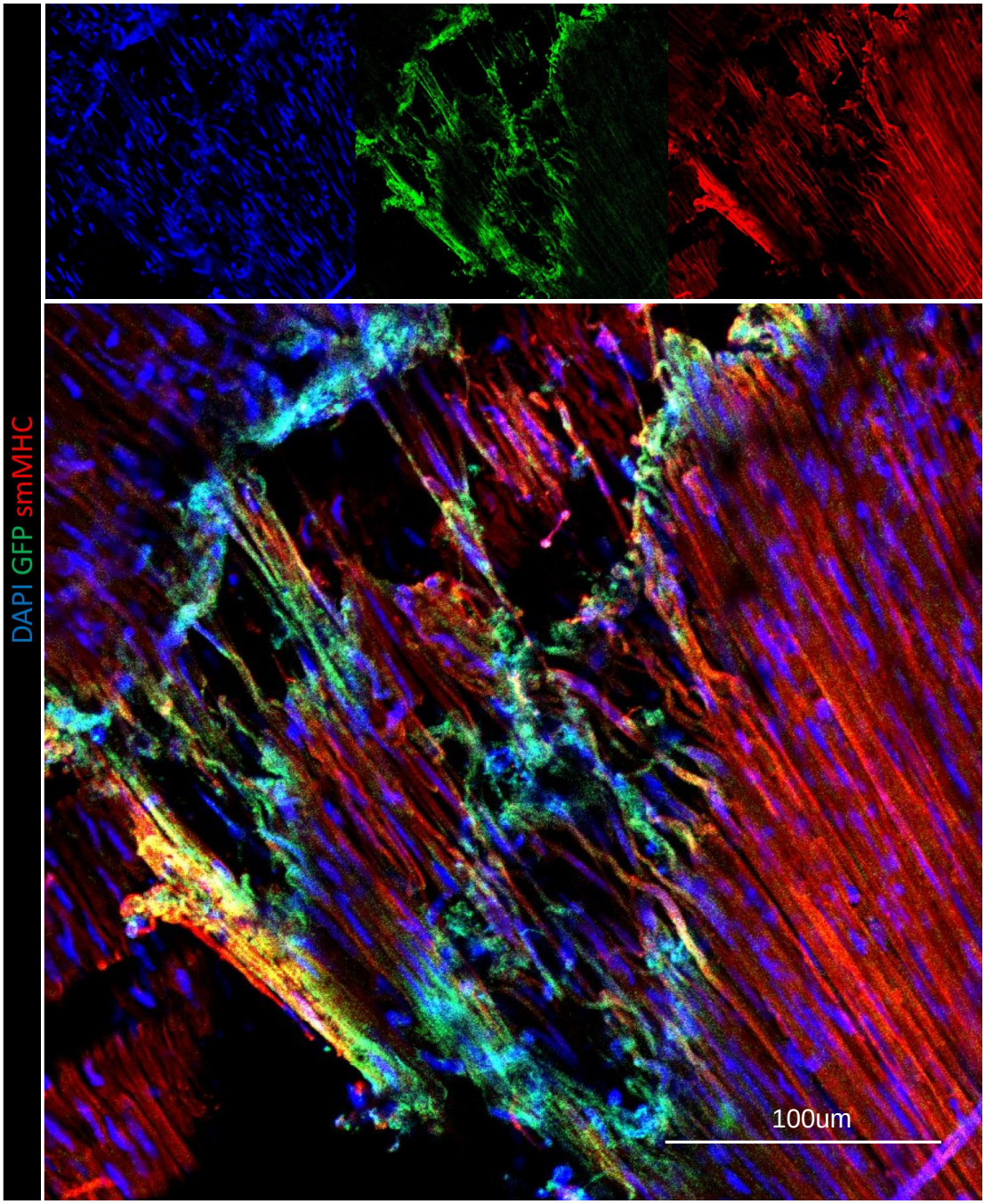

Fig 5.10: Whole mount staining for Smooth muscle MHC (Red) on mouse intestines retrieved 1 month after MABs GFP+ (green) injection. The staining was performed only on the visceral smooth muscle layer that was isolated after the harvest of the intestine. MABs05 resulted integrate into the visceral smooth muscle layer expressing the mature smooth muscle marker smooth muscle MHC. 3 biopsy of MABs were used for these analyses (n=3: MABs02-04-05). Representative pictures of the results obtained with MABs02 and MABs04 are displayed in Appendix figure 5.10.

5.5. Discussion

Because microvasculature alone cannot sustain organ function, the whole spectrum of various sized vessels that comprise the vascular tree must be regenerated from a complete organ tissue engineering standpoint. Indeed, smooth muscle cells, which are the primary distinction between microvasculature and bigger vessels, play an important role in vasculature function. They deliver vaso-motiliy and contribute to the biomechanical blood flow response (Neff et al., 2011). Consequently, derivation and culture of vascular smooth muscle cells represent a significant step toward regeneration of the whole vasculature.

Co-seeding of HUVECs and MABs into the preserved vasculature of a decellularised rat intestine I resembled the same behaviour seen in 2D when HUVECs were grown with MABs, which differentiated into smooth muscle. I saw a PDGFrB positive population of cells, which I believe are undifferentiated pericytes, moved to the periphery and surrounded CD31 positive endothelial cells. In addition, I saw an SM22 distinct population around the vasculature. As a result, the newly established vasculature had cells orientated in a native manner: from the inside out, I had endothelial cells inside the vessel drawing a patent endothelium, MABs surrounding them, and a smooth muscle layer encircling the vessel derived from the pericytes precursor. This is the first time that this achievement was reported in the contest of whole organ tissue engineering.

Interestingly, SM22 positive cells appear to move outside of the specified vascular structure and to position themselves at different distances inside the scaffold, entering the compartment typically occupied by visceral smooth muscle of the gut.

I confirmed this data *in vivo* taking advantages of a *TNAP-AP-CreERT2:R26R* mouse model: this model allowed us to follow the fate of Pericytes AP+ cells after injection with Tamoxifen. I saw cells infiltrating the smooth muscle layer of the gut over time

after inducing the system, showing that pericytes might be the progenitor of the mesodermal descendant of the tissue where they dwell. Paolo Bianco pioneered the idea that ubiquitous MSCs with identical capabilities do not exist, but that “tissue-specific” mesodermal progenitors can be recruited into a mural cell destiny, giving a plausible method by which pericytes are produced and how they serve as a local progenitor cell source. (Sacchetti et al., 2016). In this concept I follow his footsteps and to my knowledge this is the first time that it was proven in the visceral smooth muscle, within a gut tissue engineering model.

This behaviour was maintained in mature mice, when cells appeared to be present in the visceral smooth muscle significantly less often, although not severely so. This implies that while the stated behaviour may be preserved in adulthood, it is not the primary approach for rebuilding visceral smooth muscle.

Our findings in the TN-AP-CreERT2 mouse model show that pericytes in the gut can serve as a source of visceral smooth muscle precursors in addition to vascular smooth muscle precursors. Other than penetrating the visceral smooth muscle compartment into a decellularised scaffold, our skeletal muscle MABs' capacity to integrate into visceral smooth muscle has yet to be harnessed. Therefore, human MABs GFP+ were injected into the visceral smooth muscle of immunocompromised mice. Significantly, after one-month post injection human MABs integrate into the visceral smooth muscle layer expressing the mature smooth muscle marker smooth muscle MHC. This represent the proof of principle that this vessel associate skeletal muscle pericytes can contribute also to generate the visceral smooth muscle for clinical applications taking advantages of their default capacity to generate vascular smooth muscle. In fact, to my knowledge, no differences have been ever reported between visceral and vascular smooth muscle.

In summary in this chapter I highlighted the following outcomes:

1. MABs co-seeded with HUVECs in the preserved vasculature of a decellularised intestinal scaffold is able to regenerate the vascular smooth muscle layer. For the first time in a whole organ tissue engineering model, I reported from inside out: endothelial cells lying the vessel drawing a patent endothelium, MABs surrounding them and a smooth muscle layer around the vessel coming from the pericytes precursor.
2. Following Paolo Bianco's footsteps, I strengthen the theory that pericytes are bi-potent progenitor of the vascular smooth muscle and of the mesodermal derivatives of the tissue where they reside. This was never seen in the visceral smooth muscle and I confirmed this hypothesis in the gut of *TN-AP-CreERT2* mice.
3. Skeletal muscle MABs can be used to generate also the visceral smooth muscle for clinical applications as confirmed by their capability to invade the compartment normally belonging to the visceral smooth muscle of the intestine into a decellularized scaffold (*in vitro*) and their capability to integrate into the visceral smooth muscle in a *in vivo* set up.

Chapter 6

Newly formed vasculature anastomoses and integrate in a mature and stable endothelium *in vivo*

6.1. Introduction

The synthetic vasculature must be linked to the host vascular in order to function. The graft should encourage fast ingrowth of host vasculature over a short period of time to avoid graft tissue necrosis.

Whole organ vascular tissue engineering currently lacks in-vivo evaluations that last more than 15 days (Shaheen et al. 2019), and the preponderance of studies implant the repopulated scaffold in vivo for only a few days (Ren et al. 2015) or hours (Ko et al., 2015, Bao et al., 2015, Hussein et al., 2016., Gilpin et al., 2016., Zhou et al., 2017., Doi et al.,2017).

In all those works, the characterization of the vasculature post *in-vivo* implantation was either absent or limited at showing presence of cells and patency.

In this chapter I implanted scaffold seeded only with HUVECs and scaffold co-seeded with MABs and HUVECs and I maintained them *in-vivo* for up to a month. Characterization was assessed on the capacity to anastomose into the host vasculature, in the cells capacity to establish a mature and stable endothelium and in the phenomena involved in their maintenance.

6.2. Vascular-engineered intestine functionally integrate after omental implantation

To address the question whether the repopulated vasculature is able to successfully anastomose into the vasculature of a host, after 7 days of culture into the bioreactor, a segment of the repopulated scaffold was heterotypical implanted into the omentum of NOD-SCID-gamma (NSG) mice (Figure 6.1). The procedure was performed by a surgeon in the lab (Federico Scottoni): NSG mice were anesthetised and laparotomy was carried out to accede the abdominal cavity. Stomach was

exteriorised and the omental sheet was stretched. Scaffold were inserted in the omental sheet closed by stitching (Figure 7.1).

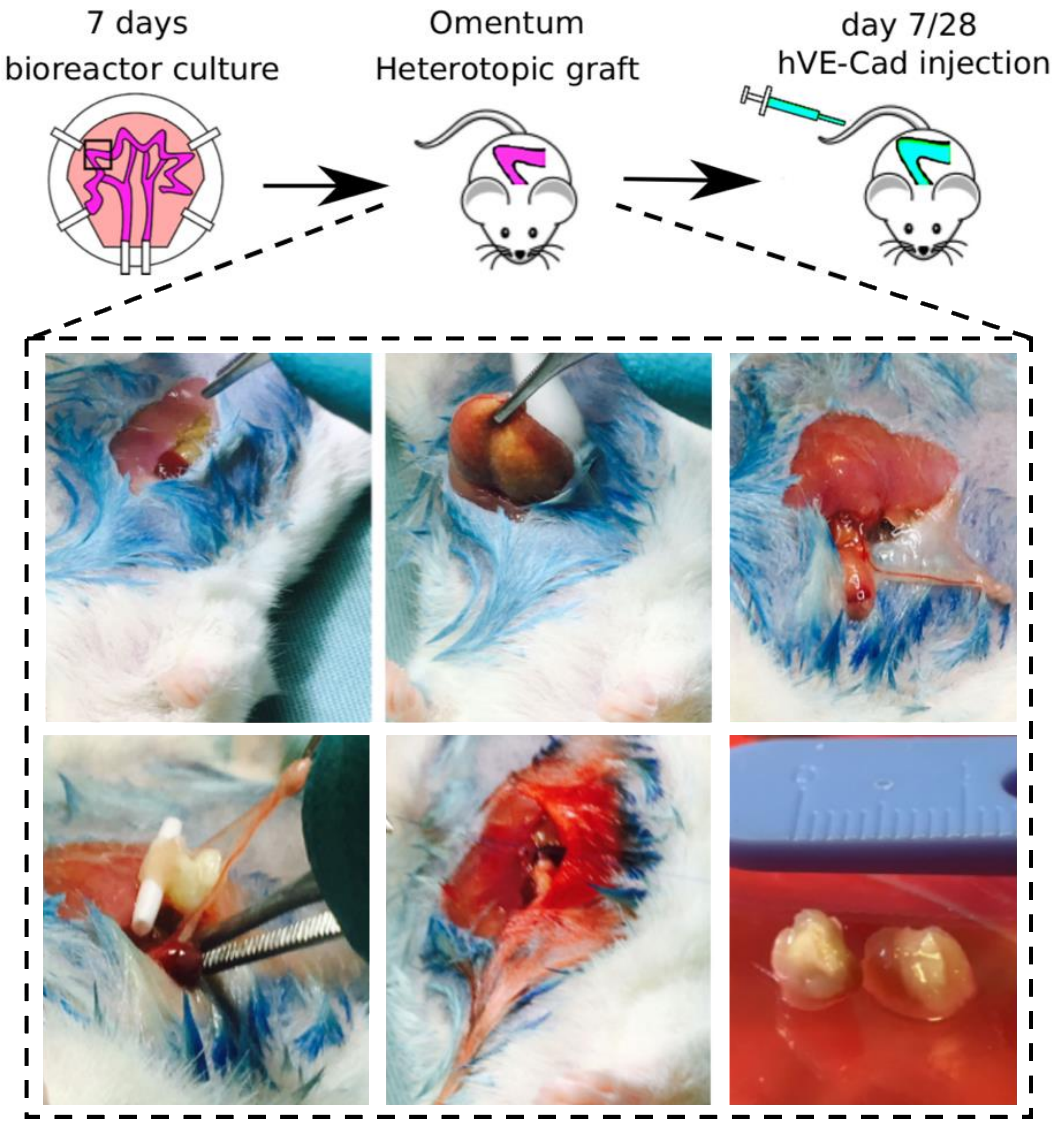

Fig 6.1: Schematic of the heterotopic experiment: after 7 days of dynamic culture into the bioreactor, scaffolds were implanted heterotopically in the mice Omentum. And after 7 days or 4 weeks intravenous injection of a FACS antibody fluorescently labelled anti human ve-caderin was performed to assess anastomoses of the newly formed vasculature of the scaffold. In the dashed panel all the different passages of the surgical procedure are displayed: laparotomy to accede the abdominal cavity. Stomach exteriorisation to stretch the omental sheet. Placement of the scaffold in the omental sheet and closure of the mice by stitching. In the last panel a macroscopic look of the scaffold after 7 days or 4 weeks is shown.

Eight mice received scaffold repopulated with both cell types whilst other 8 received the ones repopulated with HUVECs only. After either 1 week or 4 weeks mice were injected with a fluorescently labelled anti-human-VE-cadherin prior to sacrifice (Figure 6.2). If the vessel connected to the host, they would receive the antibody solution which would result in fluorescently labelled endothelial cells. Sections of both scaffolds co-seeded with HUVECs and MABs and the ones seeded with HUVECs only were stained for SM22 to identify also the smooth muscle compounds that surround mature vessels (Figure 6.2). Among those smooth muscle cells, only a few where identified as coming from human MABs progenitors while the majority appeared to be recruited from the host as shown from the human specific K80 staining (figure6.3).

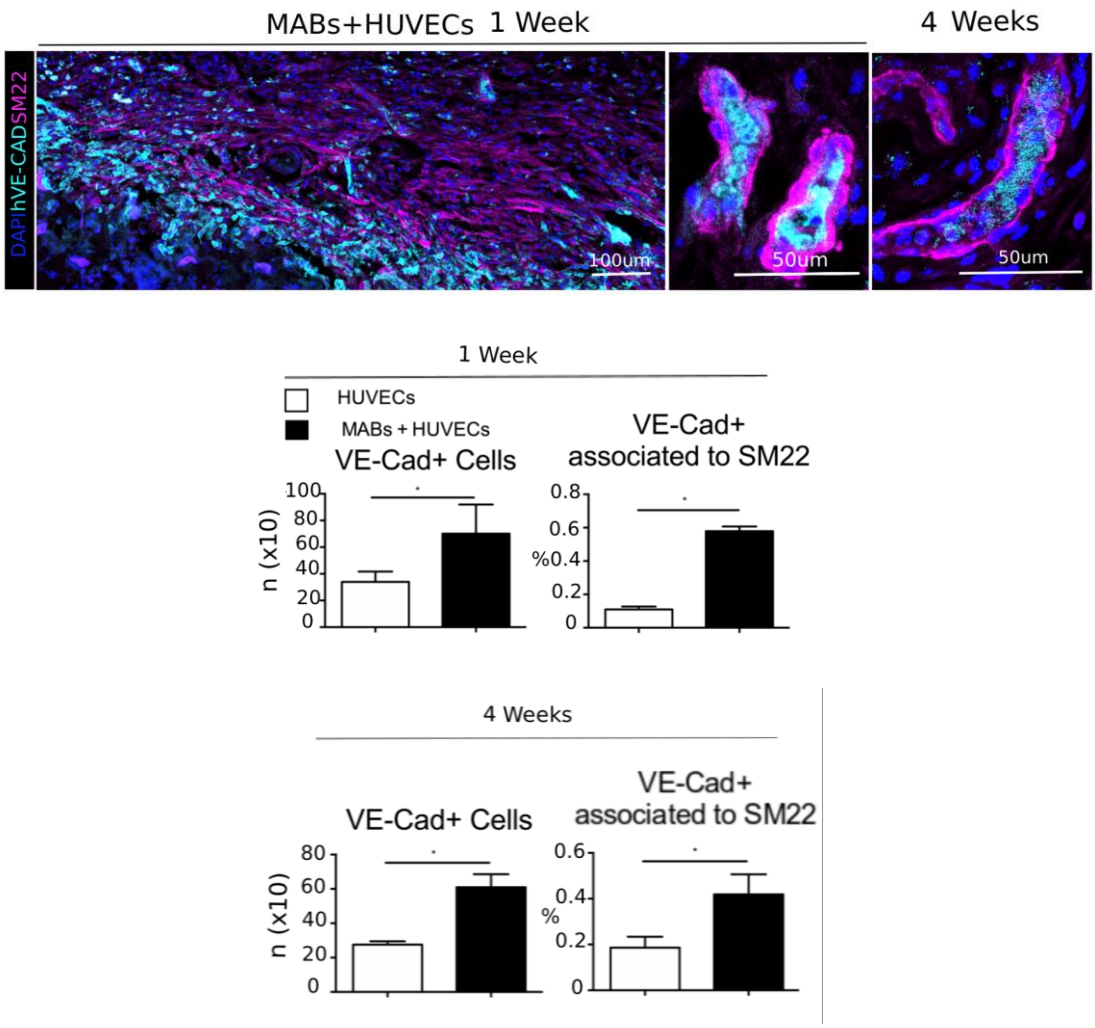

Fig 6.2. Confocal images showing Immunostaining anti SM22 of sections of scaffolds co-seeded with HUVECs and MABs at 1 week and 4 weeks (the cyan signal staining for ve-cadherin was coming from the human ve-cadherin injection performed *in vivo* e not anti ve-cadherin antibody was supplemented in this staining). 5 tile-scan images representative of a region of 1,2 mm were taken throughout the whole scaffold. Ve-cadherin positive cells and ve-cadherin positive cells associated with SM22 staining were counted for any group to evaluate the quality of the anastomosis. The final count of positive cells was an averaged value over the 5 counts. In this figure is shown the result obtained by co-seeding HUVECs with MABs04 but 4 biological replicates of MABs were used for this analyses (n=4: MABs02-03-04-05). Representative pictures of the other biological replicates are shown in Appendix figure 6.2. Unpaired T tests with equal SD were performed. P values: Ve-Cad+ at 1 week= 0.043; Ve-Cad&SM22 at 1 week= 0.0001; Ve-Cad at 4 weeks= 0.001; ; Ve-Cad&SM22 at 4 weeks= 0.015.

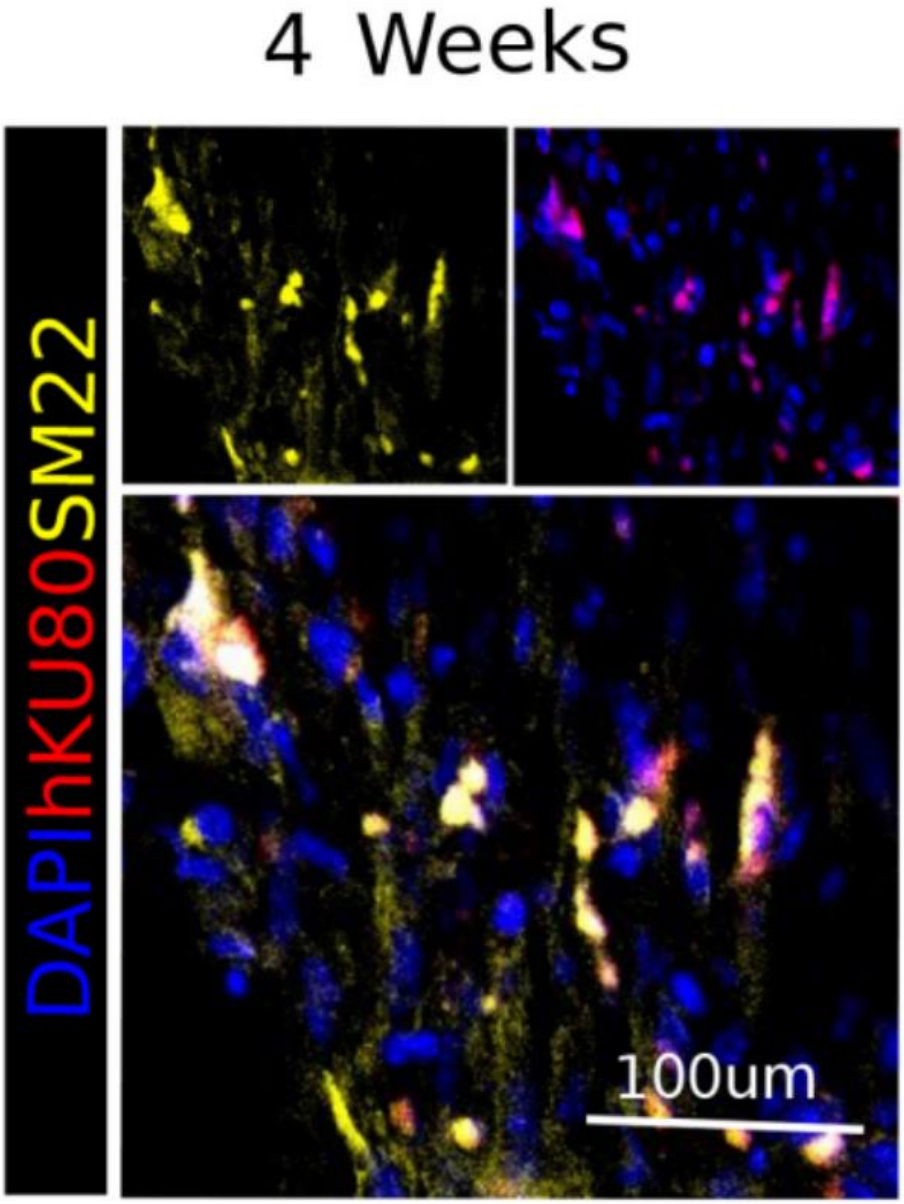

Figure 6.3 confocal images revealing presence of MABs-derived human smooth muscle. Staining for anti-human K80 show presence of MABs-derived human smooth muscle cells within the graft 4 weeks post implantation even if majority appear to be recruited from the host.

Intravenously-injected Ve-cadherin positive cells were counted to evaluate the quality of anastomosis for both groups. My results showed that in the scaffold co-seeded with both cells type a statistically significant higher number of hVE-cadherin positive cells were present both at 1 week and at 4 weeks, indicating that they could anastomose more efficiently compared to the scaffolds in which only endothelial cells

were seeded (Figure 6.2). To assess whether the hVE-cadherin antibody is specific against human cells and not mouse cells, a co-staining with mouse Endomucin (specific against mouse endothelial cells) was performed. In Figure 6.4 I clearly distinguish mouse vessel, human vessel and few chimeric vessel but mouse Endomucine signal never merge with hVE-cadherin signal (Figure 6.4).

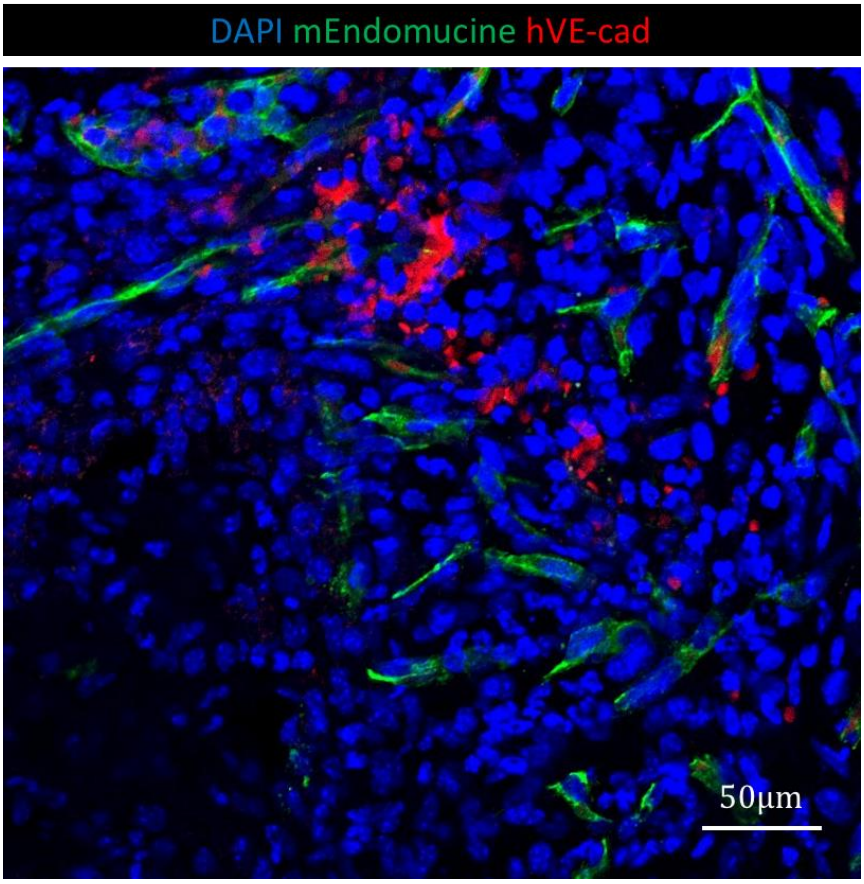

Fig 6.4: hVE-Cadherin antibody specificity: confocal image of slice of scaffold retrieved after omental implantation, stained for a specific mouse Endomucine Ab (Green) and human VE-cadherin (Red)**.** The figure display mouse vessel, human vessel and few chimeric vessel but mouse Endomucine signal never merge with hVE-cadherin signal

To evaluate whether these anastomosed vessels were able to integrate in a mature vasculature, hVE-cadherin positive cells associate with SM22 (regardless their human or mouse origin) staining were counted. These results revealed that in scaffold co-seeded with MABs and HUVECs, both at 1 week and 4 weeks, at least

50% of the cells positive for hVE-cadherin were associated to smooth muscle. Scaffolds in which only HUVECs were seeded were not able to perform in the same way and showed a statistically significant lower number of cells associated to smooth muscle, therefore a less mature and organised endothelium (Figure 6.2). Moreover, the presence of vascular smooth muscle seems to reflect the long-term outcome of the experiment. In fact, in the co-culture group the anastomosed endothelium seems to remain stable whilst in the group with HUVECs only seem to experience a decrease of cell number over time.

6.3. Mesoangioblast promote the generation of a more stable and long-lasting vasculature

In order to assess whether the great outcomes of the group with co-culture cells in comparison to the single culture was due to a proliferation process or to a stabilization effect, additional staining for Ki67 (proliferative marker) and Cleavage Caspase 3 (cell death marker) were performed. Interestingly ki67 was poorly represented even when HUVEC and MAB are co-injected, indicating that proliferation does probably occurs *in vitro*, but is suppressed *in vivo* which make the system safer. (Figure 6.4-6.5).

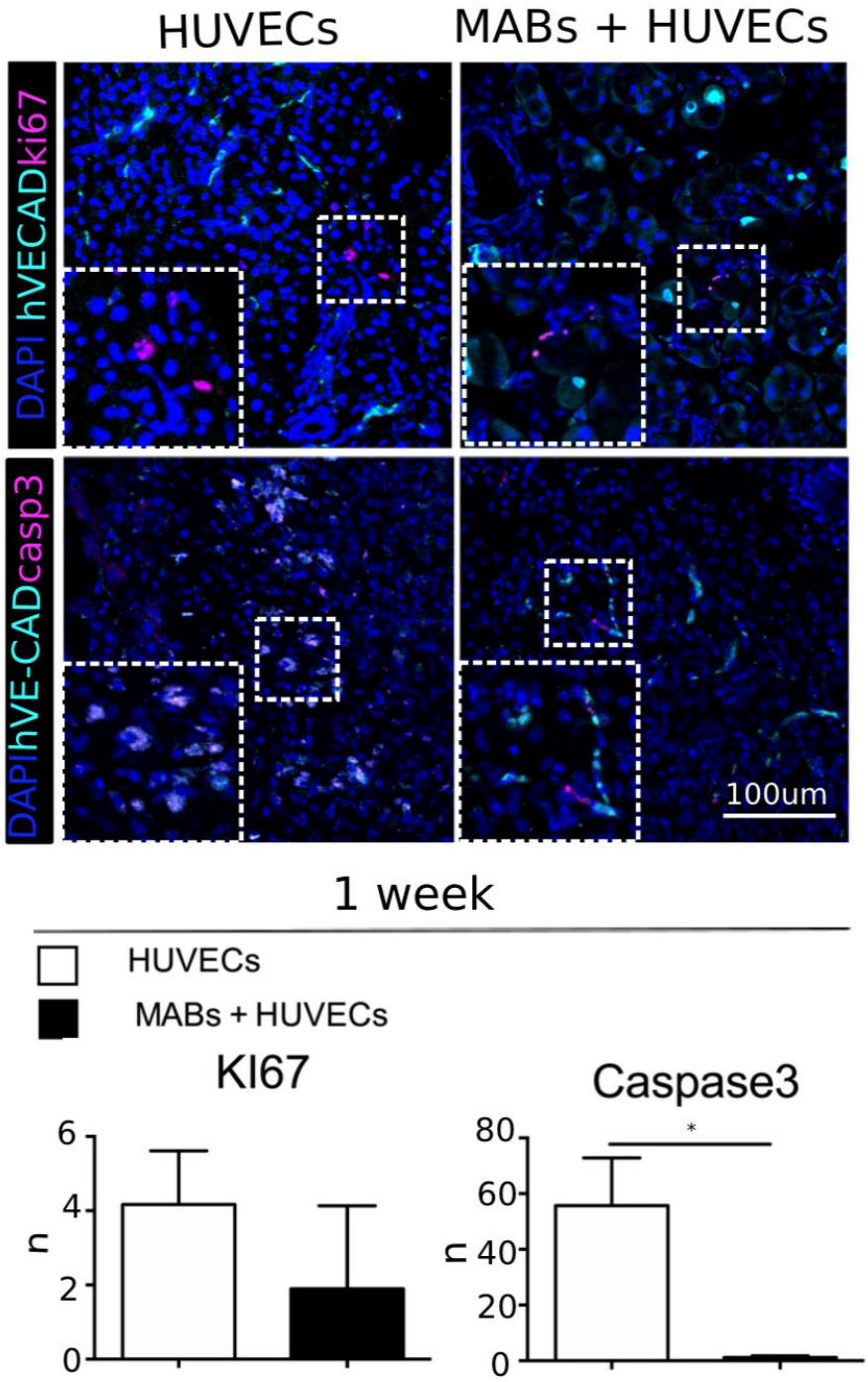

Fig. 6.4: Confocal images showing Immunostaining for Ki67 (top panels, in magenta) and Caspase 3 (bottom panels, in magenta) at1 week. 5 tile-scan images representative of a region of 1,2 mm were taken throughout the whole scaffold. Ki67 and caspase3 positive cells were counted for any group. The final count of positive cells was an averaged value over the 5 counts. In this figure is shown the result obtained by co-seeding HUVECs with MABs04 but 4 biological replicates of MABs were used for these analyses (n=4: MABs02-03-04-05). Representative pictures of the results obtained with the other MABs biopsies are displayed in Appendix figure 6.4-6.5. Unpaired T tests with equal SD were performed. P values: Ki67 at 1 week=0.1; Caspase 3 at 1 week= 0.005;.

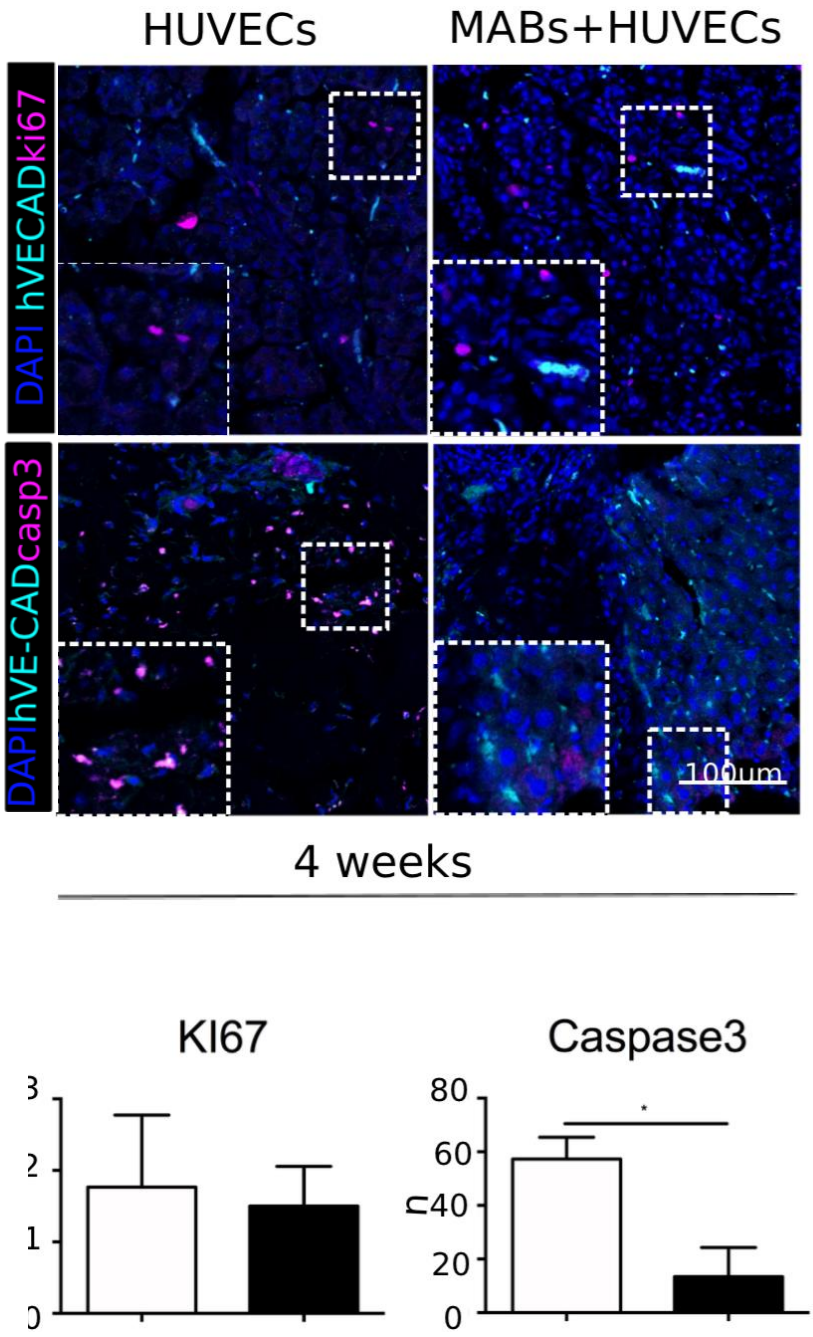

Fig. 6.5: Confocal images showing Immunostaining for Ki67 (top panels, in magenta) and Caspase 3 (bottom panels, in magenta) at 4 weeks. 5 tile-scan images representative of a region of 1,2 mm were taken throughout the whole scaffold. Ki67 and caspase3 positive cells were counted for any group. The final count of positive cells was an averaged value over the 5 counts. In this figure is shown the result obtained by co-seeding HUVECs with MABs04 but 4 biological replicates of MABs were used for these analyses (n=4: MABs02-03-04-05). Representative pictures of the results obtained with the other MABs biopsies are displayed in Appendix figure 6.4-6.5. Unpaired T tests with equal SD were performed. P values: Ki67 at 4 weeks= 0.7; Caspase 3 at 4 weeks= 0.004.

On the contrary caspase3 marker is strongly represented in the scaffold injected only with HUVECs both at 1 week and 4 weeks and basically absent in the scaffold with both cell types, indicating that apoptosis is responsible of the great cell loss in the scaffold with only HUVECs, whilst MABs stop apoptosis guaranteeing a more mature and long lasting endothelium also *in vivo* (Figure 7.4-7.5).

6.4. Discussion

The engineered vasculature produced and characterized in the chapters 5-6 need to be able to anastomose to a host *in-vivo* to exert its function.

Many works address the in-vivo evaluation only for few hours and with a heparin treatment prior seeding in order to enhance the capacity of the vascularised scaffold to be perfused *in vivo.* (Hussein et al., 2016), (Bao et al., 2015), (Ko et al., 2015), (Ren et al. 2015) (Meng et al. 2019), (Shaheen et al. 2019). Relevant for this thesis project is the work of Kitano et al. He decellularised segment of rat intestine and he repopulated it with iPSC-derived epithelial cells for 14 days and HUVECs for 3 days (Kitano et al. 2017). The intestine was subsequently implanted in a heterotopic model consisting of a subcutaneous graft in the neck, anastomosed to the vasculature and provided of two-end stomas. The graft was kept in place for four weeks; however, the quality of the re-vascularization was not assessed after the in-vivo implantation. They did examine the presence of CD31 positive cells in the scaffold, but they did not consider coverage, patency across the scaffold, or the presence of the mural compartment, which is crucial for mature endothelial cells.

After all, in my experiences scaffold repopulated with only endothelial cells resulted in a poor degree of coverage end functionality *in-vitro* which reflected the poor outcome that I would have observed also in the *in-vivo* implant

Moreover, the functionality of the graft was assessed by delivering nutrients into the lumen of the engineered intestine, via the stoma. Even though absorption of nutrient into the rat blood stream was observed, the authors could not rule out the possible free diffusion from the acellular areas of the scaffold which was not completely re-epithelialized.

I consider the perivascular compound in our work, but I am yet unable to accomplish full endothelialisation of the capillary component, which remains the major challenge of vascular tissue engineering. I did not address the re-epithelialisation of the scaffold prior to in-vivo implant due to the lack of micro-vasculature. In fact, there would be no connection to transfer nutrients absorbed from the epithelium to the macro-vasculature if there was no micro-vasculature.

I also opted not to directly anastomose the vasculature to the host due to the lack of a micro-vasculature. In reality, blood cloth would form if matrix fragments were introduced into the bloodstream.

For all these reasons I decide to implant the scaffolds heterotopically into the omental sheet of NSG mice to evaluate if the graft would promote the rapid ingrowth of the host vasculature into the scaffold to avoid tissue necrosis.

Eight mice got scaffolds repopulated with both cell types, whereas the other eight received scaffolds repopulated with just HUVECs. Prior to sacrifice, mice were injected with fluorescently labelled anti-human-VE-cadherin after 1 or 4 weeks. If the vessel was linked to the host, the antibody solution would be delivered, resulting in fluorescently labelled endothelial cells. Cell counts of human-VE-cadherin positive cells indicated that scaffold co-cultured with both cell types performed better in terms of anastomosis. Moreover, they integrated in a more mature vasculature as it was surrounded by a smooth muscle layer. As previously affirmed, the vascular smooth muscle has a pivotal role to play in providing vasculature function (Neff et al., 2011).

The latter result reflects the long-term durability of the vasculature within the scaffold co-seeded with both cell types and the loss of cells over time of the scaffolds with

HUVECs only. Remarkably, the presence of MABs promoted the recruitment of more host smooth muscle cells which is a sign of vessel maturity regardless their origin. This phenomenon contributed to tissue engraftment, sustained viability and led to a reduction in apoptosis.

Indeed, the presence of the perivascular compartment stabilises the environment of the scaffold which does not show either ki67 or Caspase 3 markers. On the contrary scaffold seeded with HUVECs only display a major degree of cell death indicated by the strong Caspase 3 signal.

Chapter 7

Discussion

7.1 Cell choice

A landmark of tissue engineering is the use of a reliable and easily available cells source. HUVECs have been chosen to address the re-endothelialisation of the preserve vasculature of a decellularised rat intestine for this study. However as previously mentioned in the introduction HUVECs failed to engraft successfully in many animal models and have several limitations. HUVECs alone showed limited capacity to form vessels and failed to survive in the long term when they were embedded in a three-dimensional fibronectin-type 1 collagen gel and then inserted into mice (Koike et al., 2004). In addition, Mummery's group reported that HUVECs could not incorporate the xenograft model into the zebrafish vasculature but were attached to the vasculature or scattered throughout the embryo. HUVECs alone resulted therefore an inadequate source of cells for the engineering of vascular tissue, making it necessary to investigate other options (Orlova et al., 2014). In the same work they reported how iPSC-derived ECs were able to outperform HUVECs instead. However, that still does not change the fact that still there is a lot of concerns on the safety and characterization of iPS also for their capacity to form teratoma *in vivo*. Moreover, HUVECs are an easy to access source and they can deliver high yield following isolation; therefore, they still represent a gold standard for the vascular field. Finding a way for adult primary cells, such as HUVECs, to improve their performance without requiring genetic changes would be extremely useful for tissue engineering and would make the access to clinic easier. In this work I want to overcome one of the main problems of tissue engineering which is the long-term durability *in vitro* and *in vivo* of endothelial cells only, in particular HUVECs, and I addressed this problem by using a perivascular cell source. Here I proposed the use of human Mesoangioblasts (MABs), blood vessel-associated bi-potent mesodermal progenitors (Minasi et al. 2002) (Dellavalle et al. 2011),which are considered a subset of

pericytes. The name Mesoangioblast come from the fact that embryonically they are isolated from the embryonic murine dorsal aorta and assigned to the perivascular lineage (CD34, Flk-1, SMA and c-Kit expression), however they are also capable to generate in-vivo both vascular and extra vascular mesodermal derivatives. This capability is lost in the adult counterpart: they are only able to generate the extravascular compound losing the endothelial features and therefore are consider pericytes. Since I aim at the revascularization of an intestinal scaffold, the ideal candidate would be the adult MABs' counterpart resident in the intestine. However, there is not a well characterised source of pericytes resident in the intestine that represent a safe choice for clinical translation.

Mesoangioblast isolated from skeletal muscle biopsies, though, have been extensively characterised in literature and they are currently used in a clinical trial for dystrophy (Cossu et al. 2016). Indeed, these cells can be easily harvested from skeletal muscle tissue biopsies, cultured under standard condition and differentiated towards either skeletal muscle or smooth muscle, the latter via TGFβ administration(Dellavalle et al. 2007) (Cossu and Biressi 2005) (Tagliafico et al. 2004).

An important point to highlight is that Dellavalle et al reported that the percentage of cells expressing both AP and CD56, following digestion of human's skeletal muscle, was less than 0.1%. However, some clones derived from the AP+/CD56- fraction were heterogeneous with cells positive for AP and/or Myf5, another marker of activated satellite cells (Charge 2004). The same heterogeneity was observed in some clones derived from AP-/CD56+ population (Dellavalle et al. 2007), suggesting that cells might switch their phenotype *in vitro*. The reason why we observe an higher number of CD56+ cells might lay on the fact that we use different muscle types and donor age compared to Dellavalle et al. Dellavalle isolated MABs from biceps brachialis of adult patients while our investigation focus on muscle taken from head, neck, and abdominal wall of patient aged from 1 week and 8 years. Moreover we

need to take in account that our FACS analyses were performed after expansion whereas Dellavalle et al. sorted the cells immediately after digestion (Dellavalle et al.2007).

In addition to these considerations, FACS analyses performed in our lab by Carlotta Camilli prior this project, demonstrated that both CD56+ and CD56- population express pericyte markers such NG2, AP and CD146. Moreover, a population of CD56+ cells was found within the original CD56- population following sorting, revealing a continuous switch in marker expression *in vitro*. These observations, together with the capacity of CD56+ cells to generate Calponin+ smooth muscle cells (Characterization performed by Carlotta Camilli prior this project), sustained the decision not to sort out this group from our study. In fact, sorting would compromise the fitness of the cells which might be a limit for the long-term aim of this project which is the clinical translation.

The capability of MABs to differentiate down to smooth muscle is another important feature of interest to us. In 2017 Urbani and Camilli also exploited their potential to generate smooth muscle for clinical applications. Theirs is the first study reporting smooth muscle regeneration by combining mesoangioblasts and decellularised scaffolds with daily administration of TGFβ. These considerations all together make MABs an ideal source for recapitulating the vascular smooth muscle compartment of the macro-vasculature which is one of the aims of this PhD project.

It is also important to highlight the contribution of Rafii's laboratory that identified an alternative source of human lineage-committed amniotic fluid (AC) cells that can be reprogrammed into proliferative functional ECs without utilizing pluripotency factors. Importantly, in 2007 was reported a rare AC subpopulation c-Kit+ (≤1%) that is multipotent (De Coppi et al. 2007). However, the majority of ACs are c-Kit- and are a more lineage committed. They showed that enforcing the expression of few ETS factors (ETV2, FLI1, ERG1) is possible to reprogram mature amniotic cells into ECs with clinical scale expansion potential (Ginsberg et al. 2015). This is very important

for clinical translational purposes; however, the potential of this cell source has never been exploited in a tissue engineering so far. In future, an interesting way to approach decellularised scaffold re-vascularization should be done by taking in account amniotic fluid derived ECs (for the endothelial compartment) and the mesenchymal portion of amniotic fluid as perivascular supporting cells. However, a lot of controversies are associated to the characterization of AFc and to the fact that they change a lot during the different stage of pregnancy and during their culture (Loukogeorgakis et al. 2017). Moreover, whether any cell of the mesenchymal compartment can serve as perivascular supporting cells for any district of the body is not sure yet. I could speculate that those cells might have different potential according on their foetal origin. All these considerations deserve to be taken in account and surely more studies should be done to characterize the very diverse pool of amniotic fluid stem cells.

7.2. Standardising vascular tissue engineering approaches: co-culture

One of the aims of this project is to enhance the tissue engineering potential of HUVECs by co-culturing them with a perivascular supporting cell. Moreover, I wanted to standardise the re-vascularization approach which seems to be very inconsistent in the vascular tissue engineering arena.

Therefore, I cultured HUVEC independently or in co-culture with MABs in a growth factor reduced Matrigel coating and EBM2 media (a basal media for endothelial cells without any growth factor) implemented with FBS.

In this set-up HUVECs without the addition of any cues, except for 3D environment of the Matrigel, started forming an interconnected web of tubing that resemble the microvasculature. In normal conditions those vessels like structure would start regressing after 24 hours till when they would completely disappear after 4-5 days.

In the co-culture MABs disposed themselves in a perivascular location supporting the vessel like structure and keeping them in culture for a longer time point up to 28 days. Another important point of this chapter is the fact that cells were able to form and maintain vessel like structures in a basal media without the addition of any growth factor and just the implementation of FBS.

The ability of cells in co-culture to emancipate from traditional growth factor-rich media is an important message because tissue engineering should aim to recapitulate the finely regulated complex of signalling guiding organ regeneration, which is difficult to achieve with traditional approaches in which cells are pulsed by cocktail of growth factors and small molecules. To move further in this approach, researchers should look for alternate growth conditions that would allow cells to be free of FBS. Although FBS contains numerous growth factors that are necessary for the maintenance and development of cultured cells, it is also well recognised that its undefined composition contains many fibrotic signals. This might explain perhaps the unconventional behaviour of the two cells in culture in the long run (after 7 days), when endothelial cells lose their harmonic organisation and MABs over-proliferate into the Matrigel (also consisting of a very undefined composition). Despite this, my interpretation of the experiment's message is that the presence of MABs allows endothelial cells to survive despite changes in their geometry. In a complete organ decellularised scaffold with more structural signals, this may not be a critical issue.

The stabilizing effect of mesenchymal cells on HUVECs is not a concept completely novel. In fact, in 2004, HUVECs and mesenchymal cells were embedded in a three-dimensional fibronectin-type 1 collagen gel and then inserted into mice. In this experiment, HUVECs were able to form tubes that connected to the host vasculature and remained patent up to 1 year (Koike et al., 2004).

However, whole organ tissue engineering often requires long period of culture into the bioreactor and therefore is important to make sure that vessel like structures can be maintained for long time points also in *in vitro.*

Maintenance of HUVECs for up to 28 days was never reported in previous reports. For this reason, the co-culture system appears to be the ideal way to approach the whole organ re-endothelialisation.

Ott's group published in 2015 a pioneer study introducing this concept and seeding through both arterial and venous routes in a rat decellularised lung (Ren et al. 2015). With this strategy, they reported a 75% endothelial coverage leading to a good barrier function. In this work the characterization of repopulated scaffolds was limited to asses presence of cells and barrier functions but not much was reported about the mechanisms lying between endothelial and perivascular cells in organ re-endothelialisation: whether perivascular cells had a beneficial effect on the re-endothelialisation in this context has not been elucidated.

Nevertheless, still many works attempted organ revascularisation without taking in account the perivascular compound.

Ott's laboratory itself published two later studies in the lung to proof scalability to human size decellularizing pig and human lungs and using epithelial and endothelial cells. In those occasions the perivascular compartment was not taken in account (Gilpin et al., 2016; Zhou et al., 2017). Seeding HUVECs only was the main re-vascularisation strategy used also in many works in the liver (Baptista et al., 2011; Shirakigawa et al., 2013; Takebe et al., 2014; Bao et al., 2015; Verstegen et al., 2017), kidney (Song et al. 2013, Du et al. 2016). and intestine (Kitano et al. 2017.).

The latter paper is a work published by Ott's laboratory where decellularised segment of rat intestine were repopulated with iPSC-derived epithelial cells for 14 days and HUVECs for 3 days (Kitano et al. 2017). Even though this is a work published after the one of 2015 in lung, they did not take in account the perivascular compound and other imitations of this work will be discussed later in this paragraph. The number of papers after the work of (Ren et al. 2015) that address the whole organ re-vascularization without the involvement of a perivascular cell source reflect the

confusion present in the field and the lack of awareness on how the perivascular compound is pivotal to regenerate an organ vasculature.

The first intent of this PhD thesis is clarifying this issue and my outcomes remarkably encourage the use of a co-culture approach to address organ re-vascularization.

In fact, this project aims at the repopulation and functional evaluation of the vasculature of a rat intestine. For this reason, I assessed whether the data achieved in plastic were valid also into the preserved vasculature of a decellularised rat intestine.

I developed a seeding method that allowed cells to distribute evenly throughout the scaffold. Moreover, my data shows that by co-seeding MABs and HUVECs is possible to achieve a better coverage compared with the seeding of HUVECs only. HUVECs, when they were seeded without the support of MABs, appeared scattered in the scaffold and they displayed remarkable cells death after 7 days of dynamic culture onto the bioreactor. On the contrary the presence of MABs allow the system to outperform the previous strategy. The co-culture allowed the endothelium to be stable after 7 days of dynamic culture and that resulted in a better endothelial coverage. This was consistent with the results in Matrigel.

One of the main hurdles of the vascular tissue engineering is the possibility of recreating a lumenalised endothelium. My data show that seeding HUVECs and MABs into the preserved vasculature of a decellularised intestine resulted in HUVECs lining the vessels while MABs surrounded them and disposed themselves in a typical perivascular position. The vasculature was also patent in many areas of the scaffold.

Finally, one of the most important function of the endothelium is to promote the formation of a barrier. Scaffold repopulated with MABs and HUVECs retained small molecules similarly to the intestine freshly isolated and therefore were able to outperform scaffold seeded only with HUVECs.

In this chapter, finally, I report the use of the perivascular compartment as pivotal for generating a patent vasculature with good barrier function and durability, with poor

results obtained instead when only HUVECs were used. Therefore, the co-culture approach should be the best way to choose for whole organ vascular tissue engineering.

All this seem very promising however reaching the capillary compound is still one of the main troubleshoots. The fact that I could not repopulate this compound represent definitely a no go for clinical translation. In fact, re-endothelialisation needs to be achieved at 100% to guarantee its function. Indeed, even a little fragment of matrix exposed would lead to cloths when blood flow would occur. Moreover, the capillary compound represents the main area of communication between the organ and the resto of the body both for driving its regeneration and for gas and nutrient exchange. Therefore, a lot of work need to be addressed to tackle this problem.

One of the things to take in account is that I am addressing the re-vascularization process into an adult decellularised scaffold. The rationale behind the use of decellularised scaffold is the fact that they are able to retain all the molecular cues that drive cells to behave as in their native environment. If this is true, the signal retained in a mature adult vasculature is a homeostatic signal rather than proliferative signal. Endothelial cells seeded into the adult vascular matrix may not receive the signals necessary to drive a sprouting angiogenesis as they do in in the first hours into Matrigel. Homeostasis is also necessary in the vasculature, however, understanding the mechanisms that drive cells to make the suitable changes to invade and form the capillary compound must be a pivotal aim for the field.

A possible way to do that is studying furtherly the components of the vascular matrix. More work should be done in order to understand what component of the vascular matrix (also in different developmental stages or in tumours) might boost a sprouting angiogenesis rather than homeostasis:

I. *In vitro* experiments on functionalised plate with vascular associated extracellular matrix proteins.

II. qPCR analyses on angiogenic or quiescence genes

III. Coating of those proteins on the preserved vasculature of the decellularised organ.

Moreover, in future works, other stimuli should be taken in account. Gradience of hypoxia and VEGF are two important factors for sprouting angiogenesis nut they have never been taken in account in studies that address whole organ vascular tissue engineering.

7.3. Vascular smooth muscle in whole organ vascular tissue engineering

From a whole organ tissue engineering perspective, the overall range of differently sized vessels which form the vascular tree must be regenerated because microvasculature alone cannot support organ function. Indeed, smooth muscle cells, which represent the main difference between microvasculature and larger vessels, have a crucial role in delivering vasculature function. They deliver vaso-motiliy and contribute to the biomechanical blood flow response (Neff et al., 2011). Consequently, derivation and culture of vascular smooth muscle cells represent a significant step toward regeneration of the whole vasculature.

Different approaches have been exploited in order to find a suitable and reliable cell source that could give rise to the vascular smooth muscle compartment. Nevertheless, while in the specific field of blood vessel tissue engineering, which is intended to reconstruct a single vascular grafting, a great deal of effort has been made to create a smooth muscle layer (Jung et al., 2015, Tresoldi et al., 2015, Zhao et al., 2010) the field of whole organ revascularization has concentrated on regenerating pericytes to provide a robust microvasculature.

Transforming growth factor-beta 1 (TGFβ) seems to be the principal pathway involved in smooth muscle differentiation process.

As mentioned previously, the human Mesoangioblasts (hMABs) used in this work, is able to differentiate down to smooth muscle by stimulating this pathway. In fact this blood vessel-associated mesodermal progenitors is bi-potent (Minasi et al. 2002) (A. Dellavalle et al. 2011): it is easily harvested from skeletal muscle tissue biopsies, cultured under standard condition and differentiated towards either skeletal muscle or smooth muscle, the latter via TGFβ administration(Arianna Dellavalle, Sampaolesi, Tonlorenzi, et al. 2007) (Cossu and Biressi 2005) (Tagliafico et al. 2004)

In chapter 3 I established that MABs can also differentiate down towards smooth muscle without TGFβ administration when they are in co-culture with HUVECs. I didn't know yet whether they retained this capability also into the decellularised scaffold. Co-seeding of HUVECs and MABs into the preserved vasculature of a decellularised rat intestine resembled the same behaviour observed in 2D when HUVECs were cultured together with MABs and the latter differentiated towards smooth muscle. In particular I observed a PDGFRβ positive population of cells, that represent the undifferentiated pericytes, relocated in a peripheral position surrounding CD31 positive endothelial cell. Moreover, I observed a SM22 differentiated population surrounding the vasculature. Therefore, the newly formed vasculature featured cells oriented in a native manner: from inside out I had endothelial cells lying the vessel drawing a patent endothelium, MABs surrounding them and a smooth muscle layer around the vessel coming from the pericytes precursor. This is the first time that this achievement was reported in the contest of whole organ tissue engineering.

However, this work requires a scale-up in order to understand if the newly generated smooth muscle layer is able to sustain the mechanical stress and pressure of big vessels. The pulsatile nature of the blood flow, indeed, expose smooth muscle cells to a mechanical stress which is also important to stimulate other functions such phenotypic switching, migration, alignment, and vascular remodelling (Mantella, et al.

2015). Moreover, the whole full layer of smooth muscle of the tunica media (and the one present in the tunica externa in the veins) has to be repopulated to guarantee the correct functions of the vasculature.

Another aspect that is important to highlights is that in this work I use a vein source of endothelial cells (HUVECs) but I try to repopulate both the vein and the arterial branch. Has never been investigated whether the cues into the scaffold drives the suitable arterial versus venous endothelial cell fate specification.

A rising number of paper reports that endothelial cells identity is plastic towards arterial or venous differentiation and therefore arterial cells contribute to venous vessels, and venous cells may differentiate into arteries (Basac et al. 2017).

In 2014 Cong et al. reported both in Zebrafish and in mouse retina that endothelial tip cells not only invade avascular tissues during the sprouting angiogenesis, but that they can change their direction of migration and ultimately migrate against the advancing vascular front. They showed that this behaviour is necessary for artery development (Xu et al. 2014). More recently Pitulescu et al. confirm this theory and observed that Dll4–Notch signalling induces an endothelial fate switch towards arterial ECs the angiogenic growth front (Pitulescu et al. 2017). All those studies say that endothelial cells are plastic and that artery are form by vein-derived endothelial cells tips. This encourages the use of a vein EC source for tissue engineering proposes.

Future works involve:

I. Scale up experiment on pig aortas should be performed in order to understand if the smooth muscle layer generated is able to sustain the mechanical stress and pressure of big vessels.

II. Functional assays on the smooth muscle.

III. Assess the vein artery specification of ECs into the preserved vasculature of the decellularised organ.

8.4. Unveiling, in vitro, the mechanisms behind the endothelial driven smooth muscle differentiation by MABs

Then, I tried to unveil *in vitro* the mechanisms that are behind smooth muscle differentiations by MABs when they are co-cultured with HUVECs

When I co-cultured HUVECs and MABs in plastic in EGM2 media, MABs showed expression of smooth muscle markers such SM22 and Calponin after seven days of culture.

Surprisingly this phenomenon happened without the administration of TGFβ which is the canonical pathway used to drive MABs' smooth muscle differentiation (Arianna Dellavalle, Sampaolesi, Tonlorenzi, et al. 2007) (Cossu and Biressi 2005) (Tagliafico et al. 2004). TGFβ is not contained in the EGM media but endothelial cells may produce it and guide MABs smooth muscle differentiation. To assess that, I co-culture HUVECs and MABs in presence of a TGFβ inhibitor and I observed that smooth muscle differentiation decreases only slightly and still a lot of differentiated Calponin positive cells were present.

How do MABs decide between pericytes and smooth muscle fate?

Many reports have implied that endothelial cells and mural cells are closely associated, and that their interactions are necessary for the control of vessel development, stability, remodelling, and function in vivo and in vitro. However, the mechanism through which endothelial and mural cells communicate with one another is only partially known. Several ligand-receptor systems have been involved in heterotypic cell interactions to govern vascular formation and maintenance. Endothelial cell-secreted PDGF-B is known to be required for pericyte recruitment to newly formed vasculature via PDGFR-BB.

Relevant for this thesis, Cappellari et al. demonstrated that DLL4 and PDGF-BB activation causes embryonic myoblasts to transition to the perivascular lineage without erasing its myogenic memory (Cappellari et al. 2013).

Moreover, the Notch ligand DLL4 has been shown essential for vascular formation. When DLL4 is inhibited in developing mouse retinas, excessive proliferation of non-functional vasculature occurs. Blood vessels become unorganized and display increased sprouting and microvessel density, but decreased perfusion and function (Pitulesku et al. 2017). The microvessels created by the hyperproliferation of endothelial cells in the absence of DLL4 are immature and they lack coverage by α-smooth muscle actin (α-SMA) cells, which ultimately lead to this paradoxical scenario in which there are more vessels yet less perfusion and functionality. While this paper shows a clear correlation between the absence of Dll4 and absence of a mature smooth muscle layer, it doesn't provide a clear observation of how smooth muscle cells invade the vasculature and if they come from the pericyte. An hypothesis which would combine previous reports and the data of this thesis is that endothelial cells recruit other stromal cells (such committed muscle cells) from the avascular tissue through PDGR-BB and commit them to a pericyte lineage thanks the contribution both of notch signalling (through Dll4) and PDGF-BB signalling (as described in Cappellari et al. 2013). The bidirectional plasticity between a committed myoblast and pericyte might be extended also to the smooth muscle phenotype which is a default capacity of pericytes (such MABs, used in this thesis).

The signal provides by the presence of DLL4 and absence of PDGF-BB (which may be switch off in a stabilised vascular tissue) represents one of the signals that might drive MABs decision to switch into a smooth muscle phenotype. This hypothesis guided the investigations conducted in this thesis, however, does not exclude the possibility that other signals might influence this decision.

To test this hypothesis, I co-culture MABs with HUVECs ablating notch signalling: *we knew that one of our collaborators could provide a cell line knock out for jagged 1.*

Unfortunately, there wasn't another cell line also knock out for dll4 and therefore we use the antibody. This was the best way in our hands to test our hypothesis.

in particular I design a co-culture setting which involved MABs with HUVECs Jagged1 -/- or with HUVECs in presence of Dll4 antibody or a combination of the 2 conditions. Interestingly, when jagged1 was ablated I did not observe and significant decrease of smooth muscle markers. However, when Dll4 or both ligands were absent, MAB smooth muscle differentiation was completely inhibited.

Since Dll4 is an important endothelial component, its lack may affect other cellular compounds leading endothelial cells to lose the capacity to drive MABs smooth muscle differentiation. I sectioned the problem by coating Notch ligand Dll4 and jagged1 in the presence or absence of PDGF-BB in tissue culture dishes. Culturing MABs on those coated dishes, I mimicked the endothelial Notch signal without taking in account all the other endothelial compounds. qPCR analyses confirmed that smooth muscle differentiation is orchestrated by Dll4 and in particular it follows Dll4 - Notch 3 axes.

7.5. Pericytes: "tissue-specific" mesodermal progenitors

An inspected data was that the SM22 positive cells population (coming from the pericyte precursor) appeared to migrate outside the defined vasculature structure and to disposed themselves at various distances within the scaffold invading the compartment normally belonging to the visceral smooth muscle of the intestine.

To the best of my knowledge, very little is known about the formation of gut smooth muscle in both humans and mice. Two theories are the most widely accepted in the field: one reports the presence of a cKit+ progenitor capable of giving rise to both longitudinal smooth muscle and Cajal's myenteric interstitial cells; the other reports the presence of a cKit+ progenitor capable of giving rise to both longitudinal smooth muscle and Cajal's myenteric interstitial cells (ICC) (Torihashi et al. 1997, Cluppel et

al. 1998). The second identifies mesothelial cells (a kind of epithelial cell found on the coelomic cavity) as playing a key role in the development of visceral smooth muscle via an epithelial-mesenchymal transaction (Rinkevich et al. 2012). However, none of these hypotheses account for the probable contribution of a pericyte precursor, which is the surprising finding shown in our tissue engineered gut vasculature.

taking advantages of a *TNAP-AP-CreERT2:R26R* mouse model I corroborated my initial hypothesis that pericyte can, indeed, be the progenitor of the mesodermal derivative of the tissue where they reside. This theory was first enounced by Paolo Bianco: he was pioneer in the concept that ubiquitous MSCs with equal capacities do not exist, but that “tissue-specific” mesodermal progenitors can be recruited into a mural cell fate, providing a plausible mechanism by which pericytes are generated, and how they act as a local progenitor cell source (Sacchetti et al., 2016). In this concept, I follow his footsteps and to my knowledge this is the first time that it was proven in the visceral smooth muscle, within a gut tissue engineering model.

I also tested whether this behaviour was maintained also in the adult mice, therefore two months old mice were also induced with tamoxifen and sacrificed after one month. In this case cells appeared to be in the visceral smooth muscle much more infrequently showing that this behaviour is conserved in the adult life but is not the main strategy for regenerating the visceral smooth muscle.

This is comparable to what Cossu's laboratory reported in earlier skeletal muscle research. (Arianna Dellavalle, Sampaolesi, Tonlorenzi, et al. 2007).

They discovered that vessel-associated skeletal muscle pericytes (MABs) are a second myogenic precursor with equal myogenic potency to satellite cells but a different phenotype. In addition, in a subsequent study, they employed TN-AP-CreERT2 mice (the same model used in this study) to track the destiny of vessel-associated cells during postnatal muscle development. They discovered that their contribution to postnatal skeletal muscle occurs mostly during the first month of postnatal development and thereafter becomes sporadic in adult mice (Arianna

Dellavalle, Sampaolesi, Tonlorenzi, et al. 2007). My experiments in the *TN-AP-CreERT2* mice model indicate finally that pericytes in the intestine represent an alternative source of visceral smooth muscle precursors, other than only vascular smooth muscle precursors. However, the capability of my skeletal muscle MABs to integrate into visceral smooth muscle, other than invading the visceral smooth muscle compartment into a decellularised scaffold, hasn't been exploited yet. Therefore, human MABs GFP+ were injected into the visceral smooth muscle of immunocompromised mice. Significantly, after one month post injection human MABs integrate into the visceral smooth muscle layer expressing the mature smooth muscle marker smooth muscle MHC. This represent the proof of principle that this vessel associate skeletal muscle pericytes can contribute also to generate the visceral smooth muscle for clinical applications taking advantages of their default capacity to generate vascular smooth muscle. In fact, to my knowledge, no differences have been ever reported between visceral and vascular smooth muscle. After all, what I reported is actually very analogue to what happen in the mesothelium.

Initially mesothelial cells were reported to convert to a mesenchymal cell phenotype and migrate to contribute to the vascular smooth muscle of the intestine (William et al 2005). Only subsequently Rinkevich et al. demonstrated, by genetic lineage tracing, that mesothelial cells have an important role also in the visceral smooth muscle generation both in development and post-natal growth (Rinkevich et al. 2012). Equally to what I have observed, this is another indication that visceral and vascular smooth muscle feature very close identity and that cells that are able to differentiate towards smooth muscle can contribute to both visceral and vascular SMC.

It's fascinating how this phenomenon was unveiled in a tissue engineering set-up within a decellularised scaffold. This reveals that tissue engineering could be used to test cells behaviour in their natural environment and dissect complicated process to fewer variables, in a more controlled fashion, without the interference of the effects other compounds or problems related to promiscuity of markers.

Future works:

I. Are MABs able to rescue the normal smooth muscle phenotype of an injured mice?

II. Confirming this phenomenon in other organs

7.6. In vivo anastomoses

Whole organ vascular tissue engineering still lacks a long term in-vivo characterization. In fact, many are the number of papers that describe the implantations of revascularized scaffolds *in-vivo* but only for short time points or with a very poor *in vivo* characterization. Many works address the in-vivo evaluation only for few hours and with a heparin treatment prior seeding in order to enhance the capacity of the vascularised scaffold to be perfused *in vivo.*

For instance, the endothelial cell line EA HY926 was used to recellularise an acellular pig liver lobe, coated with heparin gel that facilitated cell adhesion and grafting. This scaffold did not cause thrombosis when it was grafted heterotopically into pigs for 1h (Hussein et al., 2016). Bao et al. functionalized pig decellularised scaffolds with heparin over 3 days prior seeding of the cells. With this technique, they demonstrated how the liver did not cause sudden thrombosis when grafted in the piglets ' infra-hepatic space for 1 hour (Bao et al., 2015).

Atala's group used MS1 endothelial cells to re-vascularize porcine livers and they were able to sustain perfusion for 24h after Orthotopic liver transplant *in vivo*. (Ko et al., 2015).

Ren et al. (2015) co-seeded HUVECs and hMSCs, or iPSC-derived ECs and PCs, onto a decellularised lung scaffold in 2015. In this example, the lungs were orthotopically implanted in-vivo for three days, and in-vivo evaluation was restricted to demonstrating the existence of cells and perfusability. Furthermore, the

mechanism that exists between endothelial cells and perivascular cells in this situation has not been identified.

Meng et al. implanted rat sinusoidal endothelial cells onto a rat liver scaffold in 2019. They were able to identify blood flow after 8 days of implantation thanks to Doppler ultrasonography (Meng et al. 2019).

Significantly, Shaheen et al. re-vascularized decellularised whole porcine livers with HUVECs and implanted them heterotopically into immunosuppressed pigs, sustaining perfusion for up 15 days. (Shaheen et al. 2019).

Relevant for this thesis project is the work of Kitano et al. He decellularised segment of rat intestine and he repopulated it with iPSC-derived epithelial cells for 14 days and HUVECs for 3 days (Kitano et al. 2017). The intestine was subsequently implanted in a heterotopic model consisting of a subcutaneous graft in the neck, anastomosed to the vasculature and provided of two-end stomas. The graft was maintained for 4 weeks however the quality of the re-vascularization was not evaluated after the in-vivo implantation. They did assessed presence of CD31 positive cells into the scaffold but coverage, patency throughout the whole scaffold and presence of mural compartment important for a mature endothelium was not taken in account.

After all, in my experience scaffold repopulated with only endothelial cells resulted in a poor degree of coverage end functionality *in-vitro* which reflected the poor outcome that I would have observed also in the *in-vivo* implant

Moreover, the functionality of the graft was assessed by delivering nutrients into the lumen of the engineered intestine, via the stoma. Even though absorption of nutrient into the rat blood stream was observed, the authors could not rule out the possible free diffusion from the acellular areas of the scaffold which was not completely re-epithelialized.

In my work I do take in account the perivascular compound, but I still are not able to achieve the full endothelialisation of the capillary compartment that still represent the main hurdle of vascular tissue engineering. Due to the lack of the micro-vasculature

I did not address the re-epithelialisation of the scaffold prior *in-vivo* implant. In fact, without micro-vasculature there wouldn't be a link able to deliver the nutrient absorbed from the epithelium to the macro-vasculature.

Also, for the lack of a micro-vasculature I decided not to directly anastomose the vasculature to the host. In fact, blood cloth would occur if pieces of matrix are exposed to the blood stream.

For all this reasons I decide to implant the scaffolds heterotopically into the omental sheet of NSG mice to evaluate if the graft would promote the rapid ingrowth of the host vasculature into the scaffold to avoid tissue necrosis.

This experiment revealed that scaffold co-cultured with both cell types anastomosed better. Remarkably, the presence of MABs promoted the recruitment of more host smooth muscle cells which is a sign of vessel maturity regardless their origin. As previously affirmed, the vascular smooth muscle has a pivotal role to play in providing vasculature function (Neff et al., 2011).

The latter result reflects the long term durability of the vasculature within the scaffold co-seeded with both cell types and the loss of cells over time of the scaffolds with HUVECs only.

The presence of the perivascular compartment stabilises the environment of the scaffold which does not show either ki67 or Caspase 3 markers. On the contrary scaffold seeded with HUVECs only display a major degree of cell death indicated by the strong Caspase 3 signal

Finally, all this study has a great potential that need to be exploited and scaled-up. However still a big gap stands between tissue engineering and the clinical translation. One of the biggest achievements would be long-term perfusion in orthotopic models, while current studies showed short time points limited to a few days. I could speculate that this is due to the fact that blood clothing occurs after the first stages of implantation. In fact, to date no studies achieved a fully confluent regenerated

endothelium including the capillary compound. This become a problem also when it gets to test the functionality of the vasculature that can't resemble the physiological one. In order to reach long term patency of the blood vessel network, researcher should focus on delivering ex-vivo a stable and functional vasculature that provides an adequate and confluent endothelial layer.

In conclusion, has come the time for tissue engineering for scaling up to functional human sized and preclinical models and vascularisation will be the fundament to achieve this aim.

7.7. Final remarks

Someone may argue that the fact that pericytes and endothelial cells form more stable vascularization is not particularly novel. Indeed, the goal of our research is not just to demonstrate that perivascular cells are required for a stable vascular tree; this is a well-established notion in the literature.

Here, we aimed at using this pivotal concept to serve the ambitious purpose of having a long lasting and functional vascular tree in a tissue engineered organ. In fact, several works attempted organ revascularisation without taking in account the perivascular compound. As we discussed extensively in this thesis, Harald Ott's group was the first to publish a pioneer research introducing this in 2015 by seeding iPSC-derived endothelium and perivascular cells in a decellularised lung (Ren et al. 2015). Moreover, the group published two follow up studies to prove scalability to human sized lungs, using epithelial and endothelial cells. In these papers, the perivascular compartment was not taken in account (Gilpin et al., 2016; Zhou et al., 2017). Ott's studies are a microcosm of the confusion in the field: while co-culture of endothelial and perivascular cells is a well-established concept, there is still work to be done to translate this technique into organ tissue engineering using primary adult cells and

validate a standard technique for revascularizing whole organs. Indeed, HUVECs alone, have been exploited for the re-vascularisation in several other organ engineering strategies including liver (Baptista et al., 2011; Shirakigawa et al., 2013; Takebe et al., 2014; Bao et al., 2015; Verstegen et al., 2017), in the kidney (Song et al. 2013, Du et al. 2016) as well as in the intestine (Kitano et al. 2017), with little success.

In regards of the novelty of our work, an important aspect that should be considered is the anatomical positioning of the cells that, so far, has not been addressed in the literature. Our engineered vasculature features cells oriented in a native fashion: with the endothelial cells lined the vessel, drawing a patent endothelium and the mesoangioblasts surrounding them, forming a smooth muscle layer around the vessel. In fact, while in the specific field of blood vessel engineering a great deal of effort has been made to create a smooth muscle layer (Jung et al., 2015, Tresoldi et al., 2015, Zhao et al., 2010), this is, to our knowledge, the first time that this achievement was reported in the context of whole organ tissue engineering.

Finally, possibly the most innovative message of our paper is the contribution of MABs to visceral smooth muscle development and regeneration. The mechanisms of gut smooth muscle development, both in human and mice, are still matter of debate. Two are the most accredited theories in the field: *i)* one reports the presence of a cKit+ progenitor able to give rise to both longitudinal smooth muscle and the myenteric interstitial cells of Cajal (ICC) (Torihashi et al. 1997, Cluppel et al. 1998), while the second *ii)* identifies mesothelial cells (a type of epithelial cells that lies onto the coelomic cavity) to have an important role in the generation of visceral smooth muscle via an epithelial-mesenchymal transition (Rinkevich et al. 2012). However, none of those theories take into account the possible contribution of a perivascular precursor to the visceral smooth muscle, as reported in our work. Similarly, other tissues in the body have shown a contribution of perivascular precursor towards the tissue homeostasis (Mohamed T. et al Biomaterials. 2019 Oct; 217: 119284.). Here we have

shown that these cells contribute to the formation of smooth muscle during development. Further experiments will be necessary to understand if these cells can also contribute to the visceral smooth muscle, in response to a tissue damage.

Finally, the potential long term aim of our approach would be providing a platform to treat congenital new-born diseases, such as short bowel syndrome, where even a 5cm transplantation of a functional small intestine would revert the patient to a sufficient absorption of nutrients.

The scope of this thesis is therefore to provide a solid approach for organ pre-vascularisation, using two adult cell sources. A further scaling up into large animals will be certainly required to land into a preclinical study. However, this work is still very relevant to the field, since the revascularized segments measured up to the required 5cm.

While relevant to the field, our work should be taken with limitations related to the fact that HUVECs, rather than an intestinal-specific endothelium were used in the decellularised intestine. ECs are specialized to the organ of origin; while HUVECs can replace some of the more general functions they may lack some of the more specialised cell functions which resident ECs play in intestinal capillaries. Further studies may reveal an even finer orchestration of the endothelium, which would be relevant for intestinal engineering.

Furthermore, we have not yet investigated the cross-talk between the microvasculature and the intestinal mucosa which may reveal further interesting cellular interaction relevant to intestinal development and tissue engineering. Despite the clinical relevance of the mucosa, the current work focused on underpinning the mechanisms of vasculature regeneration and the role of perivascular cells.

Tissue engineering approaches, like the one used here, could help to test cell behaviour within their natural environment in a more controlled fashion by reducing variables. Importantly this would allow the dissection of complicated processes without the interference of effects of other cellular components, which is the obstacle

in animal models. Finally, after revealing some of the fundamental processes of vasculature regeneration in the gut, it will be now important to look at the contribution of other systems such as nerves, lymphatic vessels and mucosa.

Appendix figures chapter 3

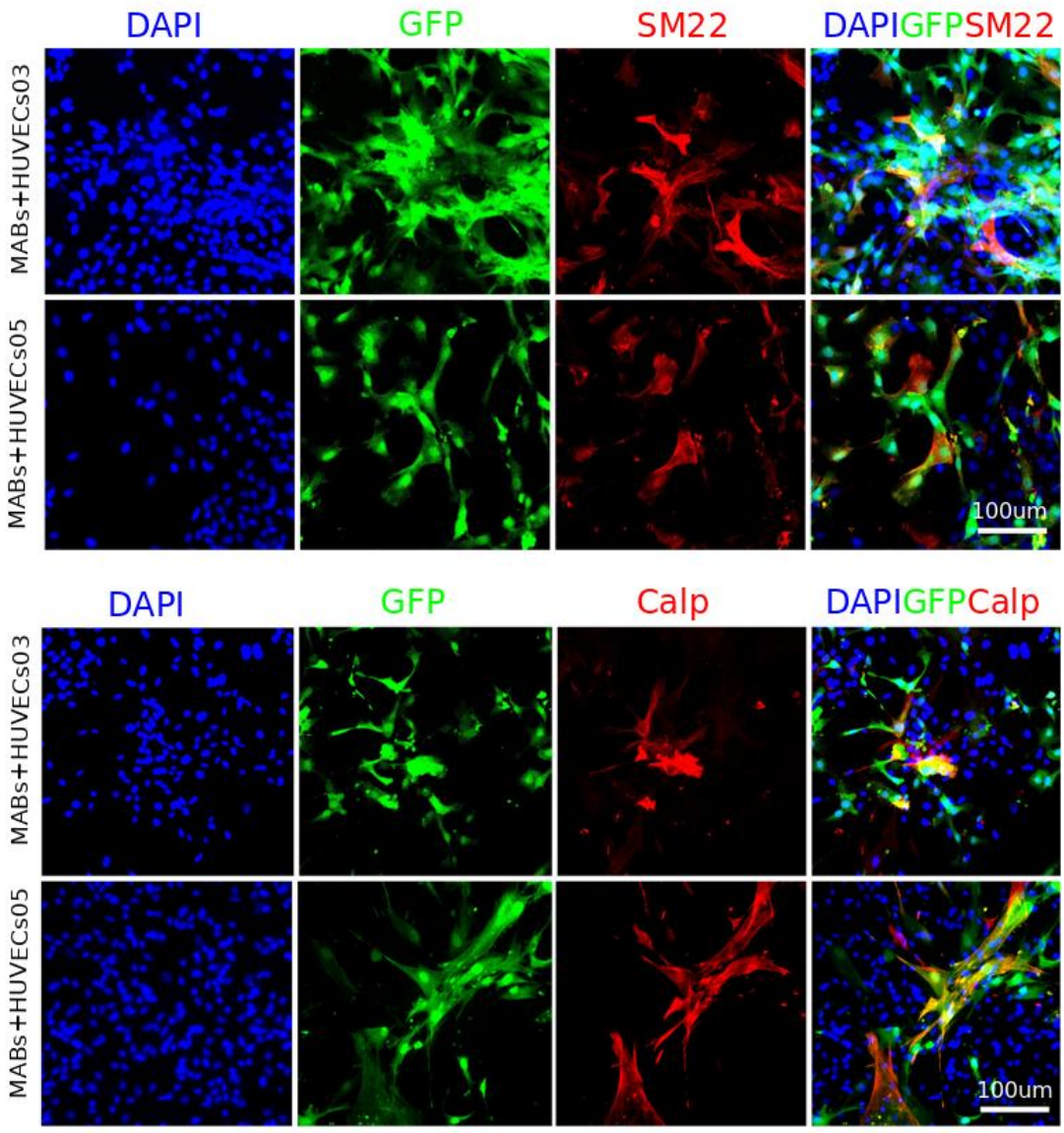

Appendix Fig 3.7: co culture of HUVECs and MABs. Immunostaining immages of MABs03-05 GFP+ (in green) cultured independently or in co-culture with huvecs (unstained blu nuclei), stained for SM22 or Calponin (in red).

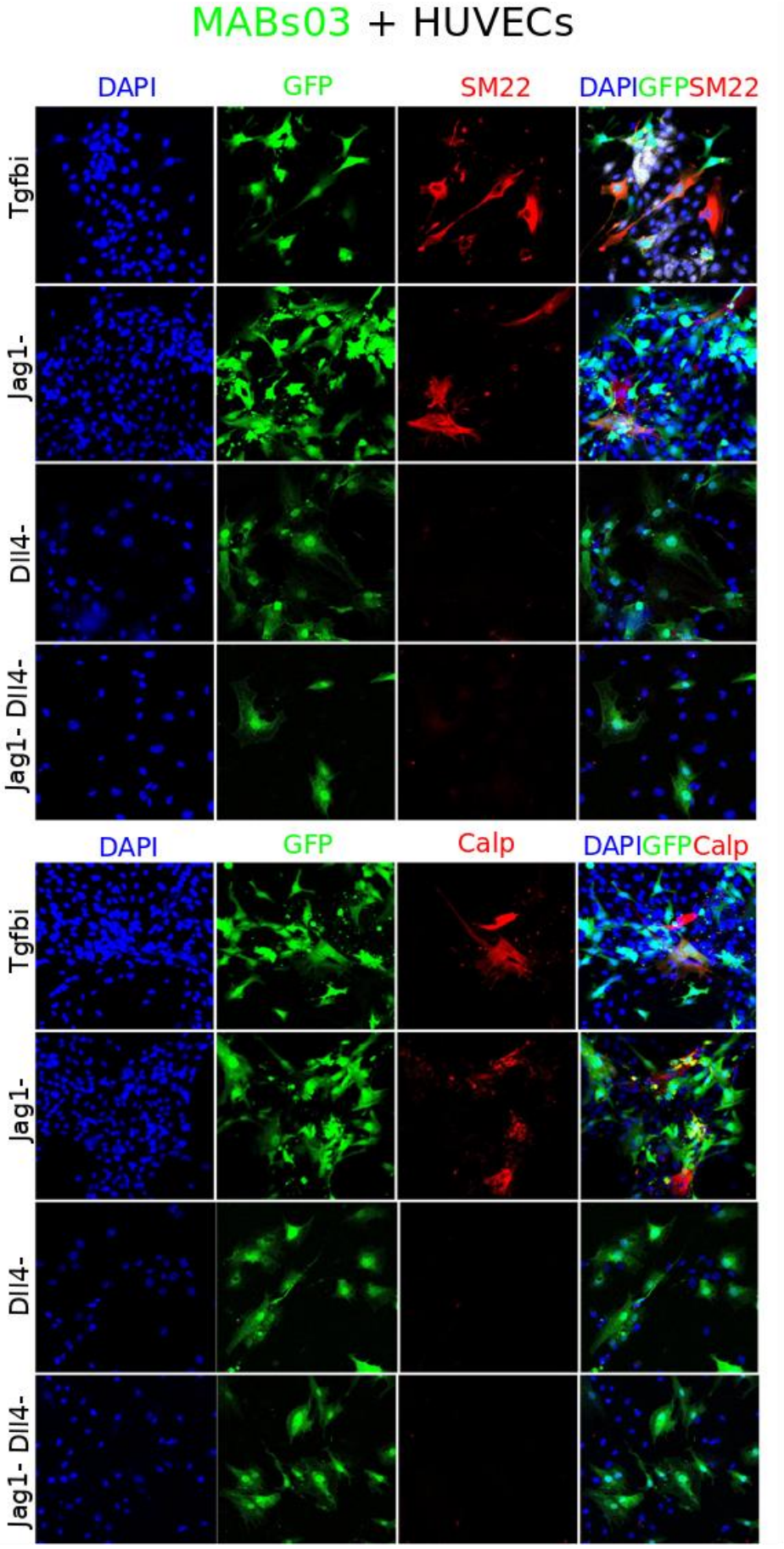
MABs03 + HUVECs
DAPI
GFP
SM22
DAPIGFPSM22
Tgfbi
Jag1-
Dll4-
Jag1- Dll4-
DAPI
GFP
Calp
DAPIGFPCalp
Tgfbi
Jag1-
Dll4-
Jag1- Dll4-

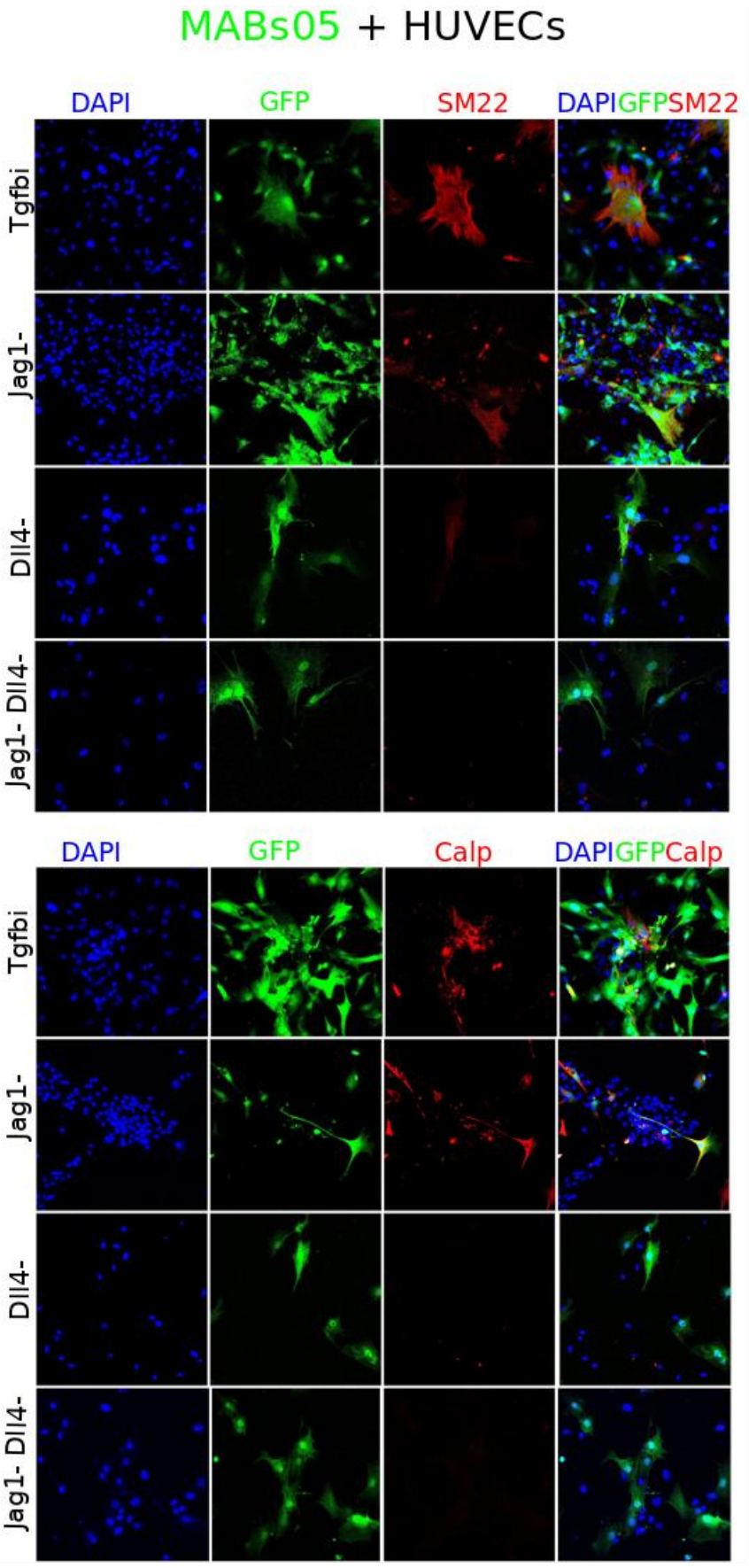
MABs05 + HUVECs
DAPI
GFP
SM22
DAPIGFPSM22
Tgfbi
Jag1-
Dll4-
Jag1- Dll4-
DAPI
GFP
Calp
DAPIGFPCalp
Tgfbi
Jag1-
Dll4-
Jag1- Dll4-

Appendix Fig. 3.8: Blocking notch pathway in MABs From top to bottom, immunofluorescence staining for SM22 and Calponin of MABs03-05 cultured with HUVECs in presence of Transforming Growth Factor beta (TGFb) inhibitor, MABs cultured with HUVECs Jagged 1 -/- or with HUVECs in presence of Dll4 antibody or a combination of the 2 conditions. These panels shows, from left to right, single channels of DAPI (in blue) MAB's GFP signal (in green), Staining for SM22 and Calponin (in red) and merges of the 3 signals.

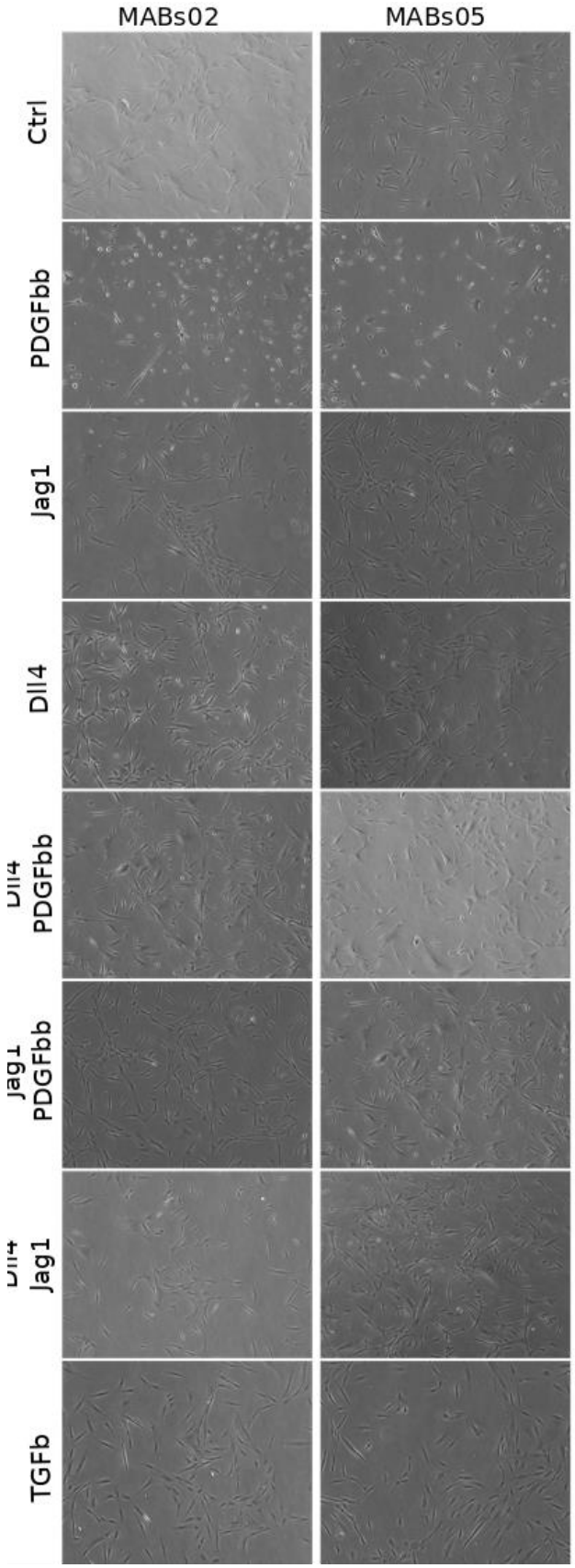
MABs02
MABs05
Ctrl
PDGFbb
Jag1
Dll4
Dll4 PDGFbb
Jag1 PDGFbb
Dll4 Jag1
TGFb

Appendix Fig. 3.9. Bright field images of MABs02 cultured on dishes coated with Dll4, jagged1, Dll4 and jagged1 , and w/o PDGF-BB, MABs were also cultured in normal condition and in presence of Transforming Growth Factor beta (TGFb) as negative and positive control.

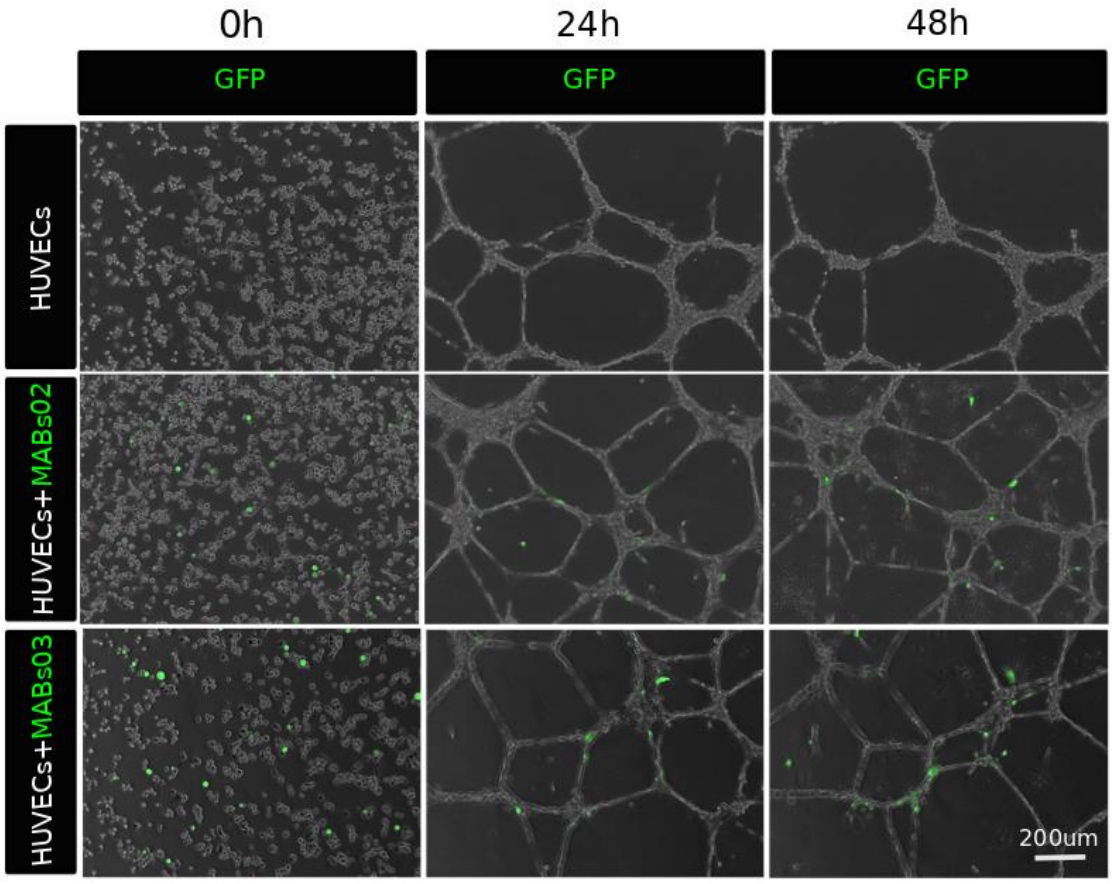

Appendix Fig. 3.14: a. Confocal images of MABs (green) and HUVECs in Matrigel cultured together at 1:5 ratio, or independently in a media without growth factor (EBM2). HUVECs branched with MABs positioned in perithelial position supporting angiogenesis. This appendix figure shows the results obtained from MABs02-03. MABs 05 is shown in Fig.3.14

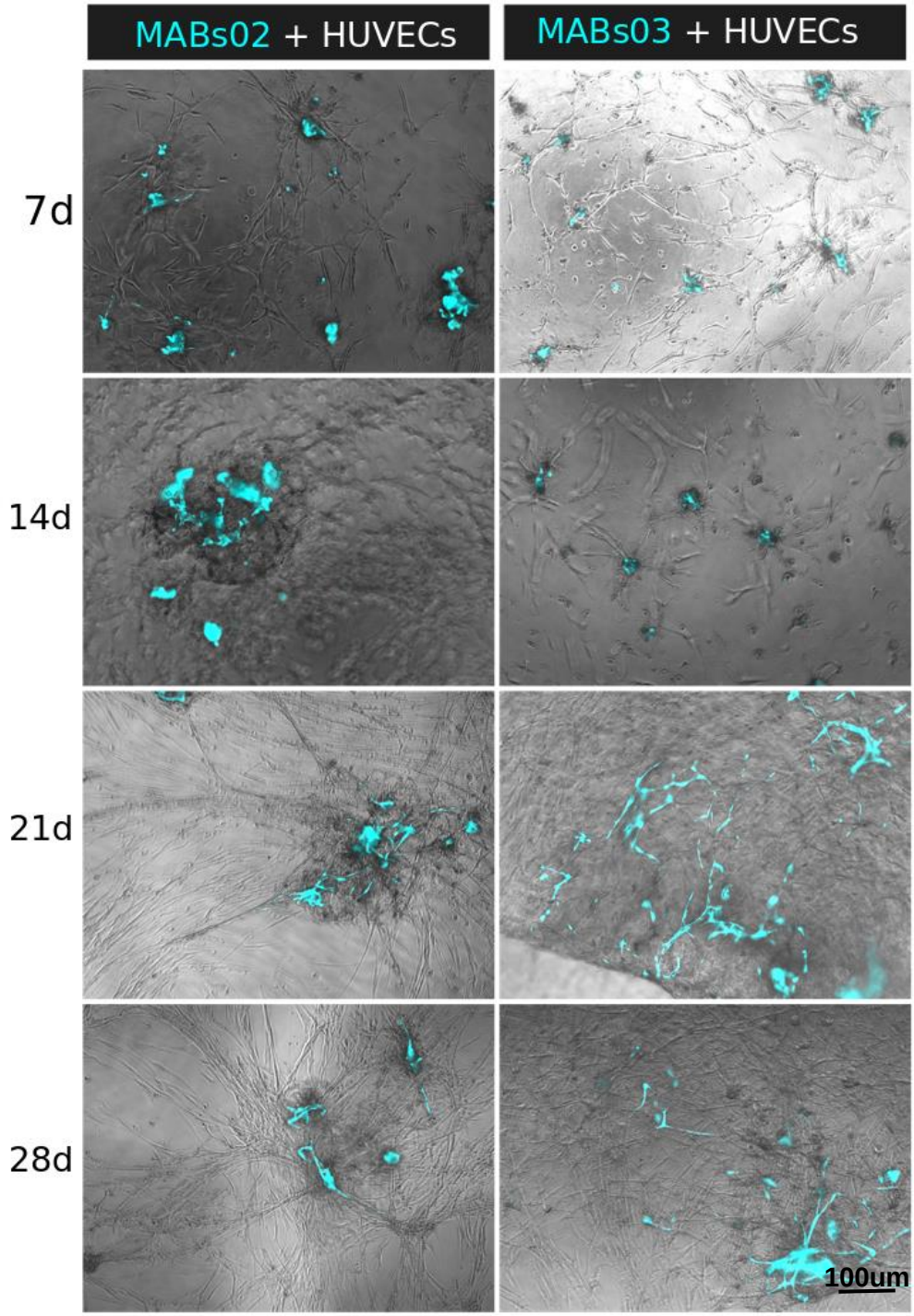

Appendix Fig. 3.15: Confocal images of MABs and HUVECs (cyan) in Matrigel cultured together at 1:5 ratio in a media without growth factor (EBM2) kept for 28 days. The figure shows the results obtained with HUVECs and MABs02-03. The other biological replicates (MABs02—03) are shown in the Appendix figure 4.2. MABs 05 and HUVECs cultures independently is shown in Fig.3.15

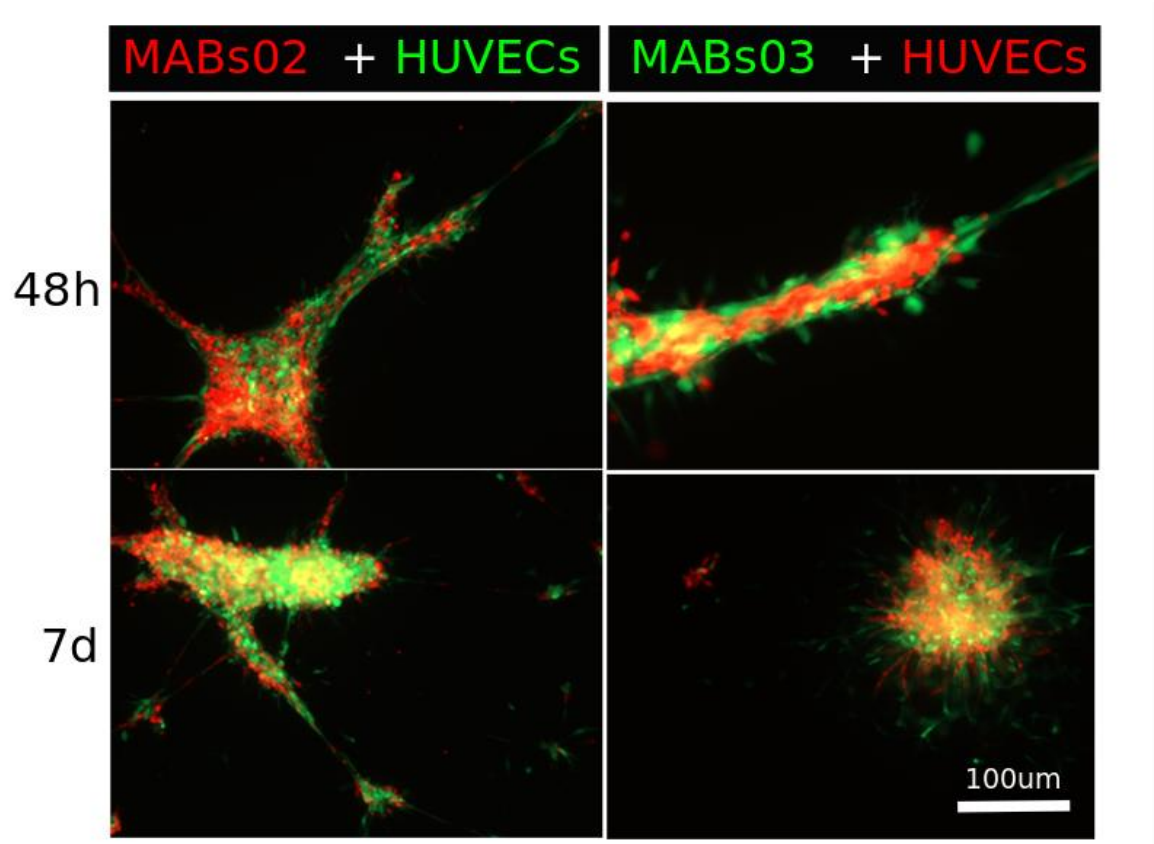

Appendix Fig 3.16: Confocal images of MABs GFP (in green) and HUVECSs mCherry (in red) in Matrigel cultured together at 1:5 ratio in a media without growth factor (EBM2) at 48h and 7 days. Images shows the interaction between MABs and HUVECs is maintained even after the loss of canonical vessel like structure organisation at 7 days. The figure shows the results obtained with HUVECs and MABs02-03. The other biological replicates (MABs05) is shown in fig. 3.16.

Appendix figures chapter 4

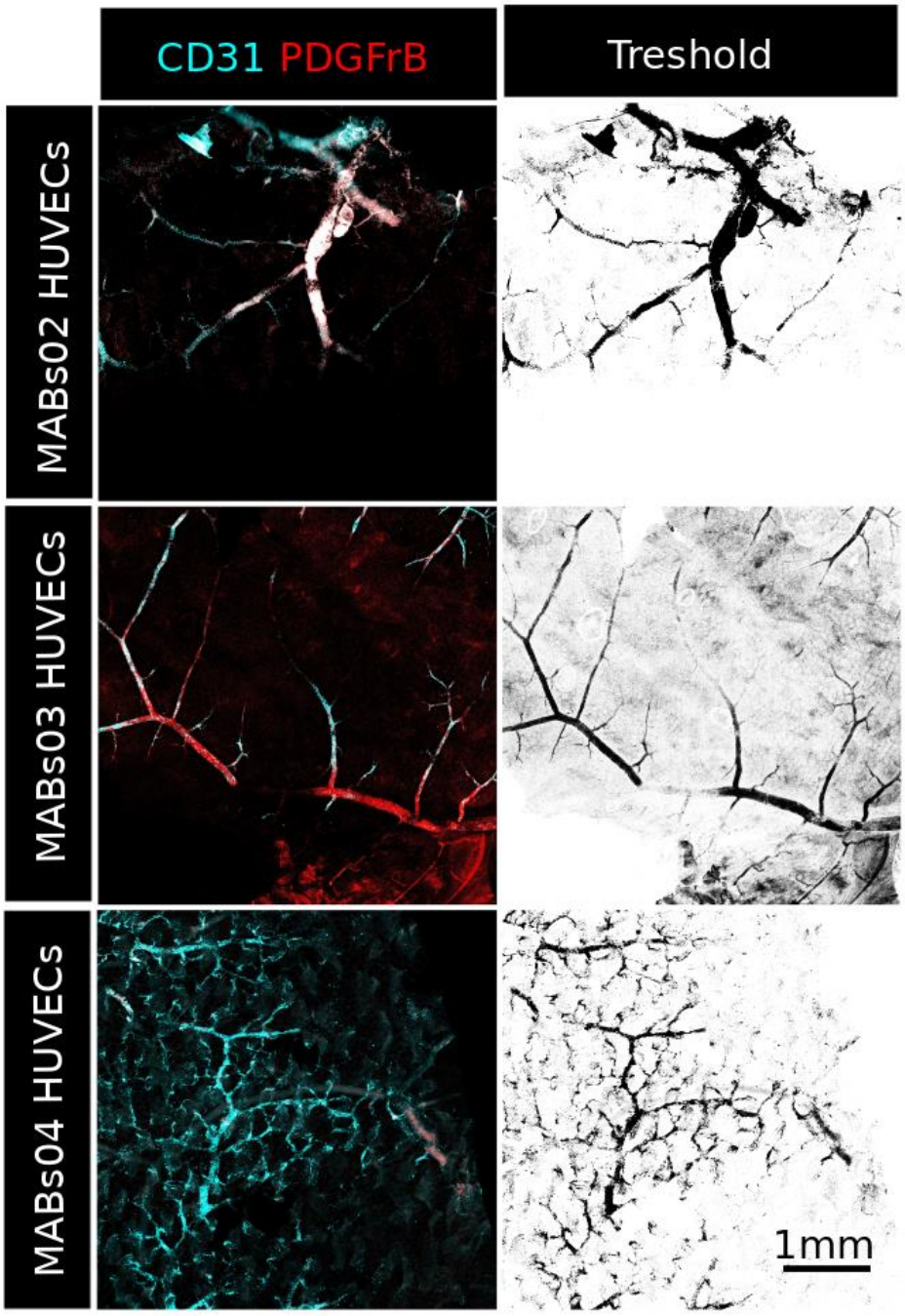

Appendix Figure 4.3 Endothelial coverage into the preserved vasculature of a decellularized rat intestine. whole mount staining for PDGFrB and CD31 (staining respectively MABS02-03-04 and HUVECs) performed on scaffold co-seeded with HUVECs and MABs02-03-04, and they were imaged through confocal microscope. The images are representative of 4 mm^2 of scaffold (tile scan 5 field of view times 5 at 20x magnification). Those imaged were

thresholded through ImageJ in the same way to calculate the coverage. Biopsy MABs05 and the control scaffold seeded only with HUVECs is shown in figure 4.3.

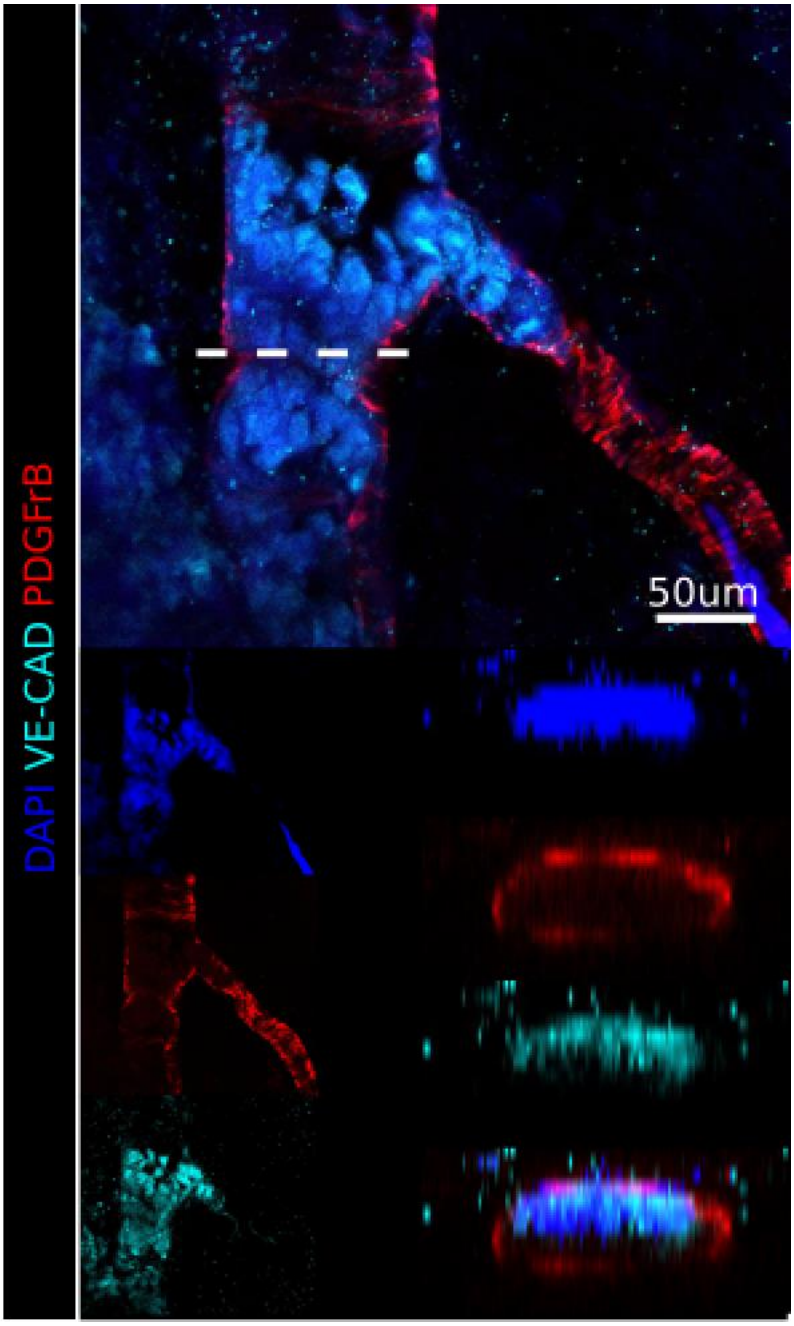
DAPI VE-CAD PDGFrB
50um

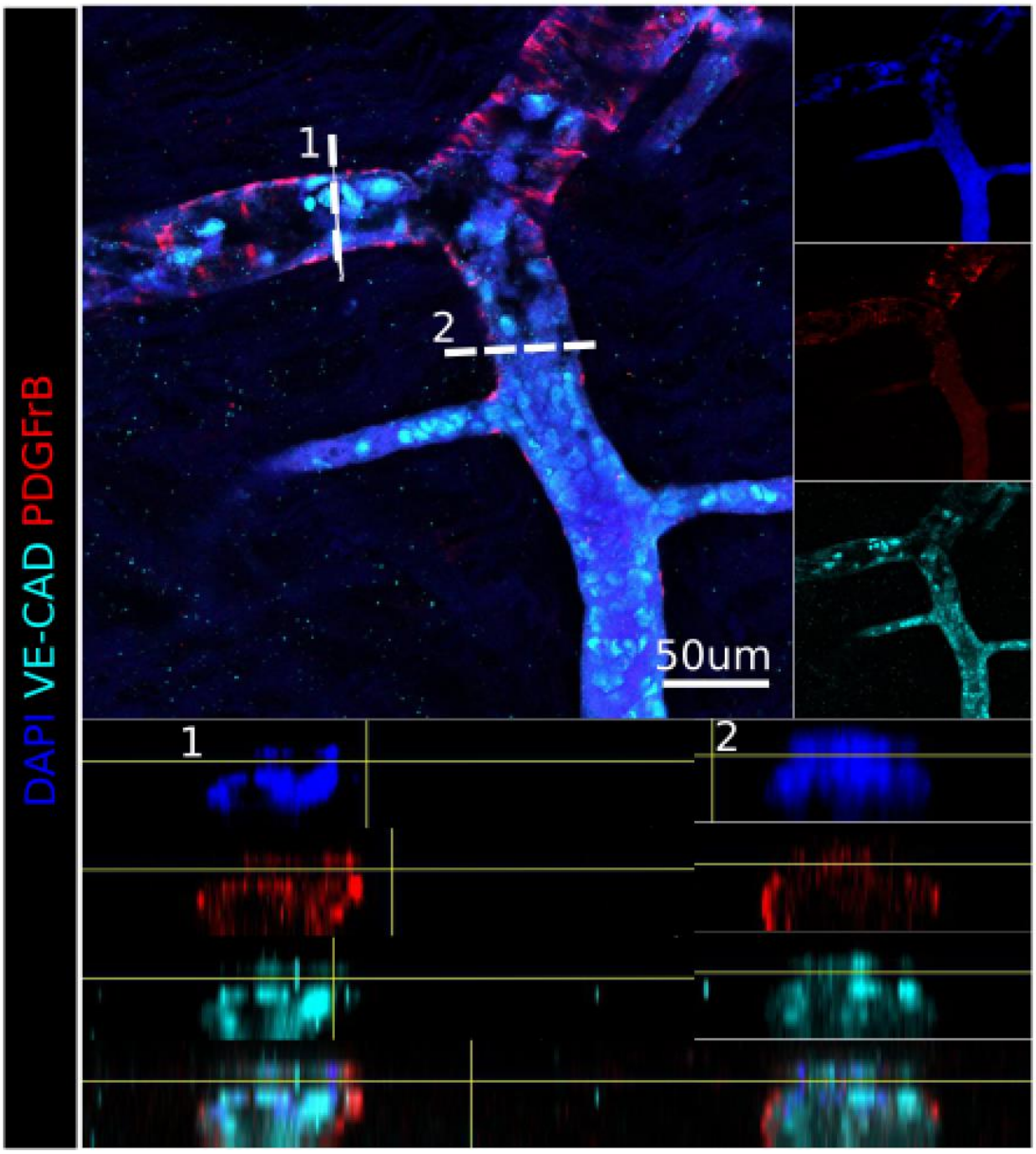

Appendix figure 4.5a. Assessment of the vessel patency after re-vascularization. In Figure 4.5a the patency of the repopulated scaffold (with HUVECs and MABs05) has been shown through LDL uptake. Here are displayed confocal images of repopulated scaffold with HUVECs and MABs02 (top image) and MABs04 (bottom image) stained for VE-Caderin and PDGFrB. Orthogonal views of the dashed areas of the z-stak confocal images shows the vasculature featuring a patent lumen with endothelial cells lying the vessel and Pericytes surrounding it. In the bottom panels of both images are displayed the individual channels of the 3 lumen dashed above.

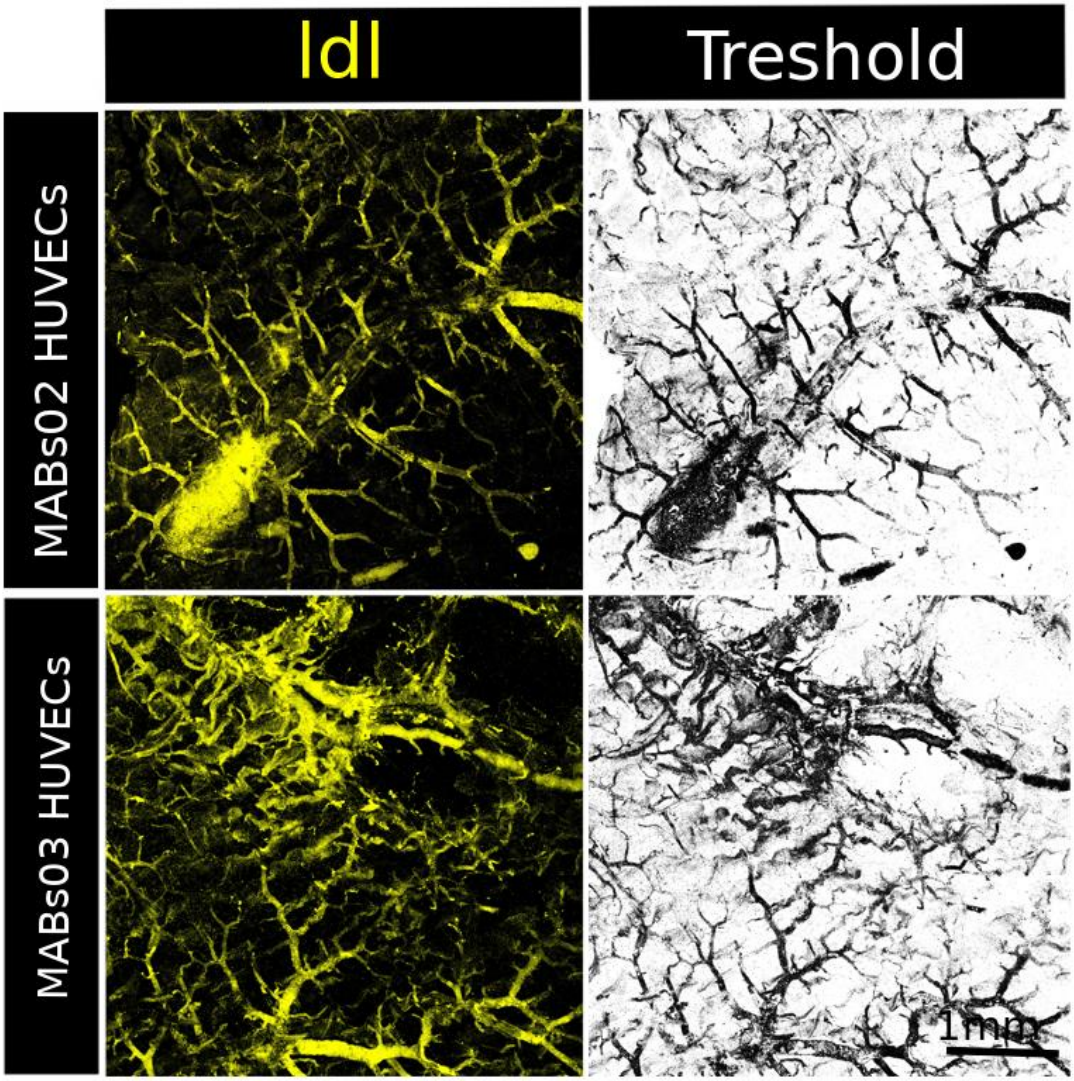

Appendix Figure 4.5b. Assessment of the vessel patency after re-vascularization. injection of labelled LDL through the mesenteric artery and vein of the re-populated vasculature reveals presence of endothelial cells (yellow, since they have uptaken the fluorescent LDL), and the areas of the scaffold that are perfused. Confocal images representative of 4 mm^2 of scaffold (tile scan 5 field of view times 5 at 20x magnification). Those imaged were thresholded through ImageJ in the same way as I previously described for the endothelial coverage. These are representative images of repopulated scaffold with HUVECs and MABs02-03.

Appendix figures 5

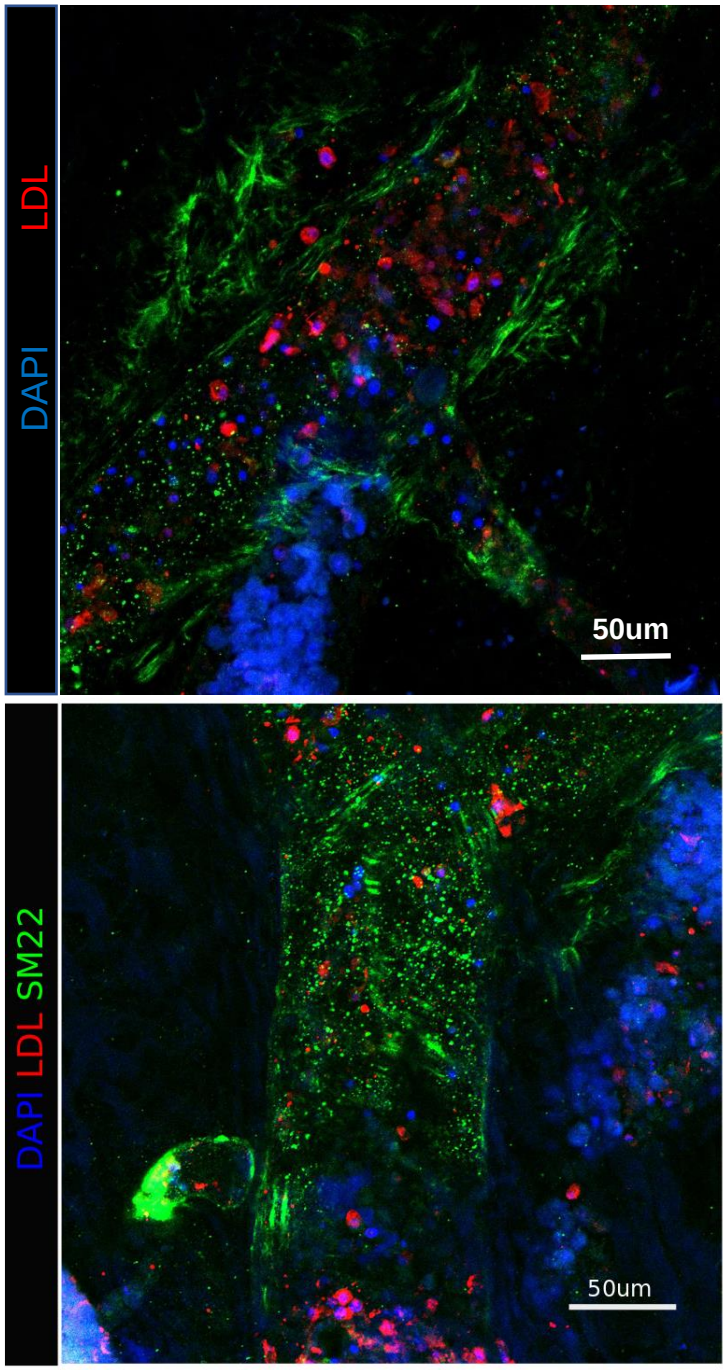

Appendix figure 5.2: **confocal images of the re-vascularized scaffold with both MABs and HUVECs shows presence of smooth muscle into the scaffold**. This appendix figures displays similar results of the Fig 5.2 obtained with MABs02 (top image) and MABs04 (bottom image). In this case the presence of HUVECs within the scaffold was assessed by LDL uptake, whereas SM22 staining demonstrates MABs03's ability to differentiate down to

smooth muscle within the scaffold. The SM22 marker is found along the vasculature's edge, as well as in a section of the scaffold that belongs to the visceral smooth muscle.

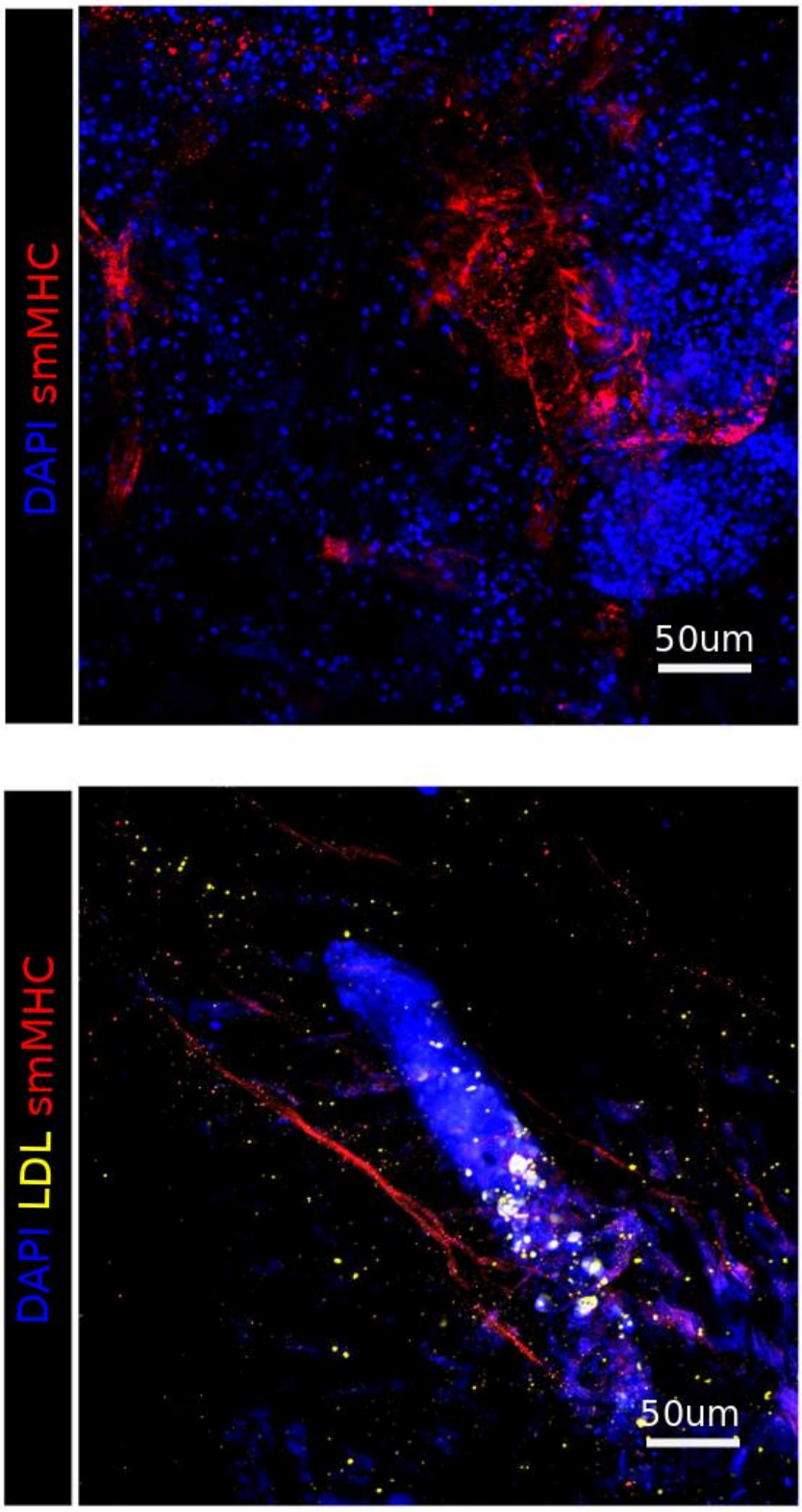

Appendix figure 5.4: Confocal image of a re-vascularized vessel with HUVECs and MABs. This appendix figures displays similar results of the Fig 6.4 obtained with MABs02 (top image) and MABs04 (bottom

image). Both MABs biopsies co-seeded into the preserved vasculature of a decellularized rat intestine could differentiate and shows mature smooth muscle marker such smooth muscle MHC.

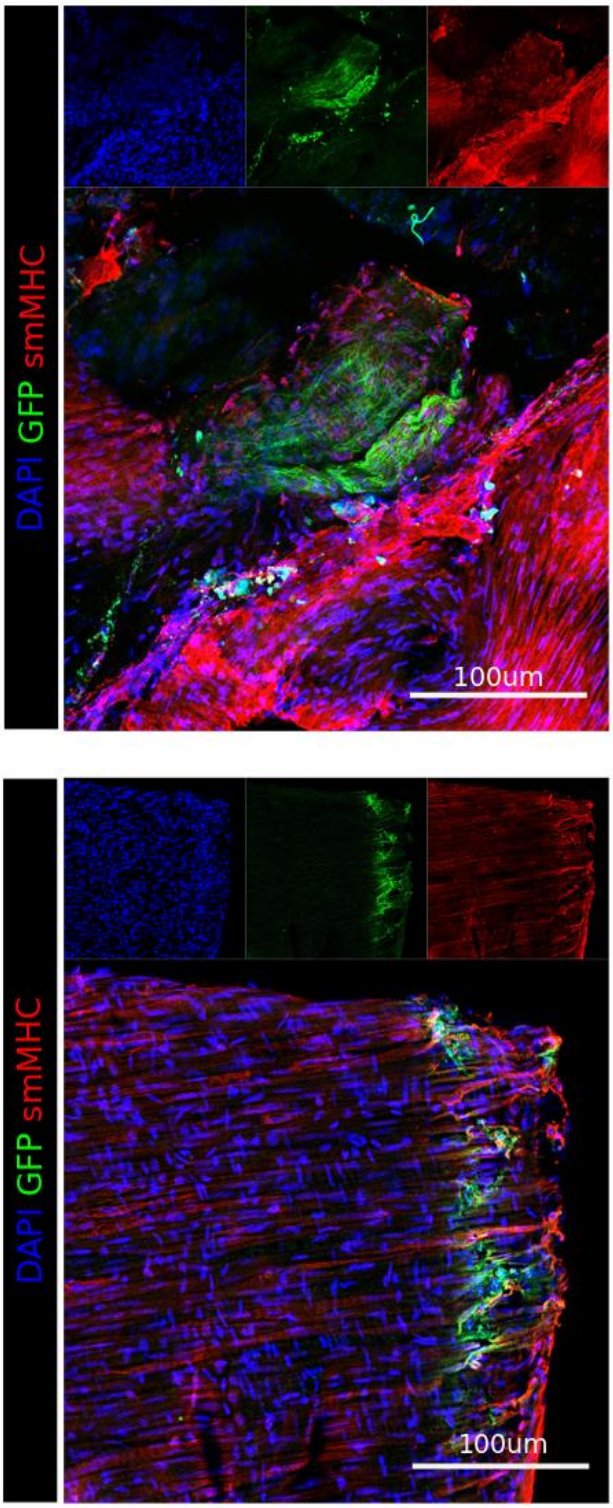

Appendix figure 5.10: Whole mount staining for Smooth muscle MHC (Red) on mouse intestines retrieved 1 month after MABs GFP+ (green) injection. The staining was performed only on the visceral smooth muscle layer that was isolated after the harvest of the intestine. MABs02 (top image) and MABs04 (Bottom image) resulted

integrate into the visceral smooth muscle layer expressing the mature smooth muscle marker smooth muscle MHC.

Appendix figures 6

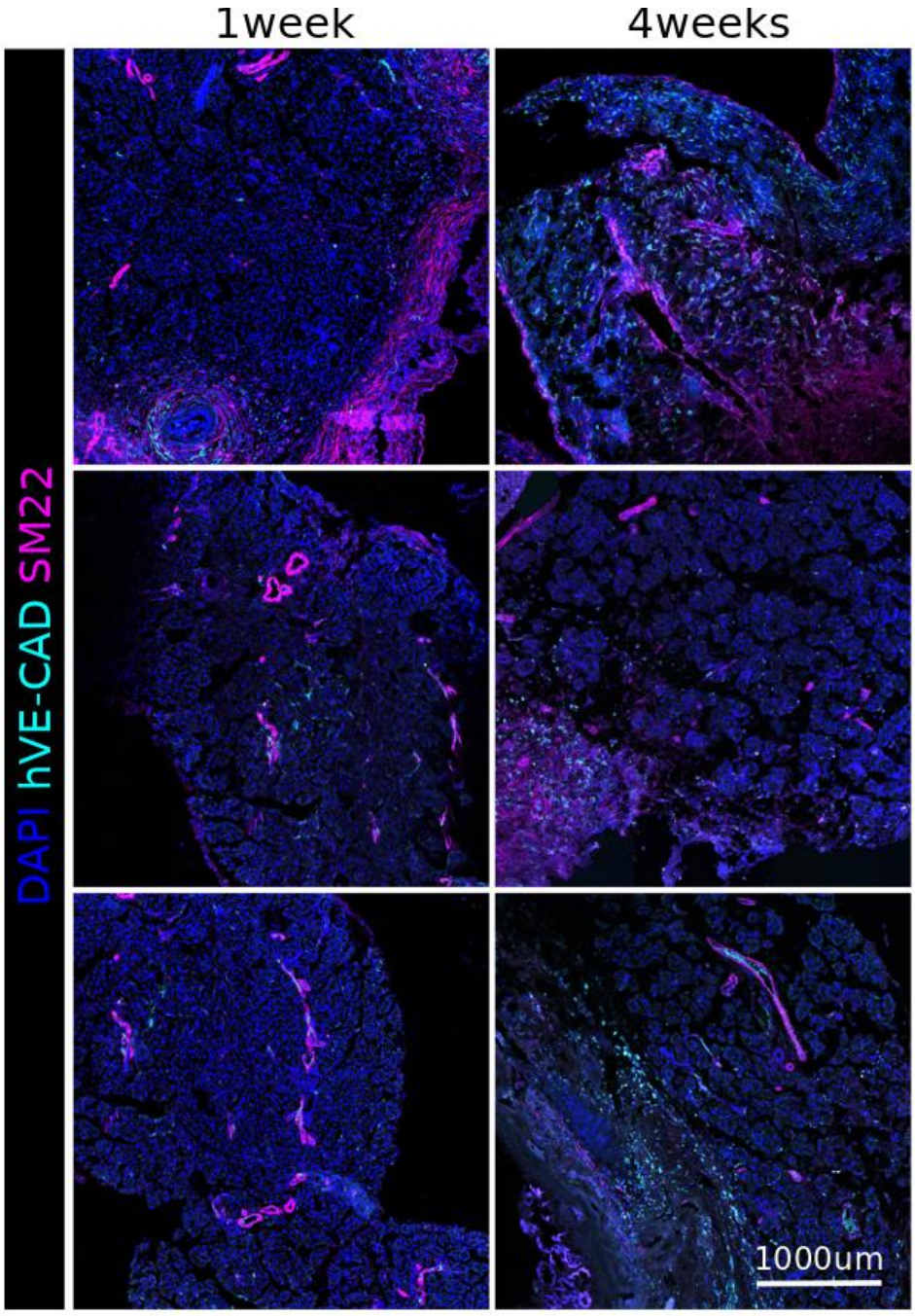

Appendix figure 6.2. Confocal images showing Immunostaining anti SM22 of sections of scaffolds co-seeded with HUVECs and MABs at 1 week and 4 weeks (the cyan signal staining for ve-cadherin was coming from the human ve-cadherin injection performed in vivo e not anti ve-cadherin antibody was supplemented in this staining). This appendix figure shows the results obtained by seeding (from top to bottom) MABs02, MABs03, MABs05.

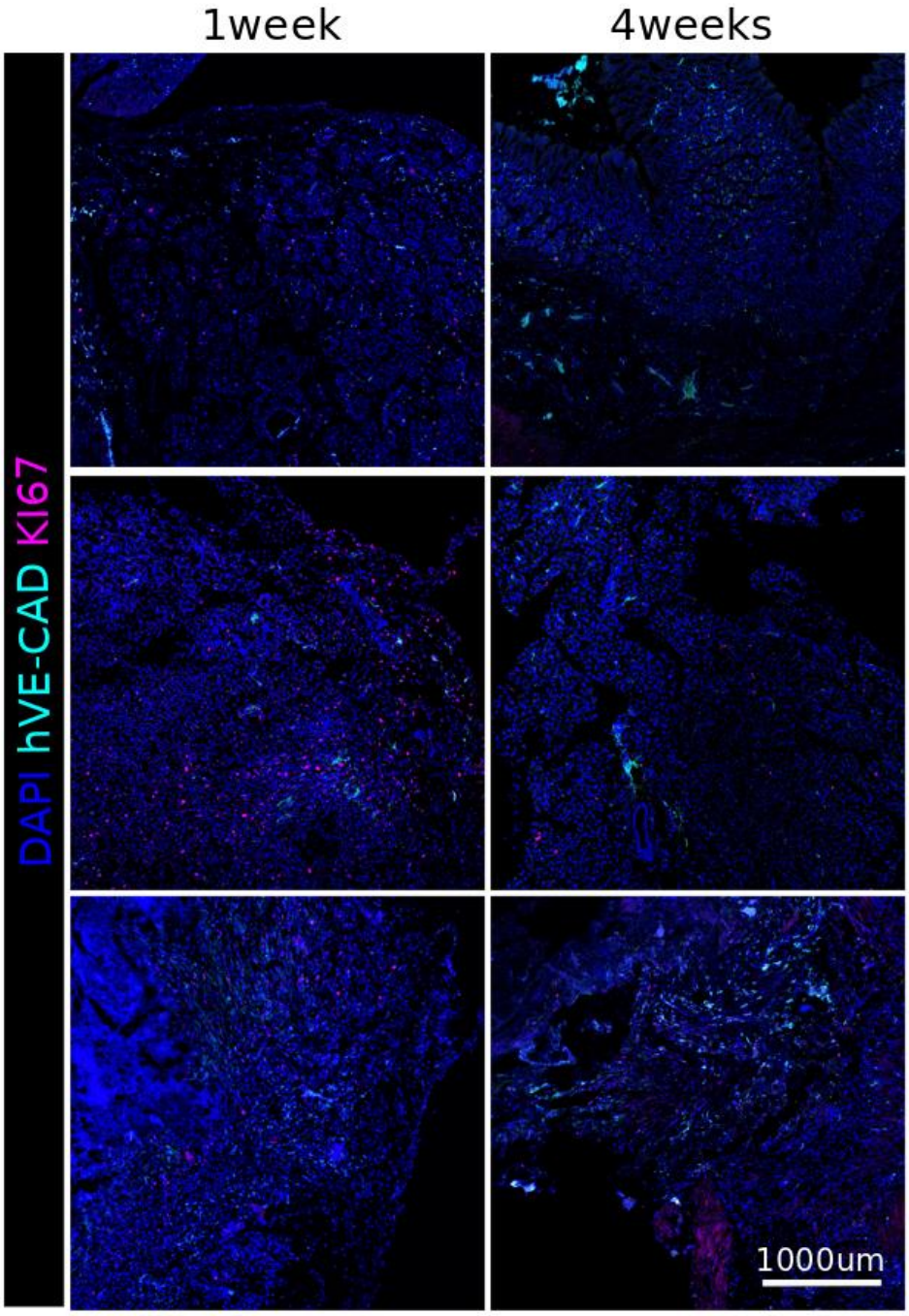

Appendix figure 6.4: Confocal images showing Immunostaining for Ki67 (in magenta) at 1 week and 4 weeks.

This appendix figure shows the results obtained by seeding (from top to bottom) MABs02, MABs03, MABs05.

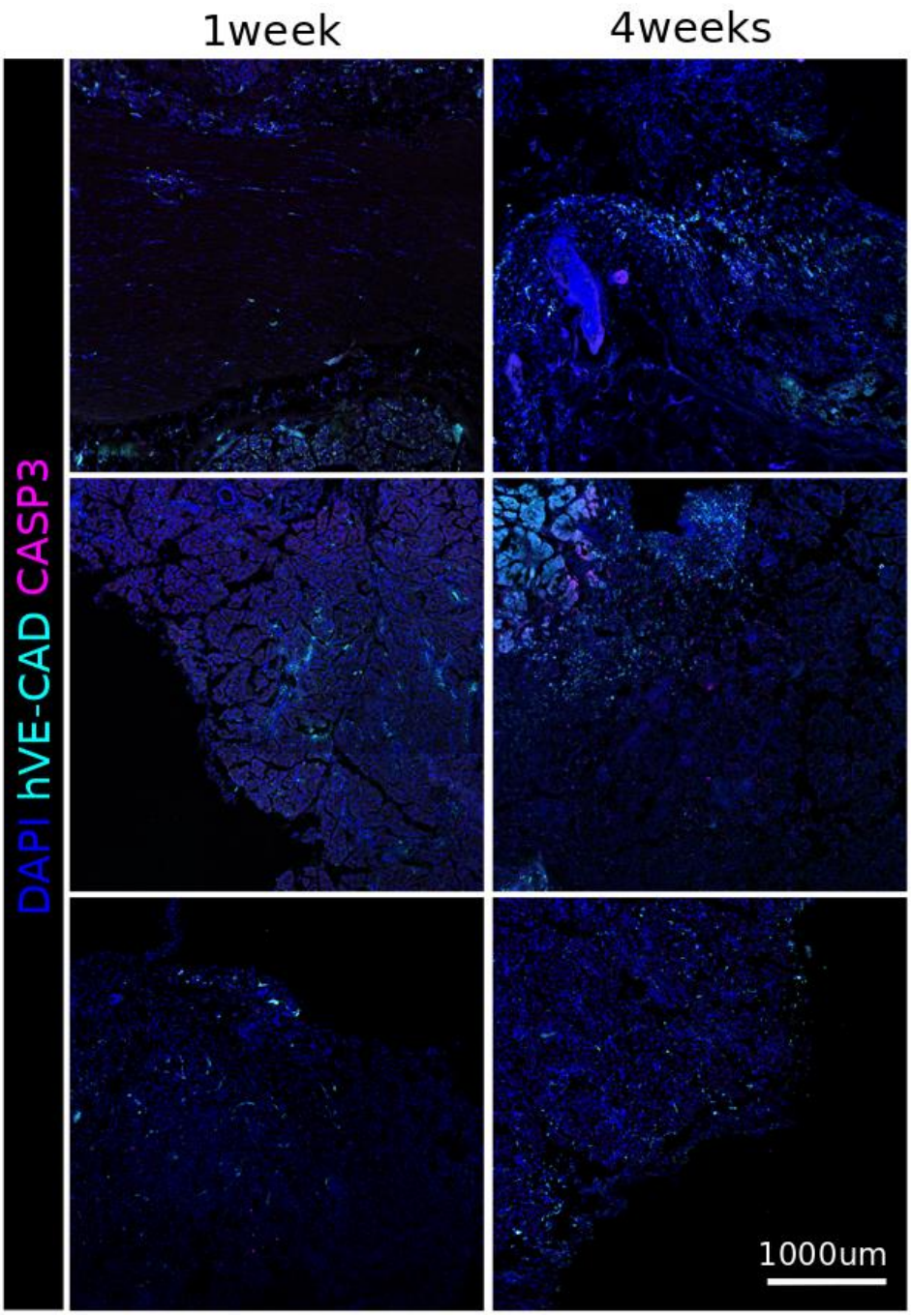

Appendix figure 6.5: Confocal images showing Immunostaining for Caspase-3 (in magenta) at 1 week and 4 weeks. This appendix figure shows the results obtained by seeding (from top to bottom) MABs02, MABs03, MABs05.

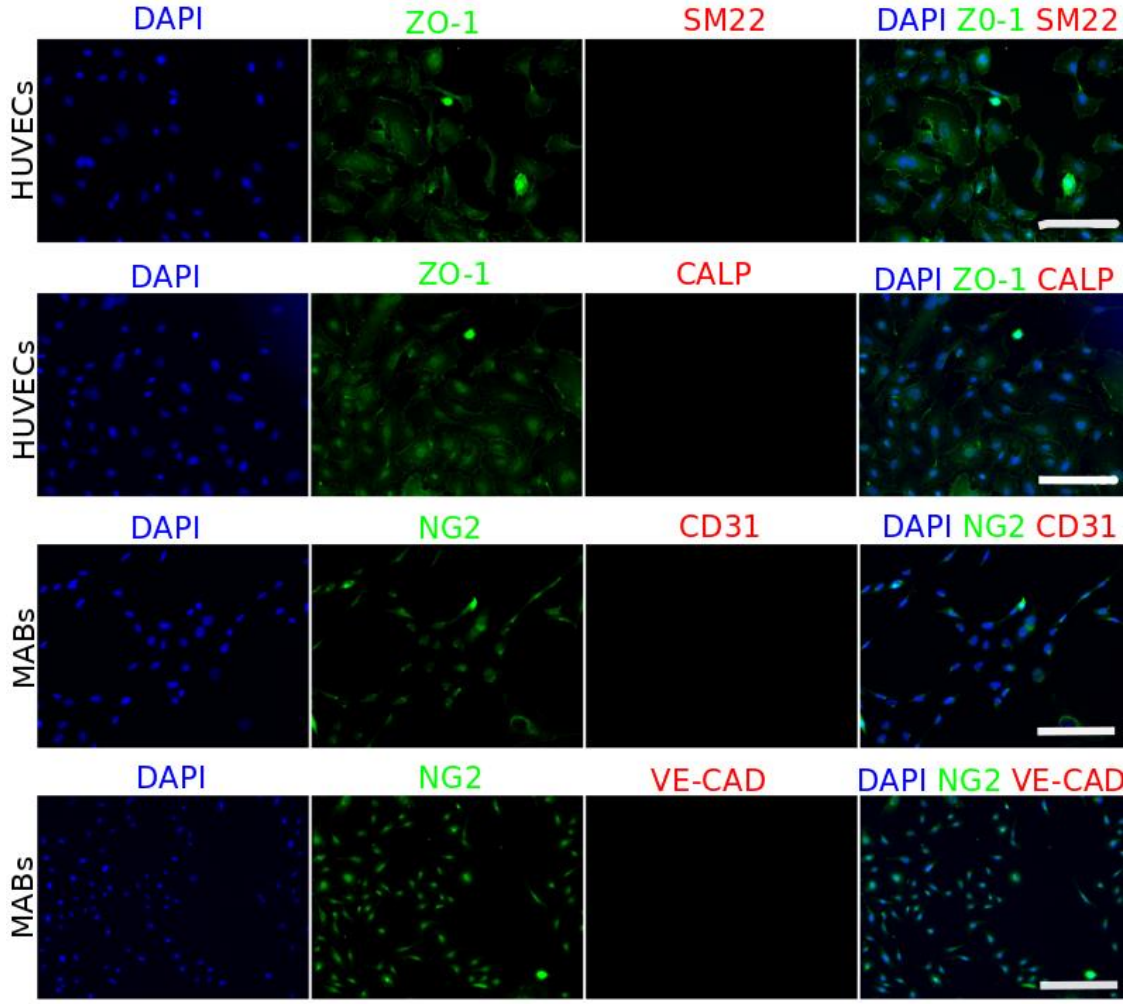

Appendix figure 7: Control staining to check non-specific signal of SM22 CALP CD31 and VE-CAD staining. HUVECs stained for zo-1 (typical endothelial cells marker) have been stained for smooth muscle markers such SM22 and Calponin (2 top panels) that endothelial cells are not supposed to express. MABs stained for NG-2 (a typical pericyte marker) have been stained for endothelial markers such CD31 and VE-CAD, that MABs are not supposed to express. This type of negative control has been used to set the right exposure of confocal images of the staining in plastic, in order to discern the real signal of the bounded antibody from non-specific signal.

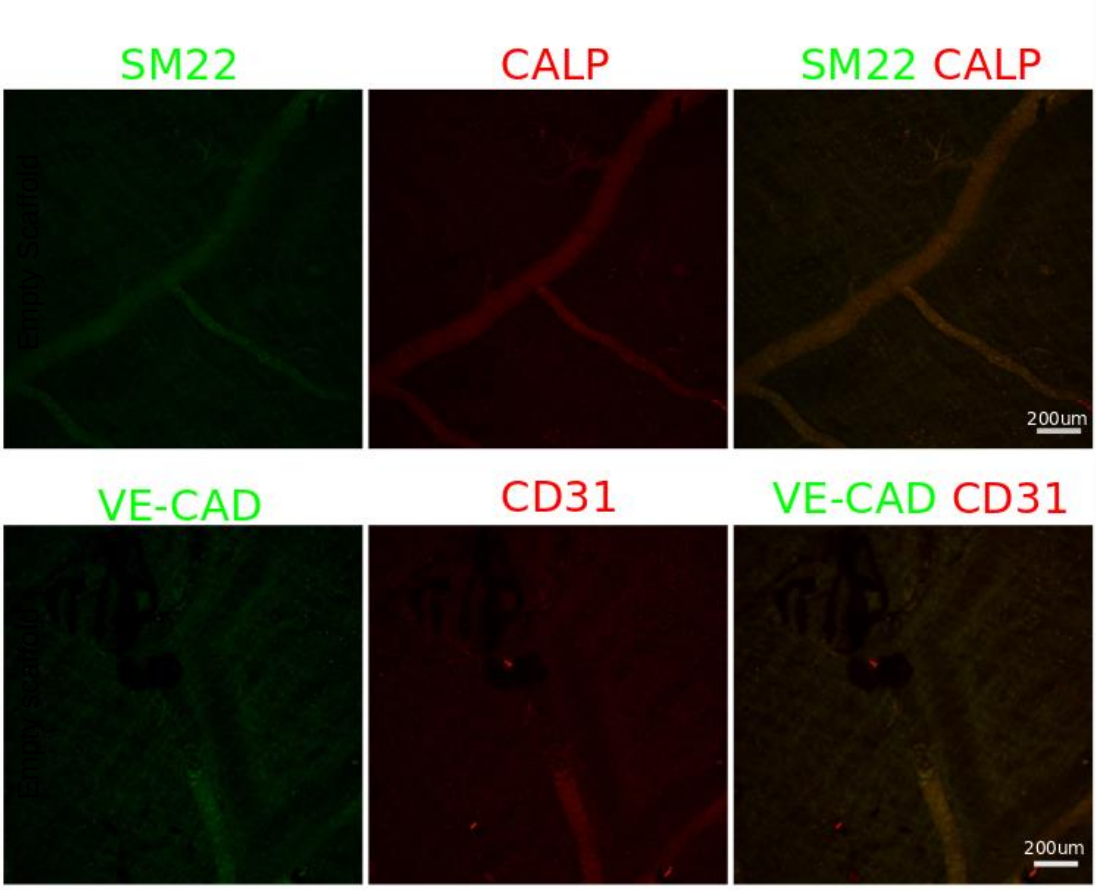

Appendix figure 7: Control staining to check non-specific signal of SM22, CALP, VE-CAD and CD31 on the decellularused intestinal scaffold. Decellularuised scaffold with no cells seeded were stained for SM22, CALP,VE-CAD and CD31 (all markers that a decellularuised scaffold is not supposed to express). This type of negative control has been used to set the right exposure of confocal images of the staining on the scaffolds, in order to discern the real signal of the bounded antibody from non-specific signal.

References

Abboud, H.E. et al. 1995. Role of platelet-derived growth factor in renal injury. Annual review of physiology *57*, 297-309.

Aird ,W C. et al. 2007. “Phenotypic heterogeneity of the endothelium: I. Structure, function and mechanisms.” Circ Res 100: 158–73. 10.1161/01.RES.0000255691.76142.4a.

Aird WC. Et al. 2001. “Vascular bed-specific hemostasis: role of endothelium in sepsis pathogenesis.” Crit Care Med. 29: S28–S35

ANDREW J. et al. 2001. Invited review. *J Appl Physiol* **138**, 377.

Armulik, A. et al 2011. “Pericytes:Developmental, Physiological, and Pathological Perspectives, Problems, and Promises.” Developmental Cell 21(2): 193–215. http://linkinghub.elsevier.com/retrieve/pii/S1534580711002693 (October 16, 2017).

Asahara, T. et al 1997. “Isolation of Putative Progenitor Endothelial Cells for Angiogenesis.” Science (New York, N.Y.) 275(5302): 964–67. http://www.ncbi.nlm.nih.gov/pubmed/9020076.

Asahara, T. et al. 1997. ”Isolation of putative progenitor endothelial cells for angiogenesis” Science 275(5302):964–966.

Askari, S. et al. 2003. “Effect of stromal-cellderived factor 1 on stem-cell homing and tissue regeneration in ischaemic cardiomyopathy” Lancet, 2003;362:675–6.

Badylak, Stephen F. et al 2002. “The Extracellular Matrix as a Scaffold for Tissue Reconstruction.” Seminars in Cell & Developmental Biology 13(5): 377–83. https://www.sciencedirect.com/science/article/pii/S1084952102000940.

Bao, Ji et al 2015. “Hemocompatibility Improvement of Perfusion-Decellularised Clinical-Scale Liver Scaffold through Heparin Immobilization.” Scientific Reports 5(1): 10756. http://www.nature.com/articles/srep10756.

Baptista, Pedro M. et al 2011. “The Use of Whole Organ Decellularization for the Generation of a Vascularized Liver Organoid.” Hepatology 53(2): 604–17.

Beamish, J. A. et al. 2010. ”Molecular regulation of contractile smooth muscle cell phenotype: implications for vascular tissue engineering”. Tissue engineering part B. Reviews. 16(5): 467-491.

Beenken, A. et al. 2009. The FGF family: Biology, pathophysiology and therapy. *Nat. Rev. Drug Discov.* **8**, 235–253.

Bergers, G. et al 2005. “The Role of Pericytes in Blood-Vessel Formation and Maintenance.” Neuro-Oncology 7(4): 452–64. http://www.ncbi.nlm.nih.gov/pubmed/16212810.

Betsholtz, C. et al 2004. “Insight into the Physiological Functions of PDGF through Genetic Studies in Mice.” Cytokine & Growth Factor Reviews 15(4): 215–28. https://www.sciencedirect.com/science/article/pii/S1359610104000152?via%3Dihu .

Betsholtz, C. et al. 2004. “Role of platelet-derived growth factor in mesangium development and vasculopathies: lessons from platelet-derived growth factor and platelet-derived growth factor receptor mutations in mice.” Current opinion in nephrology and hypertension *13*, 45-52.

Brandt, J. E. et al. 1999. ”Ex vivo expansion of autologous bone marrow CD34+ cells with porcine microvascular endothelial cells results in a graft capable of rescuing lethally irradiated baboons.” Blood 94, 106–113.

Brohl, D. et al. 2012. Colonization of the satellite cell niche by skeletal muscle progenitor cells depends on Notch signals. Developmental cell *23*, 469-481.

Butler, J. M. et al. 2010. “Instructive role of the vascular niche in promoting tumour growth and tissue repair by angiocrine factors” Nature Rev. Cancer 10, 138–146.

Butler, Jason M. et al 2010. “Instructive Role of the Vascular Niche in Promoting Tumour Growth and Tissue Repair by Angiocrine Factors.” Nature Reviews Cancer 10(2): 138–46. http://www.ncbi.nlm.nih.gov/pubmed/20094048.

Cappellari, O. et al 2013. “Dll4 and PDGF-BB Convert Committed Skeletal Myoblasts to Pericytes without Erasing Their Myogenic Memory.” DEVCEL 24: 586–99. http://dx.doi.org/10.1016/j.devcel.2013.01.022.

Cappellari, O. et al 2013. “Pericytes in Development and Pathology of Skeletal Muscle.” Circulation Research 113(3): 341–47.

Carmeliet, P. et al 2011. “Molecular Mechanisms and Clinical Applications of Angiogenesis.” Nature 473(7347): 298–307. http://www.ncbi.nlm.nih.gov/pubmed/21593862.

Ceradini D J. et al. 2004 “Progenitor cell trafficking is regulated by hypoxic gradients through HIF-1 induction of SDF-1” Nat Med, 2004;10:858–64

Chandra, R. et al 2018. “Current Treatment Paradigms in Pediatric Short Bowel Syndrome.” Clinical Journal of Gastroenterology 11(2): 103–12. https://doi.org/10.1007/s12328-017-0811-7.

Chute, J. P. et al. 1999 “A comparative study of the cell cycle status and primitive cell adhesion molecule profile of human CD34+ cells cultured in stroma-free versus porcine microvascular-- endothelial cell cultures.” Exp. Hematol. 27, 370–379.

Collett, G D M. et al 2005. “Angiogenesis and Pericytes in the Initiation of Ectopic Calcification.” Circulation Research 96(9): 930–38. http://www.ncbi.nlm.nih.gov/pubmed/15890980.

Conboy, I.M. et al. 2002. The regulation of Notch signaling controls satellite cell activation and cell fate determination in postnatal myogenesis. Developmental cell *3*, 397-409.

Cordle, J. *et al.* 2008. A conserved face of the Jagged/Serrate DSL domain is involved in Notch trans-activation and cis-inhibition. Nature structural & molecular biology *15*, 849-857.

Cortiella, J. et al. 2010. “Influence of Acellular Natural Lung Matrix on Murine Embryonic Stem Cell Differentiation and Tissue Formation.” Tissue engineering. Part A 16(8): 2565–80.

Cossu, G. 2017. “Lancet Commission: Stem Cells and Regenerative Medicine.” The Lancet. http://www.ncbi.nlm.nih.gov/pubmed/28987452.

Cossu, G. et al. 2003. Mesoangioblasts – “vascular progenitors for extravascular mesodermal tissue”, Current opinion in genetics & development. 13(5): 537-542.

Cossu, G. et al. 2005. “Satellite Cells, Myoblasts and Other Occasional Myogenic Progenitors: Possible Origin, Phenotypic Features and Role in Muscle Regeneration.” Seminars in Cell and Developmental Biology 16(4–5): 623–31.

Cossu, G. et al. 2016. “Intra-arterial Transplantation of HLA-matched Donor Mesoangioblasts in Duchenne Muscular Dystrophy.” EMBO Molecular Medicine 8(12): 1470–71.

cytochemistry : official journal of the Histochemistry Society 41, 1813-1821.
Dejana E et al. 2009. “Organisation and signaling of endothelial cell-to-cell junctions in various regions of the blood and lymphatic vascular trees” Cell Tissue Res 335:17–25. doi:10.1007/s00441-008-0694-5.

Davis, M. P. A. et al. 2013. A set of tools for quality control and analysis of high-throughput sequence data. *Methods* **63**, 41–49.

Dellavalle, A. et al. 2007. “Pericytes of Human Skeletal Muscle Are Myogenic Precursors Distinct from Satellite Cells.” Nature Cell Biology 9(3): 255–67. http://www.nature.com/doifinder/10.1038/ncb1542 (October 17, 2017).

Dellavalle, A. et al. 2011. “Pericytes Resident in Postnatal Skeletal Muscle Differentiate into Muscle Fibres and Generate Satellite Cells.” Nature Communications 2: 499. http://www.ncbi.nlm.nih.gov/pubmed/21988915 (October 17, 2017).

Demehri, Farokh R. et al. 2015. “Enteral Autonomy in Pediatric Short Bowel Syndrome: Predictive Factors One Year after Diagnosis.” Journal of Pediatric Surgery 50(1): 131–35. http://www.ncbi.nlm.nih.gov/pubmed/25598109.

Dew, L. et al. 2016. “Investigating Neovascularization in Rat Decellularised Intestine: An *In Vitro* Platform for Studying Angiogenesis.” Tissue engineering. Part A 22(23–24): 1317–26. http://www.ncbi.nlm.nih.gov/pubmed/27676406.

Díaz-Flores, L et al. 2009. “Pericytes. Morphofunction, Interactions and Pathology in a Quiescent and Activated Mesenchymal Cell Niche.” Histology and histopathology 24(7): 909–69. http://www.ncbi.nlm.nih.gov/pubmed/19475537 (October 17, 2017).

Ding, B. S. et al. 2011. “Endothelial-derived angiocrine signals induce and sustain regenerative lung alveolarization.” Cell 147, 539–553.

Ding, Bi S. et al. 2010. “Inductive Angiocrine Signals from Sinusoidal Endothelium Are Required for Liver Regeneration.” Nature 468(7321): 310–15.

Dobin, A. *et al.* 2013. STAR: ultrafast universal RNA-seq aligner. *Bioinformatics* **29**, 15–21.

Du, C. et al. 2016. “Functional Kidney Bioengineering with Pluripotent Stem-Cell-Derived Renal Progenitor Cells and Decellularised Kidney Scaffolds.” Advanced Healthcare Materials 5(16): 2080–91. https://doi.org/10.1002/adhm.201600120.

Eklund L. et al. 2017. “Angiopoietin–tie signalling in the cardiovascular and lymphatic systems.” Clinical Science. 2017;131(1):87–103. doi: 10.1042/CS20160129)

Elliott, Martin J. et al. 2012. “Stem-Cell-Based, Tissue Engineered Tracheal Replacement in a Child: A 2-Year Follow-up Study.” Lancet (London, England) 380(9846): 994–1000.

Feinberg, B et al. 2017. “Plasticity of Arterial and Venous Endothelial Cell Identity – Some Nerve!” Physiology & behavior 176(10): 139–48. file:///C:/Users/Carla

Carolina/Desktop/Artigos para acrescentar na qualificação/The impact of birth weight on cardiovascular disease risk in the.pdf.

Félétou M. 2011. “The Endothelium: Part 1: Multiple Functions of the Endothelial Cells—Focus on Endothelium-Derived Vasoactive Mediators.” Chapter 2. https://www.ncbi.nlm.nih.gov/books/NBK57148/

Fishman, Jonathan M. et al. 2013. “Immunomodulatory Effect of a Decellularised Skeletal Muscle Scaffold in a Discordant Xenotransplantation Model.” Proceedings of the National Academy of Sciences of the United States of America 110(35): 14360–65. http://www.ncbi.nlm.nih.gov/pubmed/23940349.

Flamme I and Risau W. 1992 “Induction of vasculogenesis and hematopoiesis *in vitro*.” Development 116: 435–439.

Frigo G. et al. 2016. “Human IgGs induce synthesis and secretion of IgGs and neonatal Fc receptor in human umbilical vein endothelial cells.” Immunobiology. 221(12):1329–1342. doi: 10.1016/j.imbio.2016.08.002

Gamba, P. et al. 2002. “Experimental Abdominal Wall Defect Repaired with Acellular Matrix.” Pediatric Surgery International 18(5–6): 327–31. http://www.ncbi.nlm.nih.gov/pubmed/12415348.

Garg, M. et al. 2011. “Intestinal Transplantation: Current Status and Future Directions.” Journal of Gastroenterology and Hepatology 26(8): 1221–28. http://doi.wiley.com/10.1111/j.1440-1746.2011.06783.x.

Geckil, H. et al. 2010. “Engineering Hydrogels as Extracellular Matrix Mimics.Geckil, H., Xu, F., Zhang, X., Moon, S., & Demirci, U. (2010). Engineering Hydrogels as Extracellular Matrix Mimics. Nanomedicine (London, England), 5(3), 469–84.

Gerhardt H. et al. 2003 “VEGF guides angiogenic sprouting utilizing endothelial tip cell filopodia.” J Cell Biol 161:1163–77. doi:10.1083/jcb.200302047

Gerhardt, H. et al. 2003. “Endothelial-Pericyte Interactions in Angiogenesis.” Cell and Tissue Research 314(1): 15–23. http://www.ncbi.nlm.nih.gov/pubmed/12883993.

Gerli, Mattia F M. et al. 2014. “Transplantation of Induced Pluripotent Stem Cell-Derived Mesoangioblast-like Myogenic Progenitors in Mouse Models of Muscle Regeneration.” Journal of visualized experiments : JoVE (83): e50532. http://www.ncbi.nlm.nih.gov/pubmed/24472871 (October 17, 2017).

Geudens I. et al 2011 “Gerhardt H. Coordinating cell behaviour during blood vessel formation.” Development 138:4569–83. doi:10.1242/dev.062323

Gilbert, T. et al. 2006. “Decellularization of Tissues and Organs.” Biomaterials 27(19): 3675–83.

Gilpin, A. et al. 2017. “Decellularization Strategies for Regenerative Medicine: From Processing Techniques to Applications.” BioMed Research International 2017: 1–13. https://www.hindawi.com/journals/bmri/2017/9831534/.

Gilpin, Sarah E. et al. 2014. “Perfusion Decellularization of Human and Porcine Lungs: Bringing the Matrix to Clinical Scale.” The Journal of heart and lung transplantation : the official publication of the International Society for Heart Transplantation 33(3): 298–308.

Gilpin, Sarah E. et al. 2016. “Regenerative Potential of Human Airway Stem Cells in Lung Epithelial Engineering.” Biomaterials 108: 111–19. http://dx.doi.org/10.1016/j.biomaterials.2016.08.055.

Ginsberg, M. et al. 2015. “Direct Conversion of Human Amniotic Cells into Endothelial Cells without Transitioning through a Pluripotent State.” Nature Protocols 10(12): 1975–85. http://www.nature.com/doifinder/10.1038/nprot.2015.126.

Goulet, O J et al. 1991. “Neonatal Short Bowel Syndrome.” The Journal of pediatrics 119(1 Pt 1): 18–23. http://www.ncbi.nlm.nih.gov/pubmed/1906099.

Grber K. et al 2015. “Suspends first clinical trial involving induced pluripotent stem cells.” Nature Biotechnology; 33(9): 890-1.

Gridley, T. et al. 2007. Notch signaling in vascular development and physiology. Development *134*, 2709-2718.

Grim, M. et al. 1990. “Alkaline phosphatase and dipeptidylpeptidase IV staining of tissue components of skeletal muscle: a comparative study.” The journal of histochemistry and cytochemistry : official journal of the Histochemistry Society 38, 1907-1912.

Hamilton, D. et al. 2004. “Characterization of the Response of Bone Marrow-Derived Progenitor Cells to Cyclic Strain: Implications for Vascular Tissue-Engineering Applications.” Tissue Engineering 10(3–4): 361–69. http://www.liebertonline.com/doi/abs/10.1089/107632704323061726.

Harris, Lisa J et al. 2011. “Differentiation of Adult Stem Cells into Smooth Muscle for Vascular Tissue Engineering.” The Journal of surgical research 168(2): 306–14.

Heldin, C.H. (1992). Structural and functional studies on platelet-derived growth factor. The EMBO journal *11*, 4251-4259.

Heldin, C.H., and Westermark, B. (1999). Mechanism of action and *in vivo* role of platelet-derived growth factor. Physiological reviews *79*, 1283-1316.

Hellstrom, M. et al. 1999. Role of PDGF-B and PDGFR-beta in recruitment of vascular smooth muscle cells and pericytes during embryonic blood vessel formation in the mouse. Development *126*, 3047-3055.

Hofmann, J.J. et al. 2007. Notch signaling in blood vessels: who is talking to whom about what? Circulation research *100*, 1556-1568.

Höllwarth, Michael E. et al. 2017. “Surgical Strategies in Short Bowel Syndrome.” Pediatric surgery international 33(4): 413–19. http://www.ncbi.nlm.nih.gov/pubmed/28039510.

Howell, Jonathan C et al. “Generating Intestinal Tissue from Stem Cells: Potential for Research and Therapy.” https://www.ncbi.nlm.nih.gov/pmc/articles/PMC3236565/pdf/nihms-339822.pdf.

Hussein, Kamal H. et al. 2016. “Heparin-Gelatin Mixture Improves Vascular Reconstruction Efficiency and Hepatic Function in Bioengineered Livers.” Acta biomaterialia 38: 82–93.

Hussey, George S. et al. 2018. “Extracellular Matrix-Based Materials for Regenerative Medicine.” Nature Reviews Materials 3(7): 159–73. http://dx.doi.org/10.1038/s41578-018-0023-x.

Hynes, Richard O. et al. 2009. “The Extracellu.” Science 326(5957): 1216–19.

Jain, Rakesh K. et al. 2005. “Engineering Vascularized Tissue.” Nature Biotechnology 23(7): 821–23. http://www.ncbi.nlm.nih.gov/pubmed/16003365.

Jeremy J S. et al. 2017. “Regeneration and Experimental Orthotopic Transplantation of a Bioengineered Kidney Jeremy.” Physiology & behavior 176(5): 139–48.

Jiang, H. et al. 2014. A fast and accurate adapter trimmer for next-generation sequencing paired-end reads. *BMC Bioinformatics* **15**, 182

Jung, Y. et al. 2015. “Scaffold-Free, Human Mesenchymal Stem Cell-Based Tissue Engineered Blood Vessels.” Scientific reports 5: 15116.

Kadota, Y. et al. 2014. “Mesenchymal Stem Cells Support Hepatocyte Function in Engineered Liver Grafts.” Organogenesis 10(2): 268–77.

Kelly, Darlene G. et al. 2014. “Short Bowel Syndrome.” Journal of Parenteral and Enteral Nutrition 38(4): 427–37. http://doi.wiley.com/10.1177/0148607113512678.

Kennedy M. et al. 2007. “Development of the hemangioblast defines the onset of hematopoiesis in human ES cell differentiation cultures.” *Blood.* 2007;109(7):2679–2687. doi: 10.1182/blood-2006-09-047704.

Kitano, K. et al. 2017. “Bioengineering of Functional Human Induced Pluripotent Stem Cell-Derived Intestinal Grafts.” https://www.nature.com/articles/s41467-017-00779-y.pdf.

Kluppel, M. et al. 1998. “Developmental Origin and Kit-Dependent Development of the Interstitial Cells of Cajal in the Mammalian Small Intestine.”

Ko, In K. et al. 2015. “Bioengineered Transplantable Porcine Livers with Re-Endothelialized Vasculature.” Biomaterials 40: 72–79.

Koike, N. et al. 2004. “Creation of Long-Lasting Blood Vessels.” Nature.

Kopan, R. et al. 1994. The intracellular domain of mouse Notch: a constitutively activated repressor of myogenesis directed at the basic helix-loop-helix region of MyoD. Development *120*, 2385-2396.

Kovacic, Jason C. et al. 2009. “Resident Vascular Progenitor Cells: An Emerging Role for Non-Terminally Differentiated Vessel-Resident Cells in Vascular Biology.” Stem Cell Research 2(1): 2–15. http://www.ncbi.nlm.nih.gov/pubmed/19383404.

Kuleshov, M. V. *et al.* 2016. Enrichr: a comprehensive gene set enrichment analysis web server 2016 update. *Nucleic Acids Res.* **44**, W90–W97.

Kumpf, Vanessa J. et al 2014. “Pharmacologic Management of Diarrhea in Patients With Short Bowel Syndrome.” Journal of Parenteral and Enteral Nutrition 38(1_suppl): 38S--44S. http://www.ncbi.nlm.nih.gov/pubmed/24463352.

Lammert, E., O. et al. 2001. “Induction of Pancreatic Differentiation by Signals from Blood Vessels.” Science 294(5542): 564–67.

Langer, R. et al. 1993. “Tissue Engineering.” Science, New Series 260(5110): 920–26. http://links.jstor.org/sici?sici=0036-8075%2819930514%293%3A260%3A5110%3C920%3ATE%3E2.0.CO%3B2-G.

LeCouter, J. et al. 2003 “Angiogenesis-independent endothelial protection of liver: role of VEGFR-1.” Science 299, 890–893.

Lee, E. et al. 2017. “Decellularised Material as Scaffolds for Tissue Engineering Studies in Long Gap Esophageal Atresia.” Expert opinion on biological therapy 17(5): 573–84.

Leveen, P. et al.1994. Mice deficient for PDGF B show renal, cardiovascular, and hematological abnormalities. Genes & development *8*, 1875-1887.

Levy, M.M. et al. 2001. ”Osteoprogenitor cells of mature human skeletal muscle tissue: an *in vitro* study.” Bone *29*, 317-322.

Li, W. et al. 2003 “Primary endothelial cells isolated from the yolk sac and para-aortic splanchnopleura support the expansion of adult marrow stem cells *in vitro*.” Blood 102, 4345–4353.

Lindahl, P. et al. 1997. Pericyte loss and microaneurysm formation in PDGF-B-deficient mice. Science *277*, 242-245.

Lindsell, C.E. et al. 1995. Jagged: a mammalian ligand that activates Notch1. Cell *80*, 909-917.

Majka, Susan M et al. 2003. “Distinct Progenitor Populations in Skeletal Muscle Are Bone Marrow Derived and Exhibit Different Cell Fates during Vascular Regeneration.” Journal of Clinical Investigation 111(1): 71–79. http://www.ncbi.nlm.nih.gov/pubmed/12511590.

Mantella, Laura E. et al. 2015. “Variability in Vascular Smooth Muscle Cell Stretch-Induced Responses in 2D Culture.” Vascular Cell 7(1): 1–9. http://dx.doi.org/10.1186/s13221-015-0032-0.

Marzaro, M. et al. 2006. “*In Vitro* and in Vivo Proposal of an Artificial Esophagus.” Journal of Biomedical Materials Research Part A 77A(4): 795–801. https://doi.org/10.1002/jbm.a.30666.

Matthews W. et al. 1991 “A receptor tyrosine kinase cDNA isolated from a population of enriched primitive hematopoietic cells and exhibiting close genetic linkage to c-kit.“ *Proceedings of the National Academy of Sciences of the United States of America.*;88(20):9026–9030. doi: 10.1073/pnas.88.20.9026.

Mecham, Robert P. 2012. “Overview of Extracellular Matrix.” Current Protocols in Cell Biology 57(1): 10.1.1-10.1.16. https://doi.org/10.1002/0471143030.cb1001s57.

Meezan, E. et al. 1975. “A Simple, Versatile, Nondisruptive Method for the Isolation of Morphologically and Chemically Pure Basement Membranes from Several Tissues.” Life Sciences 17(11): 1721–32.

Meng, F. et al. 2019. “Vasculature Reconstruction of Decellularised Liver Scaffolds via Gelatin-Based Re-Endothelialization.” Journal of biomedical materials research. Part A 107(2): 392–402.

Merritt, Russell J et al. “Intestinal Rehabilitation Programs in the Management of Pediatric Intestinal Failure and Short Bowel Syndrome.” https://insights.ovid.com/pubmed?pmid=28837507.

Middleton, S. J. et al. 2005. “The Current Status of Small Bowel Transplantation in the UK and Internationally.” Gut 54(11): 1650–57.

Millauer, B. et al. 1993. “High affinity VEGF binding and developmental expression suggest Flk-1 as a major regulator of vasculogenesis and angiogenesis”Cell 72(60):835-846. https://doi.org/10.1016/0092-8674(93)90573-9.

Miller, F N. et al. 1986. “Contractile Elements in the Regulation of Macromolecular Permeability.” Federation proceedings 45(2): 84—88. http://europepmc.org/abstract/MED/3510914.

Minasi, Maria G et al. 2002. “The Meso-Angioblast: A Multipotent, Self-Renewing Cell That Originates from the Dorsal Aorta and Differentiates into Most Mesodermal Tissues.” Development (Cambridge, England) 129(11): 2773–83. http://www.ncbi.nlm.nih.gov/pubmed/12015303 (October 17, 2017).

Mizutani, A. et al. 1965. Fine structural demonstration of phosphatase activity at pH 9. Nature 206, 1001-1003.

Mourikis, P. and Tajbakhsh, S. 2014. Distinct contextual roles for Notch signalling in skeletal muscle stem cells. BMC developmental biology *14*, 2.

Mori, S. *et al.* 2013. A Dominant-Negative FGF1 Mutant (the R50E Mutant) Suppresses Tumorigenesis and Angiogenesis. *PLoS One* **8**.

Mourikis, P. et al. 2012. A critical requirement for notch signaling in maintenance of the quiescent skeletal muscle stem cell state. Stem cells *30*, 243-252.

Mowat, Allan M. et al. 2014. “Regional Specialization within the Intestinal Immune System.” Nature Reviews Immunology 14(10): 667–85.

Muller, W A. et al 2013 “Getting Leukocytes to the Site of Inflammation” Vet Pathol. 50(1): 7–22. doi: 10.1177/0300985812469883

Mulnard, J. et al. 1987. “The value of centrifugation for the study of cytoplasmic changes related to the maturation and fertilization of mammalian oocytes.“ Bulletin et memoires de l'Academie royale de medecine de Belgique 142, 507-516.
Murasawa S. et al. 2005 “ Endothelial progenitor cells for vasculogenesis, Physiology (Bethesda),” 20:36-42.

Murga, M. et al 2004. “Derivation of Endothelial Cells from CD34- Umbilical Cord Blood.” Stem Cells 22(3): 385–95. http://doi.wiley.com/10.1634/stemcells.22-3-385.

Murray P. D. F. et al. 1932. ”The development *in vitro* of the blood of the early chick embryo” Proceedings of the Royal Society B: Biological Sciences. 1932;111(773):497–521. doi: 10.1098/rspb.1932.0070.

Neff, Lucas P. et al. 2011. “Vascular Smooth Muscle Enhances Functionality of Tissue-Engineered Blood Vessels in Vivo.” Journal of vascular surgery 53(2): 426–34.

Nehls, V. et al. 1992. “Pericyte involvement in capillary sprouting during angiogenesis in situ.” Cell and tissue research 270, 469-474.
Nesmith J. E. et al. 2017 “Blood vessel anastomosis is spatially regulated by Flt1 during angiogenesis.” Development.; 144(5):889–896. doi: 10.1242/dev.145672

Nichols, Joan E et al. 2017. “Giving New Life to Old Lungs: Methods to Produce and Assess Whole Human Paediatric Bioengineered Lungs.” Journal of tissue engineering and regenerative medicine 11(7): 2136–52.

Nishikawa, S. et al. 1998 “Progressive lineage analysis by cell sorting and culture identifies FLK1+ VE-cadherin+ cells at a diverging point of endothelial and hemopoietic lineages,” Development 125(9):1747–1757.

Nofziger, D. et al. 1999. Notch signaling imposes two distinct blocks in the differentiation of C2C12 myoblasts. Development *126*, 1689-1702

Nolan, D. J. et al. 2013. ”Molecular signatures of tissue-specific microvascular endothelial cell heterogeneity in organ maintenance and regeneration” Dev. Cell 26, 204–219.

Nolan, Daniel J et al. 2013. “Molecular Signatures of Tissue-Specific Microvascular Endothelial Cell Heterogeneity in Organ Maintenance and Regeneration.” Developmental Cell 26(2): 204–19. http://www.ncbi.nlm.nih.gov/pubmed/23871589.

Nowbar, AN. Et al 2014. “Discrepancies in autologous bone marrow stem cell trials and enhancement of ejection fraction weighted regression and meta-analysis.” BMJ. ;348:g2688.

Olson, Lorin E. et al. 2011. “PDGFR$β$ Signaling Regulates Mural Cell Plasticity and Inhibits Fat Development.” Developmental Cell 20(6): 815–26. http://www.ncbi.nlm.nih.gov/pubmed/21664579.

Orlando, G. et al. 2012. “Production and Implantation of Renal Extracellular Matrix Scaffolds from Porcine Kidneys as a Platform for Renal Bioengineering Investigations.” Annals of surgery 256(2): 363–70.

Orlova, Valeria V et al. 2014. “Generation, Expansion and Functional Analysis of Endothelial Cells and Pericytes Derived from Human Pluripotent Stem Cells.” Nature Protocols 9(6): 1514–31. http://www.nature.com/doifinder/10.1038/nprot.2014.102.

Otani, A. et al. 2002. “Bone Marrow–Derived Stem Cells Target Retinal Astrocytes and Can Promote or Inhibit Retinal Angiogenesis.” Nature Medicine 8(9): 1004–10. http://www.ncbi.nlm.nih.gov/pubmed/12145646.

Ott, Harald C. et al. 2008. “Perfusion-Decellularised Matrix: Using Nature’s Platform to Engineer a Bioartificial Heart.” Nature Medicine 14(2): 213–21.

Ozeki, M. et al. 2006. “Evaluation of Decellularised Esophagus as a Scaffold for Cultured Esophageal Epithelial Cells.” Journal of Biomedical Materials Research Part A 79A(4): 771–78. http://doi.wiley.com/10.1002/jbm.a.30885.

Pardanaud, L. et al. 1989 “Relationship between vasculogenesis, angiogenesis and haemopoiesis during avian ontogeny.” Development 105: 473–485.

Patel-Hett, S. et al. 2011. “Signal Transduction in Vasculogenesis and Developmental Angiogenesis.” The International Journal of Developmental Biology 55(4–5): 353–63. http://www.ncbi.nlm.nih.gov/pubmed/21732275.

Pellegata, Alessandro F et al. 2015. “Arterial Decellularised Scaffolds Produced Using an Innovative Automatic System.” Cells, tissues, organs 200(6): 363–73.

Pellegata, Alessandro F. et al. 2018. “Whole Organ Tissue Vascularization: Engineering the Tree to Develop the Fruits.” Frontiers in Bioengineering and Biotechnology 6(MAY): 1–13.

Pitulescu, Mara E et al. 2017. “Dll4 and Notch Signalling Couples Sprouting Angiogenesis and Artery Formation.” Nature Cell Biology 19(8): 915–27. http://www.ncbi.nlm.nih.gov/pubmed/28714968.

Poulos, M. G. et al. 2015. « Vascular platform to define hematopoietic stem cell factors and enhance regenerative hematopoiesis." Stem Cell Reports 10, 881–894.

R, Kishore. et al. 2014. "The Role of Surgery in Preventing Intestinal Failure." Journal of Parenteral and Enteral Nutrition 38(1): 53–59. http://journals.sagepub.com/doi/pdf/10.1177/0148607114529446.

Rafii, S. et al. 1994 " Isolation and characterization of human bone marrow microvascular endothelial cells: hematopoietic progenitor cell adhesion." Blood 84, 10–19.

Rafii, S. et al. 1995 "Human bone marrow microvascular endothelial cells support long-term proliferation and differentiation of myeloid and megakaryocytic progenitors." Blood 86, 3353–3363.

Rafii, S. et al. 2016. "Angiocrine Functions of Organ-Specific Endothelial Cells." Nature 529(7586): 316–25. http://www.ncbi.nlm.nih.gov/pubmed/26791722.

Ramilowski, J. A. *et al.* 2015. A draft network of ligand-receptor-mediated multicellular signalling in human. *Nat. Commun.* **6**,.

Regan, J.N. et al. 2009. Building a vessel wall with notch signaling. Circulation research *104*, 419-421.

Ren, X. et al. 2015. "Engineering Pulmonary Vasculature in Decellularised Rat and Human Lungs." Nature Biotechnology 33(10): 1097–1102. http://www.ncbi.nlm.nih.gov/pubmed/26368048.

Ribatti, D. et al 2011 "the role of pericytes in angiogenesis." The international journal of developmental biology. 55(3): 261-268.

Riley, James A. et al. 1948. "A Photoelectric Drop Counter"." 108: 390–92.

Rinkevich, Y. et al. 2012. "Identification and Prospective Isolation of a Mesothelial Precursor Lineage Giving Rise to Smooth Muscle Cells and Fibroblasts for Mammalian Internal Organs, and Their Vasculature." Nature Cell Biology 14(12): 1251–60. http://dx.doi.org/10.1038/ncb2610.

Risau W. et al 1988 "Vasculogenesis and angiogenesis in embryonic stem cell-derived embryoid bodies." Development 102: 471–478.

Risau W. et al. 1997 "Mechanisms of angiogenesis." Nature 386: 671–674.

Rivron, N. C. et al. 2008. "Engineering Vascularised Tissues *in Vitro*." European Cells and Materials 15: 27–40.

Robertson, Matthew J. et al. 2014. "Optimizing Recellularization of Whole Decellularised Heart Extracellular Matrix." PloS one 9(2): e90406.

Rojkind, M. et al. 1980. "Connective Tissue Biomatrix: Its Isolation and Utilization for Long-Term Cultures of Normal Rat Hepatocytes." Journal of Cell Biology 87(1): 255–63.

Roku G. et al 2016. "Researchers plan trial transplants of retinas grown from 3rd parties" http://www.asahi.com/ ajw/articles/AJ201606070063.html.).

Ronnov-Jessen, L. et al. 1996. "ADP-ribosylation of actins in fibroblasts and myofibroblasts by botulinum C2 toxin: influence on microfilament morphology and migratory behavior." Electrophoresis 17, 1776-1780.

Rouget, C. et al. 1874 “Note Sur Le Developpement de La Tunique Contractile Des Vaisseaux. Compt Rend Acad Sci,. 59.”

Rouwkema, J. et al. 2008. “Vascularization in Tissue Engineering.” Trends in biotechnology 26(8): 434–41.

Sacchetti, B. et al. 2016a. “No Identical "Mesenchymal Stem Cells" at Different Times and Sites: Human Committed Progenitors of Distinct Origin and Differentiation Potential Are Incorporated as Adventitial Cells in Microvessels.” Stem cell reports 6(6): 897–913.

Safadi, A. et al. 1991. “Activity of alkaline phosphatase in rat skeletal muscle localized along the sarcolemma and endothelial cell membranes.” The journal of histochemistry and cytochemistry : official journal of the Histochemistry Society 39, 199-203.

Sampaolesi, M. et al. 2003. “Cell therapy of alpha-sarcoglycan null dystrophic mice through intraarterial delivery of mesoangioblasts”. Science. 301(5632):487-492.

Sampaolesi, M. et al. 2006. “Mesoangioblast stem cells ameliorate muscle function in dystrophic dogs”. Nature. 444(7119).

Saxena, Amulya K. et al. 2010. “Esophagus Tissue Engineering: In Situ Generation of Rudimentary Tubular Vascularized Esophageal Conduit Using the Ovine Model.” Journal of pediatric surgery 45(5): 859–64.

Schmidt, D. et al. 2004. “Umbilical Cord Blood Derived Endothelial Progenitor Cells for Tissue Engineering of Vascular Grafts.” The Annals of Thoracic Surgery 78(6): 2094–98. http://www.ncbi.nlm.nih.gov/pubmed/15561042.

Schmittgen, Thomas D. et al. 2008. “Analyzing Real-Time PCR Data by the Comparative CT Method.” Nature Protocols 3(6): 1101–8.

Schultz-Hector, S. et al. 1993. “Cellular localization of endothelial alkaline phosphatase reaction product and enzyme protein in the myocardium.” The journal of histochemistry and

Schuster-Gossler, K. et al. 2007. Premature myogenic differentiation and depletion of progenitor cells cause severe muscle hypotrophy in Delta1 mutants. Proceedings of the National Academy of Sciences of the United States of America *104*, 537-542.

Seandel, M. et al. 2008 “Generation of a functional and durable vascular niche by the adenoviral E4ORF1 gene.” Proc. Natl Acad. Sci. USA 105, 19288–19293.

Seddon, Annela M. et al. 2004. “Membrane Proteins, Lipids and Detergents: Not Just a Soap Opera.” Biochimica et biophysica acta 1666(1–2): 105–17.

Shaheen, Mohammed F. et al. 2019. “Author Correction: Sustained Perfusion of Revascularized Bioengineered Livers Heterotopically Transplanted into Immunosuppressed Pigs.” Nature biomedical engineering.

Shalaby, F. et al. 1995 “Failure of blood-island formation and vasculogenesis in Flk-1- deficient mice,” Nature, 376(6535): 62–66.

Shannon P. *et al.* 2003. Cytoscape: A Software Environment for Integrated Models. *Genome Res.* **13**, 426

Shi, Q. et al. 1998 “Evidence for circulating bone marrow-derived endothelial cells.” Blood.1998; 92:362–367.

Shi, Q. et al. 1998. “Evidence for Circulating Bone Marrow-Derived Endothelial Cells.” Blood 92(2): 362–67. http://www.ncbi.nlm.nih.gov/pubmed/9657732.

Shirakigawa, N. et al. 2013. “Base Structure Consisting of an Endothelialized Vascular-Tree Network and Hepatocytes for Whole Liver Engineering.” Journal of Bioscience and Bioengineering 116(6): 740–45. http://dx.doi.org/10.1016/j.jbiosc.2013.05.020.

Shirota, T. et al. 2003. “Human Endothelial Progenitor Cell-Seeded Hybrid Graft: Proliferative and Antithrombogenic Potentials *in Vitro* and Fabrication Processing.” Tissue Engineering 9(1): 127–36. http://www.ncbi.nlm.nih.gov/pubmed/12625961.

SOLWAY et al. 2005. Plasticity in Skeletal, Cardiac, and Smooth Muscle Invited Review: Molecular mechanisms of phenotypic plasticity in smooth muscle cells. *Environ. Pollut.* **138**, 377

Stefkova, K. et al. 2015. “Alkaline phosphatase in stem cells.” Stem cells international 2015, 628368.

Syedain, Zeeshan H et al. 2017. “A Completely Biological ‘off-the-Shelf’ Arteriovenous Graft That Recellularizes in Baboons.” Science Translational Medicine 9(414): eaan4209. http://stm.sciencemag.org/content/9/414/eaan4209.abstract.

Tagliafico, E. et al. 2004. “TGFβ/BMP Activate the Smooth Muscle/Bone Differentiation Programs in Mesoangioblasts.” Journal of Cell Science 117(19): 4377–88.

Takahashi, T. et al. 1999 “Ischemia- and cytokineinduced mobilization of bone marrow-derived endothelial progenitor cells for neovascularization.” Nat Med, 1999;5:434–8.

Takayuki A. et all. 1999. “Bone Marrow Origin of Endothelial Progenitor Cells Responsible for Postnatal Vasculogenesis in Physiological and Pathological Neovascularization” Circulation research 85(3): 221-228.

Takayuki, A. et al. 1999. “Bone Marrow Origin of Endothelial Progenitor Cells Responsible for Postnatal Vasculogenesis in Physiological and Pathological Neovascularization” Circulation research 85(3): 221-228.

Takebe, T. et al. 2014a. “Engineering of Human Hepatic Tissue with Functional Vascular Networks.” Organogenesis 10(2): 260–67.

Takeshi, F. et al 2019 “Endothelial Progenitor Cells do not originate from the bone marrow” Circulation 140(18): 1524-1526

Talavera-Adame, D. & Dafoe, D. C. 2015 “Endothelium-derived essential signals involved in pancreas organogenesis” World J. Exp. Med. 5, 40–49.

Tallquist, M.D. et al. 2003. Additive effects of PDGF receptor beta signaling pathways in vascular smooth muscle cell development. PLoS biology *1*, E52.

Tan, J Y. et al. 2012. “Esophageal Tissue Engineering: An in-Depth Review on Scaffold Design.” Biotechnology and bioengineering 109(1): 1–15.

Tappenden, Kelly A. et al. 2014. “Pathophysiology of Short Bowel Syndrome.” Journal of Parenteral and Enteral Nutrition 38(1_suppl): 14S--22S. http://doi.wiley.com/10.1177/0148607113520005.

Tonlorenzi, R. et al. 2007 “Isolation and characterization of Mesoangioblasts from mouse, dogs, and human tissue”. Current protocols in stem cell biology.

Totonelli, G. et al. 2012. “A Rat Decellularised Small Bowel Scaffold That Preserves Villus-Crypt Architecture for Intestinal Regeneration.” Biomaterials 33(12): 3401–10. http://www.ncbi.nlm.nih.gov/pubmed/22305104.

Totonelli, G. et al. 2013. “Detergent Enzymatic Treatment for the Development of a Natural Acellular Matrix for Oesophageal Regeneration.” Pediatric Surgery International 29(1): 87–95. http://www.ncbi.nlm.nih.gov/pubmed/23124129.

Tresoldi, C. et al. 2015. “Cells and Stimuli in Small-Caliber Blood Vessel Tissue Engineering.” Regenerative medicine 10(4): 505–27.

Troppmann, C. et al. 2001. “Intestinal Transplantation.” https://www.ncbi.nlm.nih.gov/books/NBK6902/.

Tura, O. et al 2013 “Late outgrowth endothelial cells resemble mature endothelial cells and are not derived from bone marrow.” Stem Cells. 2013;31:338–348.

Valentijn K. M. et al. 2013 “Weibel–Palade bodies: a window to von Willebrand disease.” Journal of Thrombosis and Haemostasis. 2013;11(4):581–592. doi: 10.1111/jth.12160.

Vasyutina, E. et al. 2007. RBP-J (Rbpsuh) is essential to maintain muscle progenitor cells and to generate satellite cells. Proceedings of the National Academy of Sciences of the United States of America *104*, 4443-4448.

Verstegen, Monique M A. et al. 2017. “Decellularization of Whole Human Liver Grafts Using Controlled Perfusion for Transplantable Organ Bioscaffolds.” Stem cells and development 26(18): 1304–15.

von Tell, D. et al. 2006. “Pericytes and Vascular Stability.” Experimental Cell Research 312(5): 623–29. https://www.sciencedirect.com/science/article/pii/S0014482705004866?via%3Dihu .

Wang, C. et al. 2010. “A Small Diameter Elastic Blood Vessel Wall Prepared under Pulsatile Conditions from Polyglycolic Acid Mesh and Smooth Muscle Cells Differentiated from Adipose-Derived Stem Cells.” Biomaterials 31(4): 621–30. http://www.ncbi.nlm.nih.gov/pubmed/19819545.

Wang, L., et al 2012. “Liver sinusoidal endothelial cell progenitor cells promote liver regeneration in rats.” J. Clin. Invest. 122, 1567–1573.

Wen, Y. et al. 2012. Constitutive Notch activation upregulates Pax7 and promotes the selfrenewal of skeletal muscle satellite cells. Molecular and cellular biology *32*, 2300-2311

Weymann, A. et al. 2014. “Bioartificial Heart: A Human-Sized Porcine Model--the Way Ahead.” PloS one 9(11): e111591.

Xu, C. et al. 2014. “Arteries Are Formed by Vein-Derived Endothelial Tip Cells.” Nature Communications 5.

Yasui, H. et al. 2014. “Excitation Propagation in Three-Dimensional Engineered Hearts Using Decellularised Extracellular Matrix.” Biomaterials 35(27): 7839–50.

Yoder, MC. et al. 2007 “Redefining endothelial progenitor cells via clonal analysis and hematopoietic stem/progenitor cell principals.” Blood. 109:1801–1809.

Yu, G. et al. 2016. ReactomePA: An R/Bioconductor package for reactome pathway analysis and visualization. *Mol. Biosyst.* **12**, 477–479.

Urbani and Camilli et al 2017. “Multi-stage bioengineering of a layered oesophagus with in vitro expanded muscle and epithelial adult progenitors” Nature Comunication. 9:4286.

Zhao, Y. et al. 2010. “The Development of a Tissue-Engineered Artery Using Decellularised Scaffold and Autologous Ovine Mesenchymal Stem Cells.” Biomaterials 31(2): 296–307. http://www.ncbi.nlm.nih.gov/pubmed/19819544.

Zhou, H. et al. 2017. “Bioengineering Human Lung Grafts on Porcine Matrix.” Annals of Surgery 267(3): 1. http://www.ncbi.nlm.nih.gov/pubmed/28085694.

Zimmermann, K.W. et al. 1923. “Der Feinere Bau Der Blutkapillaren. Z Anat Ent-Wicklungsgesch. 68.”

Acknowledgments

I wish to express my gratitude to Prof. Paolo De Coppi for offering me the chance to join his research team and to start this unbelievable adventure. Dr Alessandro Pellegata for his supervision and advice in this years.

My industrial supervisors Gianni Dal Negro and Umesh Kumar for encouraging my research during this 4 years. Communicating my work to you and to other GSK scientists was an invaluable experience that busted my self-confidence to pursue in my work. Thank you all for inspiring me through your supervision, our scientific and personal discussions.

Thanks to all the people of the lab that helped me to go through this taught project. To my office mates and friends Giulia, Marco, Giovanni, Jeo, Soichi, Koichi and Brendan. Thank you for not killing me for being the noisier, maniac control of the office temperature and dirty shaker leaver. You have been awesome!

In particular thanks to all the students that worked along with me during this journey: Justina, Simone, Susanna and Marta. Your help and friendship was incalculable.

I am extremely thankful to all my friends in Italy: Susanna, Flavio, Letizia, Siffredina, and Sbadacchio. It's been difficult at times to engage in each other's lives, but you've always made me feel as if I've never left.

Letizia and Siffredina, in particular, you have been my spiritual family. I love you to bits.

I'm grateful to all of my new London friends, both inside and beyond the lab, for becoming my new family and making this place feel like home. I'd want to thank my "sandwich's" crick (Carlotta, Marco, Giovanni, Silvia, and Sara) for just listening

whenever I felt overwhelmed, but also because special moments, laughter, and unforgettable memories are all related to any of you.
My deepest gratitude goes in particular to Sara and Silvia. You listened to me, believed in me and brought me up throughout all this path.

My heart is full of gratitude for Emre and his family. Not only my PhD, but also my life wouldn't have been the same without you. You have always reminded me that, not matter what challenges I was facing and how important my experiments were, the things that really mattered were outside the lab. Thank you for all the unforgettable adventures. Yes, Pompei's one is still one of my favourite! I care for you.

I am profoundly grateful to my grandmother and my aunty Giovanna. You have been my teachers since when I was a little naughty kid. I know, I was a pain! I didn't like being lectured for my spelling errors! You have never given up on me, no matter how often I challenged you. I owe a lot of my perseverance to you, and there is not a PhD you can learn it from.

Most importantly, my success wouldn't have been possible without my family. You have been so close to me regardless the distance. In these years, I've realised that you are the foundation of my life patterns, my important decisions, the people I decided to love and accept in my life. There is a lot of you in this PhD too. The story that entangle us is tied to my decision to join this project and how I choose to pursue it. This brought me to many things I loved, as well as many things I regret and will come to accept. Here I began the most beautiful of my researches, the one that defines who I am and it comes from you. I am eternally thankful for your love. This thesis is for you.